23236351, 23232701, 23237721, 23234116
23235733, 23232317, 23236735, 23239437

विश्वविद्यालय अनुदान आयोग
बहादुरशाह जफर मार्ग
नई दिल्ली-110 002
UNIVERSITY GRANTS COMMISSION
BAHADURSHAH ZAFAR MARG
NEW DELHI-110 002

FINAL REPORT OF THE WORK DONE ON THE MAJOR RESEARCH PROJECT

1. **Project report No. FINAL**

2. **UGC Reference No. F. UGC-41-206/2012 (SR) Dated 17 July 2012**

3. **Period of Report : from 01.07.2012 to 31.12.2015**

4. **Title of the research project: Development of organic synthetic methods using nonmetallic catalyst: Strategy towards bioactive molecules**

5. **(a) Name of the Principal Investigator** — **DR. PRODEEP PHUKAN**

   (b) Department — **Department of Chemistry, Gauhati University,**

   (c) University/College where work has progressed — **Department of Chemistry, Gauhati University, Guwahati-781014**

6. **Effective date of starting of the project : 01.07.2012**

7. **Grant approved and expenditure incurred during the period of the report:**
   (a) Total amount approved Rs. 13,58,300.00

   (b) Total expenditure Rs. 12,48,767.00

(c) Report of the work done:

(i) Brief objective of the project

The basic aim of the research proposal is to examine the catalytic activity of some nonmetallic catalyst for various organic transformations, particularly carbon – carbon bond formation reactions. We shall be interested

- To continue our investigation on the catalytic effect of Iodine for organic transformations and application of these methodologies for the synthesis of bioactive molecules.
- To develop an organocatalyst for organic transformations.
- To study the possibility of use of quaternary ammonium salts as catalyst for various organic transformations.
- To perform mechanistic investigation of these reactions using density functional based reactivity descriptors.

Proposed Methodology

Part A: Use of Iodine as catalyst and synthesis of bioactive molecules:

One of the objectives of the present investigation is to continue our study on the catalytic property of iodine for various organic transformations, C – C bond formation in particular. We intend to develop strategies for synthesis of molecular library of compounds using iodine catalyst. More specifically, following reactions were proposed to be investigated.

Our aim was to synthesize different pipyridine analogues **A** (Scheme 1) starting from a homoallylic amine synthesized via iodine catalyzed three component reaction.

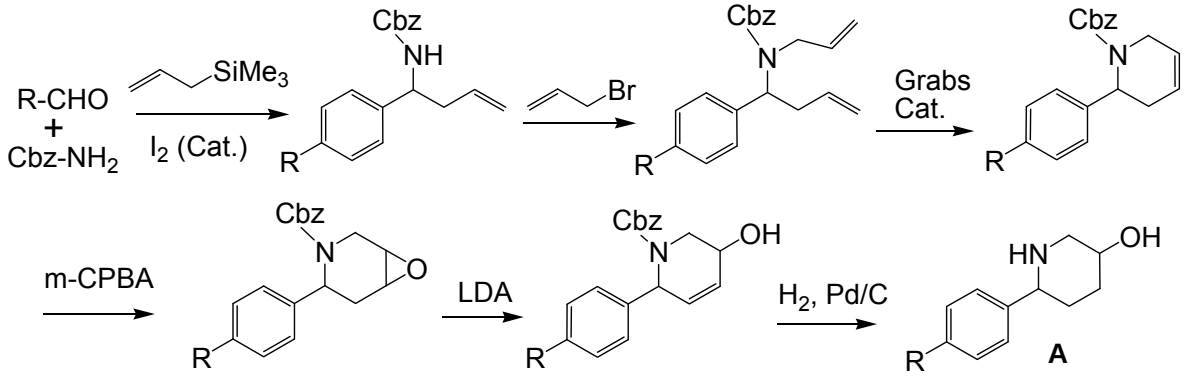

Scheme 1. Proposed work for the synthesis of pipyridine analogues

We also proposed to synthesize different cytoxazone type structures **B** (Scheme 2). First step of our strategy is sharpless asymmetric dihydroxylation of homoallyl amine made via iodine catalyzed reaction.

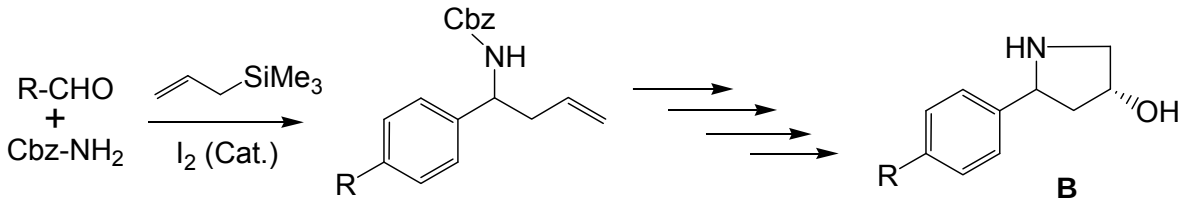

Scheme 2. Proposed work for the synthesis of cytoxazone analogues

Part B: Development of methodologies using organocatalyst and phase transfer catalyst.

Use of tetrabutyl ammonium salts especially, bisbenzoates (Figure 1) as catalyst for various organic transformations.

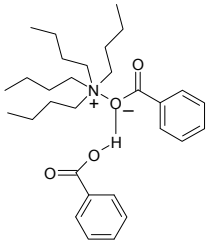

Figure 1. Tetrabutyl ammonium bisbanzoate (TBABB)

We proposed to evaluate the catalytic activity of this type of catalyst for various organic transformations. For example: Mannich type reaction (Scheme 3) to evaluate the catalytic activity of TBABB (Scheme 3).

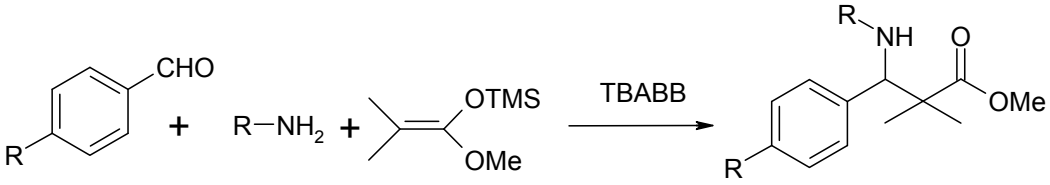

Scheme 3. Propsed scheme for Mannich type reaction using PTC

Apart from this, we would like to look for the development of new organocatalyst during the course of our investigations.

Part C: Computational studies:

Investigation on the reactivity using Density functional based reactivity descriptors. The reactivity descriptors include: global hardness, global softness, Fukui function, local softness etc.

ii. Work done

Part A: Use of Iodine as catalyst and synthesis of bioactive molecules

As per our plan to develop synthetic strategy for bioactive molecules, we opted the synthetic scheme for piperidine analogues following the reaction pathway described in Scheme 4.

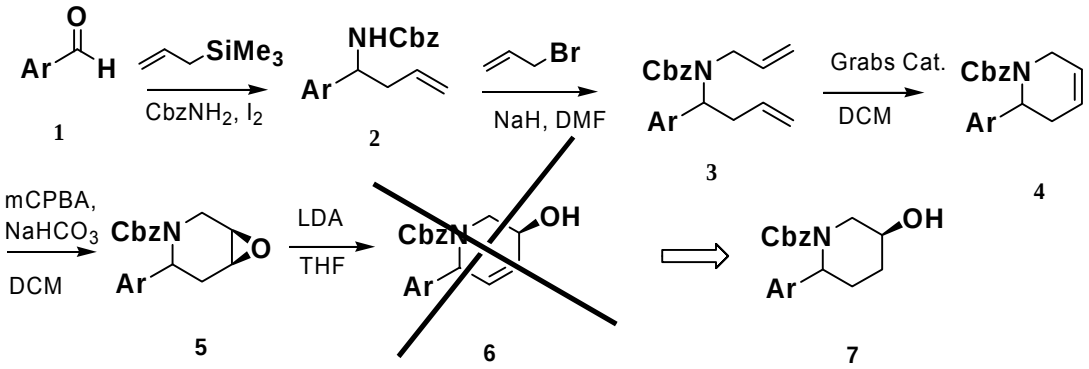

Scheme 4. Attempt for the synthesis of piperidine analogues

The first step of the synthesis is the conversion of aldehyde 1 to homoallyl amine using iodine as a catalyst. Continuing the synthetic pathway, we could synthesize epoxide **5** successfully, in good yield. The next step of the reaction is the treatment of epoxide **5** with LDA to produce the compound **6**. However, the reaction failed to produce the desired product. The reaction led to a non-isolable mixture of many products, which could not be characterized.

Hence, we planned to carry out asymmetric dihydroxylation reaction of compound 4 (Scheme 5).[1] Interestingly under the well documented and standardized Sharpless dihydroxylation protocol, asymmetric dihydroxylation failed to impart asymmetric induction in the resulting diol **8**.

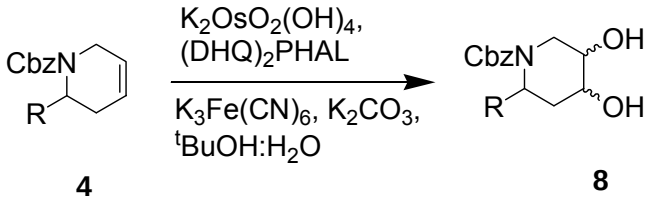

Scheme 5. Asymmetric dihydroxylation of tetrahydropyridine analouges

[1] Borah, A. J.; Phukan, P. ***Indian J. Chem.,*** **2014**, *53B*, 1417-1424

Enantiomeric excess of the products were determined from HPLC analysis. Results are shown in Table 1.

Table 1: Asymmetric dihydroxylation of alkene derivative **4**

Entry	Substrate (**4**)	Product (**8**)	Time (h)	Yield (%)	ee	$[\alpha]_D^{26}$
a	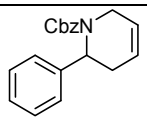	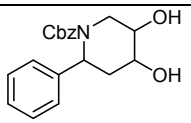	24	85	1.6	+1.1
b	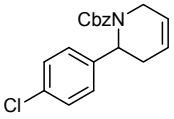	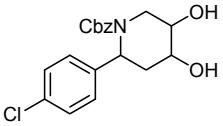	24	90	2.4	+1.2
c	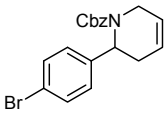	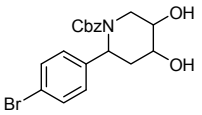	24	85	1.3	+1.7
d	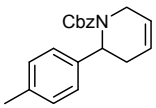	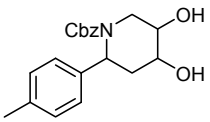	24	83	1.4	+1.4
e	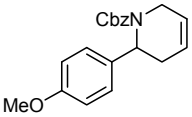	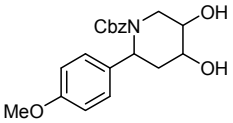	24	81	2.0	-1.5
f	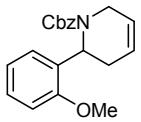	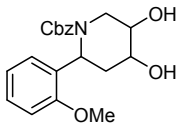	24	81	1.0	+1.6
g	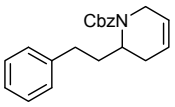	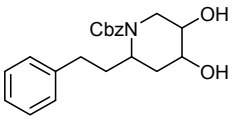	24	80	2.6	+2.5

However overall synthetic route is a convenient route for synthesis of 2,4,5-trisubstituted piperdine analogues **8**. Following the above synthetic strategy, we have synthesized seven new 2,4,5-trisubstituted piperidine analogues from corresponding Cbz-protected homoallyl amine as starting material. All the synthetic steps are very efficient and products are formed with high yield.

We have also carried out further studies to synthesize cytoxazone type structures. However, while performing Sharpless asymmetric dihydroxylation in presence of DHQD-PHAL ligand on compound 2a, we observed the formation of a complex mixture of diastereomers (Scheme 6).

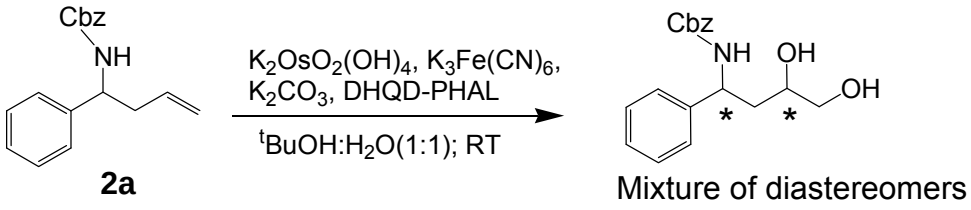

2a Mixture of diastereomers

Scheme 6. Attempt for asymmetric dihydroxylation of homoallylic amine

This may be because of remote chiral induction during asymmetric dihydroxilation which resulted in the formation of two chiral centers attached to both nitrogen and oxygen atom. We did not proceed further for the synthesis of cytoxazone analogues due to difficulty in separation of diastereomers from the mixture.

As a continuation of our work on iodine catalyzed reactions, we also developed a new protocol for the synthesis of aziridines from olefin using bromamine-T as the nitrene source (Scheme 7).[2]

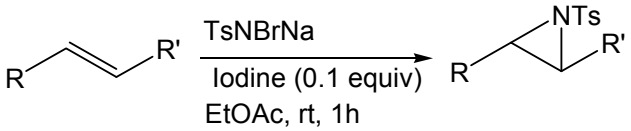

Scheme 7. Synthesis of aziridine using bromamine-T in presence of iodine catalyst

When an olefin (2 equiv.) was treated with bromamine-T (1 equiv) in presence of iodine (0.1 equiv.) at room temperature for 1h, corresponding aziridine was obtained in high yield. Results are summarized in Figure 2.

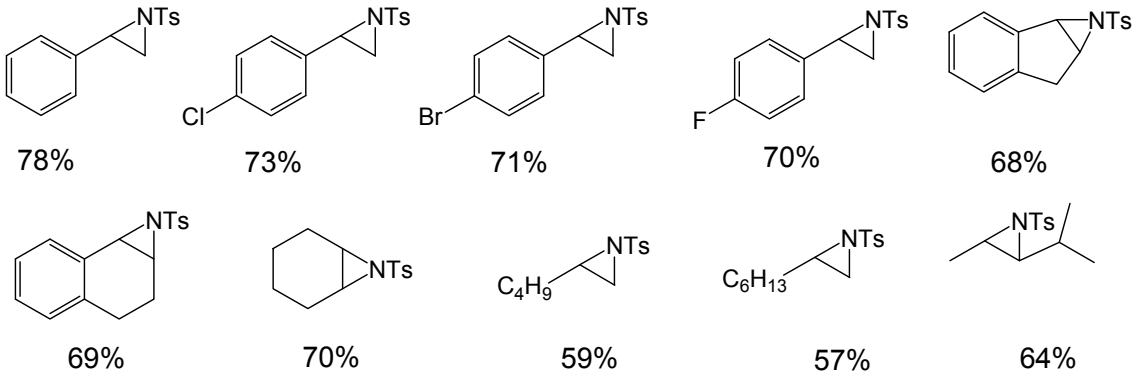

Figure 2. Aziridination of various alkenes with TsNBrNa using iodine catalyst

We also developed another methodology for the synthesis of bromohydrins using NBS in presence of Iodine catalyst (**Scheme 8**).

[2] Sharma, C. M.; Kashyap, B.; **Phukan, P**. ***Indian J. Chem.,*** **2014**, *53B*, 750-753

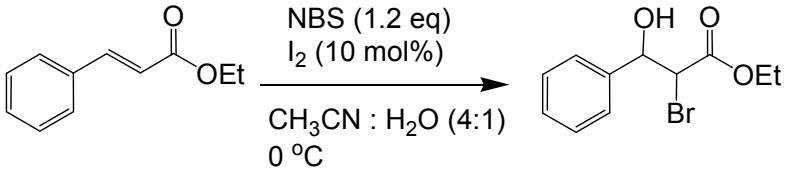

Scheme 8. Synthesis of bromohydrins in presence of iodine catalyst

Different olefins such as α, β-unsaturated carbonyl compounds, styrene etc. (1 equiv.) when treated with NBS (1.2 equiv.) in acetonitrile water mixture (4:1) in presence of iodine (0.1 equiv.) at 0 ºC, corresponding bromohydrins are formed in high yield.[3] Results are summarized in Figure 3.

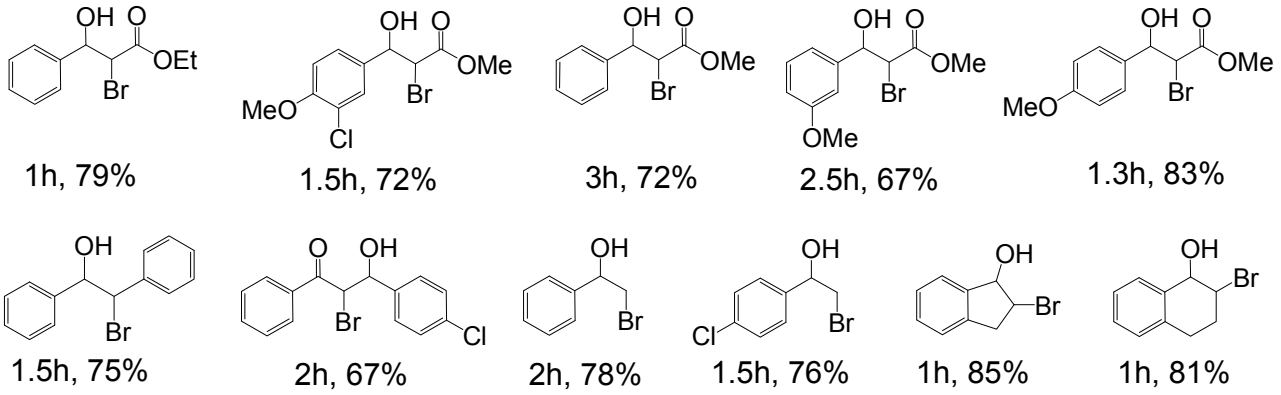

Figure 3. Synthesis of bromohydrin from olefins using NBS and iodine catalyst

Part B: Development of methodologies using organocatalyst and phase transfer catalyst

Following our proposed plan of work, we have carried out our initial studies to use tetrabutylammonium bi-benzoate (TBABB) as catalyst for Mannich reaction (Scheme 3). The reaction was carried out by treating banzaldehyde, banzyl amine and silyl ketene acetal in presence of a catalytic amount of TBABB (10 mol %) in THF at room temperature. However, the reaction did not proceed in the desired manner to produce the Mannich product. Instead, the reaction yielded simple imines as a result of the reaction of aldehyde with amine **(Scheme 9)**. Mannich reaction did not proceed in presence of TBABB.

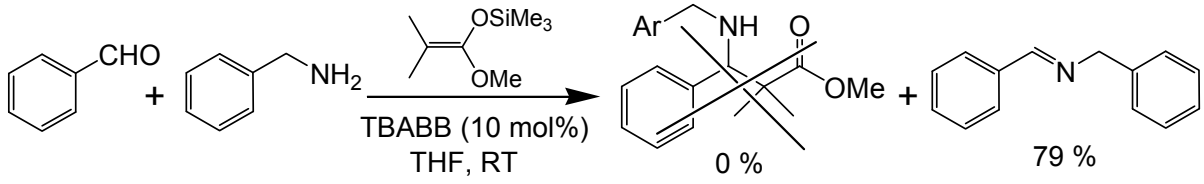

Scheme 9. Formation of immins using TBABB as catalyst

[3] Loadh, R.; Borah, A. J.; Phukan, P. ***Indian J. Chem.,*** **2014**, *53B*, 1425-1429

Finally under the optimum reaction condition, different imines are synthesized by reacting an aromatic aldehyde (1 equiv.) with benzyl amine (1.05 equiv.) in presence of catalytic amount of TBABB (15 mol%) in THF at room temperature (Figure 4).

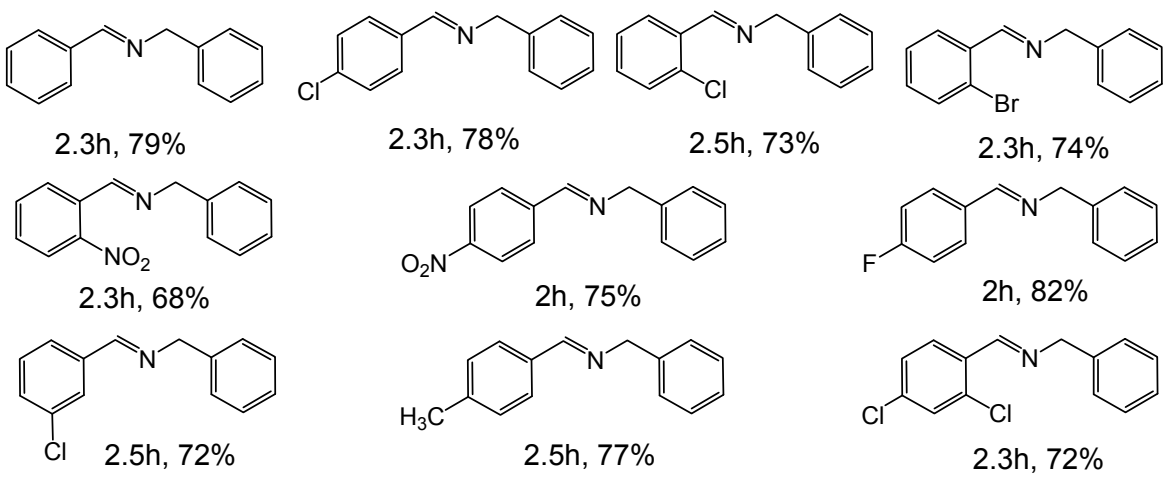

Figure 4. Synthesis of imines from various aldehydes catalyst by TBABB

Further, we have also tested this catalyst for the preparation of homoallylic alcohols from various aldehydes and allyltri(n-butyl)tin (Scheme 10). Initially, a systematic study on the synthesis of homoallylic alcohols was carried out using 4-chlorobenzaldehyde as substrate. In this reaction, allyltri(n-butyl)tin (1 mmol) was added to a mixture of 4-chlorobenzaldehyde (1 mmol) and tetrabutylammonium bi-benzoate (10 mol%) in dichloromethane at room temperature. Reaction at room temperature in DCM failed to yield the desired product after 24 h of the reaction. Further study of the reaction using DMF and THF as solvent revealed that THF is the most suitable solvent for this reaction. The reaction was further examined in presence of different amount of catalyst (10%, 15%, 20%). The yield generally increased with increasing concentration of the catalyst. However, further increase of the molar concentration of the catalyst did not significantly increase the yield of the product. Reaction at higher temperature produced poor yield of the product

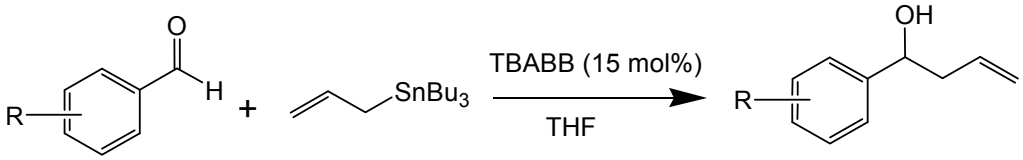

Scheme 10. Synthesis of homoallylic alcohols using TBABB

Finally, the reaction was extended by reacting 1 mmol of aldehyde with allyltributyltin in presence of catalytic amount of TBABB (15 mol%) in THF to produce corresponding homoallyl alcohols in good yield (Figure 5).

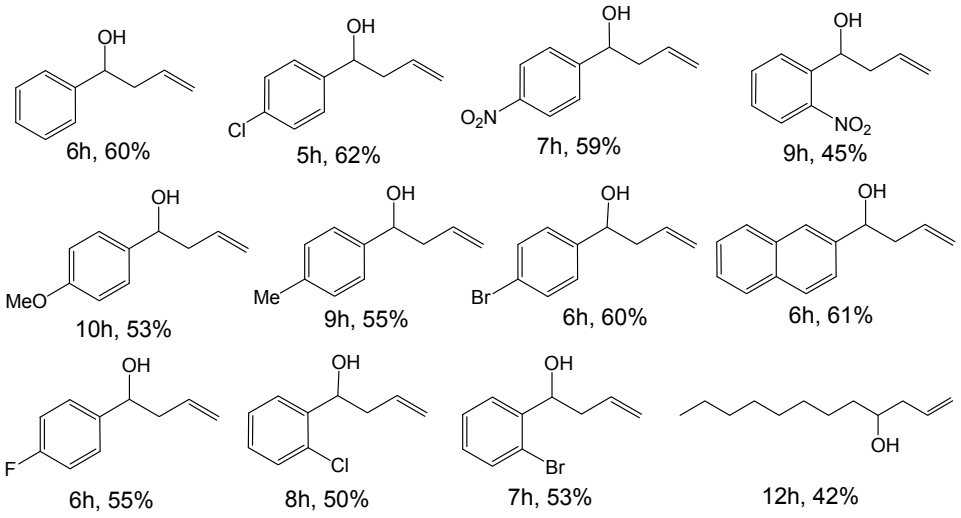

Figure 5. Synthesis of homoallylic alcohols using the TBABB/ THF system

However, the catalytic performance of the phase transfer catalyst TBABB was not impressive in this case.

Our study was further extended for nitroaldol reaction in presence of phase transfer catalyst (Scheme 11). In this study, we have tested tetrabutyl ammonium hydroxide (TBAOH) and Ambersep 900-OH along with TBABB for the reaction. Among all the three catalysts, Ambersep 900-OH was found to be the best catalyst for nitroaldol reaction. The catalyst (a commercially available resin) could be used as reusable heterogeneous catalyst for the synthesis of various nitro alcohols.

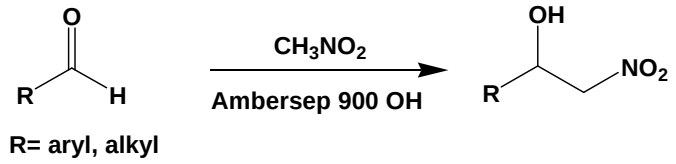

Scheme 11. Nitroaldol reaction using phase transfer catalyst

The reaction between aldehyde and nitromethane was performed under solvent-free condition at room temperature within a short time (1.2h - 2.5h) in the presence of 10 wt % of Ambersep 900-OH to produce corresponding nitroalcohols in high yield (72–91 %).[4] The catalyst could be reused (3 cycles) without appreciable loss of its activity.

[4] Loadh, R.; Sarma, M. J.; Borah, A. J.; **Phukan, P**. ***Monatsh. Chem.,*** **2015**, *146*, 969-972

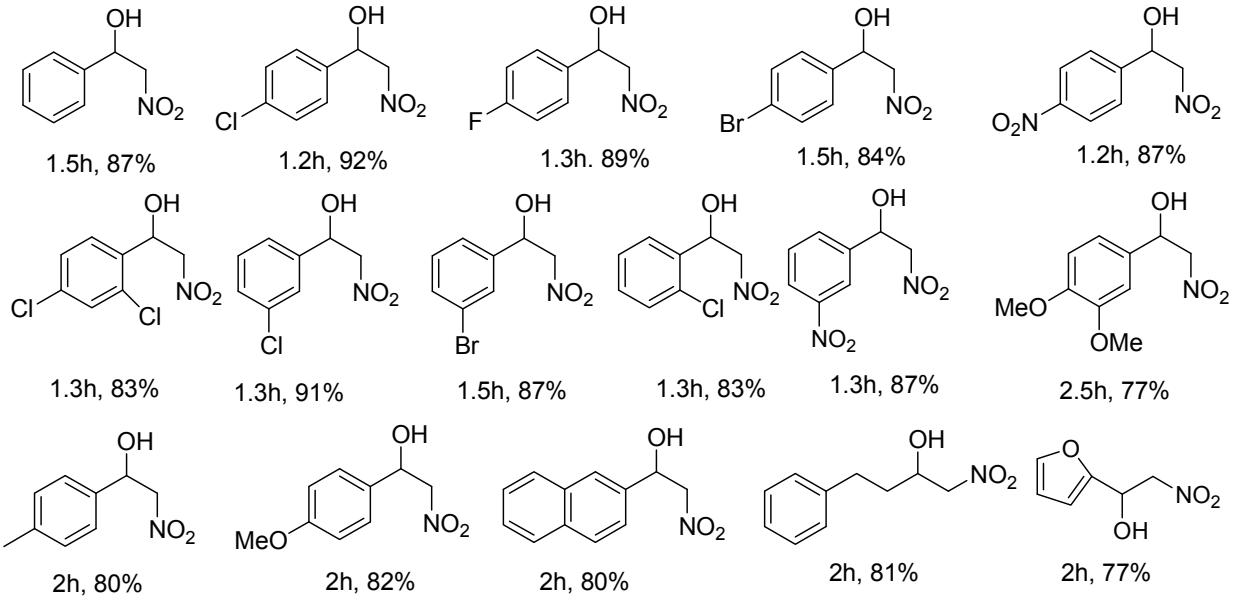

Figure 6: Henry reaction of nitromethane with various aldehydes

The catalyst was recovered from the reaction mixture just by filtration using copious amount of CH_2Cl_2. We have tested the recyclability of the catalyst for the Henry reaction by using *p*-nitrobenzaldehyde and nitromethane under the optimized reaction conditions in three consecutive cycles. During the first two consecutive cycles the similar yield (85%) was recorded (Figure 7). In the third round of catalytic cycle, though the yield was found to be lower (82%), however the change was not detrimental.

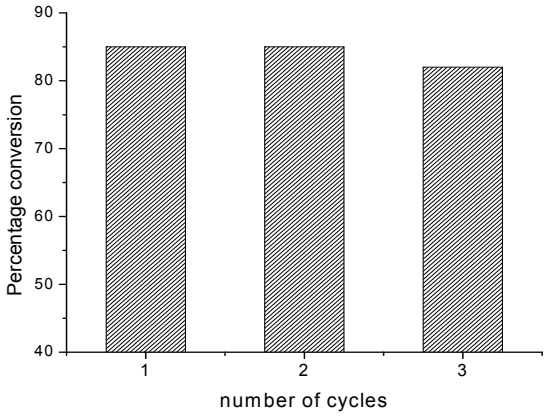

Figure 7: Bar diagram showing yield of 3 recycles of the catalyst

We have also investigated the use of different phase transfer catalysts for the synthesis of α,β-unsaturated cyanoesters from aldehydes and ethyl cyanoacetate (**Scheme 12**).

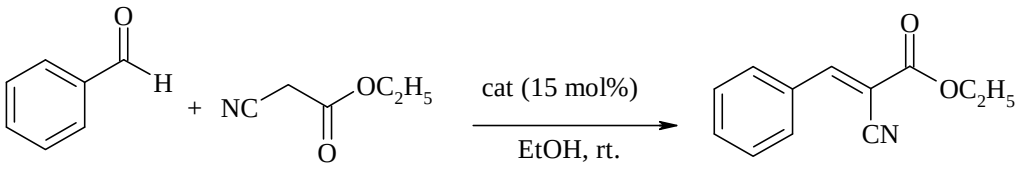

Scheme 12. Knoevenagel condensation using phase transfer catalyst

Three different phase transfer catalyst such as tetrabutyl ammonium bibenzoate, tetrabutyl ammonium hydroxide and Ambersep 900-OH were tested for this reaction. Optimization reactions are displayed in **Table 2**. Ambersep 900 OH was found to be the best choice. This reaction was carried out between aldehyde (1 equiv.) and ethyl cyanoacetate (1 equiv.) in ethanol at room temperature in presence of 15 mol% of catalyst**.**

Table 2. Solvent effect on Knoevenagel Condensation at room temperature

Entry	Catalyst	Mol% of catalyst	Solvent	Time (min)	Yield
1	Ambersep 900 OH	5	Ethanol	45	75
2		10		40	82
3		15		30	88
4		10	Methanol	50	78
5	TBAH	5	Ethanol	50	65
6		10		35	75
7		15		35	80
8		10	Methanol	40	70
9	TBABB	5	Ethanol	60	62
10		10		50	68
11		15		50	70
12		10	Methanol	60	65

After optimizing the reaction condition, we have extended the process to variety of aldehyde, which are summarized in **Figure 8**. The present method works well for all types of substrate such as aliphatic, aromatic aldehyde to produce α, β-unsaturated cyanoesters in good to excellent yield.

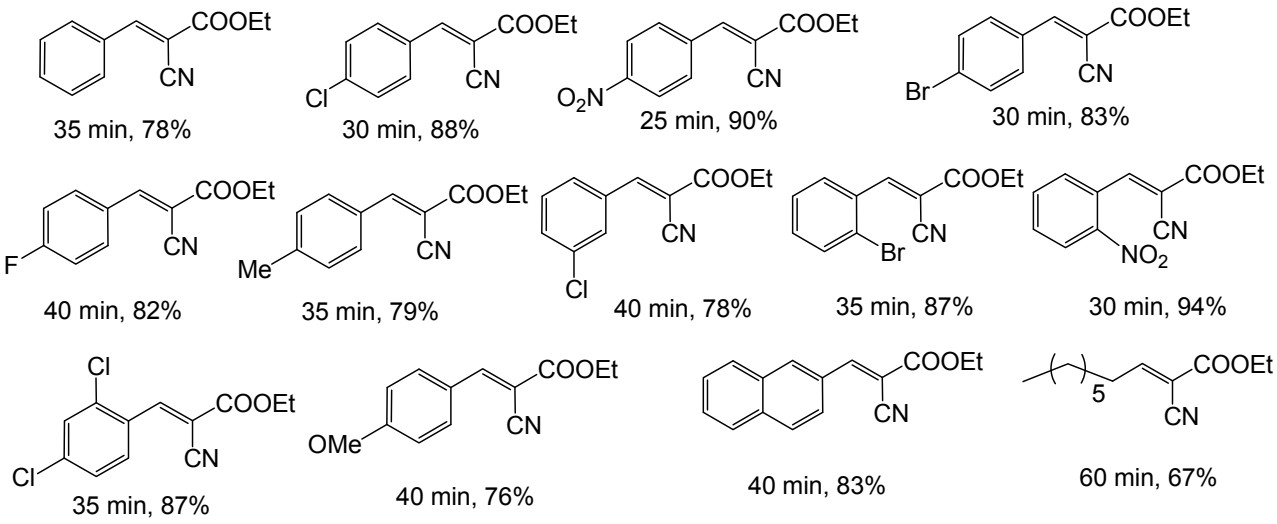

Figure 8. Knoevenagel condensation using Ambersep 900-OH as catalyst

The reusability of the catalyst was checked over several cycles by the repetition of the reaction which was carried out with 4-chloro-benzaldehyde and ethylcyanoacetate in presence of used catalyst Ambersep 900 OH (Figure 9) in ethanol as solvent.

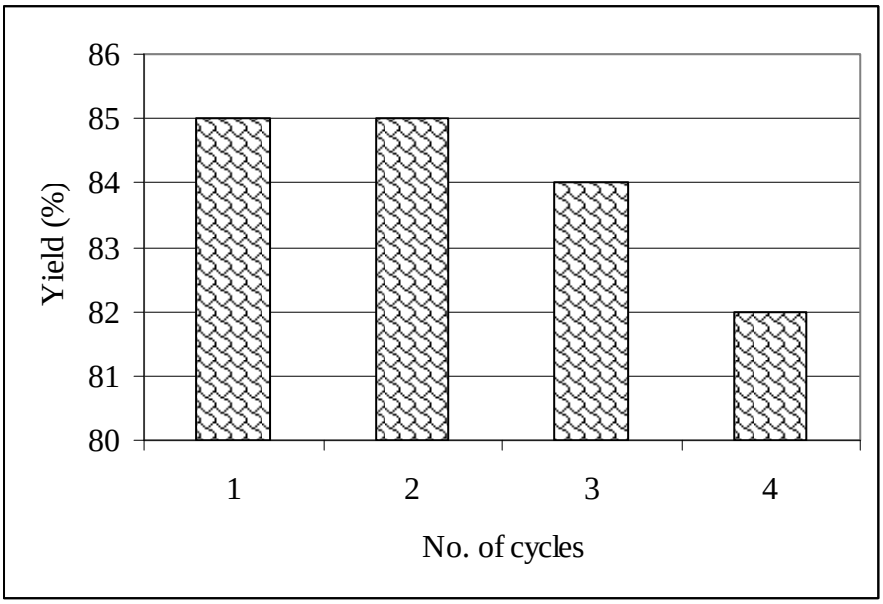

Figure 9. Recycling experiments for the Knoevenagel reaction

The catalyst did not exhibit any significant loss of catalyst activity after using four consecutive times.

Part C: Development of methodologies using Silica based organocatalyst

During our investigation, we also developed a new hybrid catalyst by immobilizing nicotinic acid onto an organomodified silica via thioesterification. The catalyst was fully characterized and applied as a heterogeneous catalyst for the synthesis of benzoylfumarate (Scheme 13).[5]

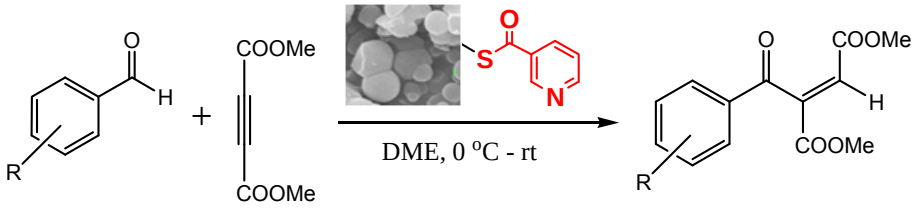

Scheme 13. Synthesis of benzoyl fumaratte using organosilica-pyridine catalyst

The supported organosilica-nicotinate catalyst was characterized by XRD, IR, N_2-adsorption and SEM analysis (Figure 10).

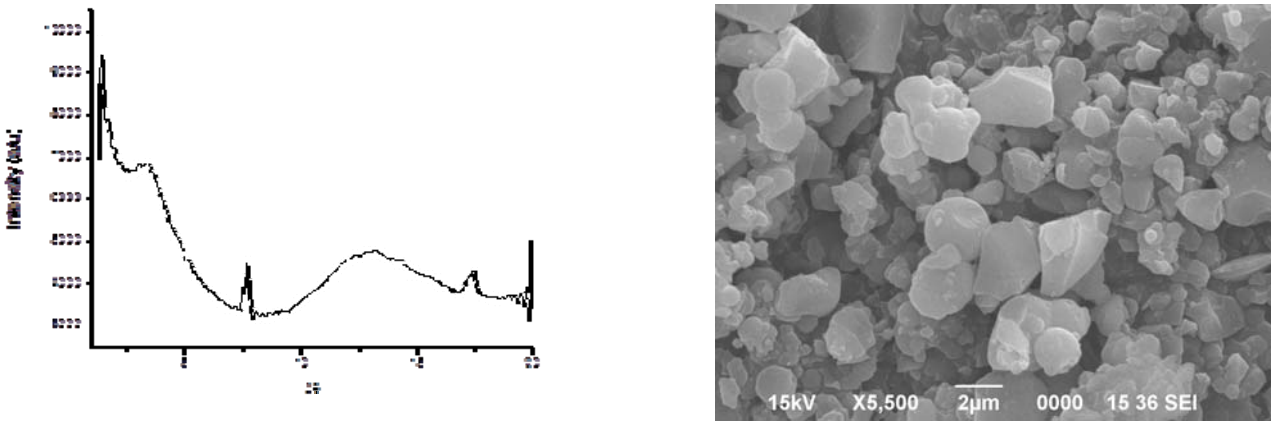

Figure 10. XRD and SEM image of the catalyst

The reactions work well in presence of 20 wt% of the catalyst at room temperature to produce the desired products in high yield after a reaction of 12h (Figure 11). The catalyst could be recovered and reused without appreciable change in activity.

[5] Singh, R. S. K.; Kashyap, B.; Phukan, P. ***Tetrahedron Lett.*** **2013**, *54*, 6687-6690

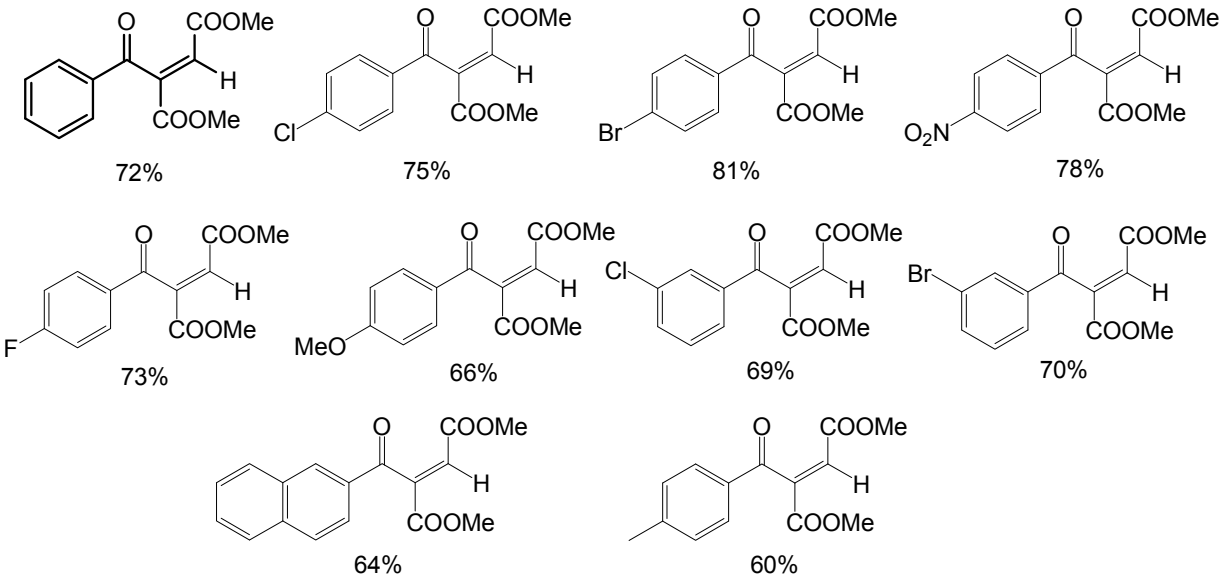

Figure 11. Synthesis of various benzoylfumarates using organomodified silica catalyst

Continuing further in this direction, we have developed a new SO3H-functionalised organomodified silica hybrid catalyst has been developed by incorporating S-sulfonic acid onto an organomodified silica (Scheme 14). The catalyst was synthesized by treating mercaptopropyl mesoporous silica with chlorosulfonic acid in CHCl3 at room temperature. The catalyst was characterized using IR, XRD, SEM, EDX, BET analysis and TGA.

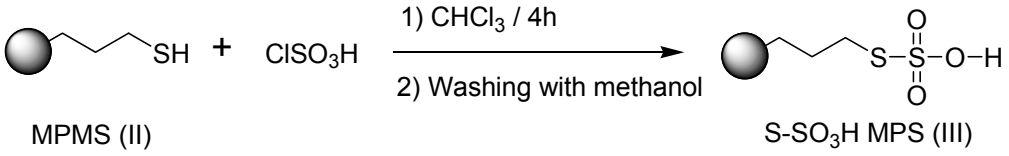

Scheme 14. Synthesis of acidic organomodified silica catalyst

The catalyst was applied as a heterogeneous catalyst for various reactions. For example, α,α-dibromo ketones were synthesized directly from alkynes and NBS at room temperature (Scheme 15). The reactions work well in the presence of 10 wt % of the catalyst in a mixture of acetonitrile and water (4:1 ratio) at room temperature to produce the desired products in high yield. The catalyst could be recovered and reused without appreciable change in activity

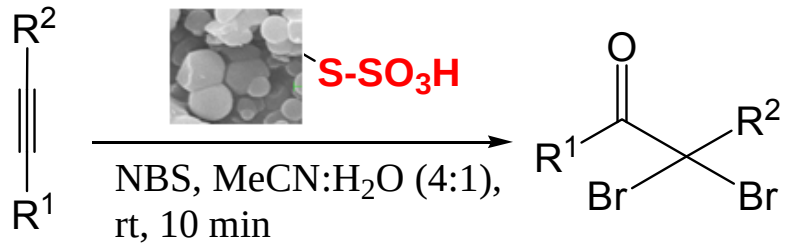

Scheme 15. Synthesis of α,α-dibromo ketones directly from alkynes and NBS

Initially investigation for the reaction between phenylacetylene and NBS revealed that the best results can be achieved by using 2.3 equivalents of NBS in presence of 10 wt % of catalyst in a mixture of acetonitrile and water (4:1 ratio). Figure 12 displayes the scope of the reaction for various alkynes under the optimum reaction condition. The reaction completes within 10 min at room temperature.

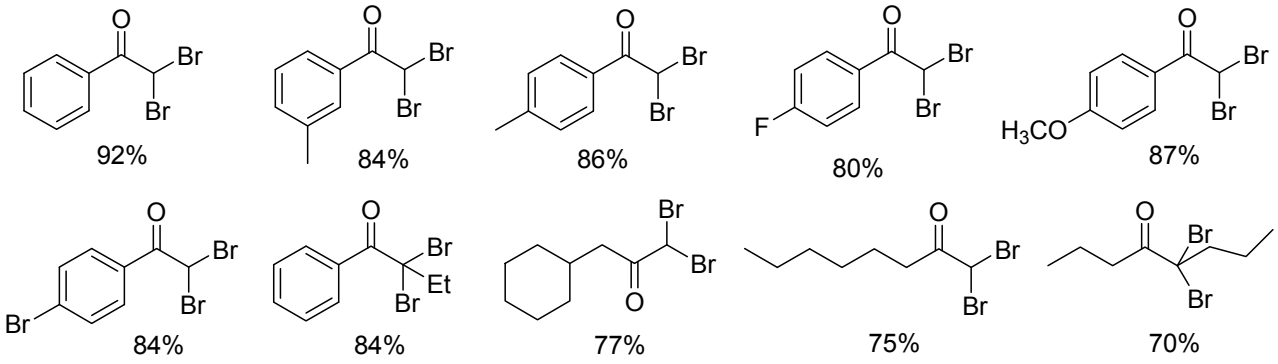

Figure 12. Synthesis of α,α-dibromoketones from alkynes using S-sulphonic acid functionalised organosilica

Reusability of the catalyst was tested with phenylacetylene. To reuse, the catalyst was filtered after completion of the reaction, washed with methanol and petroleum ether, dried under vacuum, and then kept in a desiccator overnight before reuse. It was observed that the catalyst could be reused three times without appreciable loss in activity (Figure 13).

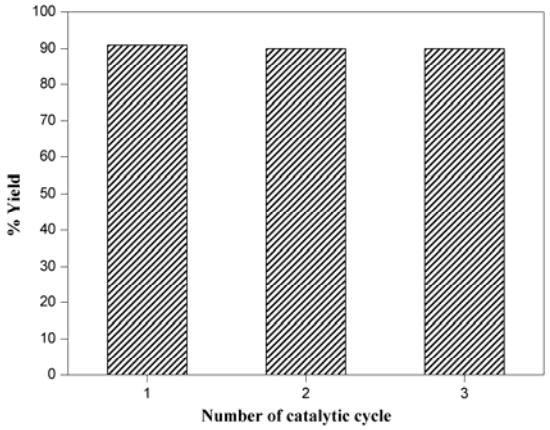

Figure 13. Bar diagram showing yield of 3 recycles of the catalyst.

Part D. Synthetic methodologies using pyridine based catalyst

Pyridine has been used as an excellent solvent for acetylating reaction. We intended to carry out a study on the catalytic efficiency of pyridine for acetylation of alcohol using acetic anhydride. For comparison, DMAP and 44′-di-*tert*-butyl-22′-dipyridyl (DTBDP) were also chosen for initial study. The catalytic efficiency was evaluated in presence of an equimolar amount of acetic anhydride in presence of catalytic amount of the pyridine derivatives at room temperature under solvent free condition (Scheme 16).

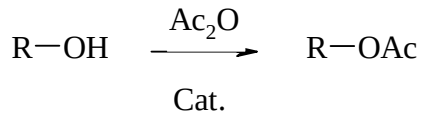

Catalyst = pyridine, DMAP, DTBDP

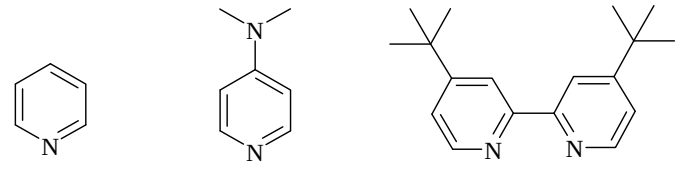

Pyridine DMAP DTBDP

Scheme 16. Acetylation of alcohols in presence of pyridine derivatives

Initial experiments for acetylation of benzyl alcohol (1 mmol) with acetic anhydride (1 mmol) at room temperature under solvent free condition revealed that the use of 15 mol % of catalyst was the best in terms of yield and reaction time. The reaction was further extended the procedure using different alcohols. The results are summarized in **Table 3**.

Table 3. Acetylation of alcohols under solvent free condition

Entry	Substrate	Product	Pyridine		DMAP		DTBDP	
			Time min	Yield (%)	Time min	Yield (%)	Time min	Yield (%)
1.	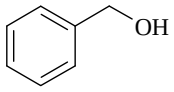	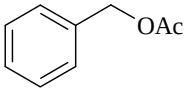	10	98	5	95	60	68
2.	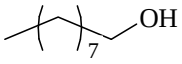	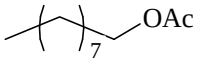	20	91	10	88	60	65
3.	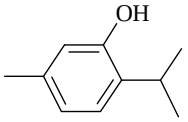	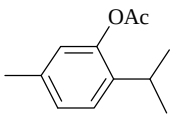	20	80	10	90	45	60
4.	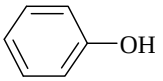	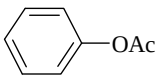	5	97	3	88	35	50
5.	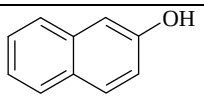	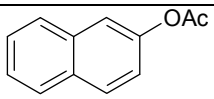	25	95	12	92	60	60
6.	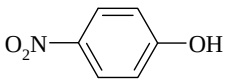	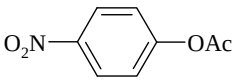	15	96	7	95	40	52
7.	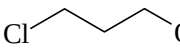	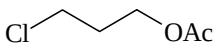	10	93	5	87	40	70
8.	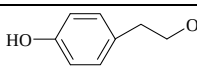	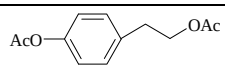	15	58	10	70	40	65
9.	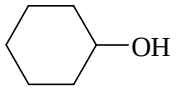	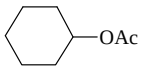	20	92	10	96	40	70
10.	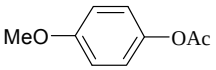	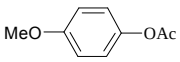	20	60	10	98	60	60
11.	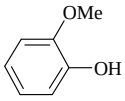	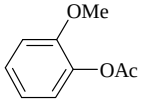	60	No reaction	60	No reaction	60	No reaction
12.	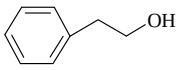	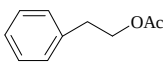	15	88	5	92	40	70
13.	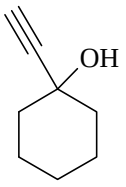	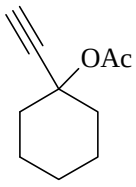	60	No reaction	30	80	60	No reaction

DMAP has been found to be a very effective catalyst for acetylation of alcohols and phenols, under solvent free condition using acetic anhydride as the acetylating agent. The order of catalytic activity of pyridine derivatives under consideration was found to be

DMAP > Pyridine > DTBDP

After getting success in the use of pyridine anchored organosilica catalyst, we have also examined the catalytic efficiency of poly(4-vinylpyridine-co-ethylvinylbenzene) 25% cross-linked (with divinylbenzene) as a heterogeneous catalyst for the synthesis of benzoyl fumarate from aldehyde and dimethyl acetylenedicarboxylate. Our intension was to find out an alternative commercially available catalyst for the reaction. Various aromatic aldehydes undergo this reaction with good yield in presence of 15 wt% of the catalyst (**Table 4**).

Table 4. Synthesis of benzoyl fumarates using PVPEVB catalyst[a]

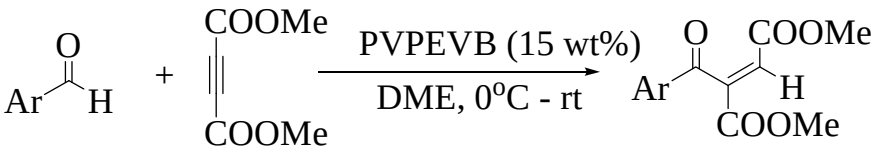

Entry	Ar	Yield (%)[b]
1	C_6H_5 (**1a**)	60
2	4-BrC_6H_4 (**1b**)	79
3	4-ClC_6H_4 (**1c**)	74
4	4-FC_6H_4 (**1d**)	70
5	4-$NO_2C_6H_4$ (**1e**)	80
6	4-$MeOC_6H_4$ (**1f**)	68
7	4-MeC_6H_4 (**1g**)	53
8	$C_{10}H_7$ (**1h**)	61
9	3-BrC_6H_4 (**1i**)	68
10	3-ClC_6H_4 (**1j**)	70

[a]Reaction condition: aldehyde (1 mmol), DMAD (1 mmol), PVPEVB (15 wt %), DME (5 mL), 0 °C to rt, 8h. [b]Isolated yield.

The catalyst was recovered and reused for six times without appreciable alternation in activity (Table 5).

Table 5. Reusability of the catalyst[a]

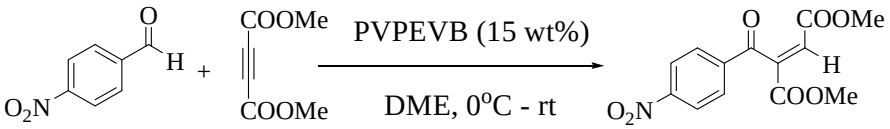

Entry	Catalyst reused	Catalyst recovered (%)[b]	Yield (%)[c]
1	1st	98	80
2	2nd	97	79
3	3rd	95	79
4	4th	92	78
5	5th	91	77
6	6th	89	76

[a]Reaction condition: 4-nitrobenzaldehyde (1 mmol), DMAD (1 mmol), DME (5 mL), 0 °C to rt, 8h. [b]With respect to first use. [c]Isolated yield.

Part E: Computational Studies:

DFT studies on ring opening pathways of 2-substituted non activated aziridine

Conceptual Density Functional Theory (DFT) based descriptors have been used to rationalize the observed activation and regioselectivity in the ring opening of 2-substituted non activated aziridines via aziridinium intermediate (Scheme 17).[6]

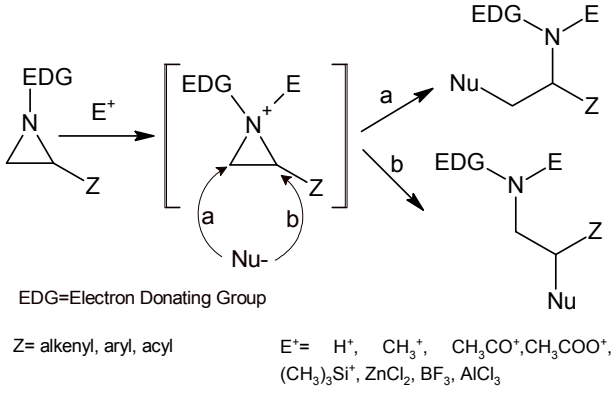

Scheme 17. Electrophilic activation and ring opening pathways of 2-substituted aziridine

All the aziridines and their aziridinium complexes with the electrophiles considered in this study are depicted in Figure 14. For convenience of treatment each of the four

[6] Baruah, B.; Deuri, S.; Phukan, P., ***Comput. Theo. Chem***, **2014**, *1027*, 197-202

aziridines (designated by A, B, C and D), their corresponding aziridinium species are put into four representative series, namely Series I, Series II, Series III and Series IV.

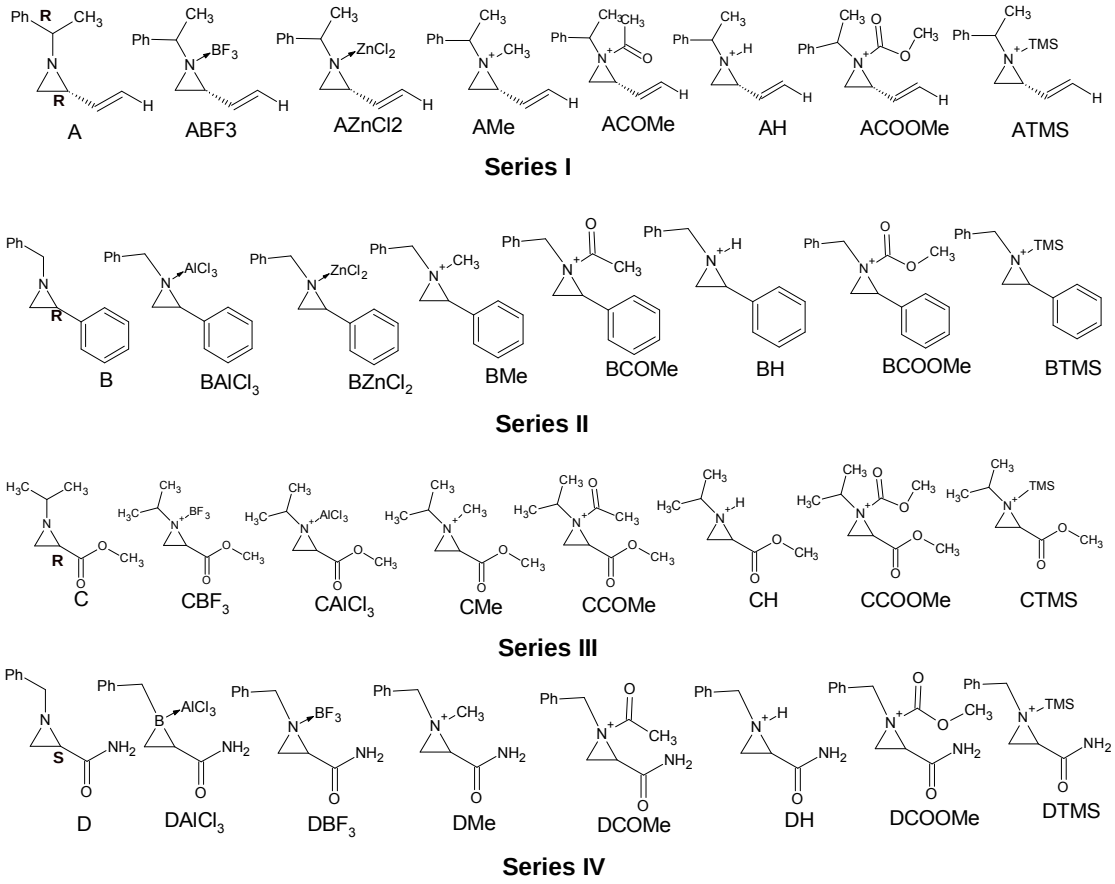

Figure 14. Non activated aziridines and their aziridinium species

Substantial increase in electrophilicity values was observed in going from aziridine to the aziridinium species via *N*-complexation. Irrespective of the type of aziridine, the same order of electrophilic activation is observed among each series of complexes. The order of electophilic activation can be generalized as shown in the Scheme 18.

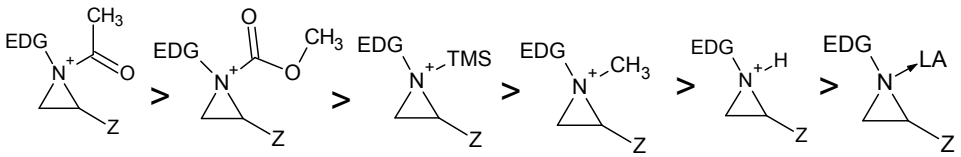

Scheme 18. The order of electrophilic activation

DFT analysis of the nucleophilicity of substituted pyridines

While working on the use of pyridines as catalyst for acetylation of alcohols, we found that DMAP is very effective for such reactions. So, we intended to carry out a study

on the nucleophilic behavior of different substituted pyridines. Accordingly, some commonly used 3-substituted, 4-substituted and 3,4,5-substituted pyridines were examined using DFT to predict the nucleophilicity behaviour based on four different methods known in the literature (Figure 15-17). Altogether 125 numbers of commonly available pyridines and another 29 number of newly designed 4-substituted pyridine (hitherto not synthesized) were tested to find out superior nucleophilic pyridines. HOMO-LUMO energy calculations were done using DFT/B3LYP/6-311G+(d,p) level of theory. To establish the most suitable nucleophilicity scale for all the ranges of pyridines covered herein, either Hammett substituent constant (σ) or experimental nucleophilicity values were computed. On the basis of this study, some new 4-substituted pyridines with enhanced nucleophilicity have been proposed. Nucleophilic behaviour of few predicted analogues was found to be better than that of 4-pyrrolidino pyridine.[7]

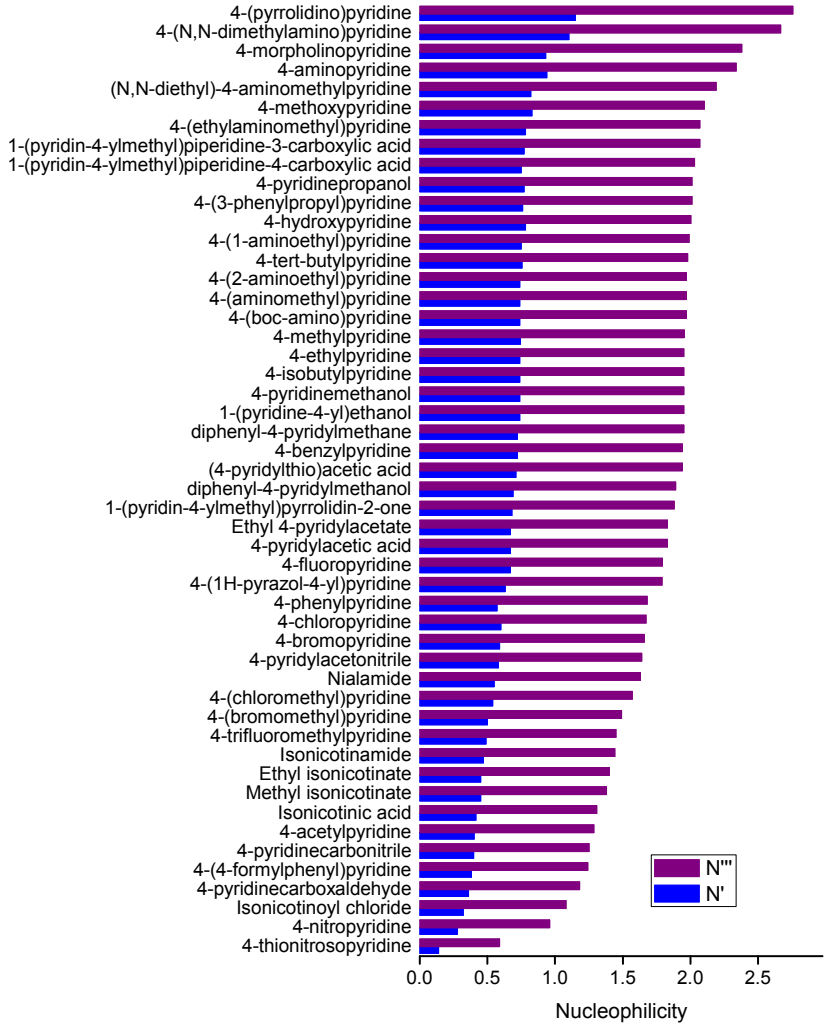

Figure 15. Nucleophilicity scale of 50 numbers of 4-substituted pyridine based on gas phase calculation

[7] Deka, K.**; Phukan, P.** ***J. Chem. Sci***. **2016**,*128*, 633-647

Initially, the goodness and linearity of all the four methods of present study for 3-substituted, 4-substituted and 3,4,5-substituted pyridines were established. Amongst the three categories of pyridine, only 4-substituted pyridine shows very good correlation with experimental as well as Hammett substituent constant. The predictive performance of all the four models were found to follow a declining trend when substitutions are present in 3-position of the pyridine ring. This may be due to the different electronic effect operating in the pyridine ring for *meta*-substitution.

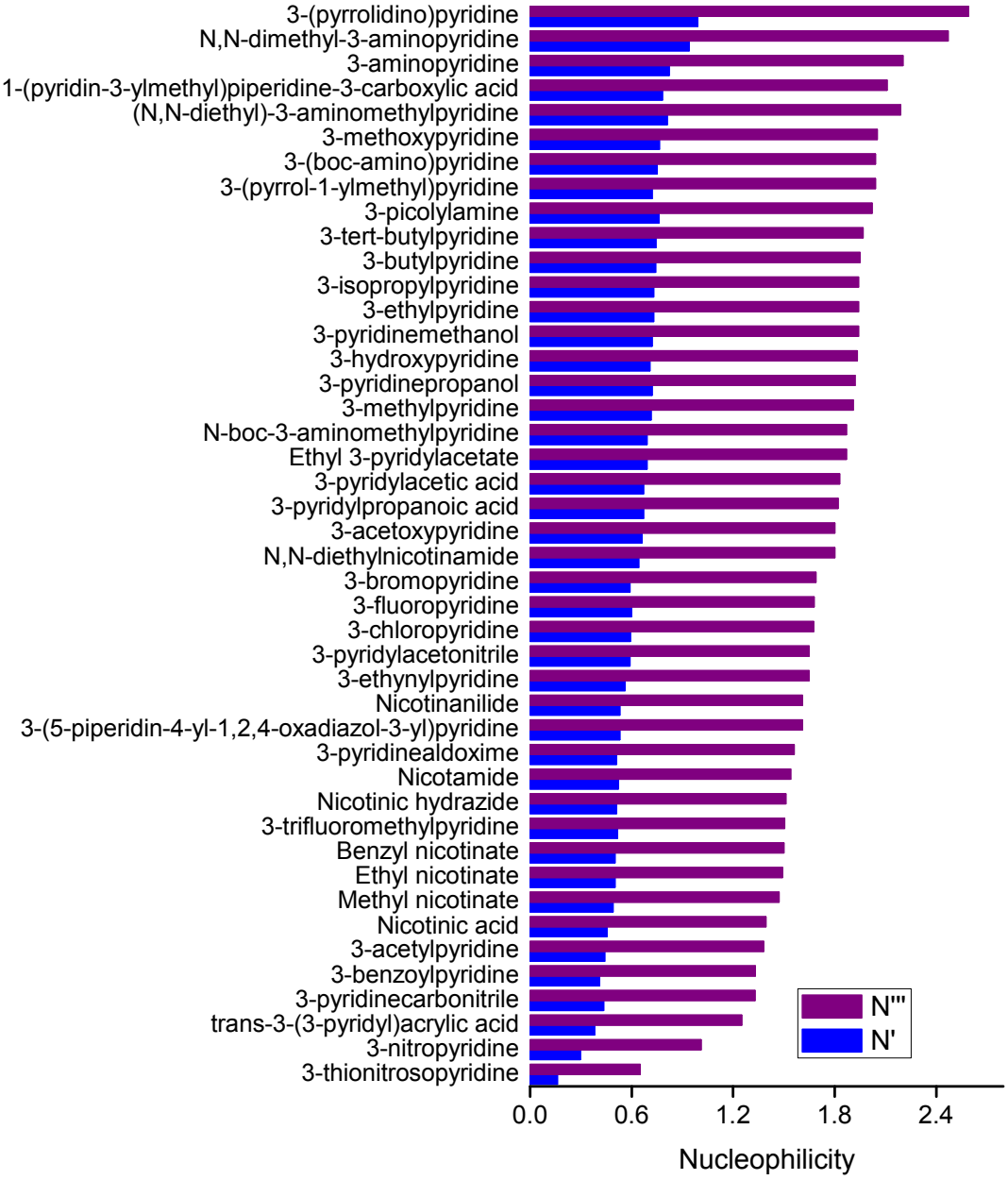

Figure 16. Nucleophilicity scale of 3-substituted pyridine based on gas phase calculation

Gas phase calculation for 4-substituted pyridine shows method I give poor R^2 values with Hammett substituent constant, whereas R^2 values are similar for all methods

with Mayr's experimental values. Inclusion of solvent model increases the linearity between calculated and experimental values for 4-substituted and 3,4,5-substituted pyridines.

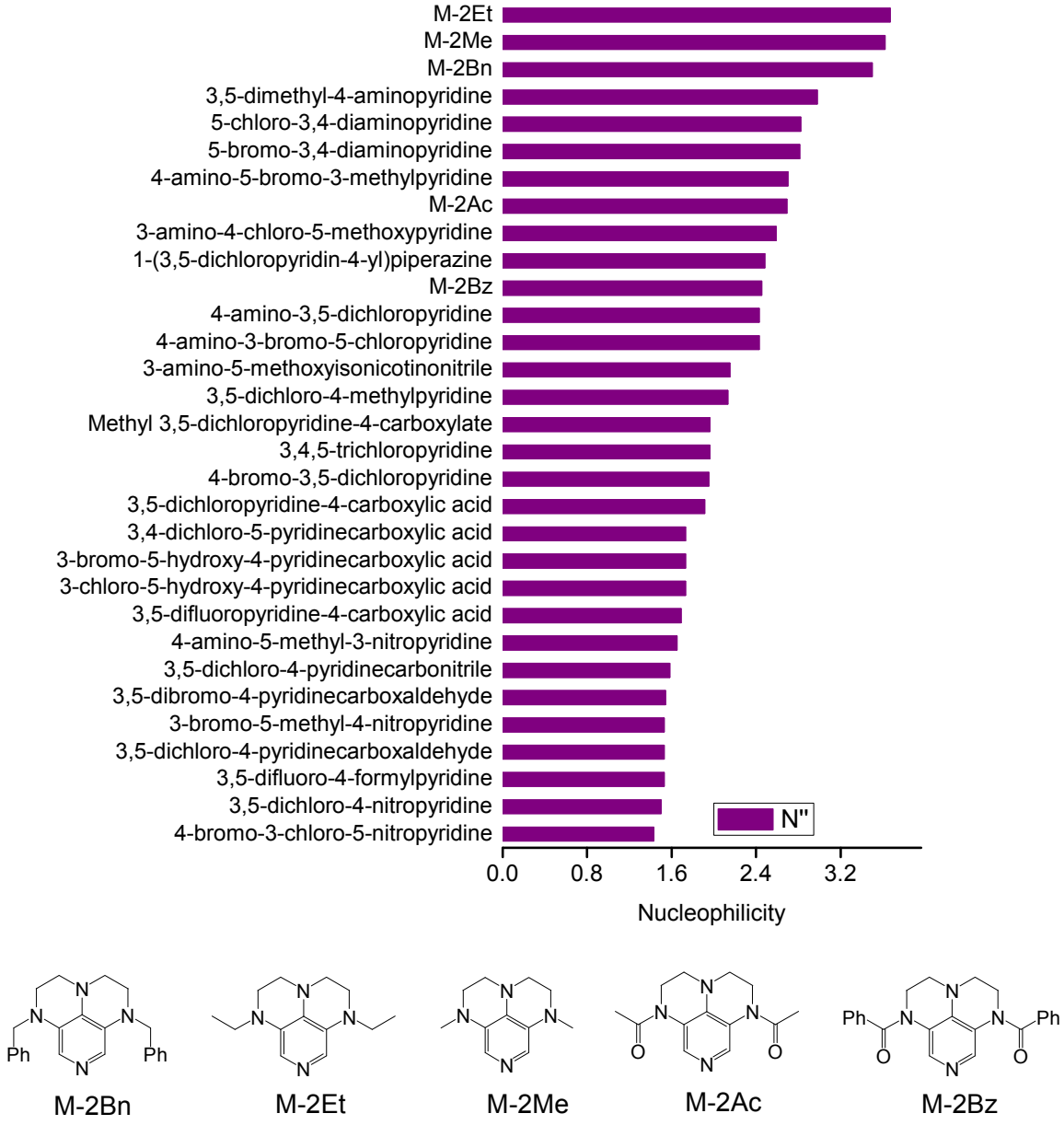

Figure 17. Nucleophilicity scale of 26 numbers of 3,4,5-substituted pyridine based on gas phase calculation

After a thorough study on the nucleophilicity of different pyridines, we proposed some new analogues of pyridines which are shown in Figure 18. With the help of this model, gas phase nucleophilicity values for 29 new 4-substituted pyridine (Figure 18) molecules were evaluated.

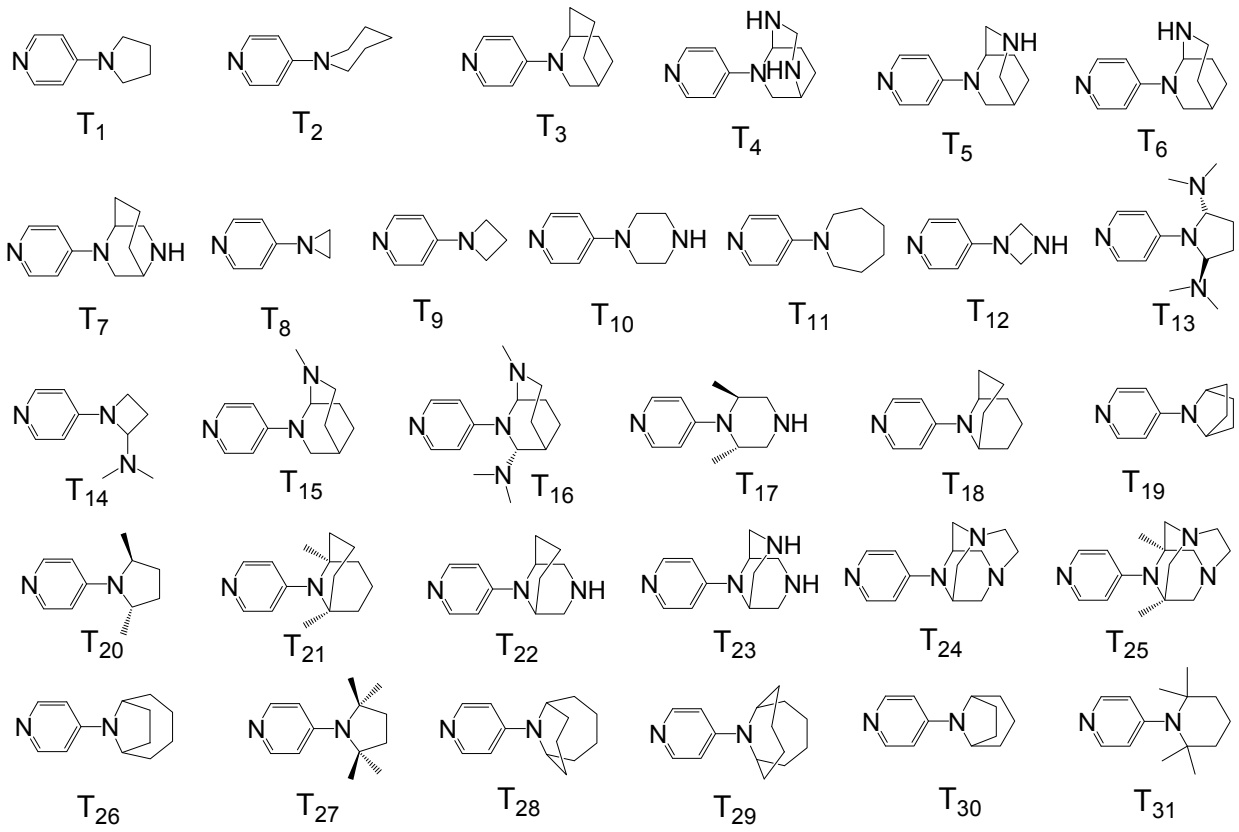

Figure 18. Some newly designed pyridines analouges

The nature of substitution and ring size of the substituent has great influence on the nucleophilicity of 4-substituted pyridines. On the basis of our study, molecules T_{20}, T_{24}, T_{26}, T_{27}, T_{28} and T_{29} are found to be more nucleophilic in nature (Figure 19). These molecules deserve the experimental validation of nucleophilicity as well as effectiveness as organocatalyst.

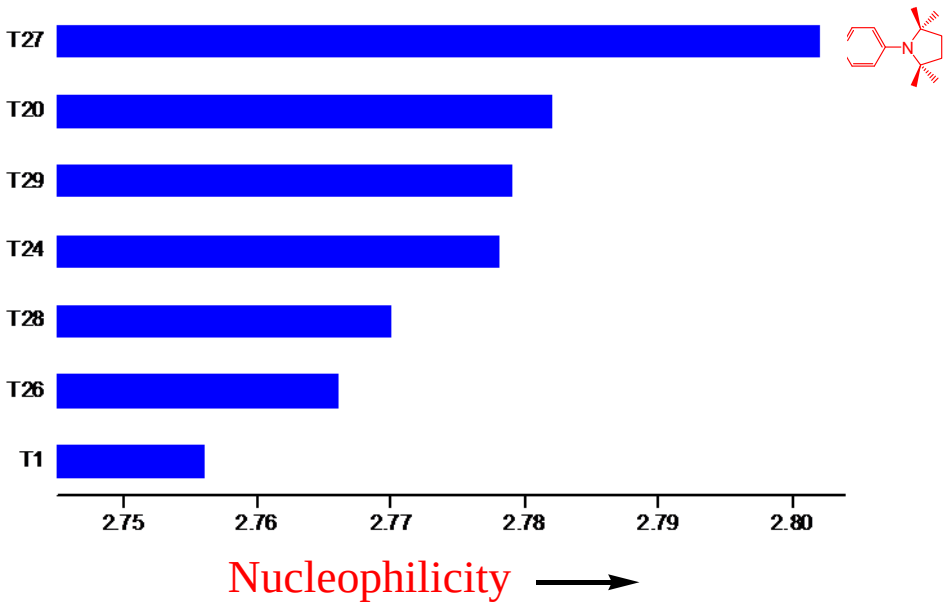

Figure 19. Nucleophilicity scale of proposed more nucleophilic molecules

Nucleophilicity studies on imidazole nucleophiles

We have investigated the nucleophilicity parameter of some imidazole nucleophiles and predicted some new imidazole molecules with very high nucleophilicity as suitable candidates for organocatalysts. A total of 31 molecules have been investigated using DFT/B3LYP/6-311G(d,p) level of theory. For the calculation of nucleophilicity of imidazoles, recently proposed inverse of the electrodonating power model has been identified as the best model from its comparison with Mayr's experimental nucleophilicity values taking a test set of 14 molecules (**Figure 20**).

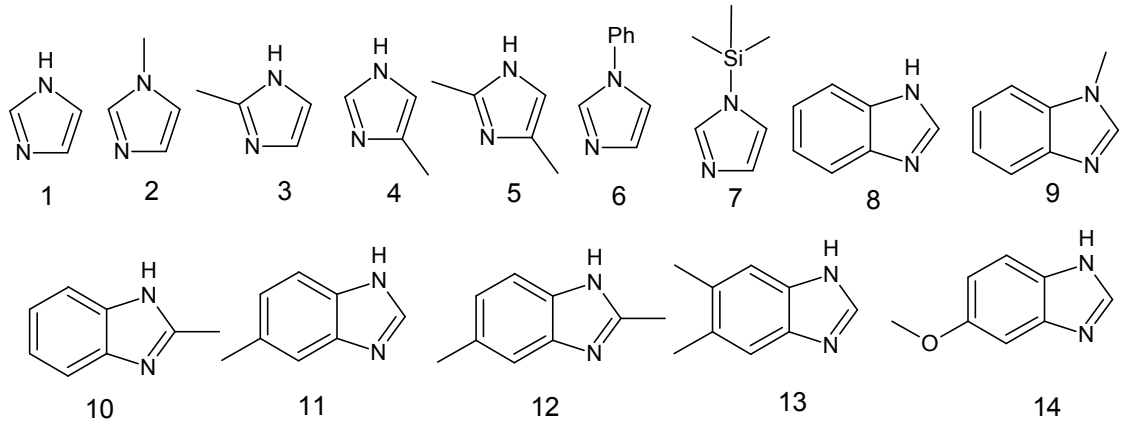

Figure 20. Imidazoles with known neucleophilicity value.

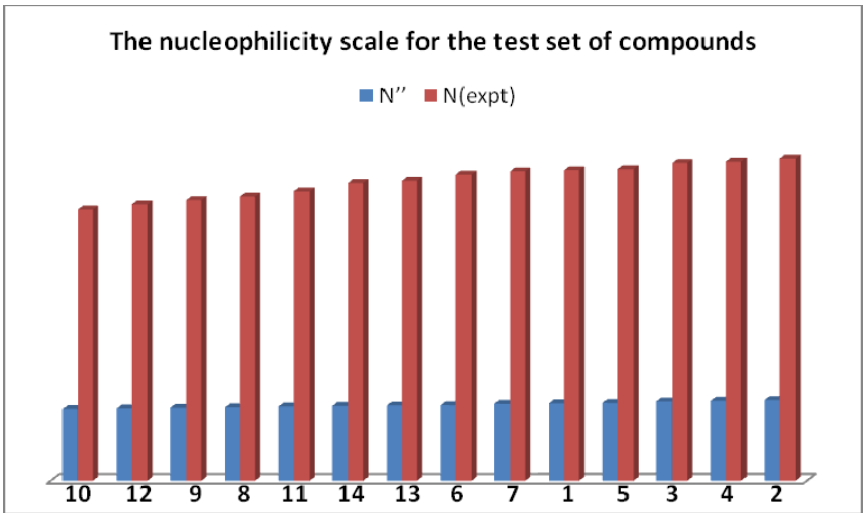

Figure 21. The nucleophilicity scale for the test set of 14 imidazole nucleophiles based on the inverse of electrodonating power model *N″* compared with the Mayr's experimental nucleophilicity scale

On the basis of this study, we have proposed some new molecules with very high nucleophilicity value as suitable candidates for organocatalyst. We have identified the

inverse of electrodonating power model as the best theoretical nucleophilicity model ahead of the ionisation potential based nucleophilicity index *N* and the inverse of electrophilicity index model for the evaluation of nucleophilicity of imidazoles. With the help of this model nucleophilicity of 31 target molecules have been calculated to see the effect of various substituents on the nucleophilic reactivity of imidazoles (Figure 22).

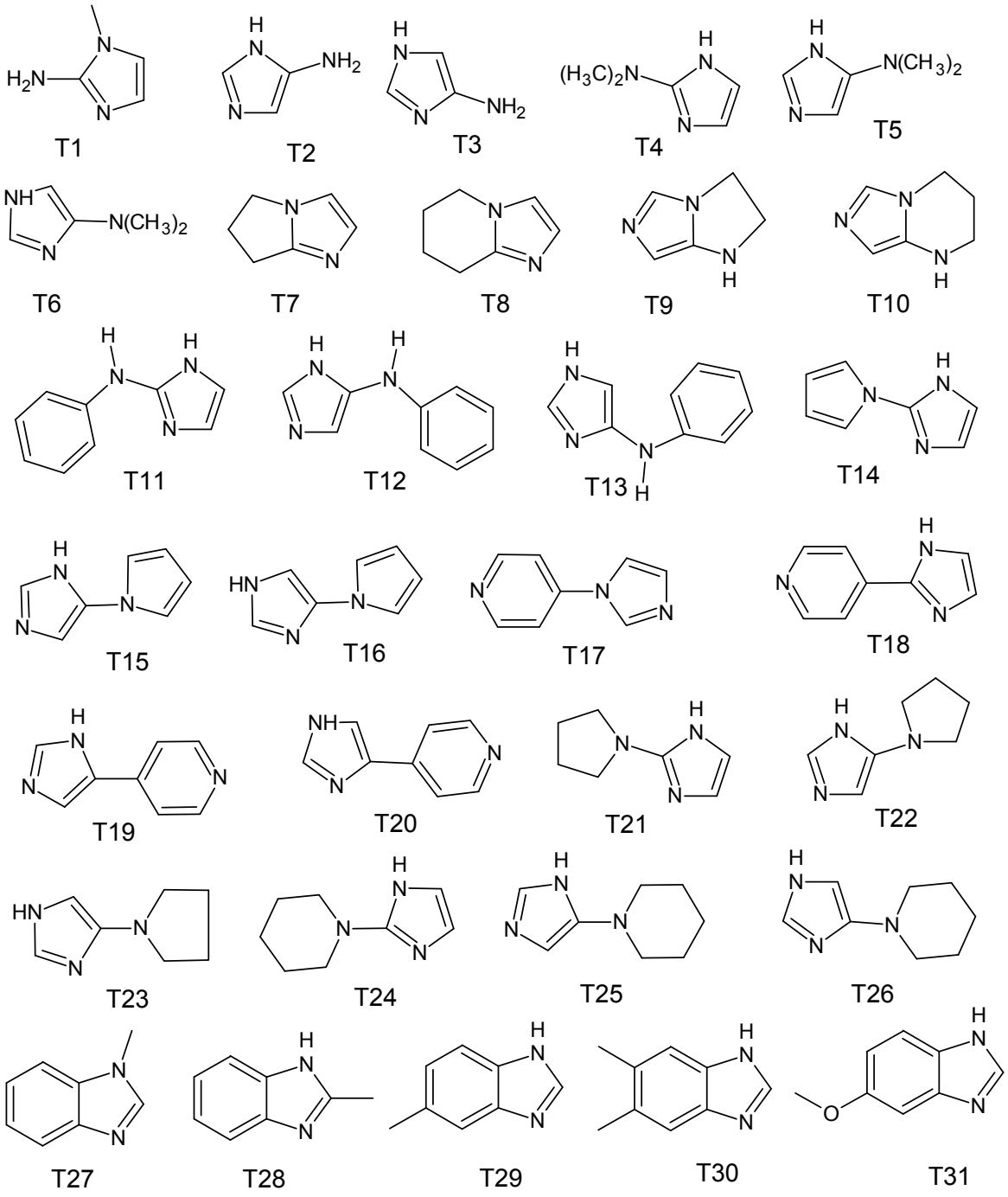

Figure 22. Target imidazole molecules under study

It is well known that the introduction of amino group to the pyridine ring changed the nucleophilicity of pyridine dramatically. Encouraged by the results of amino substitution on pyridine, we also intended to study the effect of amino substitution on imidazole. Substitution of the imidazole ring with the C-end of the $–(CH_2)_n$-NH- bridge on the N(1) position and the N-end of the same on the C(5) position improves the nucleophilicity to the greatest extent. The Nucleophilicity scale for the target imidazole nucleophiles was prepared based on the inverse of electrodonating power model *N″*. After a correlation of the calculated nucleophilicy values, molecules T9, T10, T24 and T26 were identified as potential candidate for imidazole organocatalysts.

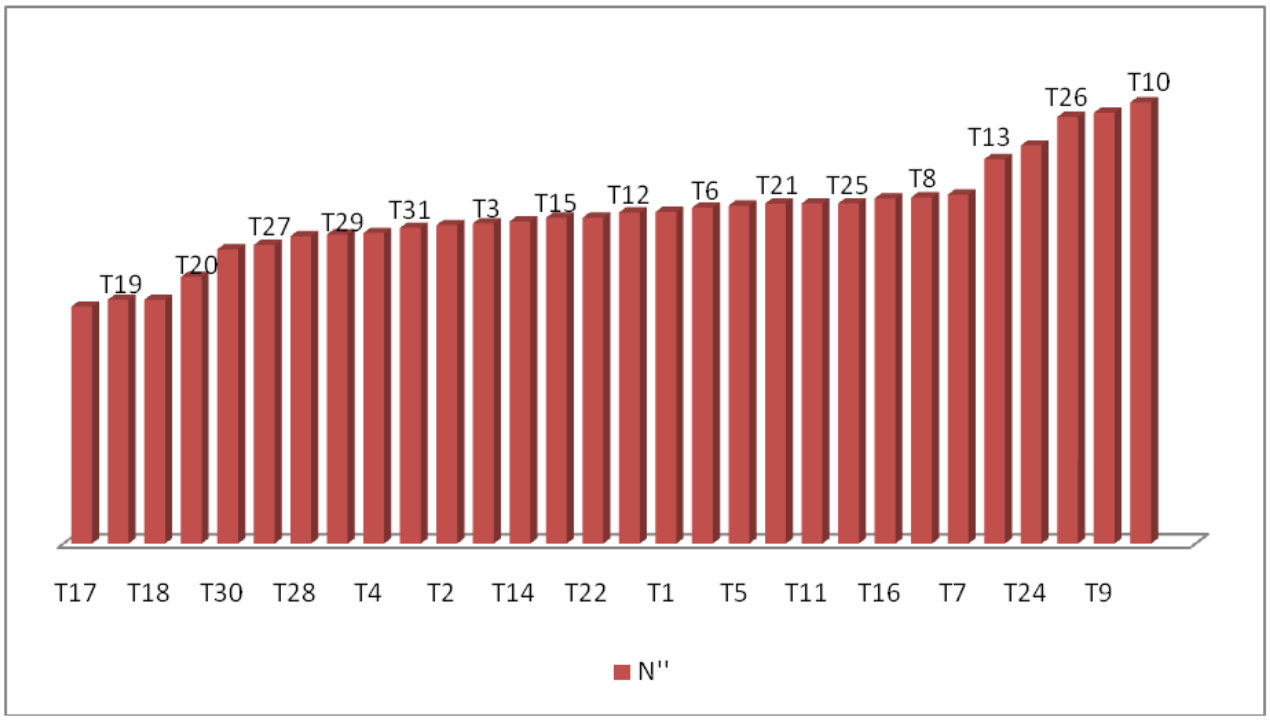

Figure 23 The Nucleophilicity scale for the target imidazole nucleophiles based on the inverse of electrodonating power model *N″*

Theoretical Insights on the Interaction of N-Heterocyclic Carbenes with Tetravalent Silicon Reagents

Lewis acid-base type interaction between *N*-heterocyclic carbene (NHC) and tetravalent silicon reagent (SiR) has been investigated computationally. This NHC-Si interaction is of fundamental importance to the understanding of variety of NHC catalyzed organic transformations involving silicon compounds such as cyanosilylation,

trifluoromethylsilylation, etc. Geometry of 24 NHCs, 10 silicon reagents and their 61 Lewis acid-base complexes have been optimized using B3LYP/6-31+G(d,p) and M05-2X/6-31+G(d,p) level of theory.

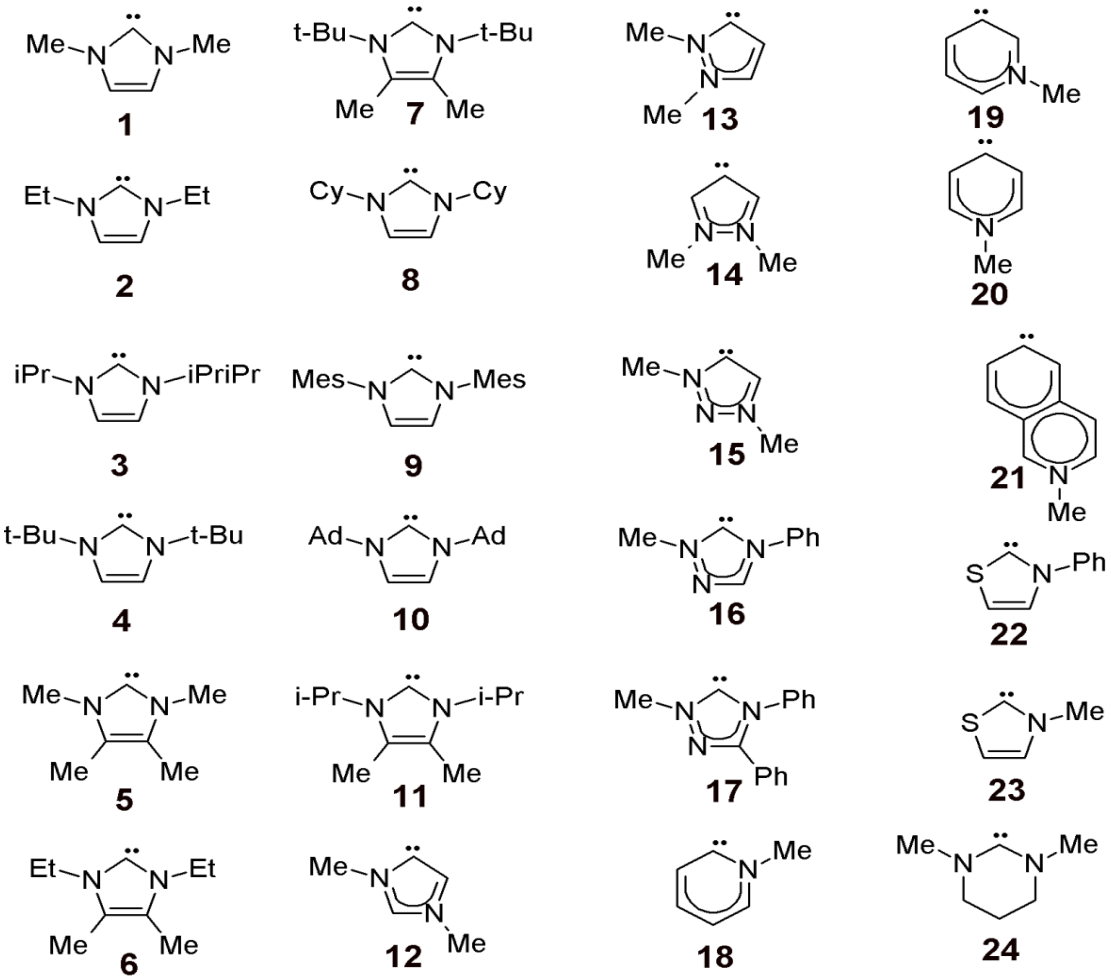

Figure 24. NHCs considered in this study

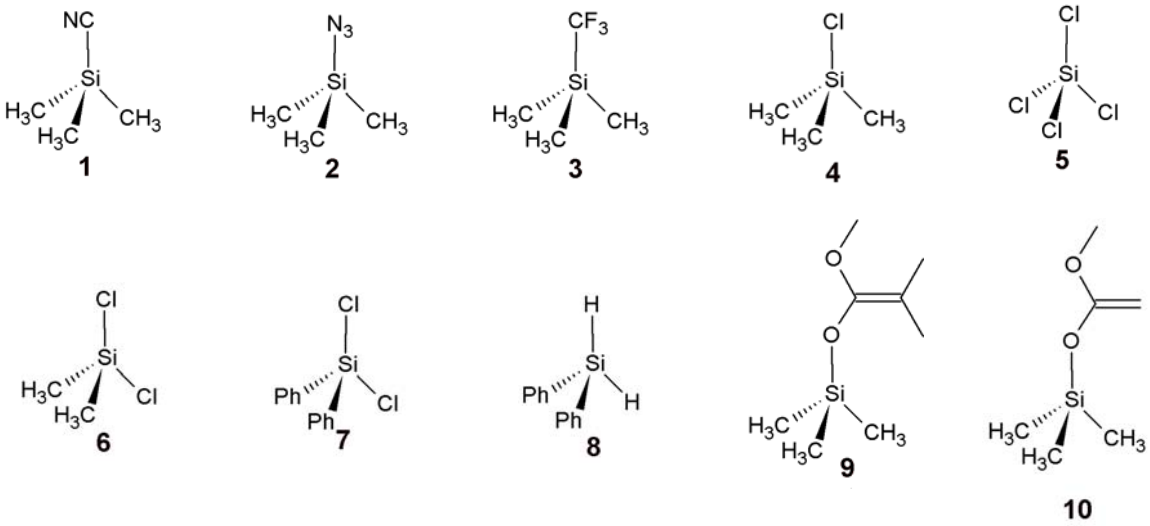

Figure 25. Silicon reagents considered in this study

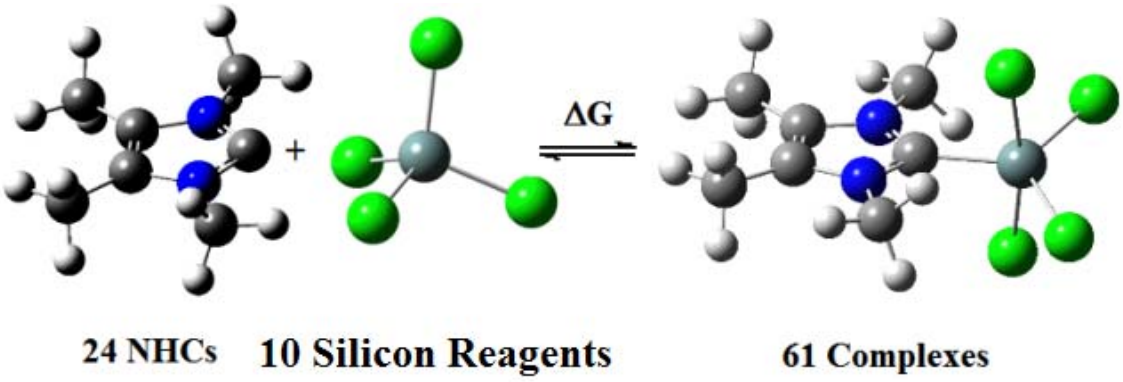

Scheme 19. NHC-Silicon reagent adduct

A variety of NHC-Silicon reagent adducts (Scheme 19) have been investigated. Strength of NHC-Si interaction has been assessed in terms of binding energy of the complexes, charge transfer (CT) and the length of Si–C_{NHC} bond. Energy decomposition analysis (EDA) and Natural Bond Orbital (NBO) analysis at M052X/6-31+G(d,p) level of theory has been carried out to get a deeper understanding of the nature of bonding and charge delocalization. Proton affinity of the NHCs and fluoride affinity of the SiRs have been calculated and correlated with the binding energy of the resulting complexes.

Most of the strong binding complexes (Figure 26) identified here (hitherto not synthesized) have stability comparable to that of the synthesized ones. High charge transfer has been observed with the formation of the stable adducts which indicates donor-acceptor nature of the complexes. A good linear correlation has been observed between charge transfer and binding energy for the complexes where steric effect is not dominant. The proton affinity values of the NHCs also correlate linearly with the binding energies of the complexes. These linear correlations suggest that the complex formation between the NHCs and the SiRs results from Lewis acid-base type interaction. Out of the ten SiRs considered, only three halosilanes were found to form strong binding NHC-SiR adducts.

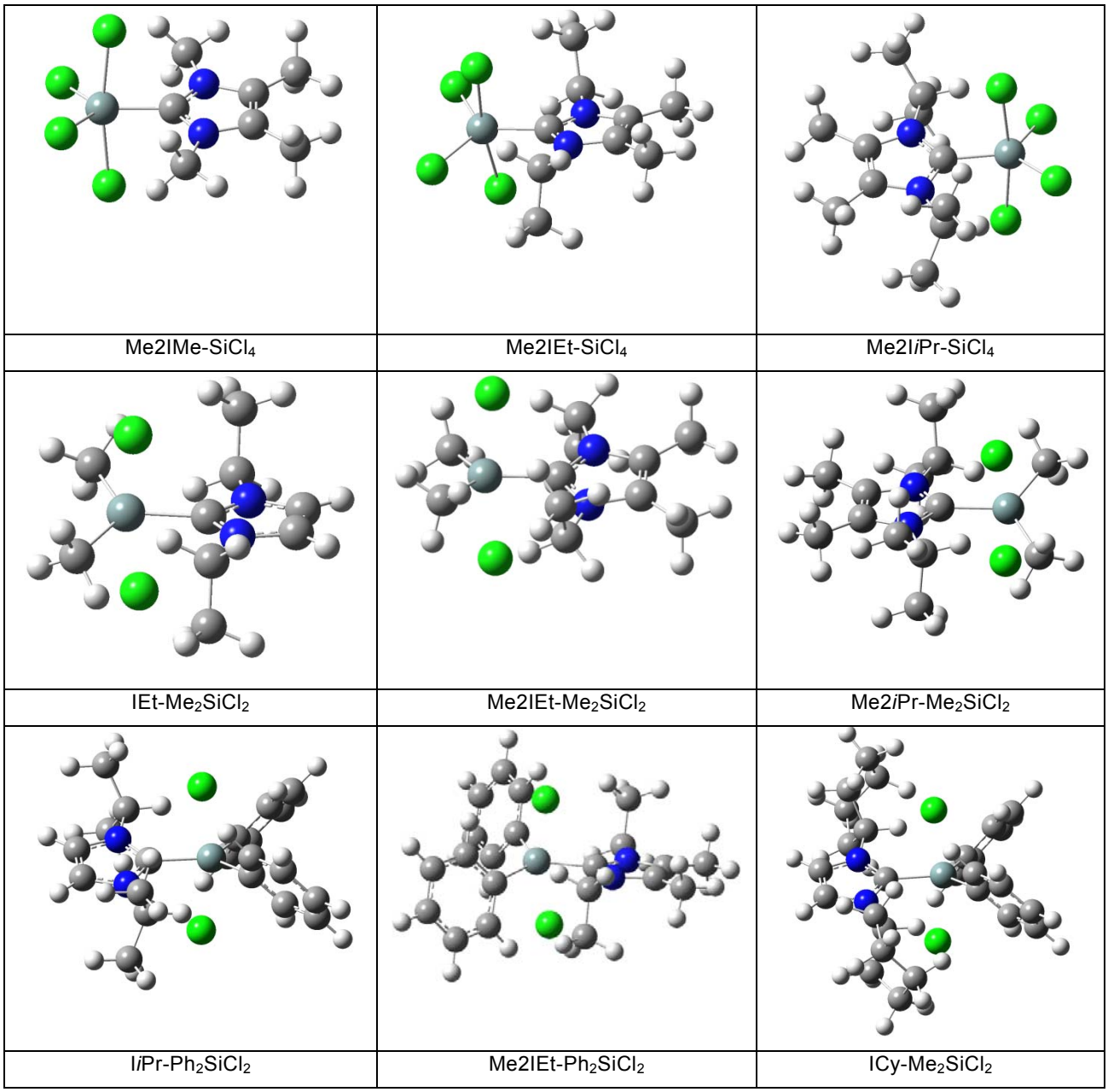

Figure 26. Optimized geometries of some strong binding complexes

In fluoride affinity scale, these three halosilanes were found to be the most Lewis acidic SiRs among the considered. Most of the SiRs used in NHC catalyzed organic transformation favour either very weak or no bonding with the NHCs. Therefore, the possibility of involvement of a NHC-SiR complex in the relevant NHC catalyzed processes was found to be very low. Steric bulk around the NHC and SiR is the most decisive factor in forming a stable NHC-SiR adduct. The most stable adducts were produced by the most electrophilic SiRs having the least steric bulk. While the steric effect was not significant, electronic effects due to the alkyl groups at the C4, C5 and the N atoms of the NHC were found to be important for the stability of the complexes.

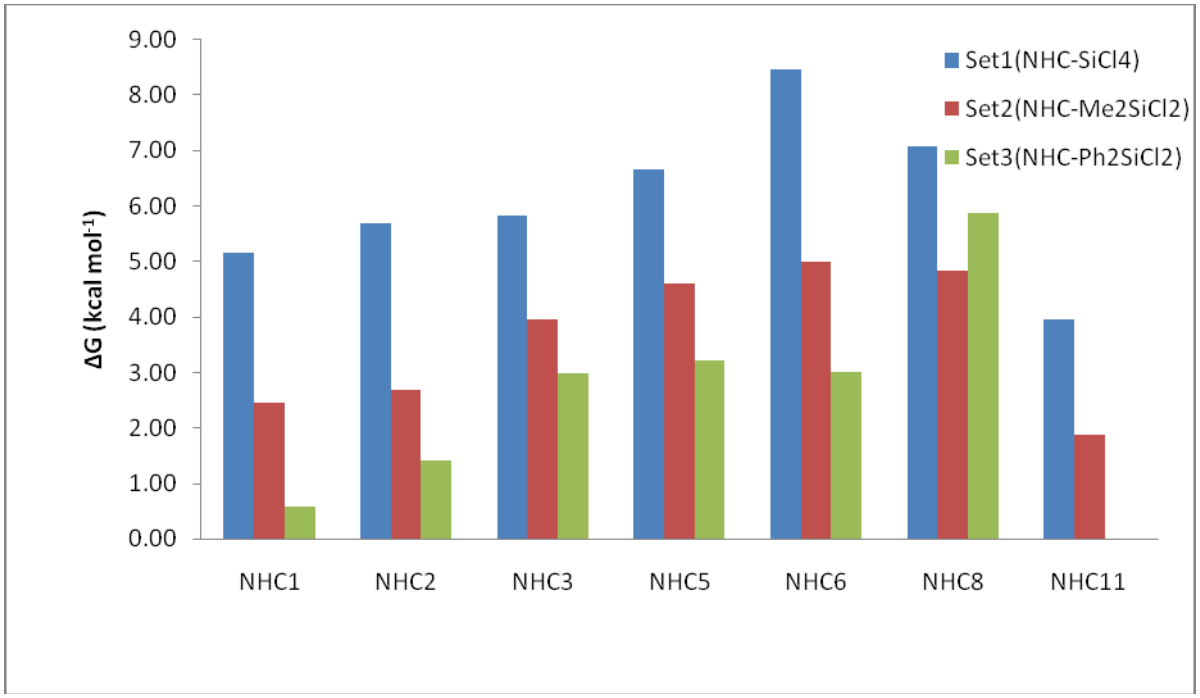

Figure 27. Comparison of stability of the strong binding NHC-SiR complexes of Set 1, Set 2 and Set 3 in terms of relative binding energy values with respect to the least stable Me2I*i*Pr-Ph_2 $SiCl_2$

Details of publications resulting from the project work

1. Nicotinic acid functionalized organomodified silica as an efficient heterogeneous catalyst for the synthesis of benzoylfumarate.
Singh, R. S. K.; Kashyap, B.; **Phukan, P**. ***Tetrahedron Lett.*** **2013**, *54*, 6687-6690. **(Highlighted in SYNFACTS, 2014, 10, 0223)**

2. Reactivity and Regioselectivity in the Ring opening of 2-substituted non-activated Aziridines: a Density Functional Theory based analysis.
Baruah, B.; Deuri, S.; **Phukan, P.**, ***Comput. Theo. Chem***, **2014**, *1027*, 197-202.

3. Aziridination of olefins with bromamine-T in presence of iodine as catalyst. Sharma, C. M.; Kashyap, B.; Phukan, P. ***Indian J. Chem.,*** **2014**, *53B*, 750-753.

4. Synthesis of some new 2-substituted 4,5-dihydroxypiperidines via Sharpless asymmetric dihydroxylation. Borah, A. J.; Phukan, P. ***Indian J. Chem.,*** **2014**, *53B*, 1417-1424.

5. Synthesis of bromohydrins using NBS in presence of iodine as catalyst. Loadh, R.; Borah, A. J.; Phukan, P. ***Indian J. Chem.,*** **2014**, *53B*, 1425-1429.

6. Selective synthesis of nitroalcohols in presence of Ambersep 900 OH as heterogeneous catalyst. Loadh, R.; Sarma, M. J.; Borah, A. J.; Phukan, P. ***Monatsh. Chem.,*** **2015**, *146*, 969-972.

7. Poly (4-vinylpyridine-co-ethylvinylbenzene), as heterogeneous reusable catalyst for the synthesis of benzoyl fumarate. Kashyap, B.; Phukan, P. ***Monatsh. Chem.,*** **2016**, *147*, 797-800.

8. Theoretical Insights on the Interaction of N-Heterocyclic Carbenes with Tetravalent Silicon Reagents. Pathak, D.; Deuri, S.; Phukan, P. ***J. Phy. Chem. A*** **2016**, *120*, 128-138.

9. DFT analysis of the nucleophilicity of substituted pyridines and prediction of new analogues having nucleophilic character stronger than 4-pyrrolidino pyridine. Deka, K.; Phukan, P. ***J. Chem. Sci***. **2016**,*128*, 633-647.

iii. Has the progress been according to original plan of work and towards achieving the objective.

YES

iv. Please indicate the difficulties, if any, experienced in implementing the project.

Sometimes, we find difficulties in collecting data from various sources from different parts of the country. In many cases, we need full data to support our observation which is difficult and time consuming.

v. Any other information which would help in evaluation of work done on the project

a. Ph. D. awarded

1. Mr. Manas Jyoti Sarma
2. Mr. Rajsekhar Loadh (as part time scholar)
3. Mr. Ranasanjay K. Singh (as part time scholar)
4. Mr. Kaustavmoni Deka (as part time scholar)

b. Publication of results

A total of **nine** (**9**) **papers** (***Tetrahedron Lett.* 2013**, *54*, 6687-6690; ***Comput. Theo. Chem*, 2014**, *1027*, 197-202; ***Indian J. Chem.*, 2014**, *53B*, 750-753; ***Indian J. Chem.*, 2014**, *53B*, 1417-1424; ***Indian J. Chem.*, 2014**, *53B*, 1425-1429; ***Monatsh. Chem.*, 2015**, *146*, 969-972; ***Monatsh. Chem.*, 2016**, *147*, 797-800; ***J. Phy. Chem. A* 2016**, *120*, 128-138 and ***J. Chem. Sci*. 2016**,*128*, 633-647) have been published from the work carried out under this project so far.

The details of publications have been given in the previous section.

c. Other impact, if any

Our paper entitled "Nicotinic acid functionalized organomodified silica as an efficient heterogeneous catalyst for the synthesis of benzoylfumarate" published in Tetrahedron Letters (2013) has been **highlighted in SYNFACTS** (*SYNFACTS*, **2014**, 10, 0223).

SIGNATURE OF THE PRINCIPAL INVESTIGATOR

5/10/2020

(Dr. Prodeep Phukan)
Professor in Chemistry, Gauhati University,
Guwahati-781014, Assam

DR. PRODEEP PHUKAN
Professor in Chemistry
Gauhati University
Guwahati-781014, Assam

REGISTRAR
Gauhati University

(Seal)

পঞ্জীয়ক
গুৱাহাটী বিশ্ববিদ্যালয়, গুৱাহাটী-১৪
Registrar
Gauhati University, Guwahati-14

23236351, 23232701, 23237721, 23234116
23235733, 23232317, 23236735, 23239437

विश्वविद्यालय अनुदान आयोग
बहादुरशाह जफर मार्ग
नई दिल्ली-110 002
UNIVERSITY GRANTS COMMISSION
BAHADURSHAH ZAFAR MARG
NEW DELHI-110 002

LIST OF PUBLICATIONS from major research project

UGC Reference No. F. UGC-41-206/2012 (SR) Dated 17 July 2012

Title of the research project: **Development of organic synthetic methods using nonmetallic catalyst: Strategy towards bioactive molecules**

Principal Investigator **DR. PRODEEP PHUKAN**
Department of Chemistry,
Gauhati University, Guwahati-781014

Details of publications

1. Nicotinic acid functionalized organomodified silica as an efficient heterogeneous catalyst for the synthesis of benzoylfumarate.
   Singh, R. S. K.; Kashyap, B.; Phukan, P. ***Tetrahedron Lett.*** **2013**, *54*, 6687-6690. **(Highlighted in SYNFACTS, 2014, 10, 0223)**

2. Reactivity and Regioselectivity in the Ring opening of 2-substituted non-activated Aziridines: a Density Functional Theory based analysis.
   Baruah, B.; Deuri, S.; Phukan, P., ***Comput. Theo. Chem***, **2014**, *1027*, 197-202.

3. Aziridination of olefins with bromamine-T in presence of iodine as catalyst. Sharma, C. M.; Kashyap, B.; Phukan, P. ***Indian J. Chem.,*** **2014**, *53B*, 750-753

4. Synthesis of some new 2-substituted 4,5-dihydroxypiperidines via Sharpless asymmetric dihydroxylation. Borah, A. J.; Phukan, P. ***Indian J. Chem.,*** **2014**, *53B*, 1417-1424.

5. Synthesis of bromohydrins using NBS in presence of iodine as catalyst. Loadh, R.; Borah, A. J.; Phukan, P. ***Indian J. Chem.,*** **2014**, *53B*, 1425-1429.

6. Selective synthesis of nitroalcohols in presence of Ambersep 900 OH as heterogeneous catalyst. Loadh, R.; Sarma, M. J.; Borah, A. J.; Phukan, P. ***Monatsh. Chem.,*** **2015**, *146*, 969-972.

7. Poly (4-vinylpyridine-co-ethylvinylbenzene), as heterogeneous reusable catalyst for the synthesis of benzoyl fumarate. Kashyap, B.; Phukan, P. ***Monatsh. Chem.,*** **2016**, *147*, 797-800.

8. Theoretical Insights on the Interaction of N-Heterocyclic Carbenes with Tetravalent Silicon Reagents. Pathak, D.; Deuri, S.; Phukan, P. ***J. Phy. Chem. A*** **2016**, *120*, 128-138.

9. DFT analysis of the nucleophilicity of substituted pyridines and prediction of new analogues having nucleophilic character stronger than 4-pyrrolidino pyridine. Deka, K.; Phukan, P. ***J. Chem. Sci***. **2016**,*128*, 633-647.

Provided for non-commercial research and education use.
Not for reproduction, distribution or commercial use.

Vol. 54 · Issue 49 · 4 December 2013 · ISSN 0040-4039
Tetrahedron Letters
The International Journal for the Rapid Publication of all Preliminary Communications in Organic Chemistry
IN THIS ISSUE:
Intramolecular palladium mediated π-allyl cyclisation of bis-Cbz- and bis-Boc-protected guanidines
Zainab Al-Shuhaib, Henning Böckemeier, Lawrence Coghlan, Elina Dörksen, Iestyn V. Jones, Patrick J. Murphy, Robert Nash, James M. Page
Available online at www.sciencedirect.com
ScienceDirect

This article appeared in a journal published by Elsevier. The attached copy is furnished to the author for internal non-commercial research and education use, including for instruction at the authors institution and sharing with colleagues.

Other uses, including reproduction and distribution, or selling or licensing copies, or posting to personal, institutional or third party websites are prohibited.

In most cases authors are permitted to post their version of the article (e.g. in Word or Tex form) to their personal website or institutional repository. Authors requiring further information regarding Elsevier's archiving and manuscript policies are encouraged to visit:

http://www.elsevier.com/authorsrights

Author's personal copy

Tetrahedron Letters 54 (2013) 6687–6690

Contents lists available at ScienceDirect

Tetrahedron Letters

journal homepage: www.elsevier.com/locate/tetlet

Nicotinic acid functionalized organomodified silica as an efficient heterogeneous catalyst for the synthesis of benzoyl fumarate

Rana Sanjay Kumar Singh, Bishwapran Kashyap, Prodeep Phukan *

Department of Chemistry, Gauhati University, Guwahati 781014, Assam, India

ARTICLE INFO

Article history:
Received 8 August 2013
Revised 10 September 2013
Accepted 13 September 2013
Available online 24 September 2013

Keywords:
Organomodified silica
Heterogeneous catalyst
Benzoyl fumarate
DMAD
Aldehydes

ABSTRACT

A new hybrid catalyst has been developed by incorporating nicotinic acid onto an organomodified silica. The catalyst was applied as a heterogeneous catalyst for the synthesis of benzoyl fumarate. The reactions work well in the presence of 20 wt % of the catalyst at room temperature to produce the desired products in high yield. The catalyst could be recovered and reused without appreciable change in activity.

© 2013 Elsevier Ltd. All rights reserved.

The modification of silica and related materials by attachment of organic functionalities onto their surfaces is an important area of research in heterogeneous catalysis directed toward achieving green chemistry goals.[1] Surface functionalization of mesoporous silica has been widely practiced in recent years for generating active sites necessary for heterogeneous catalytic activity. Numerous strategies have been described for immobilizing inorganic and/or organic active species on or within the silica matrices.[1a] Functionalization of mesoporous silica surface via tethering of an active group generally can be done in two different ways: through the so-called 'post-synthesis' method,[2] which involves grafting an organotrialkoxysilane onto the pore surfaces after mesoporous material synthesis, and through the 'direct synthesis' method,[3] in which the functional groups are introduced during the synthesis of the mesoporous material. The pore functionalization is achieved through the co-condensation reaction occurring between the organotrialkoxysilane and the silica source in the presence of a structure-directing agent. The direct synthesis method is considered more predictable and hence valuable, because it can avoid several shortcomings of the post-grafting method, such as reduction in pore size, pore blocking at the aperture and difficulties in controlling the loadings as well as the distribution of active sites.[4]

Benzoyl fumarates and its corresponding acids are known to be an important precursor for the synthesis of many agrochemicals,[5] drugs,[6] and organic transformations.[7] Nair et al. and later Shi et al. have prepared benzoyl fumarates by one pot reaction between dimethyl acetylenedicarboxylate (DMAD) and aldehyde in presence of Lewis base as homogeneous catalyst.[8] Bayat et al. have prepared this benzoyl fumarate by multicomponent reaction between DMAD, aldehyde, and PPh_3.[9] We have also developed a ferrocene based pyridine catalyst for benzoyl furmarate synthesis under homogeneous condition.[10] In addition, there are a few more examples for the synthesis of benzoyl fumarates from aldehyde and DMAD.[11] However, till date, heterogeneous approach has not been applied for this transformation. We have developed a new nicotinic acid functionalized organomodified mesoporous silica catalyst, for the first time, which acts as heterogeneous catalyst for the synthesis of benzoyl fumarates (Scheme 1). It has been observed that the organomodified silica, which has been characterized by various methods including spectroscopy and electron microscopy, is suitable as heterogeneous catalyst for the preparation of benzoyl fumarates from aldehydes and DMAD.

To realize our goal, we have developed a new organomodified mesoporous silica by incorporating nicotinic acid to the thiol group of mercaptopropyl silica (MPMS). Initially, MPMS was prepared by mixing tetraethylorthosilicate and mercaptopropyl (triethoxy) silane with a solution of *n*-dodecylamine in aqueous ethanol.[3a,b]

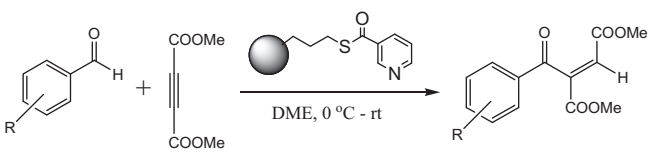

Scheme 1. Synthesis of benzoyl fumarates.

* Corresponding author.
E-mail address: pphukan@yahoo.com (P. Phukan).

0040-4039/$ - see front matter © 2013 Elsevier Ltd. All rights reserved.
http://dx.doi.org/10.1016/j.tetlet.2013.09.057

Author's personal copy

The MPMS was characterized by powder X-ray diffraction, IR spectra, TGA, SEM, and EDX. The appearance of low-angle broad XRD peaks at $2\theta = 0.5–2$ degree is the characteristic of the mesoporous nature of MPMS (Fig. 1). The observed pattern does not show well resolved diffraction peaks. The broad peaks seen for this material suggest the lack of long-range order in the structure. In the IR spectrum (Fig. S1 of SI), the presence of bands at 2950, 2560 cm^{-1}, and a broad peak at around 3300–3400 cm^{-1} confirms the presence of propyl, thiol(–S–H stretching) and Si-OH groups in the MPMS. The TGA (Fig. S3 of SI) study indicates that loss in weight up to 100 °C is due to loss of water molecule from the surface and one main weight loss in the range 340–680 °C is due to loss of the organic group from the surface. Morphology of MPMS was also analyzed by using SEM (Fig. 2) and it is obvious from the picture that the major portion of the material is made up of aggregates of smaller roughly spherical particles. A second type of structure consists of single particles, again roughly spherical, but of a much larger size. Some of these are aggregated into groups of two or three, but not into larger aggregates. The spherical structures present are often seen in a range of mesostructured materials. EDX data (Fig. S2 of SI) confirm the presence of thiol moiety in the MPMS.

Nicotinic acid functionalized MPMS was prepared by simple esterification between MPMS and nicotinic acid in DCM (Scheme 2). Functionalization was carried out by stirring a mixture of MPMS, nicotinic acid, dicyclohexylcarbodiamide, and DMAP in dry DCM under N_2 atmosphere at room temperature for 48 h. The resulting white solid was separated by filtration, washed several times with DCM and dried in vacuum.

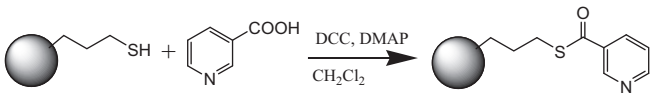

Scheme 2. Synthesis of Nicotinic acid functionalized MPMS.

The X-ray diffraction patterns (Fig. 3) were also measured for nicotinic acid functionalized MPMS and as expected, these materials do not display the degree of a long range order associated with the MCM-41 class of silicates. Unlike MPMS, it shows a sharp peak at around $2\theta = 7°$. The IR spectra of nicotinic acid functionalized MPMS show bands at around 1360–1310 cm^{-1} and 1725–1700 cm^{-1} which indicate the presence of aromatic C–N vibration of the pyridine ring and carbonyl group respectively. The SEM picture (Fig. 4) indicates no significant change in morphology after functionalization of MPMS with nicotinic acid.

Pore size distributions and surface areas were measured by N_2 adsorption studies for both the MPMS and nicotinic acid functionalized MPMS (Figs. S7–S10, SI). In both cases the materials

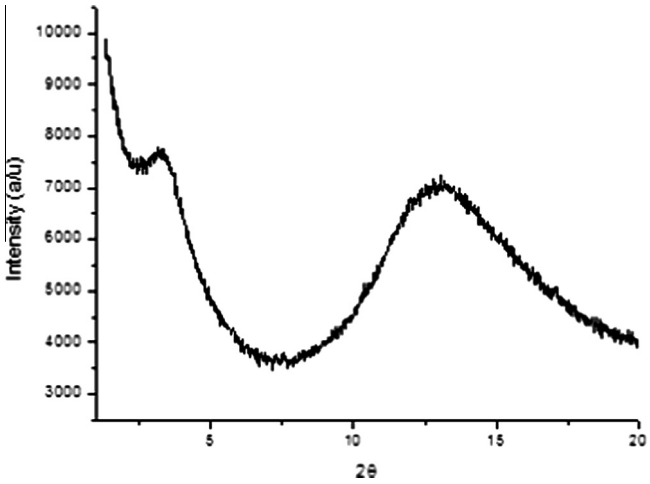

Figure 1. XRD pattern of MPMS.

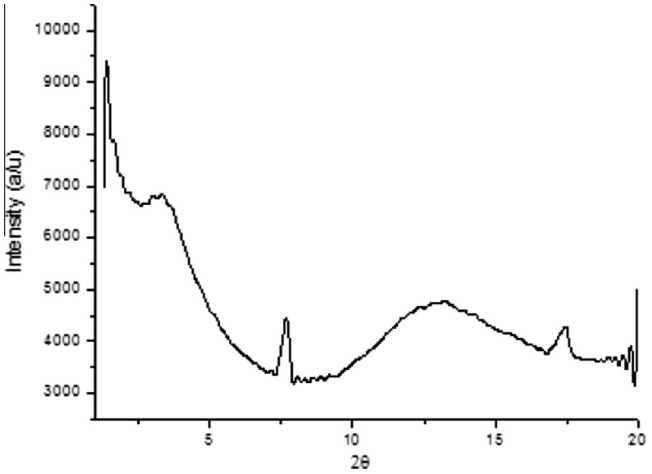

Figure 3. XRD pattern of nicotinic acid functionalized MPMS.

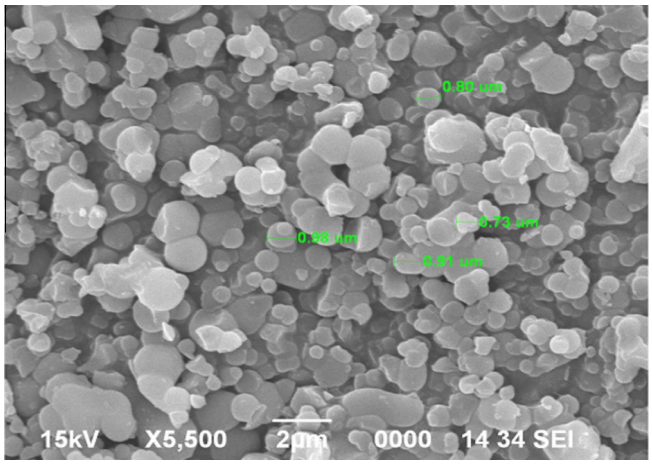

Figure 2. SEM image of MPMS.

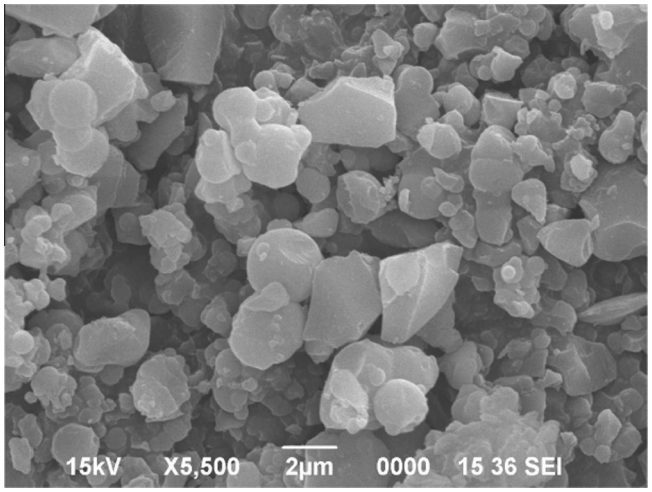

Figure 4. SEM image of nicotinic acid functionalized MPMS.

Author's personal copy

displayed isotherm with hysteresis loop of type IV (according to the scheme of classification recommended by IUPAC), which is characteristic of HMS materials with small pores and high surface areas. The isotherms of MPMS and nicotinic acid functionalized MPMS are of similar shape indicating that porous structure has been retained after functionalization. Pore size distribution is quite narrow with BJH adsorption pore average diameter between 2.17487 and 4.1727 nm. It has been observed that on functionalization of the thiol group with nicotinic acid, there is a drop in surface area as well as in average pore size.

After the confirmation of the structure and morphology of the prepared nicotinic acid functionalized MPMS we intend to test its efficiency as heterogeneous catalyst for the preparation of benzoyl fumarates from aldehydes and dimethyl acetylenedicarboxylate (DMAD). Initially, the reaction between 4-nitrobenzaldehyde and DMAD was selected as a model reaction to investigate the best reaction condition (Table 1). In a typical reaction, 10 wt% of the catalyst was added to a mixture of 4-nitrobenzaldehyde (1 mmol) and DMAD (1 mmol) in DME (5 ml) at 0 °C under N_2 atmosphere. The reaction was continued at room temperature for appropriate time

Table 1
Reaction of *p*-nitrobenzaldehyde with DMAD catalyzed by nicotinic acid functionalized MPMS catalyst in different solvents[a]

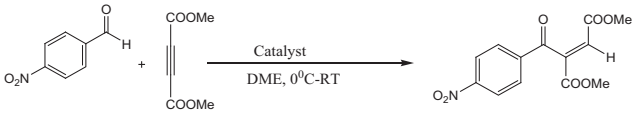

Entry	Catalyst (wt%)	Solvent	Time (h)	Yield[b] (%)
1	10	DME	7	60
2	10	DME	12	67
3	15	DME	12	72
4	15	THF	12	65
5	15	MeCN	24	30
6	15	DCM	24	Trace
7	20	DME	12	78
8	25	DME	12	79
9	0	DME	24	0

[a] Reaction condition: 4-nitrobenzaldehyde (1 mmol), DMAD (1 mmol), solvent (4 mL), 0 °C–rt.
[b] Isolated yield.

Table 2
Synthesis of benzoyl fumarates catalyzed by nicotinic acid functionalized MPMS[a]

Sl. no.	Reactant	Product	Yield[b] (%)
1	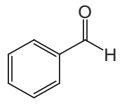 **1a**	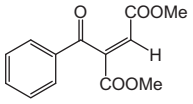 **1b**	72
2	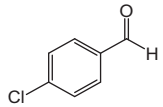 **2a**	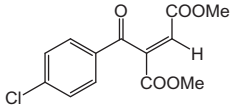 **2b**	75
3	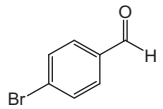 **3a**	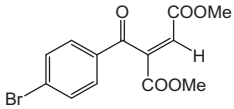 **3b**	81

Table 2 (*continued*)

Sl. no.	Reactant	Product	Yield[b] (%)
4	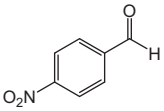 **4a**	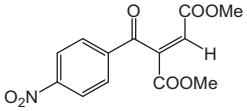 **4b**	78
5	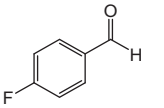 **5a**	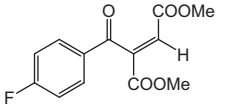 **5b**	73
6	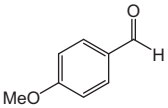 **6a**	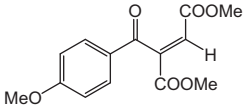 **6b**	66
7	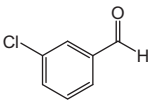 **7a**	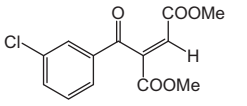 **7b**	69
8	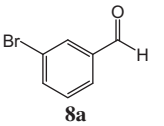 **8a**	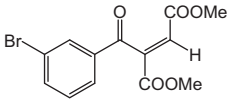 **8b**	70
9	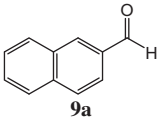 **9a**	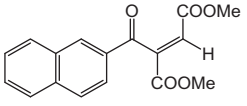 **9b**	64
10	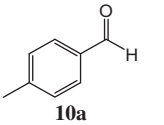 **10a**	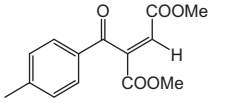 **10b**	60
11	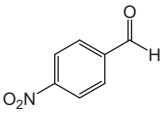	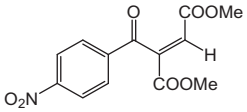	77[c]
12	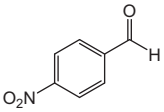	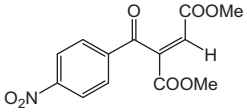	76[d]
13	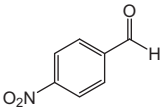	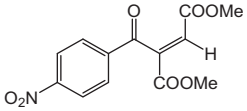	76[e]

[a] Reaction condition: aldehyde (1 mmol), DMAD (1 mmol), catalyst (20 wt%), DME (4 mL), 0 °C–rt. 12 h.
[b] Isolated yield.
[c] Catalyst reused: 1st run.
[d] Catalyst reused: 2nd run.
[e] Catalyst reused: 3rd run.

and it was found that 12 h of stirring gives the maximum yield. After usual work-up, the crude product was purified using column chromatography to get the pure product. It was observed that 20 wt% of the catalyst and 12 h of reaction time give the best result. Further reaction using 25 wt% of catalyst did not improve the reaction yield. The reaction in other solvents such as THF and acetonitrile produced lower yield. The reaction in DCM did not proceed at all. Finally, 20 wt% of catalyst was found to be the optimum amount for the best yield.

Author's personal copy

After establishing the optimum reaction condition, the scope of the reaction was examined with various aldehydes under the same reaction condition (Table 2).[12] It has been observed that various aldehydes undergo this reaction with good efficiency under the reaction condition. It was observed that, presence of electron withdrawing group in the benzene ring gives better yield (Table 2, Entries 2–8) than electron donating groups (Table 2, Entry 10).

Reusability of the catalyst was tested with 4-nitrobenzaldehyde. To reuse, the catalyst was filtered after completion of the reaction, washed with petroleum ether, dried under vacuum, and then kept in a desiccator overnight before reuse. It was observed that the catalyst could be reused three times without appreciable loss in activity (Table 2, Entry 11–13).

The mechanism of the reaction has already been discussed in detail by Shi.[8b] Accordingly, the pyridine moiety attached to the MPMS core acts as a nucleophilic promoter to form a zwitter ionic intermediate at the initial stage of the reaction.[8b] Subsequent reaction with aldehyde followed by an intramolecular proton transfer process leads to formation of the product.

In conclusion, we have effectively prepared a nicotinic acid functionalized organomodified silica catalyst from MPMS. The catalyst was characterized using XRD, SEM, IR, TGA, and EDX. It was further demonstrated that the prepared functionalized silica acts as a heterogeneous catalyst for the synthesis of benzoylfumarates from aldehydes and DMAD. The catalyst is reusable with good yield.

Acknowledgements

Financial support from UGC (Grant No. 41-206/2012/SR) is gratefully acknowledged. R.S.K.S. thanks UGC (NERO) and B.K. thanks CSIR for research fellowship.

Supplementary data

Supplementary data associated with this article can be found, in the online version, at http://dx.doi.org/10.1016/j.tetlet.2013.09.057.

References and notes

1. (a) Hoffmann, F.; Cornelius, M.; Morell, J.; Fröba, M. *Angew. Chem. Int. Ed.* **2006**, *45*, 3216–3251; (b) Melero, J. A.; van Grieken, R.; Morales, G. *Chem. Rev.* **2006**, *106*, 3790–3812; (c) Clark, J. H.; Macquarrie, D. J. *Chem. Commun.* **1998**, 853–860.
2. (a) Cauvel, A.; Renaud, G.; Brunel, D. *J. Org. Chem.* **1997**, *62*, 749–751; (b) Sutra, P.; Brunel, D. *Chem. Commun.* **1996**, 2485–2486; (c) Subba Rao, Y. V.; de Vos, D. E.; Jacobs, P. A. *Angew. Chem., Int. Ed.* **1997**, *36*, 2661–2663; (d) Subba Rao, Y. V.; de Vos, D. E.; Jacobs, P. A. *Chem. Commun.* **1997**, 355–356; (e) Feng, X.; Fryell, G. E.; Wang, L. Q.; Kim, A. Y.; Lin, J.; Kenner, K. M. *Science* **1997**, *276*, 923–926.
3. (a) Macquarrie, D. J. *Chem. Commun.* **1996**, 1961–1962; (b) Macquarrie, D. J.; Jackson, D. B.; Mdoe, J. E. G.; Clark, J. H. *New J. Chem.* **1999**, *23*, 539–544; (c) Burkett, S. L.; Sims, S. D.; Mann, S. *Chem. Commun.* **1996**, 1367–1368; (d) Richer, R.; Mercier, L. *Chem. Commun.* **1998**, 1775–1776; (e) Lim, M. H.; Blanford, C. F.; Stein, A. *J. Am. Chem. Soc.* **1997**, *119*, 4090–4091; (f) Sarma, P.; Chakrabarty, R.; Phukan, P.; Das, B. K. *J. Mol. Catal. A: Chem.* **2007**, *268*, 36–44.
4. *Characterisation and Chemical Modification of the Silica Surface*; Vansant, E. F., Van, P., der Voort, Vrancken, K. C., Eds.; Elsevier: Amsterdam, 1995; p 176.
5. (a) *Nippon Synthetic Chemical Industry Jpn. Kokai* 5838202, 1983; *Chem. Abstr.* **1983**, *99*, 1818d.; (b) Nippon Synthetic Chemical Industry Jpn. Kokai 81127302, 1981; *Chem. Abstr.* **1982**, 110, 7866k.
6. (a) Yamada, K.; Ino, K.; Takashashi, S.; Ohashi, T.; Watanabe, K. *Eur. Pat. Appl.* EP 239062, 1987; *Chem. Abstr.* **1988**, *109*, 110904z.; (b) Chosakon, Y.; Yamamoto, N. *Jpn. Kokai* 63104940, 1988; *Chem. Abstr.***1988**, *109*, 230551d.; (c) Ikeda, T.; Hirano, H.; Aoki, K. *Jpn. Kokai* 63130564, 1988; *Chem. Abstr.* **1989**, *110*, 7866k.
7. (a) Reymond, S.; Cossy, J. *Chem Rev.* **2008**, *108*, 5359–5406; (b) Kagan, H. B.; Riant, O. *Chem. Rev.* **1992**, *92*, 1007–1019; (c) Pindur, U.; Lutz, G.; Otto, C. *Chem. Rev.* **1993**, *93*, 741–761.
8. (a) Nair, A.; Sreekanth, A. R.; Abhilash, N.; Biju, A. T.; Devi, B. R.; Menon, R. S.; Rath, N. P.; Srinivas, R. *Synthesis* **2003**, 1895–1902; (b) Li, C.-Q.; Shi, M. *Org. Lett.* **2003**, *5*, 4273–4276.
9. Bayat, M.; Imanieh, H.; Hassanzadeh, F. *Tetrahedron Lett.* **2010**, *51*, 1873–1875.
10. Kashyap, B.; Phukan, P. *RSC Adv.* **2013**, *3*, 15327–15336.
11. (a) Ikeda, T.; Hirano, H.; Aoki, K. JpnKokai 63130564, 1989; *Chem. Abstr.* **1989**, *110*, 7866.; (b) Takahashi, S.; Ueda, Y.; Yanagida, Y.; Namito, Y.; Ohaska T.; Watanabe, K. European Patent Appl. EP 204286, 1986; *Chem. Abstr.* **1987**, *106*, 84179.
12. *Typical procedure:* The catalyst (20 wt % based on aldehyde) was added to a mixture of aldehyde (1 mmol) and DMAD (1 mmol) in DME (4 ml) at 0 °C under N_2 atmosphere and the reaction mixture was stirred for 12 h, (first two hours at 0 °C and then at room temperature). After completion of the reaction (TLC), the reaction mixture was filtered and the solvent from the filtrate was removed and the residue was purified with column chromatography using 20% ethyl acetate/petroleum ether as eluent to get the product. The recovered catalyst was washed with petroleum ether, dried under vacuum and then kept in a desiccator overnight before reuse.

SYNFACTS
Highlights in Current Synthetic Organic Chemistry
REPRINT

Personal Copy

Thieme

R. S. K. SINGH, B. KASHYAP, P. PHUKAN* (GAUHATI UNIVERSITY, GUWAHATI, INDIA)
Nicotinic Acid Functionalized Organomodified Silica as an Efficient Heterogeneous Catalyst for the Synthesis of Benzoyl Fumarate
Tetrahedron Lett. **2013**, *54*, 6687–6690.

Synthesis of Benzoyl Fumarates with Supported Nicotinic Acid Thioester

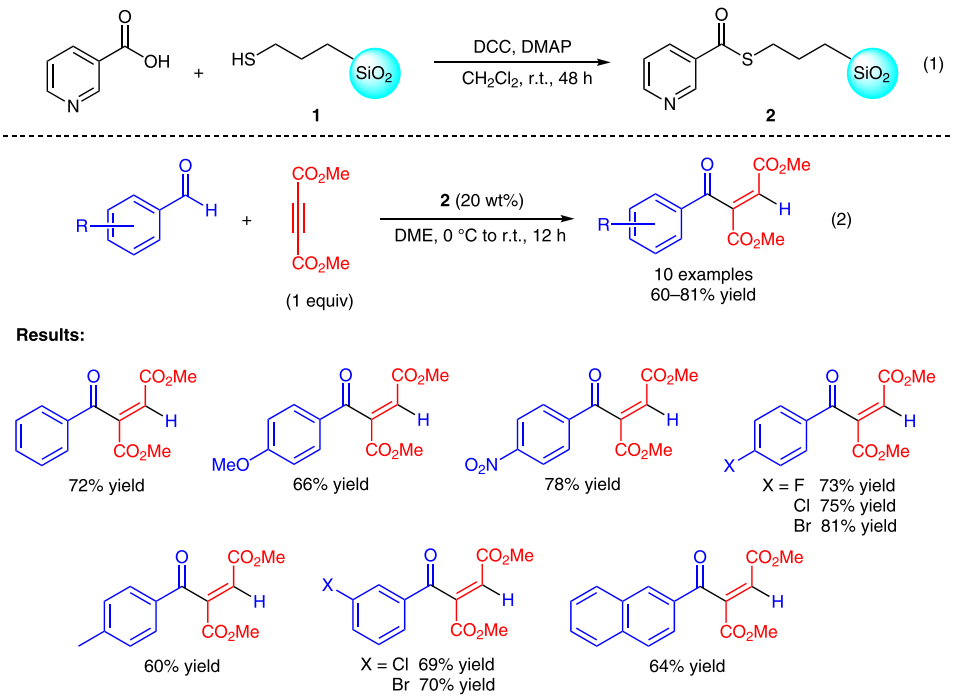

Significance: Nicotinic acid was immobilized onto a silica support via thioesterification to give the silica-supported nicotinate **2**. The reactions of benzaldehydes with dimethylacetylene dicarboxylate (DMAD) were promoted by the supported nicotinate **2** to give the corresponding benzoyl fumarate derivatives in up to 81% yield (10 examples, eq. 2).

Comment: Supported nicotinate **2** was characterized by XRD, IR, N_2-adsorption, and SEM analyses. In the reaction of 4-nitrobenzaldehyde with DMAD, the catalyst was recovered by filtration and reused three times without significant loss of catalytic activity.

SYNFACTS Contributors: Yasuhiro Uozumi, Hiroaki Tsuji
Synfacts 2014, 10(2), 0223 Published online: 20.01.2014
DOI: 10.1055/s-0033-1340541; **Reg-No.:** Y14713SF

2014 © THIEME STUTTGART • NEW YORK

Category
Polymer-Supported Synthesis
Key words
mercaptopropyl silica
nicotinic acid
benzoyl fumarates
aldehydes
dimethyl acetylenedicarboxylate

Monatsh Chem (2015) 146:969–972
DOI 10.1007/s00706-014-1395-2

ORIGINAL PAPER

Selective synthesis of nitroalcohols in the presence of Ambersep 900 OH as heterogeneous catalyst

Rajsekhar Lodh · Manas Jyoti Sarma · Arun Jyoti Borah · Prodeep Phukan

Received: 9 September 2014 / Accepted: 17 December 2014 / Published online: 21 January 2015
© Springer-Verlag Wien 2015

Abstract A green protocol has been developed for the selective synthesis of β-nitroalcohols using commercially available Ambersep 900 OH as reusable heterogeneous catalyst. The reaction between aldehyde and nitromethane was performed under solvent-free condition at room temperature within a short time (70–150 min) in the presence of 10 wt % of Ambersep 900 OH to produce corresponding nitroalcohols in high yield (72–91 %). After the reaction is over, the catalyst can be separated and reused (3 cycles) without appreciable loss in its activity.

Graphical Abstract

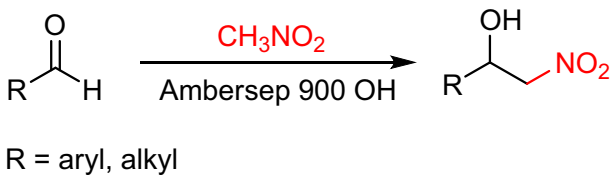

Keywords Henry reaction · Aldehyde · Nitroalcohol · Nitromethane · Ambersep 900 OH

Introduction

The Henry reaction of carbonyl compounds with alkyl nitro compounds bearing α-hydrogen atoms is one of the most fundamental and widely utilized methods for the construction of carbon–carbon bonds that leads to the formation of β-nitroalcohols which in turn can be used as valuable building blocks in organic synthesis [1–9]. From the synthetic point of view, β-nitroalcohols are very important difunctional compounds as they are versatile precursors for the preparation of a great variety of pharmaceutically active compounds such as β-aminoalcohols, α-hydroxycarboxylic acids, 2-nitroketones, or nitroalkenes [1–11]. Classical methods for preparing β-nitroalkanols include the condensation of the carbonyl compounds and a nitroalkane in the presence of a base such as alkali metal hydroxides, carbonates, bicarbonates, alkaline earth oxides, alkaline earth hydroxides or magnesium and aluminum alkoxides, rhodium complex, potassium exchanged zirconium phosphate and also organic bases such as primary, secondary, and tertiary amines [1–9]. Competitive reactions such as Cannizzaro reaction, Tishchenko reaction, and Nef-type reactions were also observed during the course of this particular reaction [1–11]. In certain cases, base catalyzed elimination of water leads to the formation of nitroalkenes which further undergo nitration to yield 1,3-dinitro compounds [12–14]. Different solid catalysts such as alumina [15, 16], alumina-KF [17], Amberlyst A21 [18, 19], SiO_2 [20], hydrotalcites [21–24], etc. were found to promote nitroaldol reaction. Some metal incorporated heterogeneous phases such as polyacrylic acid template [25], carbon nanotubes [26], and metal organic frame works [27] were also developed. Phase transfer catalyst has also been utilized for this particular reaction to improve the selectivity [28]. Some of the former approaches require

Electronic supplementary material The online version of this article (doi:10.1007/s00706-014-1395-2) contains supplementary material, which is available to authorized users.

R. Lodh · M. J. Sarma · A. J. Borah · P. Phukan (✉)
Department of Chemistry, Gauhati University,
Guwahati 781014, Assam, India
e-mail: pphukan@yahoo.com

Scheme 1

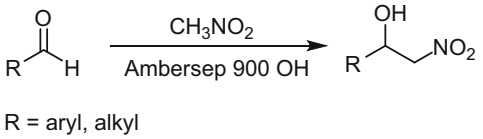

longer reaction time and in some cases, the reaction produces condensed olefin as one of the products [29–31]. Apart from these, some more catalytic systems have also been developed, which include the use of tetramethylguanidine [32], dendritic catalysts [33], rhodium complex [34], and proazaphosphatranes [3c]. Due to the importance of this particular transformation in organic synthesis, several asymmetric synthetic approaches were developed using metallic catalyst in the presence of a chiral ligand [1–9, 35–40]. There are also reports for the nitroaldol reaction in aqueous media [18, 19, 28, 41–45] and under solvent-free conditions [46–53]. However, long reaction time and formation of nitroalkene as side product are the major issues for many of these methods. Hence, the development of a convenient protocol using commercially available heterogeneous catalyst for selective synthesis of β-nitroalcohol is a prime concern for many chemical processes.

Heterogeneous catalysts are getting importance in organic transformations under solvent-free condition [54–56]. From industrial point of view, heterogeneous catalysts are important in organic transformation due to their easy separation process and economically favorable reusability. Similar to Amberlyst A21, Ambersep® 900 OH is also an anionic macromolecular ion-exchange resin, but it is strongly basic in comparison to Amberlyst A21. The utility of Ambersep 900 OH is very limited with a very few reported reactions [57–60]. Herein, we are reporting a new protocol for selective synthesis of nitroalcohols using Ambersep 900 OH as heterogeneous green catalyst (Scheme 1).

Results and discussion

To begin with, the condensation of benzaldehyde with nitromethane (1.2 equiv.) was examined at room temperature in the presence of 5 wt % of Ambersep 900 OH (Table 1, entry 1) under solvent-free condition. The reaction selectively produced corresponding nitro alcohol in 43 % yield after 2 h of reaction. When the catalyst loading was increased to 10 wt %, the reaction completes in 1.5 h with 86 % isolated yield (Table 1, entry 2).

Table 1 Optimization condition of nitroaldol reaction of benzaldehyde

Entry	Catalyst loading/wt %	Time/h	Yield/%[a]
1	5	2	43
2	10	1.5	86
3	15	1.5	84

Reaction conditions: 10 mmol benzaldehyde, 12 mmol nitromethane, room temperature

[a] Isolated yield

Further increase of catalyst amount did not improve the yield significantly. So the use of 10 wt % of the catalyst at room temperature was chosen as the best reaction condition for optimum yield.

After optimizing the reaction condition, the process was extended to a number of aldehydes. Results are summarized in Table 2. Aryl aldehydes with large -I effect (or small +R effect) requires less time than aldehydes with a large +R effect. However, the positions of substituent on the phenyl ring do not have considerable effect on rate of the reaction. Aromatic aldehydes such as 3-nitrobenzaldehyde, 4-methylbenzaldehyde, 4-methoxybenzaldehyde, and 3,4-dimethoxybenzaldehyde produced lower yield of the product. Moreover, for these particular substrates the transformations took relatively longer reaction time for completion. Reaction with heterocyclic aldehydes such as furan-2-carbaldehyde produced low yield of corresponding

Table 2 Henry reaction of nitromethane with various aldehydes (Scheme 1)

Entry	R	Prod.	Time/min	Yield/%[a]	References
1	C_6H_5	**1b**	90	86	[61]
2	4-Cl-C_6H_4	**2b**	70	91	[62]
3	4-F-C_6H_4	**3b**	80	87	[63]
4	4-Br-C_6H_4	**4b**	90	82	[62]
5	4-NO_2-C_6H_4	**5b**	70	86	[61]
6	3-Cl-C_6H_4	**6b**	80	91	[61]
7	3-Br-C_6H_4	**7b**	90	88	[61]
8	2-Cl-C_6H_4	**8b**	80	78	[61]
9	3-NO_2-C_6H_4	**9b**	80	72	[61]
10	4-CH_3-C_6H_4	**10b**	120	76	[63]
11	4-CH_3O-C_6H_4	**11b**	120	77	[63]
12	2-Naphthyl	**12b**	120	78	[61]
13	$C_6H_5CH_2CH_2$	**13b**	120	78	[61]
14	2-Furanyl	**14b**	120	72	[61]
15	3,4-$(CH_3O)_2$-C_6H_3	**15b**	150	75	[45]

Reaction conditions: 1.2 equiv. nitromethane and 10 wt % Ambersep 900 OH at room temperature

[a] Isolated yield

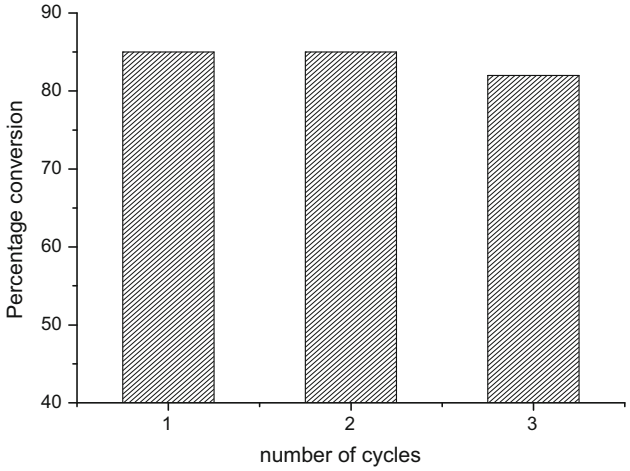

Fig. 1 *Bar diagram* representing the reproducibility of the catalyst in terms of yield after each consecutive cycles

nitroalcohol. Aliphatic aldehydes, such as 3-phenylpropanal, also produced low yield of the corresponding product.

Since we are using a solid resin catalyst, we were interested to examine the feasibility of recycling the catalyst. The catalyst was recovered from the reaction mixture just by filtration and then it was washed with ethanol for 2–3 times. The recyclability experiment was carried out for condensation of *p*-nitrobenzaldehyde and nitromethane under the optimized reaction conditions for three consecutive cycles. During the first two consecutive cycles, the similar yield (85 %) was recorded (Fig. 1). In the third round of catalytic cycle, though the yield was found to be lower (82 %), the change was not detrimental.

Conclusions

In conclusion, an efficient, green, and controlled methodology for the synthesis of β-nitroalcohols has been developed using Ambersep 900 OH as heterogeneous catalyst. Moreover, the reaction is very easy to carry out and the catalyst can be recovered just by filtration of the reaction mixture with the aid of small amount of dichloromethane. The catalyst could be recycled for the same process without having detrimental effect. Both aromatic and aliphatic aldehydes undergo the Henry reaction with high yield within a short time. The advantages of our methods can be easily realized by comparing the recent results on the use of reusable catalysts for selective synthesis of nitroalcohols via Henry reaction, which are presented in Table 3.

Table 3 Activity of different reusable catalysts for Henry reaction

Entry	Catalyst	Condition	Time/h	Yield/%	References
1	Ambersep 900 OH	r.t.	1–2.5	72–91	This work
2	Amberlyst A21	r.t.	3–20	70–95	[18, 19]
3	Phosphate buffer	r.t., pH 7	12–40	91–95	[45]
4	KF/alumina	0 °C	5–15	50–78	[17]
5	Mg-Al Hydrotalcites	Reflux	6–8	72–95	[22]
6	$Zr(KOPO_3)_2$	r.t.	6–25	62–89	[52]
7	DNA	r.t., pH 5.5	8–72	64–96	[43]

Experimental

All reagents were purchased from Sigma–Aldrich. The catalyst Ambersep 900 OH was obtained from Alfa Aesar. The solvents were purified through distillation prior to use. All reactions were carried out under indicated conditions. NMR spectra were recorded using Bruker 300 MHz instruments (300 MHz for ^{1}H, 75.3 MHz for ^{13}C). Chemical shifts are given in δ units relative to the tetramethylsilane (TMS) signal as an internal reference. IR spectra were recorded on Perkin Elmer Spectrum RX I FT-IR System.

General procedure

To a solution of aldehyde (10 mmol) in nitromethane (12 mmol) was added Ambersep 900 OH (10 wt %). The solution was stirred for appropriate time and progress of the reaction was monitored by TLC. After completion of the reaction, 5 cm^3 dichloromethane was added and the catalyst was filtered off and washed with 2 cm^3 ethanol twice. The combined organic extract was evaporated under reduced pressure and the crude product was purified by flash column chromatography using petroleum ether and ethyl acetate as eluent.

Acknowledgments Financial support from UGC, India (Grant No. 41-206/2012/SR) is gratefully acknowledged.

References

1. Rosini G (1991) The Henry (nitroaldol) reaction. In: Trost BM, Fleming I (eds) Comprehensive organic synthesis, vol 2. Pergamon Press, Oxford, p 321
2. Luzzio FA (2001) Tetrahedron 57:915
3. Kudyba I, Raczko J, Urbanczyk-Lipkowska Z, Jurczak J (2004) Tetrahedron 60:4807
4. Palomo C, Oiarbide M, Mielgo A (2004) Angew Chem Int Ed 43:5442
5. Borwga J, Gogoi N, Partha P, Barua NC (2006) Tetrahedron Asymmetry 17:3315
6. Palomo C, Oiarbide M, Laso A (2007) Eur J Org Chem 2007:2561

7. Bartók M (2006) Curr Org Chem 10:1533
8. Bartók M (2010) Chem Rev 110:1663
9. Lüthy M, Darmency V, Renaud P (2011) Eur J Org Chem 2011:547
10. Wade PA, Giuliano RM (1990) Nitro compounds: recent advances in synthesis and chemistry. VCH, Weinheim, p 137
11. Ono N (2001) The nitro group in organic synthesis. Wiley, New York, p 30
12. Motokura K, Tada M, Iwasawa Y (2008) Angew Chem Int Ed 47:9230
13. Zhou Y, Dong J, Zhang F, Gong Y (2011) J Org Chem 76:588
14. Kisanga PB, Verkade JG (1999) J Org Chem 64:4298
15. Rosini G, Ballini R, Sorrenti P (1983) Synthesis 1983:1014
16. Ballini R, Noè M, Perosa A, Selva M (2008) J Org Chem 73:8520
17. Melot JM, Texier-Boullet F, Foucaud A (1986) Tetrahedron Lett 27:493
18. Ballini R, Bosica G, Forconi P (1996) Tetrahedron 52:1677
19. Palmieri A, Gabrielli S, Ballini R (2010) Chem Commun 46:6165
20. Kumar HMS, Subba Reddy BV, Yadav JS (1998) Chem Lett 27:637
21. Choudary BM, Kantam ML, Reddy CH, Rao KK, Figueras F (1999) Green Chem 1:187
22. Bulbule VJ, Deshpande VH, Velu S, Sudalai A, Sivasankar S, Sathe VT (1999) Tetrahedron 55:9325
23. Khan FA, Dash J, Satapathy R, Upadhyay SK (2004) Tetrahedron Lett 45:3055
24. Cwik A, Fuchs A, Hell Z, Clacens JM (2005) Tetrahedron 61:4015
25. Liu C, Zhu Q, Wu Z, Zhou Z, Bhargava G, Parasher S, Rueter M, Zhou B, Chen JG (2010) Appl Catal Int Ed 389:19
26. Ogawa T, Kumagai N, Shibasaki M (2013) Angew Chem Int Ed 52:6196
27. Dhakshinamoorthy A, Opanasenko M, Čejka J, Garcia H (2013) Adv Synth Catal 355:247
28. Ballini R, Bosica G (1997) J Org Chem 62:425
29. Rosini G, Ballini R, Petrini M, Sorrenti P (1985) Synthesis 1985:515
30. Ballini R, Castagnani R, Petrinini M (1992) J Org Chem 57:2160
31. Bandager BP, Zirange MB, Wandgaokar PP (1996) Synlett 1996:149
32. Simoni D, Invidiata FP, Manfrenidi S, Ferroni R, Lampronti I, Roberti M, Pollini GP (1997) Tetrahedron Lett 38:2749
33. Morao I, Cossio FP (1997) Tetrahedron Lett 38:6461
34. Kiyooka SI, Tsutsui T, Maeda H, Kaneko Y, Isobe K (1995) Tetrahedron Lett 36:6531
35. Hashomoto K, Kumagai N, Shibasaki M (2014) Org Lett 16:3496
36. Karmakar A, Fátima M, Silva CG-D, Pombeiro AJL (2014) Dalton Trans 43:7795
37. Liu F, Gou S, Li L, Yan P, Zhao C (2013) J Mol Catal A Chem 379:163
38. Zhou Y, Gong Y (2011) Eur J Org Chem 2011:6092
39. Deng T, Cai C (2013) J Fluorine Chem 156:183
40. Qin D-D, Yu W, Zhou J-D, Zhang Y-C, Ruan Y-P, Zhou Z-H, Chen H-B (2013) Chem Eur J 19:16541
41. Reddy KR, Rajasekhar CV, Krishna GG (2007) Synth Commun 37:1971
42. Ballini R, Barboni L, Fringuelli F, Palmieri A, Pizzo F, Vaccaro L (2007) Green Chem 9:823
43. Fan J, Sun G, Wan C, Wang Z, Li Y (2008) Chem Commun 2008:3792
44. Jammi S, Ali MA, Sakthivel S, Rout L, Punniyamurthy T (2009) Chem Asian J 4:314
45. Bora PP, Bez G (2013) Eur J Org Chem 2013:2922
46. Ballini R, Castagnani R, Petrini M (1992) J Org Chem 57:2160
47. Bhattacharya A, Purohit VC, Rinalda F (2003) Org Process Res Dev 7:254
48. Gan C, Chen X, Lai G, Wang Z (2006) Synlett 2006:387
49. Tanaka K, Hachiken S (2008) Tetrahedron Lett 49:2533
50. Ballini R, Palmieri A (2006) Curr Org Chem 10:2145
51. Angelini T, Ballerini E, Bonollo S, Curini M, Lanari D (2014) Green Chem Lett Rev 7:11
52. Costantino U, Curini M, Marmottini F, Rosati O, Pisani E (1994) Chem Lett 23:2218
53. Ballini R, Bosica G, Parrini M (1999) Chem Lett 28:1105
54. Varma RS (1999) Green Chem 1:43
55. Climent MJ, Corma A, Iborra S (2011) Chem Rev 111:1072
56. Varma RS, Dahiya R, Kumar S (1997) Tetrahedron Lett 38:5131
57. Cardona F, Parmeggiani C, Faggi E, Bonaccini C, Gratteri P, Sim L, Gloster TM, Roberts S, Davies GJ, Rose DR, Goti A (2009) Chem Eur J 15:1627
58. Larsen E, Christensen LP (2005) J Agric Food Chem 53:6598
59. Mouloungui Z, Rakotondrazafy V, Valentin R, Zebib B (2009) Ind Eng Chem Res 48:6949
60. Bijttebier S, D'Hondt E, Noten B, Hermans N, Apers S, Voorspoels S (2014) Food Chem 163:147
61. Lai G, Guo F, Zheng Y, Fang Y, Song H, Xu K, Wang S, Zha Z, Wang Z (2011) Chem Eur J 17:1114
62. Kanagaraj K, Suresh P, Pitsumani K (2010) Org Lett 12:4070
63. Mayani VJ, Abdi SHR, Kureshy RI, Khan NH, Das A, Bajaj HC (2010) J Org Chem 75:6191

Monatsh Chem (2016) 147:797–800
DOI 10.1007/s00706-015-1531-7

ORIGINAL PAPER

Poly(4-vinylpyridine-*co*-ethylvinylbenzene) as heterogeneous reusable catalyst for the synthesis of benzoyl fumarate

Bishwapran Kashyap[1] · **Prodeep Phukan**[1]

Received: 14 April 2015 / Accepted: 6 July 2015 / Published online: 6 August 2015
© Springer-Verlag Wien 2015

Abstract Poly(4-vinylpyridine-*co*-ethylvinylbenzene) 25 % cross-linked (with divinylbenzene) has been found to be an effective heterogeneous catalyst for the synthesis of benzoyl fumarate from aldehyde and dimethyl acetylenedicarboxylate. Various aromatic aldehydes undergo this reaction with good yield in presence of 15 wt% of the catalyst. The catalyst was recovered and reused six times without appreciable alteration in activity.

Graphical abstract

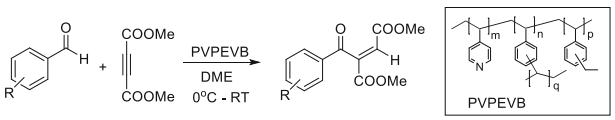

Keywords Benzoyl fumarate · Poly(4-vinylpyridine-*co*-ethylvinylbenzene) · Heterogeneous catalyst · DMAD · Aldehyde

Introduction

Benzoyl fumarates and their corresponding acids are known to be the vital precursors in the synthesis of many important agrochemicals, drugs as well as in many synthetically important reactions such as Diels–Alder reaction [1–8]. While studying the photo-oxidation of furans, Scarpati and co-workers have observed the formation of benzoyl fumarates [9, 10]. In the year 2003, a direct protocol for the synthesis of benzoyl fumarates was developed independently by Shi and Nair [11, 12]. Their approach involves the reaction between aldehyde and dimethyl acetylenedicarboxylate (DMAD) in presence of Lewis base such as pyridine and DMAP as catalyst. Recently, Bayat et al. observed the formation of similar structural features as byproduct during the synthesis of γ-butyrolactone [13]. There are also few reports in the literature for the synthesis of benzoyl fumarates [5, 14]. However, all these methods are based on the application of homogeneous catalysts which have the obvious problem of reusability. Application of reusable catalyst is important from the industrial as well as green chemistry point of view. We have recently reported a homogeneous reusable catalyst for the synthesis of benzoyl fumarates [15]. Subsequently, we made an improvement of the method by developing a nicotinic acid-based heterogeneous catalyst [16]. Although we are successful in synthesizing new reusable catalysts, these catalysts have to be made via multistep procedure. So, we looked for alternative commercially available catalyst to make the method more viable. Since DMAP has been proven to be the best catalyst for this particular reaction, we intended to examine the possibility of using poly(4-vinylpyridine-*co*-ethylvinylbenzene) 25 % cross-linked with divinylbenzene as the first case due to its commercial availability. In this paper, we describe the use of poly(4-vinylpyridine-*co*-ethylvinylbenzene) (PVPEVB) as reusable heterogeneous catalyst for the synthesis of benzoyl fumarate from aldehyde (Scheme 1).

Electronic supplementary material The online version of this article (doi:10.1007/s00706-015-1531-7) contains supplementary material, which is available to authorized users.

✉ Prodeep Phukan
pphukan@yahoo.com

[1] Department of Chemistry, Gauhati University, Guwahati, Assam 781014, India

Scheme 1

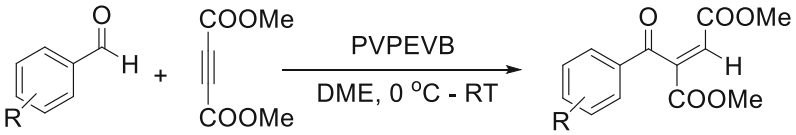

Results and discussion

The catalyst, PVPEVB (Fig. 1) is commercially available. Initially, the reaction between 4-nitrobenzaldehyde and DMAD was taken as a model reaction to find out the optimum condition for the reaction. In a typical reaction, 5 wt% (based on the aldehyde amount) of the catalyst was added to a mixture of 4-nitrobenzaldehyde (1 mmol) and DMAD (1 mmol) in 5 cm^3 DME at 0 °C under nitrogen atmosphere and the reaction was continued at room temperature for an appropriate time. After the completion of the reaction (as indicated by TLC analysis), the catalyst was separated by filtration and washed with a small amount of DCM. The reaction mixture was concentrated and the crude material was purified by column chromatography using a mixture of petroleum ether and ethyl acetate as eluent to get the pure product. Initial reaction in the absence of the catalyst fails to give the desired product even after 24 h of reaction (Table 1, entry 1). However, 5 wt% of catalyst and DME as solvent gives 70 % of benzoyl fumarate as product with 10 h of reaction time (Table 1, entry 2). It was observed that the reaction in other solvents such as acetonitrile and THF produced lower yield with longer reaction hours (Table 1, entries 3, 4). Only trace amount of the product formation was observed when DCM was used as solvent (Table 1, entry 5). The reaction was further investigated by increasing the catalyst amount. The reaction in presence of 15 wt% of PVPEVB produced 80 % of corresponding fumarate after 8 h of reaction (Table 1, entry 7). Further increase in catalyst loading did not improve the reaction (Table 1, entries 8, 9). Finally,

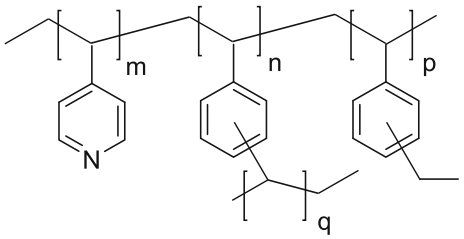

Fig. 1 Structure of poly(4-vinylpyridine-*co*-ethylvinylbenzene), 25 % cross-linked with divinylbenzene (as per Sigma-Aldrich catalogue description)

Table 1 Reaction of *p*-nitrobenzaldehyde with DMAD catalyzed by PVPEVB under different conditions

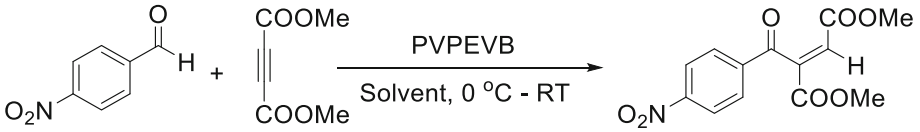

Entry	PVPEVB/wt%	Solvent	Time/h	Yield/%[a]
1	0	DME	24	0
2	5	DME	10	70
3	5	THF	14	50
4	5	CH_3CN	24	37
5	5	DCM	24	Trace
6	10	DME	8	74
7	15	DME	8	80
8	20	DME	8	80
9	25	DME	8	81

Reaction conditions: 4-nitrobenzaldehyde (1 mmol), DMAD (1 mmol), 5 cm^3 solvent, 0 °C to rt

[a] Isolated yield

Table 2 Synthesis of benzoyl fumarates using PVPEVB catalyst

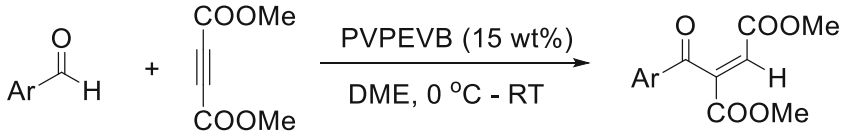

Entry	Ar	Yield/%[a]
1	C_6H_5 (**1a**)	60
2	4-BrC_6H_4 (**1b**)	79
3	4-ClC_6H_4 (**1c**)	74
4	4-FC_6H_4 (**1d**)	70
5	4-$NO_2C_6H_4$ (**1e**)	80
6	4-MeOC_6H_4 (**1f**)	68
7	4-MeC_6H_4 (**1g**)	53
8	$C_{10}H_7$ (**1h**)	61
9	3-BrC_6H_4 (**1i**)	68
10	3-ClC_6H_4 (**1j**)	70

Reaction conditions: aldehyde (1 mmol), DMAD (1 mmol), PVPEVB (15 wt%), 5 cm^3 DME, 0 °C to rt, 8 h

[a] Isolated yield

15 wt% of catalyst (based on the aldehyde amount), 1 mmol of aldehyde, 1 mmol of DMAD in DME and 8 h of reaction time was found to be the optimum condition for the reaction. After optimization the protocol has been extended to a variety of aldehydes and the results are presented in Table 2.

The efficiency of this method is evident from the high yield of benzoyl fumarates formed from various substituted benzaldehydes. It was observed that the presence of electron withdrawing group enhances the yield of the reaction (Table 2, entries 2–6). On the other hand, electron donating group results in the lower product yield (Table 2, entry 7). It was further observed that para-substituted aldehyde shows better results compared to the corresponding meta-substituted aldehyde (Table 2, entries 3, 4, 8, 9). This reaction was found to be less effective for aliphatic aldehyde.

Reusability of the catalyst was tested with 4-nitrobenzaldehyde. After the completion of the reaction, the solvent was removed and 5 cm^3 DCM was added to the crude reaction mixture. The reaction mixture was passed through a filter paper to remove the insoluble polymeric catalyst. The residue in the filter paper was washed with DCM, dried under vacuum, and kept in a desiccator for 24 h before reuse. Initially, after the first use, the recovery percentage of the catalyst was found to be 98 % in comparison to the first use of the catalyst. The recovered catalyst was reused. We have reused the catalyst six times without appreciable loss in activity. The slight decrease in yield in the subsequent step can be attributed to the small decrease in the catalyst recovery. After the sixth run, the yield was found to be 76 with 89 % of catalyst recovery (Table 3, entry 6).

Table 3 Reusability of the catalyst

Entry	Catalyst reused	Catalyst recovered/%[a]	Yield/%[b]
1	1st	98	80
2	2nd	97	79
3	3rd	95	79
4	4th	92	78
5	5th	91	77
6	6th	89	76

Reaction conditions: 4-nitrobenzaldehyde (1 mmol), DMAD (1 mmol), 5 cm^3 DME, 0 °C to rt, 8 h

[a] With respect to first use

[b] Isolated yield

The mechanism of this reaction has already been proposed by Shi et al. [11]. In this case, the pyridine moiety attached to the polymer takes part in the mechanism. Thus, the pyridine subunit of the polymeric catalyst produces a zwitterionic intermediate by interacting with DMAD, which subsequently reacts with aldehyde followed by intermolecular proton transfer. Expulsion of the catalyst at the final stage results in the formation of the product.

In conclusion, we have developed an efficient heterogeneous and reusable catalytic protocol for the synthesis of benzoyl fumarate from aldehyde and DMAD in presence of

a catalytic amount of poly(4-vinylpyridine-*co*-ethylvinylbenzene). Use of a commercially available catalyst makes this methodology convenient for direct applications. The method is suitable for various aromatic aldehydes to obtain the product in high yield. Moreover, the catalyst can be reused six times without appreciable loss in activity.

Experimental

The catalyst poly(4-vinylpyridine-*co*-ethylvinylbenzene) 25 % cross-linked (with divinylbenzene) was purchased from Sigma-Aldrich Corporation.

Typical experimental procedure for polymer catalyzed synthesis of benzoyl fumarate

A solution of 0.142 g DMAD (1 mmol) and 0.045 g 4-nitrobenzaldehyde (1 mmol) in 5 cm^3 anhydrous DME was cooled to 0 °C under nitrogen atmosphere. PVPEVB (15 wt%) was then added and the reaction was stirred at room temperature for 8 h. After the completion of the reaction, the reaction mixture was filtered and the residue was washed with DCM. The combined filtrate was concentrated and purified by column chromatography using a mixture of petroleum ether and ethyl acetate as eluent to get the pure product **1e** with 80 % yield.

Acknowledgments Financial Support from University Grants Commission, India (Grant No. 41-206/2012/SR), India, is gratefully acknowledged. BK thanks CSIR for the senior research fellowship.

References

1. Reymond S, Cossy J (2008) Chem Rev 108:5359
2. Pindur U, Lutz G, Otto C (1993) Chem Rev 93:741
3. Yamada K, Ino K, Takashashi S, Ohashi T, Watanabe K (1988) N2-(1-carboxy-3-oxo-3-phenyl)-L-lysine derivatives, their preparation, and their use as intermediates for potential antihypertensives. Eur Patent EP 239062, 30 Sep 1987; Chem Abstr 109:110904z
4. Kagan HB, Riant O (1992) Chem Rev 92:1007
5. Ikeda T, Hirano H, Aoki K (1989) Preparation of benzoylacrylic acid esters as drug and agrochemical intermediates. Jpn Kokai 63130564, 2 June 1988; Chem Abstr 110:7866
6. Chosakon Y, Yamamoto N (1988) Process for the preparation of 3-benzoylacrylic acids as intermediates for food preservatives, perfumes, and drugs. Jpn Kokai 63104940, 10 May 1988; Chem Abstr 109:230551
7. Nippon Synthetic Chemical Industry (1983) Benzoylacrylic acid esters as fungicides. Jpn Kokai 5838202, 5 Mar 1983; Chem Abstr 99:1818
8. Nippon Synthetic Chemical Industry (1981) Benzoylacrylic acid esters as acaricides. Jpn Kokai 56127302, 6 Oct 1981; Chem Abstr 96:2180
9. Iesce MR, Cermola F, Piazza A, Graziano ML, Scarpati R (1995) Synthesis 439
10. Iesce MR, Cermola F, Graziano ML, Scarpati R (1994) Synthesis 944
11. Li C-Q, Shi M (2003) Org Lett 5:4273
12. Nair A, Sreekanth AR, Abhilash N, Biju AT, Devi BR, Menon RS, Rath NP, Srinivas R (2003) Synthesis 1895
13. Bayat M, Imanieh H, Hassanzadeh F (2010) Tetrahedron Lett 51:1873
14. Takahashi S, Ueda Y, Yanagida Y, Namito Y, Ohaska T, Watanabe K (1987) Process for the preparation of trans-β-benzoylacrylic acid esters. Eur Patent Appl EP204286, 10 Dec 1986; Chem Abstr 106:84179
15. Kashyap B, Phukan P (2013) RSC Adv 3:15327
16. Singh RSK, Kashyap B, Phukan P (2013) Tetrahedron Lett 54:6687

Indian Journal of Chemistry
Vol. 53B, November 2014, pp 1417-1424

Synthesis of some new 2-substituted 4,5-dihydroxypiperidines *via* Sharpless asymmetric dihydroxylation

Arun Jyoti Borah & Prodeep Phukan*

Department of Chemistry, Gauhati University, Guwahati 781 014, India

E-mail: pphukan@yahoo.com

Received 3 December 2013; accepted (revised) 6 September 2014

Synthesis of seven new 2-substituted 4,5-dihydroxy piperidines have been reported using homoallylic carbamates as the starting material that have been synthesized *via* three-component reaction of aldehyde, allyl trimethyl silane and benzyl carbamate in presence of iodine as catalyst. Further *N*-allylation of the substrate followed by ring closing metathesis produced the corresponding 1,2,3,6-tetrahydropyridine derivatives. Subsequent Sharpless dihydroxylation of the tetrahydropyridines produced the 2-substituted 4,5-dihydroxy piperidines in high yield.

Keywords: Piperidine, homoallylic carbamates, ring closing metathesis, Sharpless asymmetric dihydroxylation, iodine

Piperidine and its analogues are ubiquitous in alkaloids and in man-made substances possessing biological activities[1]. They are important building blocks in the synthesis of pharmaceuticals and fine chemicals. The ability of piperidine analogues to act as chemotherapeutic agents is well documented[2]. Several substituted piperidines display important biological properties like antiviral[3], antidepressant[4], cytotoxic[5] and antimalarial activity[6]. Some piperidine derivatives are used as neuroleptic agents[7]. These structural moieties are found in pharmaceuticals like paroxetine, risperidone, methylphenidate, raloxifene, mixoxidil, thioridazine and in many others[1]. These compounds also find industrial applications such as raw material for hardners of epoxy resin, corrosion inhibitor, insecticides, accelerator of rubber, urethane catalysts, as antioxidant, *etc*. It is well known that the biological properties of piperidines are highly dependent on the type and location of substituents on the heterocyclic ring. Hence the search for new piperidine analogues is gaining importance in recent years. Numerous stereoselective routes to various substituted piperidines have been developed[8]. Particularly, 2,4,5-trisubstituted piperidines are common structures in natural products and synthetic compounds exhibiting potential biological activities[9-13]. Pseudodistomin alkaloids were isolated from the Okinawan tunicate *Pseudodistomina kanoko* by Kobayashi *et al*[10,12-14]. These alkaloids exhibit calmodulin antagonistic activity and potent cytotoxicity against both murine leukemia and human epidermoid carcinoma KB cells.

There are a number of methods reported in the literature for the synthesis of substituted piperidines, most of which are focused on the synthesis of piperidine based azasugars[15]. Irrespective of the starting material, tactical approaches to substituted piperidines use RCM[16] to form the 1,2,3,6-tetrahydropyridine building block from a prerequisite diene precursor. The other consequential stage in the overall synthesis is the diastereoselective dihydroxylation of the endocyclic double bond under Upjohn dihydroxylation reaction condition[15]. The selectivity is governed by presence of another chiral centre near to the double bond in the system, particularly at allylic position[17]. In continuation of the work on Sharpless dihydroxylation reactions[18] herein is reported the synthesis of some new piperidine analogues. Another objective of this work is to examine effect of Sharpless asymmetric dihydroxylation of 1,2,3,6-tetrahydropyridine on the enantioselectivity of the final diol.

Results and Discussion

The strategy begins with the synthesis of 1,2,3,6-tetrahydropyridine ring by using homoallylamine as starting material (**Scheme I**). The homoallylamines were prepared according to reported iodine catalyzed three component condensation of benzaldehyde **1**, benzyl carbamate and allyltrimethylsilane[19]. The homoallylamine **2** was subjected to *N*-allylation

reaction by using allyl bromide in presence of NaH and products **3** were isolated with very good yield in 65-98%. Then the diene precursor **3** was provided to ring closing metathesis process by using Grubb's 1st generation catalyst in CH_2Cl_2. This results in the formation of 1,2,3,6-tetrahydropyridine block **4**. The product **4** was isolated with excellent yield of between 86-92% (**Table I**).

Thereafter it was planned to carry out Sharpless asymmetric dihydroxylation reaction of the tetrahydropyridine **4** using catalytic amount of $K_2OsO_2(OH)_4$ along with $K_3Fe(CN)_6$ as cooxidant in presence of $(DHQ)_2PHAL$ as ligand (**Scheme II**)[20].

The reaction was carried out using *t*BuOH:H_2O (1:1) as solvent at low temperature. Although the formation of optically pure diols was expected, HPLC

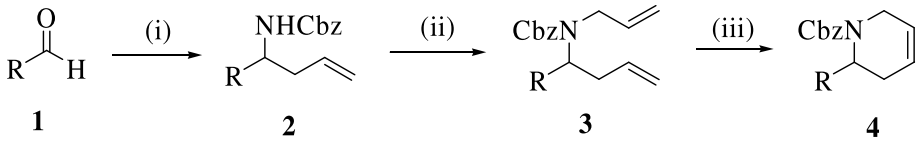

1 **2** **3** **4**

Reagents and conditions: (i) allyltrimethylsilane, benzyl carbamate, I_2, CH_3CN, RT (ii) allyl bromide, NaH, DMF, 0°C to RT (iii) Grubbs' 1st generation catalyst, CH_2Cl_2, RT.

Scheme I — Synthesis of 1,2,3,6-tetrahydropyridine **4**

Table I — Synthesis of products **2**, **3** and **4**

Entry	Homoallylamine **2**	Yield[a]	Diene **3**	Yield[a]	Tetrahydropyridine **4**	Yield[a]
a	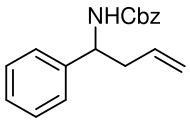	80	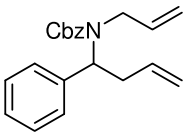	93	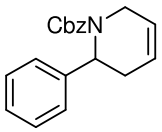	92
b	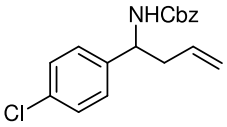	70	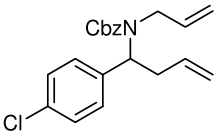	97	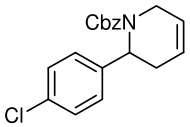	88
c	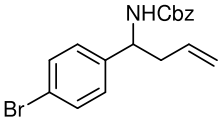	75	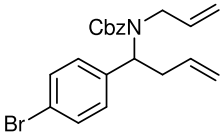	96	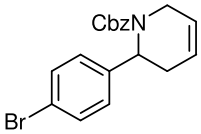	86
d	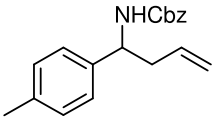	72	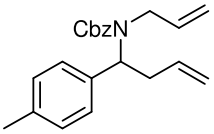	98	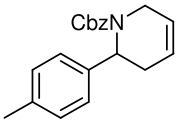	88
e	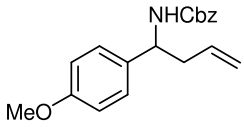	75	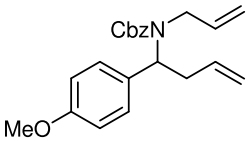	95	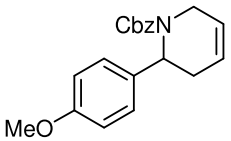	92
f	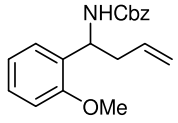	80	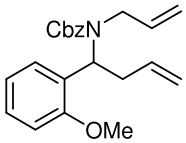	98	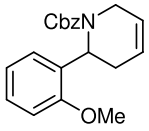	87
g	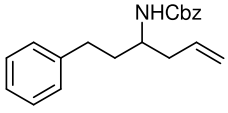	70	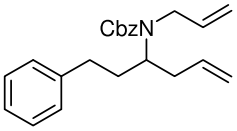	65	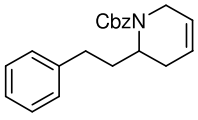	87

[a]Isolated yield

analysis revealed that the enantioselectivities of the diols **5** were very poor (**Table II**). This analysis indicated that the use of standard Sharpless asymmetric dihydroxylation condition on this type of substrates results in the formation of nearly racemic diols. The products were isolated with excellent yield of between80-90%. The ligand probably does not take part in the formation of osmium (VI) glycolate complex that is produced from 1,2,3,6-tetrahydropiperidine ring and osmium source during

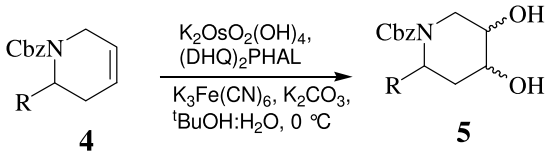

Scheme II — Synthesis of 4,5-dihydroxy piperidine **5**

Table II — Synthesis of 2-substituted 4,5-dihydroxypiperidines, **5** from alkene **4**[a]

Entry	Substrate **4**	Product **5**	Time (h)	Yield[b] (%)	*ee*[c]	$[\alpha]_D^{26}$
a	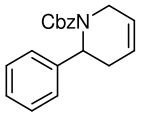	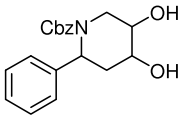	24	85	1.6	+1.1
b	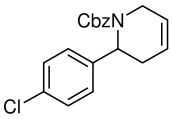	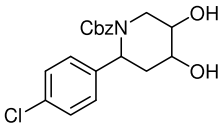	24	90	2.4	+1.2
c	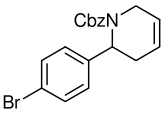	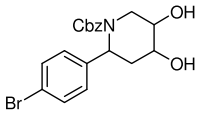	24	85	1.3	+1.7
d	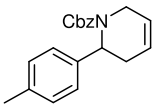	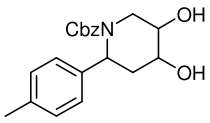	24	83	1.4	+1.4
e	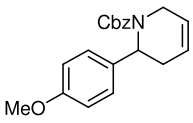	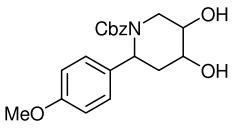	24	81	2.0	-1.5
f	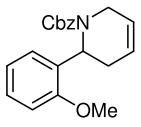	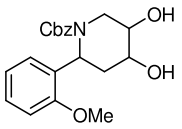	24	81	1.0	+1.6
g	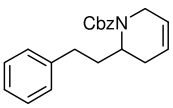	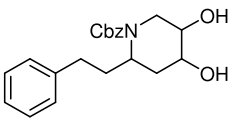	24	80	2.6	+2.5

[a] Reactions were carried out in *t*BuOH:H_2O (1:1) using 4% $K_2OsO_2(OH)_4$ and 5% $(DHQ)_2PHAL$ ligand; [b] isolated yield, [c] enantiomeric excess was determined by HPLC

dihydroxylation reaction and thereby exhibit poor enantioselectivity. These observations reveal that the structure **4** is not a suitable substrate for Sharpless asymmetric dihydroxylation process.

However, overall synthetic route is a convenient route for synthesis of 2,4,5-trisubstituted piperidine analogues. Following the above synthetic strategy, seven new 2,4,5-trisubstituted piperidine analogues were synthesized from corresponding Cbz-protected homoallyl amine as starting material. All the synthetic steps are very efficient and products are formed with high yield. All the products were characterized *via* IR and NMR spectroscopic studies.

Experimental Section

All reagents were purchased from Sigma-Aldrich. The solvents were purified by distillation prior to use. All reactions were carried out under the indicated conditions. NMR spectra were recorded using tetramethylsilane as an internal standard. IR spectra were recorded on Perkin-Elmer Spectrum RX I FT-IR System. Specific rotations were measured with Perkin-Elmer Model 343 Polarimeter. The enantiomeric excess of the products were determined by HPLC on Chiralcel OD-H column (0.46 cm diameter × 25 cm length).

Synthesis of Protected Homoallylamine, 2

Benzyl carbamate (1.5 equivalents) and allyltrimethyl silane (1 equivalent) were added to a solution of aldehyde (1 g) and iodine (10 mol %) in acetonitrile at RT. The reaction was completed within 10-20 minutes. The progress of the reaction was monitored by using TLC. After completion of the reaction, sodium thiosulphate was added to the reaction mixture. The mixture was extracted with EtOAc. The organic extract was washed with brine and dried over anhydrous sodium sulfate. The solvent was evaporated under reduced pressure. Purification of the crude product by flash chromatography over silica gel (230-400 mesh) with petroleum ether-EtOAc (10-20%) as eluent furnished the pure product (70-80% yield).

Benzyl (1-phenylbut-3-en-1-yl)carbamate, 2a: Yield 80% (colorless solid); m.p. 67-68°C; IR (Nujol): 3056, 1714, 1423, 1262, 739 cm^{-1}; ^1H NMR (300 MHz, $CDCl_3$): δ 2.55 (br, 2H), 4.90-4.71 (m, 1H), 5.15-5.03 (m, 5H), 5.75-5.61 (m, 1H), 7.60-7.17 (m, 10H); ^{13}C NMR (75MHz, $CDCl_3$): δ 41.0, 54.4, 66.7, 118.5, 126.1, 127.3, 128.1, 128.5, 128.7, 133.6, 136.3, 141.8, 155.6.

Benzyl [1-(4-chlorophenyl)but-3-en-1-yl]carbamate, 2b: Yield 70% (colorless solid); m.p. 68-70°C; IR (KBr): 3342, 3064, 2950, 1678, 1534, 1489, 1346, 1263, 1119, 1035, 752 cm^{-1}; ^1H NMR (300 MHz, $CDCl_3$): δ 2.51 (br, 2H), 4.79-4.77 (m, 1H), 5.15-5.03 (m, 5H), 5.72-5.58 (m, 1H), 7.35-7.19 (m, 9H); ^{13}C NMR (75MHz, $CDCl_3$): δ 40.8, 53.8, 66.8, 118.8, 127.5, 128.1, 128.4, 128.6, 132.9, 133.1, 136.2, 140.5, 155.5.

Benzyl [1-(4-bromophenyl)but-3-en-1-yl]carbamate, 2c: Yield 75% (colorless solid); m.p. 87-88°C; IR (KBr): 3345, 3087, 2950, 1684, 1592, 1533, 1455, 1347, 1264, 1119, 1034, 751 cm^{-1}; ^1H NMR (300 MHz, $CDCl_3$): δ 2.50 (br, 2H), 4.83-4.67 (m, 1H), 5.24-5.02 (m, 5H), 5.71-5.58 (m, 1H), 7.15 (d, J = 7.5 Hz, 2H), 7.35 (br, 5H), 7.45 (d, J = 8.4 Hz, 2H); ^{13}C NMR(75MHz, $CDCl_3$): δ 40.8, 53.9, 66.8, 118.9, 121.0, 127.9, 128.2, 128.5, 131.6, 133.1, 136.1, 141.0, 155.5.

Benzyl [1-(4-methylphenyl)but-3-en-1-yl]carbamate, 2d: Yield 72% (colorless solid); m.p. 70-71°C; IR (KBr): 3357, 3058, 2958, 1692, 1590, 1526, 1457, 1350, 1263, 1143, 1044, 732 cm^{-1}; ^1H NMR (300 MHz, $CDCl_3$): δ 2.35 (s, 3H), 2.56-2.52 (m, 2H), 4.88-4.69 (m, 1H), 5.14-5.03 (m, 5H), 5.76-5.62 (m, 1H), 7.35-7.14 (m, 9H); ^{13}C NMR(75MHz, $CDCl_3$): δ 21.0, 40.9, 54.2, 66.6, 118.2, 126.1, 128.0, 128.4, 129.2, 133.8, 136.3, 136.9, 138.8, 155.6.

Benzyl [1-(4-methoxyphenyl)but-3-en-1-yl]carbamate, 2e: Yield 75% (colorless solid); m.p. 70-71°C; IR (KBr): 3362, 3067, 2950, 1685, 1597, 1528, 1454, 1346, 1243, 1116, 1032, 748 cm^{-1}; ^1H NMR (400 MHz, $CDCl_3$): δ 2.60-2.54 (m, 2H), 3.79 (s, 3H), 4.80-4.70 (m, 1H), 5.20-5.00 (m, 5H), 5.77-5.58 (m, 1H), 6.86 (d, J = 8.6 Hz, 2H), 7.19 (d, J = 7.8 Hz, 2H), 7.41-7.29 (m, 5H); ^{13}C NMR (100 MHz, $CDCl_3$): δ 40.9, 53.9, 55.2, 66.7, 113.8, 118.2, 127.3, 128.0, 128.4, 133.9, 136.4, 155.6, 158.7.

Benzyl [1-(2-methoxyphenyl)but-3-en-1-yl]carbamate, 2f: Yield 80% (colorless solid); m.p. 88-90°C; IR (KBr): 3333, 3060, 2942, 1685, 1600, 1537, 1468, 1352, 1264, 1121, 1035, 754 cm^{-1}; ^1H NMR (300 MHz, $CDCl_3$): δ 2.58 (m, 2H), 3.86 (s, 3H), 5.14-4.94 (m, 5H), 5.76-5.63 (m, 2H), 6.95-6.88 (br, 2H), 7.17 (d, J = 7.2 Hz, 1H), 7.48-7.23 (m, 6H); ^{13}C NMR (75MHz, $CDCl_3$): δ 39.7, 52.8, 55.2, 66.6, 110.7, 117.4, 120.5, 128.0, 128.2, 128.3, 128.4, 129.3, 134.7, 136.5, 155.6,156.8.

Benzyl (1-phenylhex-5-en-3-yl)carbamate, 2g: Yield 70% (colorless solid); m.p. 70-71°C; IR (KBr): 3065, 1696, 1534, 1451, 1243, 1045, 739 cm^{-1}; ^1H NMR (300 MHz, $CDCl_3$): δ 1.90-1.69 (m, 2H), 2.36-

2.20 (m, 2H), 2.76-2.59 (m, 2H), 3.89-3.74 (m, 1H), 5.27-5.01 (m, 4H), 5.84-5.71 (m, 1H), 7.21-7.17 (m, 3H), 7.53-7.26 (m, 7H); ^{13}C NMR (75 MHz, $CDCl_3$): δ 32.3, 36.5, 39.5, 50.4, 66.5, 118.1, 125.8, 128.0, 128.3, 128.4, 128.5, 133.9, 136.5, 141.6, 155.9.

Synthesis of diene 3

To a stirred suspension of NaH (1.4 equivalents) in dry DMF (8 mL per mmol of the substrate), the homoallylamine (2.5 mmol) was added at 0°C under nitrogen atmosphere. The resulting solution was stirred for 15 min at RT. Allyl bromide (1.2 equivalents) was then added and the reaction mixture was stirred for 7 h. After completion of reaction, the reaction mixture was quenched with aq. $NaHCO_3$ and extracted with ether (2×20 mL). The combined organic extracts were washed with brine and dried over anhydrous Na_2SO_4, concentrated under reduced pressure and purified by column chromatography (hexane/EtOAc, 95:5) to afford pure product **3** (65-98% yield) as a thick yellow liquid.

Benzyl (1-phenylbut-3-en-1-yl)prop-2-en-1-ylcarbamate, 3a: Yield 93% (yellow oil); IR(neat): 3070, 2931, 1697, 1647, 1498, 1454, 1242 cm^{-1}; ^{1}H NMR (300 MHz, $CDCl_3$): δ 2.75-2.70 (m, 2H), 3.59 (dd, J_1 =15.9 Hz, J_2 = 6.6 Hz, 1H), 3.72 (br, 1H), 5.39-4.96 (m, 7H), 5.90-5.41 (m, 2H), 7.35-7.27 (m, 10H); ^{13}C NMR (75MHz, $CDCl_3$): δ 35.3, 45.9, 58.4, 67.1, 116.1, 117.5, 127.5, 127.7, 127.8, 128.0, 128.3, 128.3, 134.8, 135.1, 136.7, 139.5, 156.6.

Benzyl [1-(4-chlorophenyl)but-3-en-1-yl]prop-2-en-1-ylcarbamate, 3b: Yield 97% (yellow oil); IR (neat): 3078, 2931, 1693, 1641, 1491, 1454, 1408, 1247 cm^{-1}; ^{1}H NMR (300 MHz, $CDCl_3$): δ 2.75-2.70 (m, 2H), 3.60 (dd, J_1=15.6 Hz, J_2= 6.3 Hz, 1H), 3.70 (br, 1H), 5.41-4.96 (m, 7H), 5.82-5.61 (m, 2H), 7.39-7.28 (m, 9H); ^{13}C NMR (75MHz, $CDCl_3$): δ 35.3, 46.0, 57.9, 67.2, 116.4, 117.7, 127.7, 127.9, 128.3, 128.4, 129.3, 133.3, 134.3, 134.9, 136.5, 138.1, 156.5.

Benzyl [1-(4-bromophenyl)but-3-en-1-yl]prop-2-en-1-ylcarbamate, 3c: Yield 96% (yellow oil); IR (neat): 3074, 2931, 1687, 1643, 1495, 1454, 1404, 1246 cm^{-1}; ^{1}H NMR (400 MHz, $CDCl_3$): δ 2.77-2.73 (m, 2H), 3.63 (dd, J_1=12Hz, J_2= 4.5 Hz, 1H), 3.76 (br, 1H), 5.53-4.90 (m, 7H), 5.77-5.54 (m, 2H), 7.24 (br, 2H), 7.41-7.33 (m, 5H), 7.47 (d, J = 6 Hz, 2H); ^{13}C NMR (100MHz, $CDCl_3$): δ 35.3, 46.2, 58.1, 67.2, 116.5, 117.7, 121.4, 127.7, 127.9, 128.3, 129.7, 131.4, 134.3, 134.7, 136.5, 138.7, 156.4.

Benzyl [1-(4-methylphenyl)but-3-en-1-yl]prop-2-en-1-ylcarbamate, 3d: Yield 98% (Yellow oil); IR (neat): 3034, 2924, 1697, 1644, 1454, 1408, 1250 cm^{-1}; ^{1}H NMR (300 MHz, $CDCl_3$): δ 2.35 (s, 3H), 2.75-2.71 (m, 2H), 3.57 (dd, J_1=16.2 Hz, J_2 = 6.6 Hz, 1H), 3.71 (br, 1H), 5.52-4.85 (m, 7H), 5.88-5.62 (m, 2H), 7.36-7.12 (m, 9H); ^{13}C NMR (75MHz, $CDCl_3$): δ 21.0, 35.5, 46.1, 58.3, 67.1, 116.0, 117.4, 127.7, 127.8, 127.9, 128.3, 129.0, 134.9, 135.2, 136.5, 136.7, 137.2, 156.4.

Benzyl [1-(4-methoxyphenyl)but-3-en-1-yl]prop-2-en-1-ylcarbamate, 3e: Yield 95% (yellow oil); IR (neat): 3076, 2932, 1690, 1638, 1600, 1490, 1408, 1245 cm^{-1}; ^{1}H NMR (300 MHz, $CDCl_3$): δ 2.74-2.70 (m, 2H), 3.58 (dd, J_1=16.2 Hz, J_2= 6.3 Hz, 1H), 3.76-3.65 (m, 1H), 3.81 (s, 3H), 5.45-4.97 (m, 7H), 5.89-5.52 (m, 2H), 6.85 (d, J = 8.7 Hz, 2H), 7.36 (br, 7H); ^{13}C NMR (75MHz, $CDCl_3$): δ 35.6, 45.7, 55.1, 57.9, 67.0, 113.6, 116.2, 117.3, 127.7, 127.8, 128.3, 129.2, 129.2, 131.5, 134.9, 135.2, 136.7, 158.8.

Benzyl [1-(2-methoxyphenyl)but-3-en-1-yl]prop-2-en-1-ylcarbamate, 3f: Yield 98% (yellow oil); IR (neat): 3074, 2935, 1693, 1640, 1600, 1492, 1408, 1249 cm^{-1}; ^{1}H NMR (300 MHz, $CDCl_3$): δ 2.73 (br, 2H), 3.69 (br, 5H), 4.88 (m, 2H), 5.35-5.00 (m, 4H), 5.62-5.42 (m, 2H), 5.79 (br, 1H), 6.83 (d, J = 8.1 Hz, 1H), 6.93 (t, J = 7.5 Hz, 1H), 7.37-7.25 (m, 7H); ^{13}C NMR (75MHz, $CDCl_3$): δ 35.7, 46.4, 53.3, 55.1, 66.7, 110.3, 115.5, 117.0, 119.8, 127.1, 127.6, 127.7, 128.2, 128.8, 135.2, 137.1, 156.1, 158.0.

Benzyl (1-phenylhex-5-en-3-yl)prop-2-en-1-ylcarbamate, 3g: Yield 65% (yellow oil); IR (neat): 3066, 2927, 1697, 1641, 1498, 1484, 1404, 1234 cm^{-1}; ^{1}H NMR (300 MHz, $CDCl_3$): δ 1.95-1.59 (m, 2H), 2.42-2.20 (m, 2H), 2.69-2.47 (m, 2H), 3.97-3.68 (m, 2H), 4.35-4.06 (m, 1H), 5.26-4.84 (m, 6H), 5.81-5.61 (m, 1H), 6.04-5.84 (m, 1H), 7.46-6.91 (m, 10H); ^{13}C NMR (75MHz, $CDCl_3$): δ 32.8, 34.5, 37.9, 46.4, 56.5, 67.0, 116.4, 117.1, 125.7, 127.6, 127.7, 127.9, 127.9, 128.2, 128.3, 128.3, 134.9, 135.2, 135.6, 136.8, 141.8, 156.5.

Synthesis of tetrahydropyridine 4

To a stirred solution of diene **3** (2 mmol) in dry CH_2Cl_2 (10 mL per mmol of substrate) was added a solution of Grubbs' 1st generation catalyst (5 mol%) in dry CH_2Cl_2. The resulting purple solution becomes brown after 5-10 min. The reaction mixture was stirred for 7 h at RT under N_2 atmosphere. The progress of the reaction was monitored by TLC. After

completion of the reaction, it was concentrated *in vacuo* and the residue was purified by column chromatography (hexane/EtOAc, 90:10) to afford the pure compound **4** (86-92% yield)

Benzyl 2-phenyl-3,6-dihydropyridine-1(2*H*)-carboxylate, 4a: Yield 92% (oil); IR (neat): 3035, 2951, 1697, 1656, 1498, 1415, 1342, 1222, 1103 cm^{-1}; ^1H NMR (300 MHz, $CDCl_3$): δ 2.58 (dd, J_1= 18 Hz, J_2 =5.1 Hz, 1H), 3.50-3.36 (m, 1H), 2.77-2.66 (m, 1H), 4.40-4.24 (m, 1H), 5.26-5.16 (m, 2H), 5.66 (br, 2H), 5.91 (br, 1H), 7.37-7.22 (m, 10H); ^{13}C NMR (75MHz, $CDCl_3$): δ 27.6, 40.4, 50.9, 67.2, 123.3, 124.1, 126.8, 127.1, 127.8, 127.9, 128.3, 128.4, 136.6, 140.5, 155.6.

Benzyl 2-(4-chlorophenyl)-3,6-dihydropyridine-1(2*H*)-carboxylate, 4b: Yield 88% (oil); IR (neat): 3049, 2850, 1697, 1654, 1495, 1415, 1327, 1244 cm^{-1}; ^1H NMR (300 MHz, $CDCl_3$): δ 2.52 (dd, J_1 = 17.4 Hz, J_2 = 3.6 Hz, 1H), 2.76-2.71 (m, 1H), 3.43-3.36 (m, 1H), 4.35-4.29 (m, 1H), 5.26-5.15 (m, 2H), 5.68-5.59 (m, 2H), 5.91 (br, 1H), 7.36-7.24 (m, 9H); ^{13}C NMR (75MHz, $CDCl_3$): δ 27.6, 40.4, 50.4, 67.3, 123.0, 124.1, 127.9, 128.0, 128.3, 128.4, 128.5, 132.8, 136.5, 139.0, 155.5.

Benzyl 2-(4-bromophenyl)-3,6-dihydropyridine-1(2*H*)-carboxylate, 4c: Yield 86% (oil); IR (neat): 3035, 2850, 1697, 1651, 1485, 1415, 1330, 1222 cm^{-1}; ^1H NMR (300 MHz, $CDCl_3$): δ 2.52 (dd, J_1 =18.6 Hz, J_2 = 5.7 Hz, 1 H), 2.79-2.64 (m, 1H), 3.45-3.35 (m, 1H), 4.38-4.23 (m, 1H), 5.26-5.15 (m, 2H), 5.67-5.49 (m, 2H), 5.89 (br, 1H), 7.18 (br, 2H), 7.42-7.30 (m, 7H); ^{13}C NMR (75MHz, $CDCl_3$): δ 27.5, 50.5, 40.4, 67.3, 121.0, 123.1, 124.2, 127.9, 128.0, 128.5, 128.7, 131.4, 136.5, 139.6, 155.6

Benzyl 2-(4-methylphenyl)-3,6-dihydropyridine-1(2*H*)-carboxylate, 4d: Yield 88% (oil); IR (neat): 3032, 2943, 1689, 1654, 1423, 1346, 1246, 1207, 1103 cm^{-1}; ^1H NMR (300 MHz, $CDCl_3$): δ 2.33 (s, 3H), 2.61-2.50 (m, 1 H), 2.82-2.65 (m, 1H), 3.53-3.40 (m, 1H), 4.42-4.23 (m, 1H), 5.30-5.17 (m, 2H), 5.75-5.52 (m, 2H), 5.91 (br, 1H), 7.37-7.10 (m, 9H); ^{13}C NMR (75MHz, $CDCl_3$): δ 20.9, 27.7, 40.3, 50.7, 67.1, 123.4, 124.0, 126.7, 127.8, 127.9, 128.4, 128.9, 136.7, 137.4, 155.6.

Benzyl 2-(4-methoxyphenyl)-3,6-dihydropyridine-1(2*H*)-carboxylate, 4e: Yield 92% (oil); IR (neat): 3033, 2935, 1696, 1652, 1490, 1409, 1332, 1240, 1108 cm^{-1}; ^1H NMR (300 MHz, $CDCl_3$): δ 2.53 (dd, J_1 = 18 Hz, J_2 = 5.7 Hz, 1H), 2.79-2.64 (m, 1H), 3.42-3.35 (m, 1H), 3.79 (s, 3H), 4.38-4.23 (m, 1H), 5.26-5.16 (m, 2H), 5.71-5.51 (m, 2H), 5.91 (br, 1H), 6.82 (d, J = 8.7 Hz, 2H), 7.27-7.22 (m, 2H), 7.38-7.30 (m, 5H); ^{13}C NMR (75MHz, $CDCl_3$): δ 27.7, 40.2, 50.4, 55.1, 67.1, 113.6, 123.4, 124.0, 127.8, 127.9, 128.0, 128.4, 132.5, 136.7, 155.5, 158.5.

Benzyl 2-(2-methoxyphenyl)-3,6-dihydropyridine-1(2*H*)-carboxylate, 4f: Yield 87% (oil); IR (neat): 3035, 2939, 1697, 1654, 1492, 1411, 1334, 1242, 1111 cm^{-1}; ^1H NMR (300 MHz, $CDCl_3$): δ 2.50-2.44 (m, 1H), 2.76-2.64 (m, 1H), 3.76 (m, 4H), 4.36-4.25 (m, 1H), 5.29-5.13 (m, 2H), 5.96-5.71 (m, 3H), 6.88 (t, J = 7.8 Hz, 2H), 7.38-7.15 (m, 7H); ^{13}C NMR (75MHz, $CDCl_3$): δ 28.3, 41.8, 46.9, 55.1, 66.8, 110.8, 119.8, 123.6, 123.8, 126.7, 127.4, 127.6, 128.1, 128.2, 130.2, 137.0, 156.3, 156.7.

Benzyl 2-(2-phenylethyl)-3,6-dihydropyridine-1(2*H*)-carboxylate, 4g: Yield 87% (oil); IR (neat): 3032, 2931, 1697, 1658, 1495, 1415, 1338, 1226 cm^{-1}; ^1H NMR (300 MHz, $CDCl_3$): δ 1.86-1.66 (m, 1 H), 2.07-1.91 (m, 2H), 2.73-2.39 (m, 3H), 3.67-3.51 (m, 1H), 4.67-4.30 (m, 2H), 5.23-5.14 (m, 2H), 5.73-5.56 (m, 2H), 7.37-7.16 (m, 10H); ^{13}C NMR (75MHz, $CDCl_3$): δ 28.8, 32.6, 33.3, 39.8, 48.3, 67.0, 122.8, 123.1, 125.7, 127.8, 127.9, 128.2, 128.2, 128.4, 136.7, 141.7, 155.5.

Synthesis of 4,5-dihydroxy piperidine 5

To a RB flask containing 20 mL of a mixture of *t*BuOH and water (1:1), $K_3Fe(CN)_6$ (3 equivalents) and K_2CO_3 (3 equivalents) was added and the mixture was stirred for 5-10 min. The flask was charged with $K_2OsO_2(OH)_4$ (0.004 equivalents) and $(DHQD)_2PHAL$ (0.02 equivalents). Subsequently, the olefin (1.5 mmol) was added and the reaction mixture was stirred for 24 h at 0°C. The progress of the reaction was monitored by TLC. After completion of the reaction, it was quenched with sodium sulfite and allowed to stir for another 30 min at RT. The reaction mixture was then washed with brine solution and extracted with EtOAc (2×20 mL). The separated organic layer was dried over anhydrous Na_2SO_4. The solvent was then evaporated under reduced pressure and the crude product was purified by column chromatography (petroleum ether/ethylacetate) (1:1) (80-90% yield). Enantiomeric excess was determined by HPLC (having an UV detector at 230 nm) with Chiralcel OD-H column using a 90:10 mixture of hexane and isopropanol with a flow rate 0.5 mL/min.

Benzyl 4,5-dihydroxy-2-phenylpiperidine-1-carboxylate, 5a: Yield 85% (colorless solid); m.p. 121-23°C; IR (KBr): 3414, 2900, 1658, 1493, 1346, 1238, 1130 cm^{-1}; ^1H NMR (300 MHz, $CDCl_3$): δ 2.30-2.19

(m, 1H), 2.48-2.34 (m, 1H), 2.98-2.82 (m, 1H), 3.71-3.62 (m, 1H), 3.81 (br, 1H), 4.40-4.25 (m, 1H), 5.25-5.17 (m, 2H), 5.65 (br, 1H), 7.37-7.24 (m, 10H); ^{13}C NMR (75MHz, $CDCl_3$): δ 29.6, 44.6, 53.3, 66.1, 67.6, 67.8, 126.0, 127.0, 127.7, 128.0, 128.4, 128.8, 136.4, 138.1, 156.9; MS: *m/z* (%) 350 (M^+ + Na, 100); t_r = 16.7 min and 25.7 min; $[\alpha]_D^{29}$: + 1.1° (c 1, $CHCl_3$).

Benzyl 2-(4-chlorophenyl)-4,5-dihydroxypiperidine-1-carboxylate, 5b: Yield 90% (colorless solid); m.p. 78-80°C; IR (KBr): 3336, 2908, 1685, 1492, 1346, 1242, 1130 cm^{-1}; ^{1}H NMR (300 MHz, $CDCl_3$): δ 2.39-2.21 (m, 2H), 2.59 (br, 2H), 2.90-2.82 (m, 1H), 3.73-3.61 (m, 1H), 3.87-3.80 (m, 1H), 4.38-4.30 (m, 1H), 5.25-5.16 (m, 2H), 5.61 (br, 1H), 7.17 (d, *J* = 8.4 Hz, 2H), 7.34-7.27 (m, 7H); ^{13}C NMR (75MHz, $CDCl_3$): δ 29.6, 44.6, 53.0, 66.0, 67.5, 67.7, 127.5, 127.8, 128.1, 128.5, 128.9, 133.0, 136.2, 136.7, 156.8; MS: *m/z* (%) 384 (M^+ + Na, 100); t_r = 18.3 min and 28.3 min; $[\alpha]_D^{29}$: + 1.2° (c 1, $CHCl_3$).

Benzyl 2-(4-bromophenyl)-4,5-dihydroxypiperidine-1-carboxylate, 5c: Yield 85% (colorless solid); m.p. 86-88°C; IR (KBr): 3379, 2924, 1678, 1495, 1319, 1246, 1127 cm^{-1}; ^{1}H NMR (300 MHz, $CDCl_3$): δ 2.34-2.19 (m, 2H), 2.84-2.79 (m, 1H), 3.35 (br, 2 OH), 3.70-3.56 (m, 1H), 3.81 (br, 1H), 4.32-4.27 (m, 1H), 5.23-5.13 (m, 2H), 5.57 (br, 1H), 7.10 (d, *J* = 8.4 Hz, 2H), 7.32-7.27 (m, 5H), 7.45 (d, *J* = 8.1 Hz, 2H); ^{13}C NMR (75MHz, $CDCl_3$): δ 29.4, 44.6, 53.0, 66.0, 67.4, 67.7, 121.0, 127.7, 127.8, 128.1, 128.5, 131.8, 136.1, 137.2, 156.8; MS: *m/z* (%) 427.8 (M^+ + Na, 98), 430.1 (M^++2+Na, 100); t_r = 19.7 min and 30.3 min; $[\alpha]_D^{29}$: + 1.7° (c 1, $CHCl_3$)

Benzyl 4,5-dihydroxy-2-(4-methylphenyl)piperidine-1-carboxylate, 5d: Yield 83% (colorless solid); m.p. 84-86°C; IR (KBr): 3402, 2908, 1685, 1593, 1435, 1350, 1246, 1126 cm^{-1}; ^{1}H NMR (300 MHz, $CDCl_3$): δ 2.28-2.21 (m, 1H), 2.33 (s, 3H), 2.39 (br, 1H), 2.89-2.84 (m, 1H), 3.71-3.62 (m, 1H), 3.79 (br, 1H), 4.32-4.27 (m, 1H), 5.23-5.14 (m, 2H), 5.61 (br, 1H), 7.16-7.10 (m, 4H), 7.32-7.27 (m, 5H); ^{13}C NMR (75MHz, $CDCl_3$): δ 20.8, 29.5, 44.6, 53.1, 66.1, 67.5, 125.9, 127.6, 127.9, 128.4, 129.4, 134.9, 136.4, 136.6, 156.9; MS: *m/z* (%) 364.1 (M^+ + Na, 100); t_r = 14.9 min and 22.9 min; $[\alpha]_D^{29}$: + 1.4° (c 1, $CHCl_3$).

Benzyl 4,5-dihydroxy-2-(4-methoxyphenyl)piperidine-1-carboxylate, 5e: Yield 81% (colorless solid); m.p. 54-55°C; IR (KBr): 3513, 2943, 1687, 1595, 1488, 1341, 1236, 1108 cm^{-1}; ^{1}H NMR (300 MHz, $CDCl_3$): δ 2.25-2.15 (m, 1H), 2.44-2.33 (m, 1H), 2.91-2.86 (m, 1H), 3.76-3.70 (m, 1H), 3.80 (s, 4H), 4.37-4.25 (m, 2H), 5.26-5.17 (m, 2H), 5.61 (br, 1H), 6.86 (d, *J* = 9.3 Hz, 2H), 7.16 (d, *J* = 8.1 Hz, 1H), 7.35-7.27 (m, 5H); ^{13}C NMR (75MHz, $CDCl_3$): δ 29.8, 44.5, 52.8, 55.2, 66.1, 67.6, 67.8, 114.1, 127.2, 127.7, 128.0, 128.5, 129.8, 136.4, 156.9, 158.5; MS: *m/z* (%) 380.0 (M^+ + Na, 100); t_r = 18.0 min and 28.1 min; $[\alpha]_D^{29}$: –1.5° (c 1, $CHCl_3$).

Benzyl 4,5-dihydroxy-2-(2-methoxyphenyl)piperidine-1-carboxylate, 5f: Yield 81% (colorless solid); m.p. 81-82°C; IR (KBr): 3514, 2943, 1689, 1597, 1485, 1342, 1238, 1111 cm^{-1}; ^{1}H NMR (300 MHz, $CDCl_3$): δ 2.36-2.19 (m, 2H), 2.73 (br, 2H), 3.40-3.31 (m, 1H), 3.76 (s, 4H), 3.93 (br, 1H), 4.49-4.37 (m, 1H), 5.15-5.06 (m, 2H), 5.73 (br, 1H), 6.88 (t, *J* = 7.8 Hz, 2H), 7.06 (d, *J* = 6.9 Hz, 1H), 7.39-7.11 (m, 6H); ^{13}C NMR (75MHz, $CDCl_3$): δ 29.9, 46.6, 50.7, 55.1, 66.4, 67.2, 67.4, 110.8, 120.1, 126.1, 127.4, 127.7, 128.2, 128.3, 128.7, 136.5, 156.7, 156.8; MS: *m/z* (%) 380.2 (M^+ + Na, 100); t_r = 20.0 min and 41.6 min; $[\alpha]_D^{29}$: + 1.6° (c 1, $CHCl_3$).

Benzyl 4,5-dihydroxy-2-phenethylpiperidine-1-carboxylate, 5g: Yield 80% (yellow oil); IR (KBr): 3414, 2935, 1678, 1495, 1342, 1242, 1130 cm^{-1}; ^{1}H NMR (300 MHz, $CDCl_3$): δ 1.81-1.61 (m, 2H), 2.10-1.87 (m, 2H), 2.69-2.47 (m, 2H), 3.03-2.98 (m, 1H), 3.99-3.78 (m, 2H), 4.39-4.22 (m, 1H), 4,48 (br, 1H), 5.25-5.04 (m, 2H), 7.34-7.14 (m, 10H); ^{13}C NMR (75MHz, $CDCl_3$): δ 31.1, 32.2, 32.7, 43.5, 51.0, 66.1, 67.5, 67.4, 125.9, 127.7, 128.0, 128.1, 128.3, 128.4, 136.4, 141.2, 156.6; MS: *m/z* (%) 378.2 (M^++Na, 20), 338.1 (M-OH, 22), 320.1 (M-2 OH-1, 9); t_r = 24.5 min and 28.6 min; $[\alpha]_D^{29}$: + 2.5° (c 1, $CHCl_3$).

Conclusion

In conclusion, a synthetic strategy for the synthesis of some new 2,4,5-trisubstituted piperidine analogues from corresponding homoallylic carbamate has been developed. During the process, 1,2,3,6-tetrahydropyridine derivatives were synthesized *via* the ring closing metathesis reaction which was further subjected to Sharpless dihydroxylation to produce corresponding 2-substituted 4,5-dihydroxy piperidines in high yield. This study also revealed that the standard Sharpless asymmetric dihydroxylation condition is not effective to induce chirality on this type of tetrahydropyridine derivatives.

Acknowledgement

Financial support from UGC, India (Grant No. 41-206/2012-SR) is gratefully acknowledged. AB thanks DST-JBNSTS for providing a visiting studentship to work in the Department of Organic Chemistry, IISc, Bangalore. The authors also thank Prof. K. R. Prasad (IISc, Bangalore) for extending his laboratory facilities during the initial stage of this work.

References

1 Balasubramanian M & Keay J G, *Comprehensive Heterocyclic Chemistr*y, Vol II, edited by Katritzky A R, Ress C W, Scriven E F V (Elsevier Science, Oxford), 5, **1997**, 245.

2 (a) De Garavilla L, Greco M N, Sukumar N, Chen Z W, Pineda A O, Mathews F S, Di Cera E, Giardino E C, Wells G I, Haertlein B J, Kauffman J A, Corcoran T & Maryanoff B E, *J Biol Chem*, 280, **2005**, 18001; (b) Mosnaim A D, Ranade V V, Wolf M E, Puente J & Antonieta V M, *Am J Ther*, 13, **2006**, 261.

3 Finke P E, Oates B, Mills S G, MacCoss M, Malkowitz L, Springer M S, Gould S L, Demartino J A, Carella A, Carver G, Holmes K, Danzeisen R, Hazuda D, Kessler J, Lineberger J, Miller M, Schleif W A & Emini E A, *Bioorg Med Chem Lett*, 11, **2001**, 2475.

4 Trabaco A A, Aerts N, Alvarez R M, Andres J I, Boeckx I, Fernandez J, Gomez A, Janssens F E, Leenaerts J E, Lucas A I D, Matesanz E, Steckler T & Pullan S, *Bioorg Med Chem Lett*, 17, **2007**, 3860.

5 (a) Kobayashi J & Ishibashi M, *Heterocycles*, 42, **1996**, 943; (b) Ninomiya I, Kiguchi T & Naito T, *Alkaloids*, 50, **1998**, 317.

6 (a) Murata K, Takano F, Fushiya S & Oshima Y, *J Nat Prod*, 61, **1998**, 729; (b) Kobayashi S, Ueno M, Suzuki R, Ishitani H, Kim H S & Wataya Y, *J Org Chem*, 64, **1999**, 6833; (c) Takaya Y, Tasaka H, Chiba T, Uwai K, Tanitsu M, Kim H S, Wataya Y, Miura M, Takeshita M & Oshima Y, *J Med Chem*, 42, **1999**, 3163.

7 Boswell R F, Welstead W J, Duncan R L, Johnson D N & Funderburk W H, *J Med Chem*, 21, **1978**, 136.

8 (a) Bailey P D, Millwood P A & Smith P D, *Chem Commun*, **1998**, 633; (b) Laschat S & Dickner T, *Synthesis*, 13, **2000**, 1781; (c) Weintraub P M, Sabol J S, Kane J M & Borcherding D R, *Tetrahedron*, 59, **2003**, 2953; (d) Buffat M G P, *Tetrahedron*, 60, **2004**, 1701.

9 (a) Wagner I & Musso H, *Angew Chem Int Ed Engl*, 22, **1983**, 816; (b) Plunkett A O, *Nat Prod Rep*, 11, **1994**, 581; (c) Hashimoto K, Higashibayashi S & Shirahama H, *Heterocycles*, 46, **1997**, 581.

10 Ishibashi M, Ohizumi Y, Sasaki T, Nakamura H, Hirata Y & Kobayashi J, *J Org Chem*, 52, **1987**, 450.

11 Freyer A J, Patil A D, Killmer L, Troupe N, Mentzer M, Carte B, Faucette L & Johnson R K, *J Nat Prod*, 60, **1997**, 986.

12 Kobayashi J, Naitoh K, Doi Y, Deki K & Ishibashi M, *J Org Chem*, 60, **1995**, 6941.

13 (a) Clinch K, Vasella A & Schauer R, *Tetrahedron Lett*, 28, **1987**, 6425; (b) Glänzer B I, Györgydeák Z, Bernet B & Vasella A, *Helv Chim Acta*, 74, **1991**, 343.

14 (a) Kiguchi T, Yuumoto Y, Ninomiya I, Naito T, Deki K, Ishibashi M & Kobayashi J, *Tetrahedron Lett*, 33, **1992**, 7389; (b) Ishibashi M, Deki K & Kobayashi J, *J Nat Prod*, 58, **1995**, 804.

15 (a) Martín R, Alcón M, Pericás M A & Riera A, *J Org Chem*, 67, **2002**, 6896; (b) Han H, *Tetrahedron Lett*, 44, **2003**, 1567; (c) Takahata H, Banba Y, Sasatani M, Nemoto H, Kato A & Adachi I, *Tetrahedron*, 60, **2004**, 8199; (d) Pearson M S M, Mathé-Allainmat M, Fargeas V & Lebreton J, *Eur J Org Chem*, **2005**, 2159; (e) Pyun S-J, Lee K-Y, Oh C-Y, Joo J-E, Cheon S-H & Ham W-H, *Tetrahedron*, 61, **2005**, 1413; (f) Reddy M S, Narender M & Rao K R, *Tetrahedron*, 63, **2007**, 331; (g) Epple R, Urbina H D, Russo R, Liu H, Mason D, Bursulaya B, Tumanut C, Li J & Harris J L, *Bioorg Med Chem Lett*, 17, **2007**, 1254; (h) Dragutan I, Dragutan V, Mitan C, Vosloo H C M, Delaude L & Demonceau A, *Beilstein J Org Chem*, 7, **2011**, 699; (i) Dragutan I, Dragutana V & Demonceau A, *RSC Adv*, 2, **2012**, 719.

16 Armstron S K, *J Chem Soc*, *Perkin Trans 1*, **1998**, 371; (b) Fu G C & Grubbs R H, *J Am Chem Soc*, 114, **1992**, 7324.

17 (a) Cha J K, Christ W J & Kishi Y, *Tetrahedron Lett*, 24, **1983**, 3943; (b) Cha J K & Kim N-S, *Chem Rev*, 95, **1995**, 1761.

18 (a) Nandanan E, Jaychandran B, Phukan P, Pais G C G & Sudalai A, *Indian J Chem*, 37B, **1998**, 1221; (b) Nandanan E, Phukan P & Sudalai A, *Indian J Chem*, 38B, **1999**, 283; (c) Phukan P & Sudalai A, *J Chem Soc*, *Perkin Trans I*, **1999**, 3015; (d) Nandanan E, Phukan P & Sudalai A, *Indian J Chem*, 38B, **1999**, 893; (e) Phukan P, Jagtap J H & Sudalai A, *Indian J Chem*, 39B, **2000**, 950; (f) Borah A J, Goswami P, Barua N C & Phukan P, *Tetrahedron Lett* 53, **2012**, 7128; (g) Borah A J & Phukan P, *J Chem Sci*, 125, **2013**, 1503.

19 Phukan P, *J Org Chem*, 69, **2004**, 4005.

20 Kolb H C, VanNieuwenhze M S & Sharpless K B, *Chem Rev*, 94, **1994**, 2483.

Indian Journal of Chemistry
Vol. 53B, June 2014, pp 750-753

Notes

Aziridination of olefins with bromamine-T in presence of iodine as catalyst

Chinta Mani Sharma, Bishwapran Kashyap & Prodeep Phukan*

Department of Chemistry, Gauhati University, Guwahati 781 014, India

E-mail: pphukan@yahoo.com

Received 1 May 2013; accepted (revised) 4 April 2014

A strategy for achieving synthesis of aziridine employing iodine catalysed aziridination of alkenes with bromamine-T as nitrene source has been described. Ethyl acetate has been found to be the most suitable solvent and the strategy has been extended to various kinds of olefins to produce the corresponding aziridines in high yield.

Keywords: Aziridine, bromamine-T, iodine, catalyst, olefin

Aziridines, the smallest group of the nitrogen-containing heterocycles, are an important class of compounds having synthetic and biological significance[1]. They exhibit highly regio-and stereoselective ring opening reactions which provide a convenient entry to the stereoselective preparation of functionalized amino compounds, heterocycles, and alkaloids[1]. Many bioactive natural products contain this three-membered ring heterocycle as an important subunit. A general strategy for achieving the synthesis of aziridine is the metal-catalyzed aziridination of alkenes with proper nitrene sources[2]. Iminoiodinane derivatives such as [*N*-(*p*-tolylsulfonyl) imino]phenyliodinane (PhI=NTs) (Ref 3) and its variants have been extensively used as nitrene source in presence of several transition metal catalysts[4]. However, due to some limitations associated with the use of PhI=NTs, alternative nitrogen sources such as organic azides (RN_3) (Ref 5) chloramine-T [TsN(Cl)Na] (Ref 6), bromamine-T (TsN(Br)Na) (Ref 7) and others[8] have been employed. Among these nitrogen sources, bromamine-T has been proven to be the most efficient one[7]. However, many of the methods for aziridination reaction using bromamine-T (BAT), have limitations such as use of more amount of the substrate, long reaction time, high reaction temperature, *etc*. As a part of the work on iodine catalysed reactions[9], herein is reported a fast method of aziridination reaction using BAT in presence of iodine as catalyst (**Scheme I**).

Results and Discussion

Initially, the study was carried out by using styrene as a model substrate. The reaction was carried out by adding BAT (1 equiv.) to a mixture of styrene (2 equiv.) and iodine (0.1 equiv.) in dichloromethane at RT. The whole process was carried out at RT under nitrogen atmosphere and the progress of the reaction was monitored by TLC. It was observed that the reaction takes 4 hr for completion to produce corresponding aziridine in 61% isolated yield. To evaluate the optimum reaction condition, a series of reactions were performed with different solvents and amount of bromoamine-T to get the best possible result (**Table I**). When acetonitrile was used as solvent in the reaction, the yield of the product was improved to 69% after 3 hr at RT. Further investigation on the reaction using ethyl acetate as a solvent gave the better result of 78% isolated yield of the product after 1 hr of reaction. However, increase of BAT amount could not improve the yield. Finally, use of styrene and BAT in the molar ratio 2:1 was found to be optimum for the best result.

After optimizing the reaction conditions, the process was extended to a variety of olefins. Results are summarized in **Table II**. Various kinds of olefins such as indene, 1,2-dihydronaphthalene, cyclohexene, 1-hexene, 1-octene, and *trans*-2-butene-1-ol produced the corresponding aziridine in high yields (**Table II**).

Experimental Section

General procedure for synthesis of aziridine

To a solution of olefin (2 mmol) and BAT (1 mmol) in dry ethyl acetate (5 mL), iodine (0.1 mmol) was added and the reaction stirred at RT under nitrogen

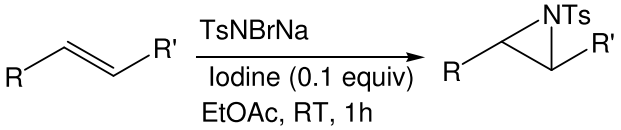

Scheme I — Synthesis of aziridines using TsNBrNa

Table I — Aziridination of styrene under different reaction conditions

Sl. No.	Solvent	TsNBrNa (mmol)	Time (hr)	Yield[b] (%)
1	DCM	1	4	61
2	CH_3CN	1	2	69
3	EtOAc	1	1	78
4	EtOAc	2	1	70

[a]Reaction conditions: styrene (2 mmol), solvent (2 mL), iodine (0.1 mmol), RT. [b]Isolated yield.

Table II — Aziridination of various alkenes with TsNBrNa[a]

Sl. No	Substrate (a)	Product (b)	Yield[b] (%)
1	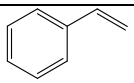	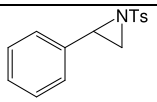	78
2	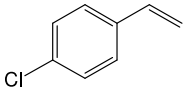	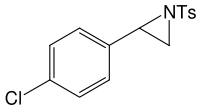	73
3	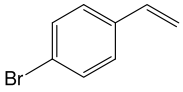	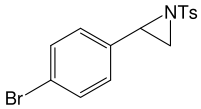	71
4	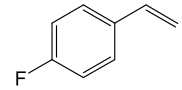	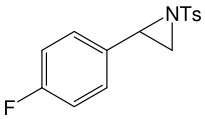	70
5	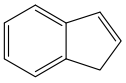	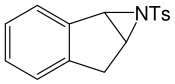	68
6	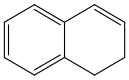	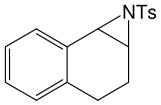	69
7		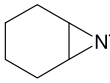	70
8	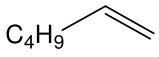	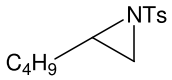	59
9	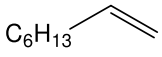	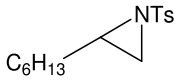	57
10	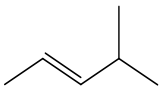	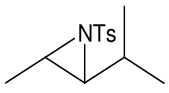	64

[a]Reaction conditions: olefin 2 mmol, TsNBrNa (1 mmol), EtOAc (10 mL), RT, 1hr. [b]Isolated yield based on BAT

atmosphere for appropriate time (TLC). After completion of the reaction, an aqueous solution of 10% sodium thiosulfate (5 mL) was added and the organic layer separated. The aqueous layer was extracted with ethyl acetate, and the combined organic layer was washed with brine and dried over anhydrous sodium sulfate and concentrated. The crude product was purified by flash chromatography over silica gel (230-400 mesh) with petroleum ether/ethyl acetate as eluent.

2-Phenyl-1-(toluene-4-sulfonyl)-aziridine, 1b (Ref 3c, 6f). m.p. 88-89°C (Lit.[3c] 88-89°C); ^{1}H NMR ($CDCl_3$, 400 MHz): δ 7.81 (d, *J* = 8.4 Hz, 2H), 7.27-7.14 (m, 7H), 3.71 (dd, *J* = 4.6 Hz, 7.1 Hz, 1H), 2.92 (d, *J* =7.2, 1H), 2.36 (s, 3H) 2.32 (d, *J* = 4.4 Hz, 1H); ^{13}C NMR ($CDCl_3$, 100 MHz): δ 152.9, 143.2, 143.1, 137.9, 136.7, 136.5, 136.1, 134.7, 49.2, 44.1, 29.8.

2-(4-Chloro-phenyl)-1-(toluene-4-sulfonyl)-aziridine, 2b (Ref 3c, 6f). m.p. 113-14 °C (Lit.[3c] 115-16°C); ^{1}H NMR ($CDCl_3$, 400 MHz): δ 7.86 (d, *J* = 8.4 Hz, 2H), 7.35-7.14 (m, 6H), 3.73 (dd, *J* = 4.4 Hz, 4.7 Hz, 1H), 2.98 (d, *J* =9.2 Hz, 1H), 2.44 (s, 3H) 2.34 (d, *J* = 4.4 Hz, 1H); ^{13}C NMR ($CDCl_3$, 100 MHz): δ 144.8, 134.7, 133.5, 129.8, 128.7, 127.9, 127.9, 40.2, 36.0, 30.9, 21.7.

2-(4-Bromo-phenyl)-1-(toluene-4-sulfonyl)-aziridine, 3b (Ref 6h). m.p. 126-27°C (Lit.[6h] 127-29°C); ^{1}H NMR ($CDCl_3$, 300 MHz): δ 7.86 (d, *J* = 8.1 Hz, 2H), 7.42 (d, *J* = 8.4 Hz, 2H), 7.34 (d, *J* = 8.4 Hz, 2H), 7.09 (d, *J* = 8.1 Hz, 2H), 3.74-3.70 (m, 1H), 2.98 (d, *J* = 7.2 Hz, 1 H), 2.44 (s, 3H), 2.347 (d, *J* = 4.2 Hz, 1H); ^{13}C NMR ($CDCl_3$, 75 MHz): δ 144.8, 134.6, 134.1, 131.6, 129.7, 128.1, 127.8, 122.2, 40.2, 35.9, 21.6.

2-(4-Fluoro-phenyl)-1-(toluene-4-sulfonyl)-aziridine, 4b (Ref 6h). m.p. 134-35°C (Lit.[6h] 136-38°C); ^{1}H NMR ($CDCl_3$, 300 MHz): δ 7.83 (d, *J* = 8.4 Hz, 2H), 7.28 (d, *J* = 7.8 Hz, 2H), 7.17-7.13 (m, 2H), 6.94-6.89(m, 2H), 3.7295 (dd, *J* = 4.5 Hz, 7.1 Hz, 1H), 2.92 (d, *J* = 7.2 Hz, 1H), 2.354 (s, 3H), 2.32 (d, *J* = 4.5 Hz, 1H). ^{13}C NMR ($CDCl_3$, 75 MHz): δ 144.6, 134.3, 129.5, 128.1, 128.0, 127.6, 115.3, 115.0, 40.0, 35.7, 21.2.

1-[(4-Methylphenyl)sulfonyl]-1, 1a,6, 6a-tetrahydroindeno[1,2-*b*]azirene, 5b (Ref 6h). m.p. 164-65°C (Lit.[6h] 164-66°C); ^{1}H NMR ($CDCl_3$, 400 MHz): δ 7.82 (d, *J* = 8.1 Hz, 2H), 7.39 (d, *J* = 7.4 Hz, 1H), 7.31 (d, *J* = 8.1 Hz, 2H), 7.24-7.23 (m, 3H), 4.29 (d, *J* = 5.3 Hz, 1H), 3.15-3.12 (m, 2H), 2.43 (s, 3H); ^{13}C NMR ($CDCl_3$, 100 MHz): δ 144.4, 143.5, 138.2, 135.5, 129.7, 128.7, 127.7, 126.7, 125.6, 125.1, 50.1, 44.9, 34.6, 21.6.

1-[(4-Methylphenyl)sulfonyl]-1a, 2,3,7b-tetrahydro-1*H*-naphtho[1,2-*b*]azirene, 6b (Ref 3c). m.p. 122-23°C (Lit.[3c] 123-24°C); ^{1}H NMR ($CDCl_3$, 400 MHz): δ 7.81 (d, *J* = 8.4 Hz, 2H), 7.34-7.1 (m, 6H), 7.12-7.04 (m, 2H), 7.04 (d, *J* = 7.4 Hz, 1H), 3.81 (d, *J* =

7.1 Hz, 1H), 3.60-3.50 (m, 1H), 2.85-2.68 (m, 1H), 2.58-2.48 (m, 1H), 2.41 (s, 3H), 2.30-2.18 (m, 1H), 1.72-1.60 (m, 1H); ^{13}C NMR ($CDCl_3$, 100 MHz): δ 144.2, 136.6, 135.6, 130.0, 129.7, 129.4, 128.6, 128.4, 127.6, 126.3, 42.1, 41.7, 24.7, 21.6, 20.0.

7-[(4-Methylphenyl)sulfonyl]-7-azabicyclo[4.1.0]heptane, 7b (Ref 6h). m.p. 53-54°C (Lit.[3c] 55.3-55.9°C); ^{1}H NMR ($CDCl_3$, 400 MHz): δ 7.78 (d, *J* = 8.1 Hz, 2H,), 7.29 (d, *J* =7.9 Hz, 2H), 2.98-2.88 (m, 2H), 2.41 (s, 3H), 1.82-1.65 (m, 4H), 1.40-1.10 (m, 4H); ^{13}C NMR ($CDCl_3$, 100 MHz): δ 143.9, 135.8, 129.5, 127.5, 39.7, 21.5.

2-Butyl-1-[(4-methylphenyl)sulfonyl]aziridine, 8b (Ref 6b). Oil; ^{1}H NMR ($CDCl_3$, 400 MHz): δ 7.81 (d, *J* = 8.4 Hz, 2H,), 7.32 (d, *J* = 8.1 Hz, 2H), 2.75-2.65 (m, 1H), 2.61 (d, *J* = 6.9 Hz, 1H,) 2.43 (s, 3H), 2.04 (d, *J* = 4.6 Hz, 1H,) 1.58-1.45 (m, 1H), 1.38-1.14 (m, 5H), 0.79 (t, *J* = 6.9 Hz, 3H); ^{13}C NMR ($CDCl_3$, 100 MHz): δ 144.4, 135.2, 129.6, 128.0, 40.4, 33.8, 31.0, 28.8, 22.1, 21.6, 13.8.

2-Hexyl-1-[(4-methylphenyl)sulfonyl] aziridine, **9b** (Ref 6b). Oil; ^{1}H NMR ($CDCl_3$, 400 MHz): δ 7.82 (d, *J* = 8.4 Hz, 2H), 7.32 (d, *J* = 8.1 Hz, 2H), 2.75-2.65 (m, 1H), 2.62 (d, *J* = 7.1 Hz, 1H), 2.43 (s, 3H), 2.04 (d, *J* = 4.6 Hz, 1H,) 1.58-1.44 (m, 1H), 1.37-1.15 (m, 9H), 0.84 (t, *J* = 7.1 Hz, 3H); ^{13}C NMR ($CDCl_3$, 100 MHz): δ 144.4, 135.2, 129.6, 128.0, 40.5, 33.8, 31.6, 31.3, 28.7, 26.7, 22.4, 21.6, 14.0.

2-Isopropyl-3-methyl-1-tosylaziridine, 10b (Ref 1f). m.p. 67-68°C (Lit.[1f] 70°C); ^{1}H NMR ($CDCl_3$, 400 MHz): δ 7.77 (d, *J* = 8.24 Hz, 2H), 7.24 (d, *J* = 7.8 Hz, 2H), 2.62-2.61 (m, 1H), 2.49-2.47 (m, 1H), 2.36 (s,3H), 1.59 (d, *J* = 4.12 Hz, 3H) 1.39 (m, 1H), 0.81 (d, *J* = 6.88 Hz, 3H), 0.66 (d, *J* = 6.88 Hz, 3H); ^{13}C NMR ($CDCl_3$, 100 MHz): δ 143.7, 137.9, 129.3, 127.4, 54.9, 45.3, 30.0, 21.4, 19.7, 19.3, 14.2.

Conclusion

In conclusion, iodine has been found to catalyse aziridination of olefin with bromamine-T as the nitrene source. The procedure is fast, easy to perform at RT and applicable to various olefins to give corresponding aziridines in high yield.

Acknowledgement

Financial support from UGC, India (Grant No. 41-206/2012-SR) is gratefully acknowledged. BK thanks CSIR for research fellowship.

References

1 *Aziridines and Epoxides in Organic Synthesis*, edited by A K Yudin (Wiley-VCH, Weinheim), **2006**; (b) Pearson W H, Lian B W & Bergmeier S C, *Comprehensive Heterocyclic Chemistry II*, Vol IA, edited by A Padwa (Pergamon Press, New York), **1996**, pp 1-6; (c) Tanner D, *Angew Chem Int Ed*, 33, **1994**, 599; (d) Hu X E, *Tetrahedron*, 60, **2004**, 2701; (e) Davis F A & Coull S M, *Synthesis*, **2000**, 1347;(f) Sureshkumar D, Koutha S M & Chandrasekaran S, *J Am Chem Soc*, 127, **2005**, 12760.

2 Fantauzzi S, Caselli A & Gallo E, *Dalton Trans*, **2009**, 5434; (b) Davies H M L & Manning J R, *Nature*, 451, **2008**, 417; (c) Diaz-Requejo M M & Perez P J, *Chem Rev*, 108, **2008**, 3379; (d) Watson I D G, Yu L & Yudin A K, *Acc Chem Res*, 39, **2006**, 194; (e) Müller P & Fruit C, *Chem Rev*, 103, **2003**, 2905.

3 Yamada Y, Yamamoto T & Okawara M, *Chem Lett*, **1975**, 361; (b) Evans D A, Faul M M & Bilodeau M T, *J Org Chem*, 56, **1991**, 6744; (c) Evans D A, Faul M M & Bilodeau M T, *J Am Chem Soc*, 116, **1994**, 2742.

4 Mahy J P, Battioni P & Mansuy D, *J Am Chem Soc*, 108, **1986**, 1079; (b) Conser Z, Li K R & Jacobsen E N, *J Am Chem Soc*, 115, **1993**, 5326; (c) Evans D A, Faul M M, Bilodeau M T, Anderson B A & Barnes D M, *J Am Chem Soc*, 115, **1993**, 5328; (d) Li Z, Quan R W & Jacobsen E N, *J Am Chem Soc*, 117, **1995**, 5889; (e) Müller P, Baud C, Jacquier Y, Moran M & Naegeli I, *J Phys Org Chem*, 9, **1996**, 341; (f) Dauban P & Dodd R H, *J Org Chem*, 64, **1999**, 5304; (g) Au S-M, Huang J-S, Yu W-Y, Fung W-H & Che C-M, *J Am Chem Soc*, 121, **1999**, 9120; (h) Liang J-L, Yuan S-X, Chan P W H & Che C-M, *Org Lett*, 4, **2002**, 4507; (i) Cui Y & He C, *J Am Chem Soc*, 125, **2003**, 16202; (j) Man W-L, Lam W W Y, Yiu S-M, Lau T-C & Peng S-M, *J Am Chem Soc*, 126, **2004**, 15336; (k) Li Z, Ding X & He C, *J Org Chem*, 71, **2006**, 5876; (l) Mayer A C, Salit A-F & Bolm C, *Chem Commun*, **2008**, 5975.

5 Gao G-Y, Jones J E, Vyas R, Harden J D & Zhang X P, *J Org Chem*, 71, **2006**, 6655; (b) Subbarayan V, Ruppel J V, Zhu S, Perman J A & Zhang X P, *Chem Commun*, **2009**, 4266; (c) Omura K, Uchida T, Irie R & Katsuki T, *Chem Commun*, **2004**, 2060.

6 Ando T, Minakata S, Ryu I & Komatsu M, *Tetrahedron Lett*, 39, **1998**, 309; (b) Jeong J U, Tao B, Sagasser I, Henniges H & Sharpless K B, *J Am Chem Soc*, 120, **1998**, 6844; (c) Albone D P, Aujla P S, Taylor P C, Challenger S & Derrick A M, *J Org Chem*, 63, **1998**, 9569; (d) Ali S I, Nikalje M D & Sudalai A, *Org Lett*, 1, **1999**, 705; (e) Thakur V V & Sudalai A, *Tetrahedron Lett*, 44, **2003**, 989; (f) Jain S L & Sain B, *Green Chem*, 8, **2006**, 943; (g) Cano I, Nicasio M C & Pérez P J, *Dalton Trans*, **2009**, 730; (h) Karabal P U, Chouthaiwale P V, Shaikh T M, Suryavanshi G & Sudalai A, *Tetrahedron Lett*, 51, **2010**, 6460.

7 Chanda B M, Vyas R & Bedekar A V, *Tetrahedron Lett*, 39, **1998**, 4715; (b) Chanda B M, Vyas R & Bedekar A V, *J Org Chem*, 66, **2001**, 30; (c) Antunes A M M, Marto S J M, Branco P S, Prabhakar S & Lobo A M, *Chem Commun*, **2001**, 405; (d) Vyas R, Gao G-Y, Harden J D & Zhang X P, *Org Lett*, 6, **2004**, 1907; (e) Gao G-Y, Harden J D & Zhang X P, *Org Lett*, 7, **2005**, 3191; (f) Borah A J, Phukan P, *Tetrahedron Lett*, 55, **2014**, 713.

8 Xie W, Fang J, Li J & Wang P G, *Tetrahedron*, 55, **1999**, 12929; (b) Tranchant M-J, Dalla V, Jabin I & Decroix B, *Tetrahedron*, 58, **2002**, 8425; (c) Catino A J, Nichols J M, Forslund R E & Doyle M P, *Org Lett*, 7, **2005**, 2787; (d) Han J, Li Y, Zhi S, Pan Y, Timonsc C & Li G, *Tetrahedron Lett*, 47, **2006**, 7225; (e) Zhang X-J, Yan M & Huang D, *Org*

Biomol Chem, 7, **2009**, 187; (f) Saikia I, Kashyap B & Phukan P, *Chem Commun*, 47, **2011**, 2967.

9 Phukan P, *J Org Chem*, 69, **2004**, 4005; (b) Phukan P, *Tetrahedron Lett*, 45, **2004**, 4785; (c) Phukan P, *Synth Commun*, 34, **2004**, 1065; (d) Phukan P, Kataki D & Chakraborty P, *Tetrahedron Lett*, 47, **2006**, 5523; (e) Kataki D & Phukan P, *Indian J Chem*, 45B, **2006**, 1759; (f) Kataki D, Chakraborty P, Sarmah P & Phukan P, *Indian J Chem Technol*, 13, **2006**, 519; (g) Kataki D & Phukan P, *Tetrahedron Lett*, 50, **2009**, 1958; (h) Deuri S & Phukan P, *Struct Chem*, 22, **2011**, 1075; (i) Sarma C M, Kashyap B & Phukan P, *Indian J Chem*, 51B, **2012**, 323; (j) Saikia I & Phukan P, *C R Chimie*, 15, **2012**, 688; (k) Deuri S, Kataki D & Phukan P, *Indian J Chem*, 51B, **2012**, 1163; (l) Deuri S & Phukan P, *J Phys Org Chem*, 25, **2012**, 1228; (m) Borah A J & Phukan P, *J Chem Sci*, 125, **2013**, 1503; (n) Kataki D, Bhattacharyya P, Deka M, Jha D K & Phukan P, *Indian J Chem*, 52B, **2013**, 1505.

Indian Journal of Chemistry
Vol. 53B, November 2014, pp 1425-1429

Synthesis of bromohydrins using NBS in presence of iodine as catalyst

Raj Sekhar Lodh, Arun Jyoti Borah & Prodeep Phukan*

Department of Chemistry, Gauhati University, Guwahati 781 014, India

E-mail: pphukan@ yahoo.com

Received 3 December 2013; accepted (revised) 4 September 2014

Iodine has been found to catalyze bromohydrin formation reaction using NBS as a brominating agent. The procedure is efficient and produces high yield of the product at 0°C within a short time. Cinnamic esters can easily be transformed to corresponding bromohydrins in high yield.

Keywords: Bromohydrin, NBS, catalyst, iodine

Vicinal halohydrins have been drawing interest to organic chemists because of their wide applications in the synthesis of pharmaceuticals, active intermediates[1], dyes, flame retardants[2], additives and plasticizers, agrochemicals, *etc*[3]. Various reagents have been developed by researchers for the halohydrin formation reaction over the years. A common method for the synthesis of *vic*-halohydrins is the regioselective ring opening of epoxides with hydrogen halides[4]. Several research groups have reported different methods for the synthesis of *vic*-halohydrins from oxiranes using a variety of reagents such as elemental halogen[5], metal halides[6], chlorosilanes[7], haloboranes[8], *etc*. Sharghi and his co-workers reported the ring opening halogenations of epoxides by elemental halogens (I_2 or Br_2) in the presence of thiourea or isonocotinic hydrazide under mild reaction condition to yield halohydrin[9]. In the presence of magnesium nitrate catalyst, Suh *et al*. reported a highly regioselective conversion of epoxide to bromohydrins using tetrabutyl ammonium bromide[10]. Various oxidative halogenation methods were also reported where residual HX is regenerated by various oxidants such as metals, persulfates, and hypervalent iodine oxidants[11]. In the oxidative halogenation methods[11], the halogen source requires a metal salt, an oxidizing agent and a catalyst to perform the transformations. In addition, different metal complexes in presence of haloperoxidases[12] have been introduced in the biosynthesis of many halogenated marine natural products like terpenes, indoles, phenols, *etc*. Biotransformations of alkenes by haloperoxidases for regiospecific bromohydrin formation from cinnamyl substrates in neutral aprotic media have also been reported[13].

Generally bromohydrin synthesis using *N*-bromosuccinimide (NBS) require a catalyst[14]. *N*-Bromosuccinimide generally acts as brominating agent for the synthesis of bromohydrins in moist dimethylsulfoxide as reaction medium[15]. Hydrobromination of olefins using NBS in ionic liquid has also been reported[16]. Use of molecular halogens in place of *N*-halosuccinimide has several disadvantages such as hazardous nature of molecular halogens, low yield and longer reaction time[17] and inability to transform electron deficient alkenes[18]. *N*,*N*-Dibromo-*p*-toluene-sulfonamide has also been found to be an effective reagent for bromohydrin formation[19]. However, due to commercial availability, NBS has been most widely utilized for the synthesis of bromohydrins. In continuation of the ongoing work on iodine catalyzed reactions[20], herein is reported a new methodology for the synthesis of bromohydrin using NBS in presence of iodine as catalyst (**Scheme I**). The emphasis is on the extension of the procedure for relatively inactive substrates such as cinnamic esters.

Since we are more interested in studying the process for substrates like cinnamate, initial experiments were performed using ethyl cinnamate as the model substrate (**Table I**). In a typical reaction, ethylcinnamate (1 mmol) was added to a mixture of NBS (1.2 mmol) and iodine (10 mol %) in a mixture (4:1 ratio) of acetonitrile and water (5 mL) at RT. Further improvement of yield was observed, when the reaction was performed at 0°C. The reaction without catalyst produced poor yield under these particular reaction conditions.

After optimizing the reaction conditions we extended the procedure using different olefins. The results are summarized in **Table II**. From **Table II** it

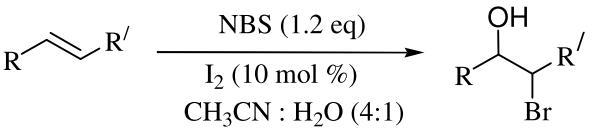

R = Ar
R/= Ar, COOEt, COOMe, H, *etc.*

Scheme I — Bromohydrin synthesis using NBS in presence iodine as catalyst

Table I — Synthesis of bromohydrin from ethylcinnamate under various conditions[a]

Entry	Catalyst (mmol)	NBS (mmol)	Temp.	Time (h)	Yield[b] (%)	% of *anti* product
1	0.1	1.2	RT	2	68	-
2	0.1	1.2	0°C	1	79	>99
3	0.1	1.1	0°C	1	70	>99
4	_	1.2	RT	10	55	-

[a]Reaction condition: ethylcinnamate (1 mmol); MeCN-H_2O (4:1, 5 mL); [b]Isolated yield.

can be concluded that the bromohydrins could be synthesized from different olefins such as ethyl cinnamate, methyl cinnamate, *trans*-stibene, styrene, indene and 1,2-dihydro naphthalene in excellent yield. In all cases, the rate of reaction is fast. However, in case of chalcone (Entry 7), the reaction produced lower yield. In all cases, the reaction displays high regioselectivity.

Mechanistically, the reaction may proceed through the iodine catalyzed formation of bromonium ion intermediate. Iodine is known to behave as a soft acid (electron acceptor) due to the presence of vacant d-orbital. Similar to other Lewis acids, iodine activates NBS by coordinating with one of the carbonyl oxygen atom of NBS. This results in weakening of N-Br bond, which finally facilitate the transfer of Br^+ species to alkenes (**Scheme II**). This is followed by the nucleophilic attack by water in an *anti*-selective fashion. Final step of the reaction is the deprotonation of the resulting complex to form the bromohydrin.

In conclusion, a general catalytic method has been developed for the bromohydrin reaction of various olefinic substrates in the presence of iodine using NBS as brominating agent with high yield. The important features of this methodology are mild reaction condition, cleaner reaction profile, operational simplicity and cheap, non-toxic and readily available catalyst. This procedure is very effective for relatively inactive cinnamic esters.

Experimental Section

All the chemicals used were that of analytical grade. IR spectra were recorded by using Perkin-Elmer Spectrum RX I FT-IR spectrometer. ^1H and ^{13}C NMR spectra were measured in $CDCl_3$ at 300 and 75 MHz respectively, using Bruker Avance 300 MHz spectrometer using TMS as internal standard.

Synthetic procedures

To a solution of olefin (1 mmol) and NBS (1.2 mmol), in acetonitrile-water (4:1) (5 mL) in a 25 mL round-bottom flask was added iodine (0.1 mmol) at 0°C. The mixture was stirred at 0°C using a magnetic stirrer for the appropriate time as found by monitoring the progress of the reaction by TLC from time to time till completion. After completion of the reaction, the reaction mixture was washed with 10% aqueous $Na_2S_2O_3$ (10 mL). Ethyl acetate was added to the reaction mixture and the organic layer was separated. The aqueous layer was extracted with ethyl acetate (2×20mL) and combined organic extract was washed with brine solution. The organic layer thus obtained was dried over anhydrous Na_2SO_4 and the solvent evaporated to give crude product. The crude product was purified by column chromatography over silica gel (230-400 mesh) with petroleum ether-EtOAC as eluent which gave the pure bromohydrin.

Spectroscopic Data

Ethyl 2-bromo-3-hydroxy-3-phenyl propanoate, **1b**: White solid m.p. 76-78°C [Lit.[9f] 76-77°C]; IR (KBr): 3450, 2979, 2930, 1719, 1599, 1430, 1285, 1020 cm^{-1}; ^1H NMR ($CDCl_3$, 300 MHz): δ 1.28 (t, J = 6 Hz, 3H), 4.22 – 4.29 (q, J = 2 H_Z, 2H), 4.36 – 4.38 (d, J = 9.6Hz, 1H), 5.03 – 5.08 (m, 1H), 7.31 (m, 5H); ^{13}C NMR ($CDCl_3$, 75 MHz): δ 13.7, 47.6, 62.2, 74.9, 126.8, 128.5, 138.9, 169.3.

Table II — Synthesis of bromohydrin from various olefins[a]

Entry	Olefin/ Styrene (**a**)	Product (**b**)	Time (h)	Yield[b] (%)
1	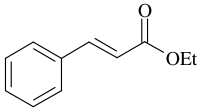	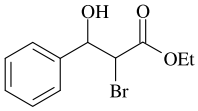	1	79
2	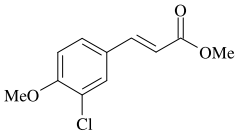	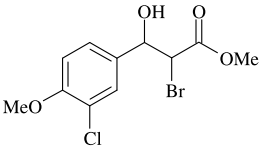	1.5	72
3	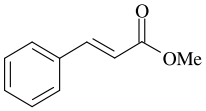	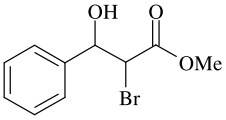	3	72
4	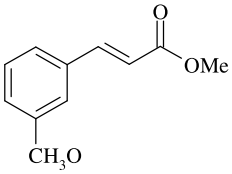	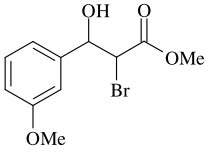	2.5	67
5	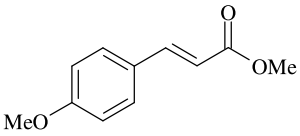	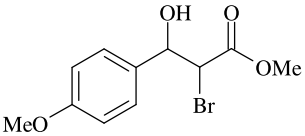	1.3	83
6	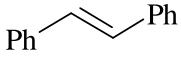	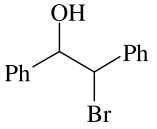	1.5	75
7	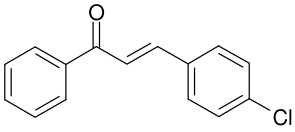	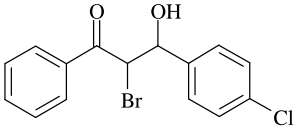	2	67
8	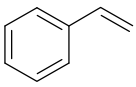	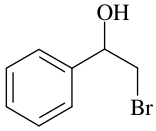	2	78
9	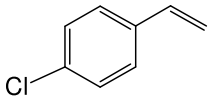	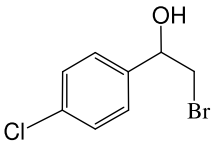	1.5	76
10	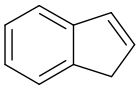	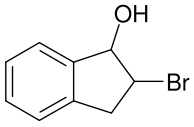	1	85
11	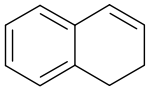	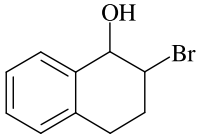	1	81

[a]Reaction condition: olefin (1 mmol); NBS (1.2 mmol), I_2 (0.1 mmol), MeCN-H_2O (4:1, 5 mL); [b]Isolated yield.

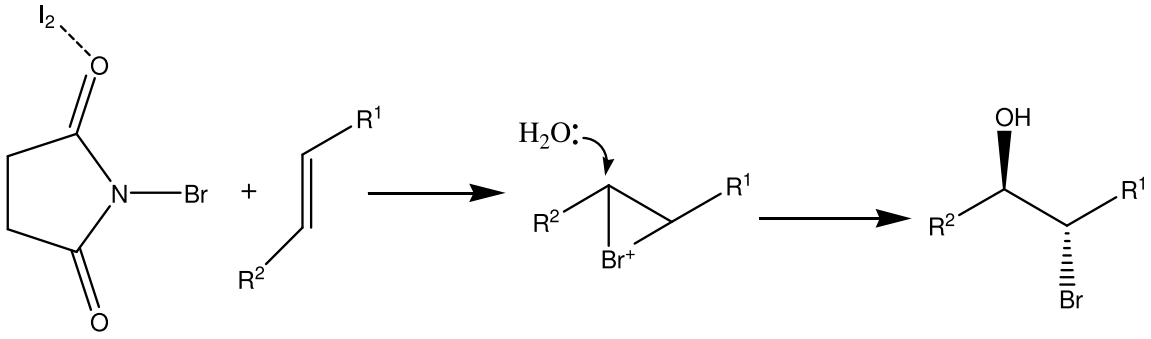

Scheme II — Plausible mechanism of iodine catalyzed bromohydrin formation

Methyl 2-bromo-3-chloro-4-methoxy phenyl-3-hydroxy propanoate, **2b**: Yellow Oil; IR (KBr): 3460, 2960, 1701, 1601, 1435, 1268, 1198, 1062, 987, 537 cm^{-1}; ^1H NMR ($CDCl_3$, 300 MHz): δ 3.70 (s, 3H), 3.73 (s, 3H) 4.23 (d, *J* = 9 Hz, 1H), 4.9 (d, *J* = 8.7 Hz, 1H), 6.84 (d, *J* = 8.4Hz, 1H), 7.16 (d, *J* = 8.4Hz, 1H), 7.34 (s, 1H); ^{13}C NMR ($CDCl_3$, 75 MHz): δ 14.1, 21.0, 47.7, 53.3, 56.1, 74.0, 111.7, 122.2, 128.8, 132.4, 154.9.

Methyl 2-bromo-3-hydroxy-3-phenyl propanoate, **3b**: White solid; m.p. 64-65°C [Lit.[9f] 63°C]; IR (KBr): 3466, 2954, 2916, 1732, 1595, 1442, 1280, 1022 cm^{-1}; ^1H NMR ($CDCl_3$, 300 MHz): δ 3.76 (s, 3H), 4.35 (d, *J* = 8.7 Hz, 1H), 5.01-5.1 (m, 1H), 7.33-7.42 (m, 5H); ^{13}C NMR ($CDCl_3$, 75 MHz): δ 47.4, 53.0, 74.9, 126.9, 128.3, 128.6, 138.9, 169.8.

Methyl 2-bromo-3-hydroxy-3-(3-methoxy phenyl)-propanoate, **4b**: White solid; m.p. 75-77°C; IR (KBr): 3450, 2970, 1708, 1602, 1440, 1260, 1195, 1055, 534 cm^{-1}; ^1H NMR ($CDCl_3$, 300 MHz): δ 3.82 (s, 6H), 6.36 (d, *J* = 15.9 Hz, 1H), 6.7–6.89 (m, 1H), 7.09–7.10 (m, 1H), 7.47 (d, 9 H_Z, 1H), 7.9 (d, 15.9 Hz, 1H); ^{13}C NMR ($CDCl_3$, 75 MHz): δ 51.7, 55.3, 112.3, 117.4, 120.5, 133.8, 143.0, 158.8, 166.6.

Methyl 2-bromo-3-hydroxy-3-(4-methoxyphenyl) propanoate, **5b**: White solid; m.p. 59°C [Lit.[9f] 59-60°C]; IR (KBr): 3440, 2950, 1715, 1600, 1430, 1265, 1195, 1065, 535 cm^{-1}; ^1H NMR ($CDCl_3$, 300 MHz): δ 3.55-3.82 (m, 6H), 4.21-4.35 (m, 1H), 4.82-5.0 (m, 1H), 6.86 (d, *J* = 6Hz, 2H), 7.26 (d, *J* = 6Hz, 2H); ^{13}C NMR ($CDCl_3$, 75 MHz): δ 47.7, 53.0, 55.0, 74.5, 113.7, 128.1, 131.1, 159.5, 169.8.

2-Bromo-1, 2-diphenylethanol, **6b**: White solid; m.p. 83-84°C [Lit.[11a] 83-84°C]; IR (KBr): 3440, 2950, 1597, 1430, 535 cm^{-1}; ^1H NMR ($CDCl_3$, 300 MHz): δ 2.47 (br, s, 1H), 5.1 (d, *J* = 6 Hz, 1H), 5.21 (d, *J* = 6H$_Z$, 1H), 7.26-7.62 (m, 10H); ^{13}C NMR ($CDCl_3$, 75 MHz): δ 56.8, 78.0, 127.8, 128.1, 128.4, 128.7, 128.8, 128.9, 139.6, 139.9.

2-Bromo-3-(4-chloro-phenyl)-3-hydroxy-1-phenyl-propan-1-one, **7b**: White solid; m.p. 95°C [Lit.[11b] 96°C]; IR (KBr): 3440, 2950, 1715, 1597, 1430, 1065, 987, 535 cm^{-1}; ^1H NMR ($CDCl_3$, 300 MHz): δ 3.5 (bs, 1H), 5.14 (d, *J* = 8.5Hz, 1H), 5.32 (d, *J* = 8.1 Hz, 1H), 7.21-7.69 (m, 7H), 8.02 (d, *J* = 7.2 H_Z, 2H); ^{13}C NMR ($CDCl_3$, 75 MHz): δ 47.7, 74.0, 128.7, 128.8, 129.04, 134.3, 134.4, 137.9, 194.4.

2-Bromo-1-phenylethanol, **8b**: Thick oil; IR (neat): 3408, 2935, 2952, 1600, 1460, 1062, 708 cm^{-1}; ^1H NMR ($CDCl_3$, 300 MHz): δ 3.1 (bs, 1H), 3.51-3.67 (m, 2H), 4.90-4.95 (m, 1H), 7.26-7.39 (m, 5H); ^{13}C NMR ($CDCl_3$, 75 MHz): δ 40.7, 73.8, 125.9, 128.5, 128.7, 140.1.

2-Bromo-1-(4-chlorophenyl)ethanol, **9b**: White solid, m.p. 61-63°C. (lit.[9g] 61-62°C). IR (neat): 3430, 2945, 1594, 1445, 1068, 743 cm^{-1}; ^1H NMR (300 MHz, $CDCl_3$): δ 2.84 (bs, 1 H), 3.47-3.62 (m, 2 H), 4.83-4.91 (m, 1 H), 7.25-7.37 (m, 4 H); ^{13}C NMR (75 MHz, $CDCl_3$): δ 40.5, 73.5, 126.8, 129.1, 134.0, 139.1.

2-Bromo-2,3-dihydro-1*H*-inden-1-ol, **10b**: White solid; m.p. 124-125°C; IR (KBr): 3440, 2947, 1448, 565 cm^{-1}; ^1H NMR ($CDCl_3$, 300 MHz): δ 3.15-3.2 (m, 1H), 3.5-3.62 (m, 1H), 4.2-4.30 (m, 1H), 5.27-5.32 (m, 1H), 7.15-7.5 (m, 4H); ^{13}C NMR ($CDCl_3$, 75 MHz): δ 40.5, 54.5, 83.4, 124.1, 124.6, 127.6, 129.0, 139.8, 141.7.

Bromo-1,2,3,4-tetrahydron phthalen-1-ol, **11b**: White solid; IR (KBr): 3440, 2947, 2924, 1587, 555 cm^{-1}; ^1H NMR ($CDCl_3$, 300 MHz): δ 2.41-2.7 (m, 2H), 2.85-3.1 (m, 2H), 4.21-4.5 (m, 1H), 4.85-5.1 (m, 1H), 7.12-7.25 (m, 2H), 7.47-7.53 (m, 2H); ^{13}C NMR ($CDCl_3$, 75 MHz): δ 28.1, 29.8, 56.3, 74.1, 126.8, 128.2, 128.6, 135, 135.5.

Acknowledgement

Financial Support from UGC, India (Grant No. 41-206/2012-SR) is gratefully acknowledged. AJB thanks CSIR for research fellowship.

References

1 (a) Hajra S, Karmakar A & Bhowmick M, *Tetrahedron*, 61, **2005**, 2279; (b) Dong L & Miller M J, *J Org Chem*, 67, **2002**, 4959; (c) Evans D A, Ellman J A & De Vries K M, *J Am Chem Soc*, 111, **1989**, 8912; (d) Evans D A & Weber A E, *J Am Chem Soc*, 109, **1987**, 7151; (e) Tseng T C & Wu M J, *Tetrahedron Asym*, 6, **1995**, 1633; (f) Nicolaou K C, Kataoka T C, Caulfied T & Kumazawa T, *J Am Chem Soc*, 110, **1988**, 7910; (g) Sheehan J C, Mania D, Nakamura S, Stock J A & Maeda K, *J Am Chem Soc*, 90, **1968**, 462; (h) Boger D L & Memezes R E, *J Org Chem*, 57, **1992**, 4331; (i) Kawashima H & Kobayashi Y, *Org Lett*, 16, **2014**, 2598; (j) Li L, Cai P, Guo Q & Xue S, *J Org Chem*, 73, **2008**, 3516.

2 (a) Chou T-C & Yu S R, *J Chin Chem Eng*, 15, **1984**, 197; (b) Jennings R C & Ottridge A P, *J Chem Soc Perkin Trans 1*, **1984**, 1733.

3 (a) Christophersen C, *Acta Chem Scand*, 39B, **1985**, 517; (b) Ueda Y & Maynard S C, *Tetrahedron Lett*, 29, **1988**, 5197; (c) Konopelski J P, Boehler M A & Tarasow T M, *J Org Chem*, 54,**1989**, 4966; (d) Cananal-Duvillard I, Berrier J F, Royer J & Husson H P, *Tetrahedron Lett*, 39, **1998**, 5158; (f) Evans J M, Fake C S, Hamilton T C, Poyser R H & Showell G H, *J Med Chem*, 27, **1984**, 1127.

4 (a) Stewart C A &VanderWerf C A, *J Am Chem Soc*, 76, **1954**, 1259; (b) Owen L N & Saharia G S, *J Chem Soc*, **1953**, 2582; (c) Majetich G, Hicks R & Reister S, *J Org Chem*, 62, **1997**, 4321; (d) Reddy M A, Surendra K, Bhanumathi N & Rao K R, *Tetrahedron*, 58, **2002**, 6003.

5 Sharghi H & Naeimi H, *Bull Chem Soc Jpn*, 72, **1999**, 1525.

6 (a) Kotsuki H, Shimanouchi T, Ohahima R & Fujiwara S, *Tetrahedron*, 54, **1998**, 2709; (b) Kotsuki H & Shimanouchi T, *Tetrahedron Lett*, 37, **1996**, 1845; (c) Shimizu M, Yoshida A & Fujisawa T, *Synlett*, **1992**, 204; (d) Sbitha B, Satheesh R, Rajkumar M, Reddy Ch S & Yadav J S, *Tetrahedron Lett*, 42, **2001**, 3955.

7 Andrews G C, Grawford T C & Contilio Jr L G, *Tetrahedron Lett*, 22, **1981**, 3803.

8 (a) Joshi N N, Srevnik M & Brown H C, *J Am Chem Soc*, 110, **1988**, 6246; (b) Guindon Y, Therien M, Girard Y & Yoakin C, *J Org Chem*, 52, **1987**, 1680; (c) Bell T W & Ciaccio J A, *Tetrahedron Lett*, 27, **1986**, 827; (c) Roy C D & Brown H C, *J Orgenomet Chem*, 692, **2007**, 1608.

9 (a) Sharghi H & Eskandari M M, *Tetrahedron*, 59, **2003**, 8509; (b) Sharghi H & Eskandari M M & Gharami R, *J Mol Catal A Chem*, 215, **2004**, 55.

10 Suh Y G, Koo B A, Ko J A & Cho Y S, *Chem Lett*, 11, **1993**, 1907.

11 (a) Vijoy N, Sreeletha B P, Anu A, Tesmot G G, Siji T & Vairamani M, *Tetrahedron*, 57, **2001**, 7417; (b) Kabalka G W, Yang K, Reddy N K, Nice L E & Sadanandan E V, *Tetrahedron Lett*, 37, **1996**, 2377; (c) Dewkar G K, Narima S V & Sudalai A, *Org Lett*, 5, **2003**, 4501; (d) Adimurthy S, Ghosh S, Patoliya P U, Ramachandraiah G, Agrawal M, Gandhi M R, Upadhyay S C, Ghosh P K & Ranu B C, *Green Chem*, 10, **2008**, 232; (e) Patil R D, Joshi G & Adimurthy S, *Ind Eng Chem Res*, 49, **2010**, 8100; (f) Anand N, Kapoor M, Koul S, Taneja S C, Sharma R L & Qazi G N, *Tetrahedron Asym*, 15, **2004**, 3131; (g) Patil R D, Joshi G, Adimurthy S & Ranu B C, *Tetrahedron Lett*, 50, **2009**, 2529; (h) Macharla A K, Nappunni R C & Nama N, *Tetrahedron Lett*, 53, **2012**, 1401,

12 Mantinez J S, Carroll G L, Tschirret-Guth R A, Altenhoff G, Little R D & Bulter A, *J Am Chem Soc*, 123, **2001**, 3289.

13 (a) Caughlin P, Roberts S, Rush C & Willetts A, *Biotechnol Lett*, 15, **1993**, 907; (b) Bhuvaneswari N, Balasubramanian K K & Venkatachalam C S, *J Electronal Chem*, 354, **1993**, 223.

14 (a) Narender M, Reddy M S, Nageswar Y V D & Rao K R, *J Mol Catal A: Chem*, 258, **2006**, 10; (b) Bar S, *Can J Chem*, 88, **2010**, 605.

15 Dalton D R & Jones D C, *Tetrahedron Lett*, 8, **1967**, 2875.

16 Yadav J S, Reddy B V S, Baishya G, Harshavardhan S J, Chary Ch J & Gupta M K, *Tetrahedron Lett*, 46, **2005**, 3569.

17 Filler R, Camara B R & Naqvi S M, *J Am Chem Soc*, 81, **1959**, 658.

18 Guss C O & Rosenthal R, *J Am Chem Soc*, 77, **1955**, 2549.

19 (a) Kharasch M S & Priestley H N, *J Am Chem Soc*, 61, **1939**, 3425; (b) Paul R & Tchelitcheff S, *Bull Soc Chim France*, **1948**, 896; (c) Phukan P, Chakraborty P & Kataki D, *J Org Chem*, 71, **2006**, 7533.

20 (a) Phukan P, *J Org Chem*, 69, **2004**, 4005; (b) Phukan P, *Tetrahedron Lett*, 45, **2004**, 4785; (c) Phukan P, *Synth Commun*, 34, **2004**, 1065; (d) Phukan P, Kataki D & Chakraborty P, *Tetrahedron Lett*, 47, **2006**, 5523; (e) Kataki D & Phukan P, *Indian J Chem*, 45B, **2006**, 1759; (f) Kataki D, Chakraborty P, Sarmah P & Phukan P, *Indian J Chem Technol*, 13, **2006**, 519; (g) Kataki D & Phukan P, *Tetrahedron Lett*, 50, **2009**, 1958; (h) Deuri S & Phukan P, *Struct Chem*, 22, **2011**, 1075; (i) Sarma C M, Kashyap B & Phukan P, *Indian J Chem*, 51B, **2012**, 323; (j) Saikia I & Phukan P, *C R Chimie*, 15, **2012**, 688; (k) Deuri S, Kataki D & Phukan P, *Indian J Chem*, 51B, **2012**, 1163; (l) Deuri S & Phukan P, *J Phys Org Chem*, 25, **2012**, 1228; (m) Borah A J & Phukan P, *J Chem Sci*, 125, **2013**, 1503; (n) Kataki D, Bhattacharyya P, Deka M, Jha D K & Phukan P, *Indian J Chem*, 52B, **2013**, 1505; (o) Sharma C M, Kashyap B & Phukan P, *Indian J Chem*,53B, **2014**, 750.

Computational and Theoretical Chemistry 1027 (2014) 197–202

Contents lists available at ScienceDirect

Computational and Theoretical Chemistry

journal homepage: www.elsevier.com/locate/comptc

Reactivity and regioselectivity in the ring opening of 2-substituted non-activated aziridines: A density functional theory based analysis

Bhupen Baruah [a], Sanjib Deuri [b], Prodeep Phukan [a,*]

[a] Department of Chemistry, Gauhati University, Guwahati 781 001, Assam, India
[b] Departmentn of Chemistry, M.C. College, Barpeta 781 301, Assam, India

ARTICLE INFO

Article history:
Received 23 July 2013
Received in revised form 30 October 2013
Accepted 6 November 2013
Available online 16 November 2013

Keywords:
Non-activated aziridine
Conceptual DFT
Electrophilicity index
Fukui function
Local electrophilicity index

ABSTRACT

Non-activated aziridines are the aziridines with an electron-donating group at nitrogen. Conceptual Density Functional Theory (DFT) based descriptors have been used to rationalize the observed activation and regioselectivity in the ring opening of 2-substituted non-activated aziridines via aziridinium intermediate. Reactivity indices such as electrophilicity index (ω), condensed Fukui function for nucleophilic attack (f_k^+) and local electrophilicity index (ω_k^+) have adequately and efficiently rationalized the observed activation and regioselectivity.

© 2013 Elsevier B.V. All rights reserved.

1. Introduction

Amines with a large variety of important functional groups [1,2] can be synthesized via ring opening of non-activated aziridines. Non-activated aziridines are the ones with electron donating groups at the nitrogen atom. Prior to the ring opening via nucleophilic attack, non-activated aziridines are activated using an electrophile. In a common activation strategy, aziridine moiety is first converted to an aziridinium ion via *N*-complexation with the electrophile which consequently undergoes a regioselective nucleophilic attack to produce the target amines. Aziridinium ions are usually obtained through six different methodologies i.e., *N*-alkylation, *N*-alkoxycarbonylation, *N*-acylation, *N*-protonation, *N*-silylation and *N*-complexation with Lewis acids [2]. Activation strategies and ring opening pathways for the non-activated aziridines are depicted in Scheme 1. The nucleophile can attack the aziridinium species either at the unsubstituted carbon atom (path a) or at the substituted carbon atom (path b) leading to two regioisomeric amines. Therefore issue of regioselectivity is vital to the synthesis of functionalized amines via aziridinium intermediate.

Regio- and stereochemical selectivity in the ring opening of non-activated aziridine have been the subject of several computational studies [3–6]. Conceptual DFT [7] based descriptors have been successfully implemented by Berger in a recent study [8] of ring opening reactions of activated aziridine; both FMO theory and the Fukui function were able to rationalize the experimentally observed ratios of isomeric products emphasizing once again the growing importance of conceptual DFT based reactivity descriptors in organic chemistry. In the present work conceptual DFT based method has been adopted to rationalize the experimentally observed activation and regioselectivity in the ring opening reactions of non-activated aziridine. Electrophilicity index (ω) [9,10] has been used to assess the various experimental approaches towards enhancing reactivity of the aziridine substrate in terms of electrophilic activation. We have used condensed Fukui function for nucleophilic attack (f_k^+) [11] and local electrophilicity index (ω_k^+) [12] to find out the most preferable site for nucleophilic attack in the aziridinium species. Four aziridine molecules belonging to the family of 2-alkenyl, 2-aryl, 2-acyl and 2-carbamoyl aziridine (designated as A, B, C, D) have been considered in this study. We have chosen these molecules because experimental data on ring opening reactions of these types of substrates are available in the literature (Table S3 of the supplementary data). Also, the choice of these substrates will enable us to observe the role of 2-substituents on electrophilic activation and regioselectivity. In order to assess the role of electrophiles in various activation strategies, we have modeled the aziridinium complexes with the following electrophiles: H^+(*N*-protonation), CH_3^+(*N*-methylation), CH_3CO^+(*N*-acylation), CH_3COO^+(*N*-alkoxycarbonylation), $(CH_3)_3Si^+$(*N*-silylation). For modeling of *N*-complexation of the aziridines with Lewis acids, $ZnCl_2$, BF_3, and $AlCl_3$ have been chosen. We have considered seven substrate-electrophile combinations for each type of substrate making 28 combinations all together. Since only a few of these substrate-electrophile combinations have been examined experimentally, we believe, this work will be helpful to predict

* Corresponding author. Tel.: +91 361 2570535 (O); fax: +91 361 2700311 (O).
E-mail address: pphukan@yahoo.com (P. Phukan).

2210-271X/$ - see front matter © 2013 Elsevier B.V. All rights reserved.
http://dx.doi.org/10.1016/j.comptc.2013.11.005

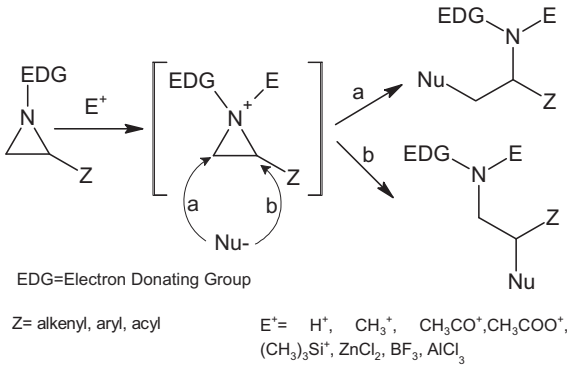

Scheme 1. Electrophilic activation and ring opening pathways of 2-substituted non-activated aziridine.

the regioselectivity preference for many of the hitherto unexamined cases. All the aziridines and their aziridinium complexes with the electrophiles considered in this study are depicted in Scheme 2. For convenience of treatment each of the four aziridines (designated by A, B, C and D), their corresponding aziridinium species are put into four representative series, namely Series I, Series II, Series III and Series IV.

2. Theory and computational details

The reactivity descriptors used here, namely the electrophilicity index (ω), condensed Fukui function for nucleophilic attack (f_k^+) and local electrophilicity index (ω_k^+) are defined within the context of conceptual density functional theory [10–12]. The global descriptors chemical potential (μ) and hardness (η) are approximated [9,10] in the finite difference approach as

$$\mu = \frac{-(I+A)}{2} \tag{1}$$

and

$$\eta = I - A \tag{2}$$

Using Janak's theorem [13], ionization potential and electron affinity can be replaced with molecular energies of HOMO (ε_H) and LUMO (ε_L), respectively. Thus, for the HOMO–LUMO approach μ and η can be expressed as

$$\mu \approx \frac{\varepsilon_L + \varepsilon_H}{2} \tag{3}$$

and

$$\eta = \varepsilon_L - \varepsilon_H \tag{4}$$

Global electrophilicity index is a combined descriptor involving chemical potential and hardness which expresses propensity of a species to accept electron. This index [9,10] is expressed as

$$\omega = \frac{\mu^2}{2\eta} \tag{5}$$

Fukui functions for nucleophilic attack on an atom, k, in an N–electron system was introduced by Yang and Mortier [11] as

$$f_k^+ = q_k(N+1) - q_k(N) \tag{6}$$

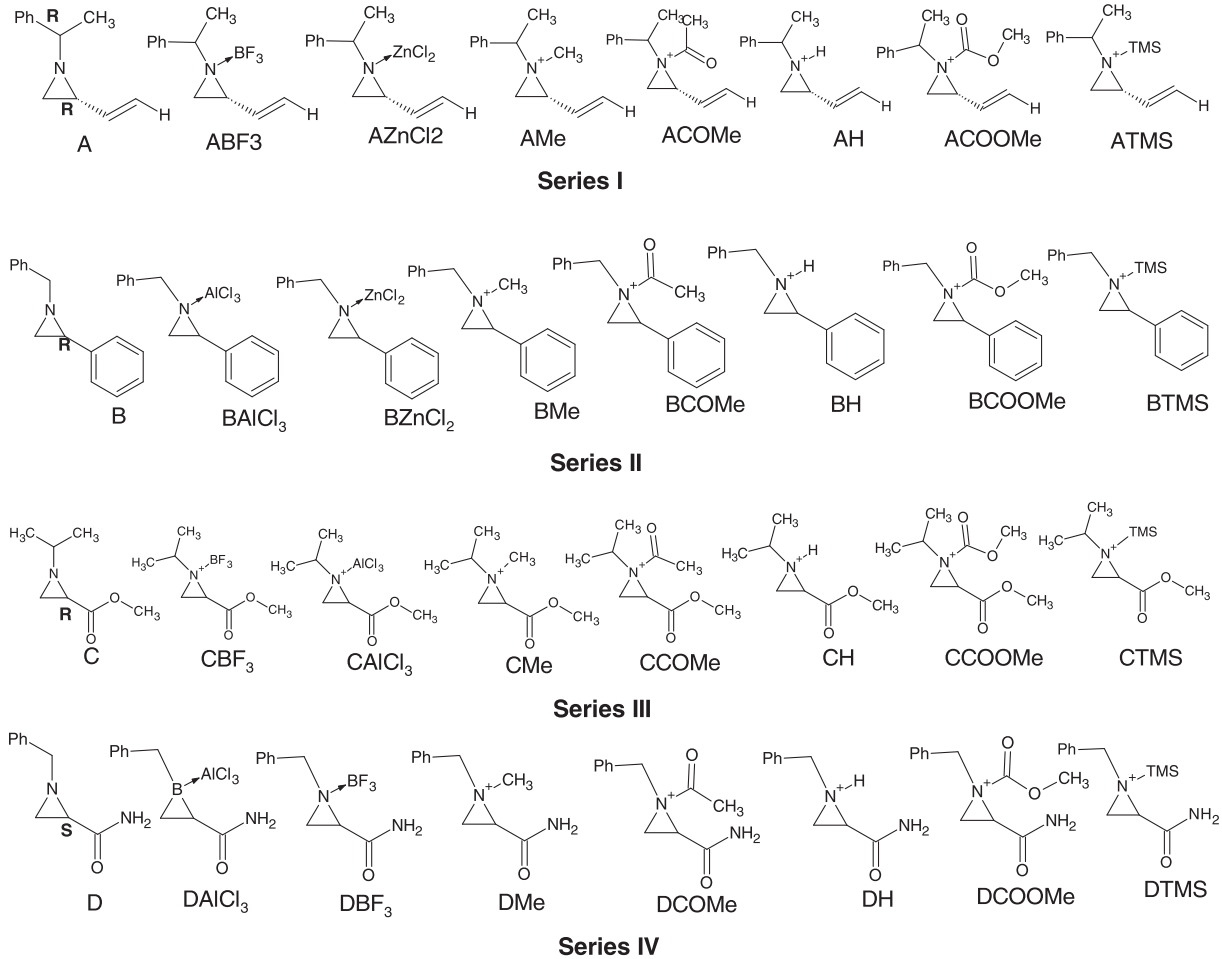

Scheme 2. Non-activated aziridines and their aziridinium species considered in this study.

Condensed-to-atom variant for local electrophilicity index [12] is defined as

$$\omega_k^+ = f_k^+ \omega \quad (7)$$

Geometries of all the aziridines and their aziridinium species are optimized using density functional three-parameter hybrid model (DFT/B3LYP) [14,15]. All calculations are carried out using the GAUSSIAN03 [16] program. For optimization part standard split valence basis set, 6-31G (d) is used for all the atoms. HOMO–LUMO energies used for the evaluation of μ, η are obtained from the energy calculation of the *N*-electron species done at DFT/B3LYP/6-31G++(d, p) level. Condensed Fukui functions are calculated using NPA populations [17] obtained from the single point energy calculations performed at DFT/B3LYP/6-31++G(d,p) level for the *N*-electron species as well as the *N + 1* electron species. All energy calculations are done at the optimized geometry of the *N*-electron species obtained from DFT/B3LYP/6-31G (d) calculations. Solvent effects were introduced through the Integral Equation Formalism version of the Polarizable Continuum Model (IEF-PCM) [18]. Choice of solvents has been made on the basis of relevant experimental studies (Table S3 of the supplementary data). For the systems ATMS, CBF3, DALCL3 and DBF3, solvents employed are dichloromethane, methanol, ethanol and methanol respectively, for the rest of the systems the most common solvent acetonitrile is used.

3. Results and discussion

3.1. Electrophilic activation via N-complexation with electrophiles

For the aziridines and their corresponding aziridinium species calculated electrophilicity index (ω) values, electrophilic activation ($\Delta\omega$) and the HOMO–LUMO energies obtained at DFT/B3LYP/6-31++G (d, p) level of theory are displayed in Table 1. Electrophilic activation ($\Delta\omega$) values are measured by subtracting ω value of an aziridine from that of the corresponding aziridinium species. A comparison of electrophilic activation ($\Delta\omega$) of non-activated aziridines by various methods employed in ring opening reactions of non-activated aziridines is depicted in Fig. 1. This parameter ($\Delta\omega$) serves as an indicator of performance of various *N*-complexation methods in activating an otherwise non-activated aziridine. Results of both the gas phase and solvent phase calculations are presented in Table 1. In the following discussion we present our analysis based on the results of solvent phase calculations. As a result of *N*-complexation, both HOMO and LUMO energy decrease substantially in the case of all the aziridines. While in the case of 2-alkenyl (A) and 2-aryl (B) aziridines maximum HOMO energy lowering is observed with *N*-silylation, in the case of 2-acyl aziridines (C and D), maximum lowering is achieved through *N*-alkoxycarbonylation and *N*-acylation respectively. Electrophilic activation of the aziridines with *N*-complexation is very much evident from the $\Delta\omega$ values. There is a substantial increase in electrophilicity

Table 1
HOMO–LUMO energies, electrophilicity (ω), and electrophilic activation ($\Delta\omega$)[b] computed at DFT/B3LYP/6-31++G(d,p) level.

System	Gas phase		Solvent phase[a]		Gas phase		Solvent phase	
	ε_H	ε_L	ε_H	ε_L	ω (eV)	$\Delta\omega$ (eV)	ω (eV)	$\Delta\omega$ (eV)
Series I								
A	−0.2413	−0.0156	−0.2400	−0.0143	0.99		0.97	
ABF3	−0.2610	−0.0443	−0.2535	−0.0314	1.46	0.47	1.24	0.27
AZnCl2	−0.2684	−0.0482	−0.2660	−0.0426	1.55	0.55	1.45	0.48
AMe	−0.3777	−0.1745	−0.2701	−0.0505	5.10	4.11	1.59	0.62
ACOMe	−0.3837	−0.2061	−0.2739	−0.0888	6.66	5.67	2.42	1.44
AH	−0.3810	−0.1761	−0.2684	−0.0445	5.15	4.16	1.49	0.51
ACOOMe	−0.3780	−0.1791	−0.2722	−0.0614	5.31	4.31	1.80	0.82
ATMS	−0.3725	−0.1658	−0.2780	−0.0616	4.77	3.77	1.81	0.84
Series II								
B	−0.2369	−0.0259	−0.2388	−0.0219	1.11		1.07	
BAlCl3	−0.2743	−0.0567	−0.2611	−0.0394	1.71	0.60	1.39	0.32
BZnCl2	−0.2705	−0.0533	−0.2587	−0.0406	1.64	0.53	1.40	0.33
BMe	−0.3771	−0.1681	−0.2687	−0.0536	4.84	3.73	1.64	0.58
BCOMe	−0.3729	−0.2059	−0.2708	−0.0911	6.82	5.71	2.48	1.41
BH	−0.3790	−0.1732	−0.2660	−0.0501	5.04	3.92	1.57	0.51
BCOOMe	−0.3700	−0.1984	−0.2707	−0.0848	6.41	5.29	2.31	1.25
BTMS	−0.3683	−0.1588	−0.2764	−0.0626	4.51	3.40	1.83	0.76
Series III								
C	−0.2428	−0.0186	−0.2494	−0.0245	1.04		1.13	
CAlCl3	−0.2959	−0.0624	−0.3087	−0.0533	1.87	0.83	1.74	0.61
CBF3	−0.3110	−0.0528	−0.3090	−0.0475	1.74	0.71	1.65	0.52
CMe	−0.4443	−0.1875	−0.3276	−0.0645	5.29	4.25	1.99	0.85
CCOMe	−0.4425	−0.2180	−0.3297	−0.0946	6.61	5.57	2.60	1.47
CH	−0.4686	−0.2083	−0.3269	−0.0592	5.99	4.95	1.89	0.76
CCOOMe	−0.4424	−0.1921	−0.3313	−0.0749	5.47	4.43	2.19	1.05
CTMS	−0.4395	−0.1860	−0.3305	−0.0730	5.25	4.21	2.15	1.02
Series IV								
D	−0.2388	−0.0214	−0.2420	−0.0185	1.06		1.03	
DAlCl3	−0.2722	−0.0555	−0.2643	−0.0426	1.68	0.63	1.44	0.41
DBF3	−0.2595	−0.0456	−0.2596	−0.0349	1.48	0.42	1.31	0.28
DMe	−0.3787	−0.1795	−0.2712	−0.0530	5.32	4.26	1.64	0.61
DCOMe	−0.3839	−0.2150	−0.3297	−0.0946	7.22	6.16	2.53	1.50
DH	−0.3822	−0.1830	−0.2700	−0.0482	5.45	4.40	1.55	0.52
DCOOMe	−0.3713	−0.2002	−0.2716	−0.0767	6.49	5.43	2.12	1.08
DTMS	−0.3697	−0.1683	−0.2710	−0.0542	4.89	3.83	1.66	0.63

[a] For the systems ATMS, CBF3, DALCL3 and DBF3 solvents employed are dichloromethane, methanol, ethanol and methanol respectively, for the rest acetonitrile.
[b] obtained by subtracting ω values of an aziridine from that of the corresponding aziridinium species.

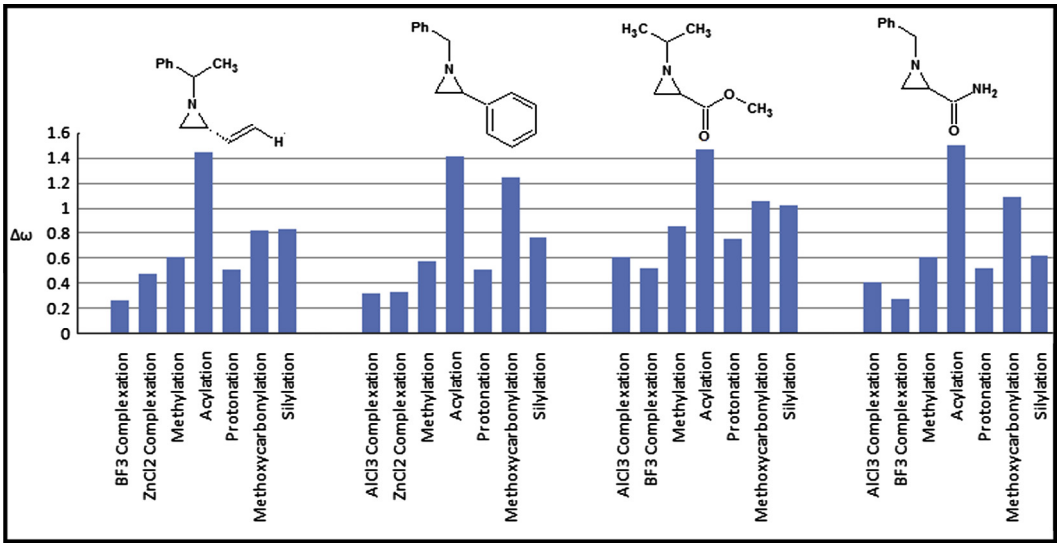

Fig. 1. Comparison of electrophilic activation ($\Delta\omega$) of non-activated aziridines by various methods employed in ring opening reactions (based on solvent phase $\Delta\omega$ values).

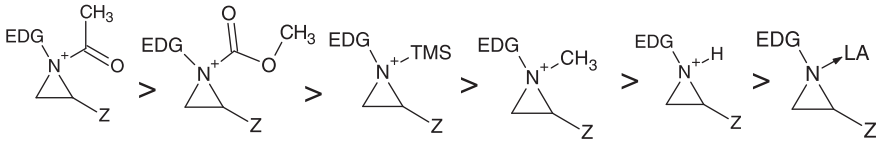

Scheme 3. The order of electrophilic activation.

values in going from aziridine to the aziridinium species via *N*-complexation. Irrespective of the type of aziridine, the same order of electrophilic activation (Fig. 1) is observed among each series of aziridine complexes. The order of electophilic activation can be generalized as shown in the Scheme 3.

From the $\Delta\omega$ values in Table 1 it is clear that maximum activation of a non-activated aziridine can be achieved with *N*-acylation and Lewis acids activate the substrates minimally.

3.2. Analysis of regioselectivity issues using local reactivity descriptor

Fukui function (f_k^+) and local electrophilicity (ω_k^+) values at the substituted carbon atom C2 and the unsubstituted carbon atom C3 of the aziridine ring of all the systems considered in this study computed at DFT/B3LYP/6-31++G(d,p) level are displayed in Table 2. Although results of calculations in both the gas phase and the solvent phase are presented in Table 2, following discussion is based on the solvent phase results. Let us first look at the regioselectivity issue with respect to the non-activated systems A, B, C, and D. For the 2-alkenyl aziridine A and 2-carbamoyl aziridine D, local indices have higher value at the C2 carbon than at the C3 carbon which implies C2 position to be the more preferable site of nucleophilic attack in aziridines A and D. For the 2-aryl aziridine B, C2 carbon has a negative value of Fukui function. As no orbital relaxation was observed in the substrate [19], negative value of Fukui function detected here might be an artifact of the NPA scheme. However, gas phase calculations predict the C2 carbon as favorable site for nucleophilic attack. In the 2-acyl aziridine C, local index values indicate C3 to be the more preferable site of nucleophilic attack. This shift in regioselectivity from C2 to C3 atom results from comparatively higher electronic population at C3 atom with respect to C2 atom (Table S2 of the supplementary data). Higher electronic population at C3 may be a consequence of stronger electron releasing effect from the isopropyl group.

Experimentally it has been found that 2-(1-alkenyl) aziridines undergo nucleophilic attack at the substituted C2 center during ring opening irrespective of the type of nucleophile and electrophile employed. Three reports [20–22] of ring opening of 2-(1-alkenyl) aziridines have been found in the literature wherein the aziridinium ions were obtained via *N*-alkoxycarbonylation, *N*-methylation and *N*-silylation respectively (Table S2). In all the three cases, nucleophilic attack occurs at the C2 carbon. All solvent phase Fukui function values are found to be higher at C2 carbon of the aziridinium species ACOMe, AMe, ATMS, there by correctly reproducing the experimental findings. Although gas phase calculation predicts C3 site as the preferred site of nucleophilic attack in the aziridinium species $AZnCl_2$, AH, ATMS, in presence of solvents C2 site is found to have higher values of local indices in all the aziridinium species in complete conformity with the experimental finding. These results also highlight the role played by the solvent on regioselectivity. Since all the aziridinium species are found to have higher local indices at the C2 atom, electrophiles may not have any substantial effect on regioselectivity. Only in the case of ACOOMe, local indices fail to predict the experimentally observed regioselectivity wherein calculated Fukui function values for the C2 and C3 atoms are found to be nearly equal.

Another point needs to be mentioned here. If one look at the NPA charges (Table S2) at C2 and C3 for all the systems considered in this study, the picture is completely opposite. C3 atom always has higher charge than that of C2 atom. Therefore, here the charge is not a true indicator of regioselectivity. This also negates the possibility of a hard-hard type interaction being operative.

Although in the case of 2-(1-alkenyl) aziridines no experimental data of regioselectivity for Lewis acid complexation and protonation are found in the literature, calculation predicts C2 carbon as the preferred site of nucleophilic attack in those cases. Another case of negative Fukui function is encountered in the system A1BF3.

Table 2
Fukui function (f_k^+) and local electrophilicity (ω_k^+) values on the relevant carbon atoms computed at DFT/B3LYP/6-31++G(d,p) level.

Systems	Centers	Gas phase		Solution phase[a]	
		f_k^+	ω_k^+	f_k^+	ω_k^+
Series I					
A	C2	0.0122	0.0121	0.0104	0.0102
	C3	0.0025	0.0025	0.0052	0.0051
ABF3	C2	−0.0063	−0.0093	−0.0025	−0.0032
	C3	0.0113	0.0166	0.0075	0.0093
AZnCl2	C2	0.0006	0.0010	0.0065	0.0094
	C3	0.0181	0.0280	0.0015	0.0021
AMe	C2	0.0286	0.1462	0.0254	0.0405
	C3	0.0263	0.1340	0.0190	0.0302
ACOMe	C2	0.0260	0.1732	0.0195	0.0471
	C3	0.0104	0.0692	0.0082	0.0198
AH	C2	0.0424	0.2183	0.0261	0.0388
	C3	0.0225	0.1159	0.0205	0.0304
ACOOMe	C2	0.0343	0.1821	0.0614	0.1101
	C3	0.0764	0.4054	0.0631	0.1133
ATMS	C2	0.0209	0.0994	0.0233	0.0423
	C3	0.0243	0.1160	0.0178	0.0323
Series II					
B	C2	0.0113	0.0126	−0.0015	−0.0016
	C3	0.0042	0.0047	0.0047	0.0050
BAlCl3	C2	0.0158	0.0271	0.0177	0.0245
	C3	0.0104	0.0178	0.0054	0.0075
BZnCl2	C2	0.0178	0.0292	0.0119	0.0167
	C3	0.0133	0.0218	0.0032	0.0044
BMe	C2	0.0694	0.3360	0.0526	0.0864
	C3	0.0124	0.0600	0.0116	0.0190
BCOMe	C2	0.1053	0.7185	0.1013	0.2512
	C3	0.0165	0.1126	0.0149	0.0369
BH	C2	0.0578	0.2909	0.0506	0.0797
	C3	0.0159	0.0803	0.0115	0.0182
BCOOMe	C2	0.1863	1.1932	0.2541	0.5874
	C3	0.0189	0.1212	0.0210	0.0485
BTMS	C2	0.0365	0.1645	0.0382	0.0698
	C3	0.0091	0.0411	0.0104	0.0190
Series III					
C	C2	0.0025	0.0026	0.0227	0.0257
	C3	0.0122	0.0126	0.0733	0.0831
CAlCl3	C2	0.0170	0.0318	0.0442	0.0770
	C3	0.0230	0.0430	0.0458	0.0799
CBF3	C2	0.0015	0.0026	0.0390	0.0645
	C3	0.0187	0.0327	0.0567	0.0937
CMe	C2	0.0746	0.3942	0.0693	0.1377
	C3	0.0587	0.3101	0.0560	0.1114
CCOMe	C2	0.0344	0.2275	0.0798	0.2077
	C3	0.0562	0.3718	0.0921	0.2397
CH	C2	0.0490	0.2936	0.0661	0.1253
	C3	0.0276	0.1656	0.0551	0.1045
CCOOMe	C2	0.0696	0.3806	0.0658	0.1440
	C3	0.0267	0.1461	0.0278	0.0609
CTMS	C2	0.0661	0.3469	0.0645	0.1387
	C3	0.0315	0.1653	0.0319	0.0685
Series IV					
D	C2	0.0023	0.0024	0.0157	0.0162
	C3	0.0080	0.0085	0.0054	0.0056
DAlCl3	C2	0.0532	0.0896	0.0523	0.0756
	C3	0.0215	0.0362	0.0151	0.0218
DBF3	C2	0.0148	0.0219	0.0466	0.0611
	C3	0.0105	0.0155	0.0233	0.0306
DMe	C2	0.0944	0.5024	0.0735	0.1205
	C3	0.0374	0.1990	0.0259	0.0424
DCOMe	C2	0.0618	0.4465	0.1141	0.2885
	C3	0.0304	0.2192	0.0283	0.0715
DH	C2	0.0723	0.3944	0.0673	0.1045
	C3	0.0257	0.1402	0.0216	0.0335
DCOOMe	C2	0.1107	0.7186	0.1104	0.2337
	C3	0.0403	0.2615	0.0377	0.0798
DTMS	C2	0.0809	0.3955	0.0751	0.1245
	C3	0.0244	0.1193	0.0237	0.0393

[a] For the systems ATMS, CBF3, DALCL3 and DBF3 solvents employed are dichloromethane, methanol, ethanol and methanol respectively, for the rest acetonitrile.

In the case of 2-arylaziridines, a large number of studies confirmed the preference of nucleophilic attack for the substituted C2 carbon atom of the aziridinium species [2]. When 2-phenyl aziridines were treated with different nucleophiles and Lewis acids, amines resulted from the nucleophilic attack at the C2 carbon [23]. Similarly, the reaction of 1-benzyl-2-phenyl aziridine activated via protonation gave those amines as major product which resulted from nucleophilic attack at C2 position [24]. When we calculated the local index values of the aziridinium species obtained from 1-benzyl-2-phenyl aziridine (B) via Lewis acid complexation and protonation, we found that the C2 carbon atom is the preferred site of nucleophilic attack. This is in conformity with the results of the reported examples (Table S2) [23,24]. Moreover, we found no literature report on experimental results on the aziridinium intermediates derived from 2-aryl aziridine substrates via *N*-acylation, *N*-alkoxycarbonylation, *N*-alkylation and *N*-silylation approaches. In case of all of these strategies, the calculated local index values predicted the C2 carbon as the preferred site of nucleophilic attack in the aziridinium species.

We have also included in our study 2-acyl aziridine substrate which are, in most cases, found to execute different regioselectivity depending on the type of nucleophile and electrophile employed [2]. In the ring opening reactions of 2-(alkoxycarbonyl)aziridine using $BF_3{\cdot}Et_2O$ as electrophile and alcohols as nucleophile, nucleophilic attack takes place at the less hindered C3 carbon atom [25]. In another report Lee et al. subjected 2-acylaziridine substrates to ring opening reactions using acyl chlorides as activator [26]. In all such reactions, the nucleophile attacked the C2 position of the aziridine ring (Table S2). These two experimental cases clearly depict the effect of electrophile on the regioselectivity of ring opening in 2-acylaziridine substrate. Our calculation on the 2-acylaziridine model substrate C exactly reproduces the experimental trends both in the gas phase and the solvent phase. From Table 2 we can see that aziridinium species CBF_3 has higher f_k^+ and ω_k^+ values at the C3 carbon of the aziridine ring. Again, local indices f_k^+ and ω_k^+ have higher values at C2 carbon site in the aziridinium species CCOOMe obtained via *N*-methoxycarbonylation of 2-acyl aziridine C. This is in complete agreement with the experimental data [25,20,26]. Ring opening of 2-acyl aziridines have not been examined yet experimentally via *N*-alkylation, *N*-protonation and *N*-silylation approaches. Calculated Fukui function values for these approaches predict C2 carbon as the preferred site of nucleophilic attack in those cases. However, with $AlCl_3$ as activator, calculation predicts C3 carbon as the preferred site showing the dependence of regioselectivity on nature of electrophile in the case of 2-acyl aziridines.

Finally we considered a 2-carbamoylaziridine (D) substrate. Gotor et al. [27] observed that the substrate D when heated under reflux in methanol using $BF_3{\cdot}Et_2O$ as electrophile produced a 3:1 mixture of the C3 and C2 ring opening products. When the same substrate (D) is treated with sodium azide and $AlCl_3$ in aqueous ethanol a 1:2.5 mixture of C3 and C2 ring opening products were observed (Table S2). Although calculated local index values are in excellent agreement with the experimentally observed regioselectivity in the $AlCl_3$–EtOH approach, they have failed to rationalize the experimentally observed product ratio in the case of BF_3–MeOH approach. Failure of DFT based local indices in the later case is acceptable because the ring opening was performed under heated condition. So far, no experimental data on the ring opening of 2-carbamoyl aziridine via *N*-alkylation, *N*-acylation, *N*-alkoxycarbonylation, *N*-silylation and *N*-protonation approaches are available in the literature. The Fukui function values obtained from this work predict C2 carbon as the preferred site of nucleophilic attack in all these cases.

4. Conclusion

Conceptual DFT based reactivity descriptors have presented a strong rationale for the observed activation and regioselectivity in the ring opening of non-activated aziridines. In terms of electrophilic activation, *N*-acylation has been found to be the best approach; Lewis acids activate the substrates minimally. Regioselectivity in the ring opening reactions has been assessed from the condensed Fukui function for nucleophilic attack (f_k^+) and local electrophilicity index (ω_k^+). Local indices used here have reproduced the experimentally observed regioselectivity for a vast range of substrates and electrophiles.

Acknowledgements

Financial Support from UGC, India (Grant No. 41-206/2012-SR) is gratefully acknowledged. BB thanks UGC (NERO) for teacher fellowship.

Appendix A. Supplementary material

Supplementary data associated with this article can be found, in the online version, at http://dx.doi.org/10.1016/j.comptc.2013.11.005.

References

[1] T.-X. Métro, B. Duthion, D. Gomez Pardo, J. Cossy, Rearrangement of β-amino alcohols via aziridiniums: a review, Chem. Soc. Rev. 39 (2010) 89–102.
[2] S. Stanković, M. D'hooghe, S. Catak, H. Eum, M. Waroquier, V.V. Speybroeck, N.D. Kimpe, H.-J. Ha, Regioselectivity in the ring opening of non-activated aziridines, Chem. Soc. Rev. 41 (2012) 643–665.
[3] M. D'hooghe, S. Catak, S. Stanković, M. Waroquier, Y. Kim, H.-J. Ha, V. Van Speybroeck, N.D. Kimpe, Systematic study of halide-induced ring opening of 2-substituted aziridinium salts and theoretical rationalization of the reaction pathways, Eur. J. Org. Chem. (2010) 4920–4931.
[4] S. Catak, M. D'hooghe, T. Verstraelen, K. Hemelsoet, A. Van Nieuwenhove, H.-J. Ha, M. Waroquier, N.D. Kimpe, V. Van Speybroeck, Opposite regiospecific ring opening of 2-(cyanomethyl)aziridines by hydrogen bromide and benzyl bromide: experimental study and theoretical rationalization, J. Org. Chem. 75 (2010) 4530–4541.
[5] M. D'hooghe, V. Van Speybroeck, M. Waroquier, N.D. Kimpe, Regio- and stereospecific ring opening of 1,1-dialkyl-2-(aryloxymethyl)aziridinium salts by bromide, Chem. Commun. (2006) 1554–1556.
[6] S.Y. Yun, S. Catak, W.K. Lee, M. D'hooghe, N.D. Kimpe, V. Van Speybroeck, M. Waroquier, Y. Kim, H.-J. Ha, Nucleophile-dependent regioselective ring opening of 2-substituted *N*,*N*-dibenzylaziridinium ions: bromide versus hydride, Chem. Commun. (2009) 2508–2510.
[7] P. Geerlings, F. De Proft, W. Langenaeker, Conceptual density functional theory, Chem. Rev. 103 (2003) 1793–1873.
[8] G. Berger, Using conceptual density functional theory to rationalize regioselectivity: a case study on the nucleophilic ring-opening of activated aziridines, Comp Theor. Chem. 1010 (2013) 11–18.
[9] R.G. Parr, L. Von Szentpaly, S. Liu, Electrophilicity index, J. Am. Chem. Soc. 121 (1999) 1922–1924.
[10] P.K. Chattaraj, U. Sarkar, D.R. Roy, Electrophilicity index, Chem. Rev. 106 (2006) 2065–2091.
[11] W. Yang, W.J. Mortier, The use of global and local molecular parameters for the analysis of the gas-phase basicity of amines, J. Am. Chem. Soc. 108 (1986) 5708–5711.
[12] L.R. Domingo, M.J. Aurell, P. Perez, R. Contreras, Quantitative characterization of the local electrophilicity of organic molecules. understanding the regioselectivity on diels-alder reactions, J. Phys. Chem. A 106 (2002) 6871.
[13] J.F. Janak, Proof that $\frac{\delta E}{\delta n_i} = \varepsilon_i$ in density-functional theory, Phys. Rev. 18 (1978) 7165–7168.
[14] A.D. Becke, Density-functional thermochemistry. III. The role of exact exchange, J. Chem. Phys. 98 (1993) 5648–5652.
[15] C. Lee, W. Yang, R.G. Parr, Development of the Colle–Salvetti conelation energy formula into a functional of the electron density, Phys. Rev. B 37 (1988) 785–789.
[16] M.J. Frisch et al., Gaussian 03, Revision E.01, Gaussian Inc., Wallingford, CT, 2004.
[17] A.E. Reed, L.A. Curtiss, F. Weinhold, Intermolecular interactions from a natural bond orbital, donor–acceptor viewpoint, Chem. Rev. 88 (1988) 899–926.
[18] .J. Tomasi, B. Mennucci, R. Cammi, Quantum mechanical continuum solvation models, Chem. Rev. 105 (2005) 2999–3093.
[19] E. Echegaray, C. Cárdenas, S. Rabi, N. Rabi, S. Lee, F.H. Zadeh, A. Toro-Labbe, J.S.M. Anderson, P.W. Ayers, In pursuit of negative Fukui functions: examples where the highest occupied molecular orbital fails to dominate the chemical reactivity, J. Mol. Model 19 (2013) 2779–2783.
[20] T.B. Sim, S.H. Kang, K.S. Lee, W.K. Lee, H. Yun, Y. Dong, H.-J. Ha, A novel synthesis of 5-functionalized oxazolidin-2-ones from enantiomerically pure 2-substituted *N*-[(*R*)-(+)-r-methylbenzyl]aziridines, J. Org. Chem. 68 (2003) 104–108.
[21] Y. Kim, H.-J. Ha, S.Y. Yun, W.K. Lee, The preparation of stable aziridinium ions and their ring-openings, Chem. Commun. (2008) 4363–4365.
[22] B.K. Lee, M.S. Kim, H.S. Hahm, D.S. Kim, W.K. Lee, H.-J. Ha, An efficient synthesis of chiral terminal 1,2-diaminesusing an enantiomerically pure [1-(10R)-methylbenzyl]aziridine-2-yl]methanol, Tetrahedron 62 (2006) 8393–8397.
[23] J.S. Yadav, B.V.S. Reddy, G. Baishya, P.V. Reddy, S.J. Harshavardhan, Bismuth triflate as novel and efficient catalyst for the synthesis of β-aminosulfides, Synthesis (2004) 1854–1858.
[24] D. Savoia, G. Alvaro, R. Di Fabio, A. Gualandi, Asymmetric synthesis of 2-(2-pyridyl)aziridines from 2-pyridineimines bearing stereogenic n-alkyl substituents and regioselective opening of the aziridine ring, J. Org. Chem. 71 (2006) 9373–9381.
[25] J. Bodenan, J. Chanet-Ray, R. Vessiere, Acid-catalyzed ring opening of 2-substituted aziridines with alcohols, Synthesis (1992) 288–292.
[26] Y. Kim, H.-J. Ha, H. Yun, B.K. Lee, W.K. Lee, Ring opening of 2-acylaziridines by acid chlorides, Tetrahedron 62 (2006) 8844–8849.
[27] R. Moran-Ramallal, R. Liz, V. Gotor, Bacterial preparation of enantiopure unactivated aziridine-2-carboxamides and their transformation into enantiopure nonnatural amino acids and *vic*-diamines, Org. Lett. 9 (2007) 521–524.

J. Chem. Sci. Vol. 128, No. 4, April 2016, pp. 633–647. © Indian Academy of Sciences.
DOI 10.1007/s12039-016-1057-5

DFT analysis of the nucleophilicity of substituted pyridines and prediction of new molecules having nucleophilic character stronger than 4-pyrrolidino pyridine

KAUSTAVMONI DEKA and PRODEEP PHUKAN*
Department of Chemistry, Gauhati University, Guwahati 781 014, Assam, India
e-mail: pphukan@yahoo.com

MS received 22 September 2015; revised 26 January 2016; accepted 1 February 2016

Abstract. Some commonly used 3-substituted, 4-substituted and 3,4,5-substituted pyridines were examined using DFT to predict the nucleophilicity behavior based on four different methods known in the literature. HOMO-LUMO energy calculations were done using DFT/B3LYP/6-311G+(d,p) level of theory. To establish the most suitable nucleophilicity scale for all the ranges of pyridines covered herein, either Hammett substituent constant (σ) or experimental nucleophilicity values were computed. On the basis of this study, some new 4-substituted pyridines with enhanced nucleophilicity have been proposed. Nucleophilic behaviour of a few predicted molecules was found to be better than that of 4-pyrrolidino pyridine.

Keywords. Density functional theory; nucleophilicity; organo-catalyst; pyridine.

1. Introduction

Since the early twentieth century, pyridine derivatives have found widespread applications as commercially important substrate. Pyridine was first synthesized in 1876.[1] Pyridine derivatives find applications in a variety of areas such as bioactive compounds,[2,3] insecticides,[4] fungicides,[5] plant growth regulators[6–8] and most extensively used as organocatalysis.[9–12] Organocatalysts have received enormous attention due to their advantages such as inertness towards moisture and oxygen, easy reaction conditions, absence of transition metals, etc.[13,14] In the recent past, there has been a significant progress in the development of more active pyridine based organocatalysts for various organic transformations.[15] The activity of the organocatalysts largely depends on their nucleophilic character.[16] The concept of nucleophile and electrophile[17] leads to the development of nucleophilicity/electrophilicity scale.

Initially, nucleophilicity trends were established on the basis of certain experimental parameters. To determine nucleophilicity quantitatively, Swain and Scott[18] introduced the first nucleophilicity scale based on linear free energy relationship as

$$\log(k/k_0) = s\,n \qquad (1)$$

where k is the rate constant for the S_N2 reaction of a substrate with a particular nucleophile, k_0 is the corresponding rate constant with reference nucleophile (water), n is the intrinsic nucleophilicity for a particular substrate and s is the sensitivity parameter of the substrate.

Later, Edwards[19,20] proposed a more general equation incorporating basicity, polarizability and oxidation potential to estimate nucleophilicy parameter. Bunnet[21] suggested that several factors that must be considered in order to quantitatively describe the nucleophilicity. Pearson[22] explained that the principle of hard and soft acids and bases (HSAB) can also be applied for determination of nucleophilicity. Legon and Millen used hydrogen bonding as a probe for electron density while determining the nucleophilicity and electrophilicity of hydrogen bonded complexes from rotational spectra.[23,24] This study was carried out specifically for hydrogen bonded dimers of the type B-HX where B is a Lewis base and HX is a molecule of electrophilic character.

Mayr and coworkers successfully developed an experimental nucleophilic scale for several 4-substituted pyridine[25] and 3,4,5-substituted pyridine.[26] They measured the rate of the reactions of corresponding substituted pyridines with benzhydrylium ions using a new linear free energy relationship

$$\log k = s(E + N) \qquad (2)$$

where electrophiles were characterized by the parameter E and nucleophiles were characterized by two parameters (N and s). The authors proved that this equation is sufficient to describe quantitatively the reaction rate

*For correspondence

of a large variety of electrophile-nucleophile combinations. To understand the mechanistic aspects such as intermolecular selectivity, intramolecular selectivity, solvation effect, etc., of chemical reactions, theoretical scales of nucleophilicity/electrophilicity[27,28] are very much desirable and helpful to experimental chemist.

Inverse relationship[29] between electrophilicity and nucleophilicity was first proposed and validate in the study of helium atom interactions with strong laser pulses. The study revealed that a particular molecular site may undergo more likely an electrophilic attack or another site undergoes nucleophilic attack. Recently, Roy *et al.,* developed a theoretical nucleophilicity scale for some commonly used arenes and heteroarenes[30] by using the inverse concept of electrophilicity and nucleophilicity. In their publication, nucleophilicity values were determined using four different available theoretical methods in literature and tested linearity between Hammett substituent constant to judge the goodness of the methods. Subsequently, they determined the nucleophilicity of organotin and allyl metal reagents[31] by applying the best methods which were evaluated in their earlier publication.[30] Domingo *et al.,*[32] recently verified the inverse of the electrophilicity and the inverse of the electron donating power proposed by Roy *et al.,* for 5-substituted indoles, para-substituted phenols and 2,5-disubstituted bicyclic[2.2.1]hepta-2,5-dienes.

To develop a theoretical nucleophilicity scale for substituted pyridine, attempts have been made for very few pyridines based on the intermolecular stretching force constant of H-bonded complexes and molecular electrostatic potential.[33] Recently, we made an effort for a theoretical evaluation of nucleophilicity values of few nitrogen nucleophiles along with six numbers of 4-substituted pyridine analogues.[34] Soliman also made an effort to determine the reactivity of some substituted pyridine ligands as nucleophile towards H^+, Cu^+ and Cu^{2+} Lewis acids as electrophile.[35] So far no elaborate study has been made for a theoretical correlation of nucleophilicity behavior of various substituted pyridines.

Within the context of density functional theory,[36,37] many global and local reactivity descriptors have been defined. Global and local reactivity descriptors are widely used to study the reactivity and selectivity of chemical species. A series of reviews has been published by Chattaraj regarding different reactivity descriptors such as chemical potential (μ), chemical hardness (η), softness (S) and electrophilicity index (ω).[37–39]

In this study, the earlier reported four methods for prediction of nucleophilicity were applied and tested for 3-substituted, 4-substituted, and 3,4,5-substituted pyridine in order to evaluate the suitability of method for each category of substituted pyridines. Based on our analysis, we made an effort to predict some new 4-substituted pyridine analogues with enhanced nucleophilicity values.

2. Computational Methods

One of the important global reactivity descriptor hardness η is defined as,[40]

$$\eta \approx (\mathrm{I} - \mathrm{A}) \tag{3}$$

Where I and A are the vertical ionization energy and electron affinity. Softness (S) is the reciprocal of hardness and defined as,

$$\mathrm{S} = \frac{1}{\eta} = \frac{1}{I - A} \tag{4}$$

Global electrophilicity index introduced by Parr *et al.,*[40,41] is expressed as,

$$\omega = \frac{\mu^2}{2\eta} \tag{5}$$

Where μ is the electronic chemical potential[42] defined as,

$$\mu = \frac{-(I + A)}{2} \tag{6}$$

Using Koopman's theorem, ionization energy (I) and electron affinity (A) can be replaced by the frontier molecular energies of HOMO (E_H) and LUMO (E_L) respectively. Therefore μ and η can be expressed as,

$$\eta = \mathrm{E_L} - \mathrm{E_H} \text{ and } \mu = \frac{E_L + E_H}{2} \tag{7}$$

In an important contribution, Gazquez *et al.,*[43] have defined electron donating power ω^- as,

$$\omega^- = \frac{I^2}{2(I - A)} \tag{8}$$

and

$$\omega^- = \frac{(3I + A)^2}{16(I - A)} \tag{9}$$

Domingo *et al.,*[44] proposed the simplest approach relating the nucleophilicity N with the highest occupied molecular orbital (HOMO) energy within the Kohn-Sham Scheme[45] as,

$$\mathrm{N} = \mathrm{E_{HOMO}} - \mathrm{E_{HOMO(TCE)}}\mathrm{eV} \tag{10}$$

Where tetracyanoethylene (TCE) was taken as a reference. In this scale, the nucleophilicity index for TCE

is N = 0.0 eV, presenting the lowest HOMO energy in a long series of organic molecules was already considered.

In order to rationalize with the general notion that "more is better" Roy *et al.*,[30] proposed the nucleophilicity index N″, as the inverse of electron donating (ω^-) power.[43] Since the nucleophilicity index obtained as $\frac{1}{\omega^-}$ was below 1, the author defined the nucleophilicity N″ & N‴ as[31]

$$N'' = \frac{1}{\omega^-} \times 10 \text{ and } N''' = \frac{1}{\omega^-} \times 10$$

Following methods[30] were adopted for the present study.

$$N = E_{HOMO} - E_{HOMO(TCE)} eV \quad (10) \quad \text{Method I}$$
$$N' = \frac{1}{\omega} \quad \text{where } \omega = \frac{\mu^2}{2\eta} \quad (11) \quad \text{Method II}$$
$$N'' = \frac{1}{\omega^-} \quad \text{where } \omega^- = \frac{I^2}{2(I-A)} \quad (12) \quad \text{Method III}$$
$$N''' = \frac{1}{\omega^-} \quad \text{where } \omega^- = \frac{(3I+A)^2}{16(I-A)} \quad (13) \quad \text{Method IV}$$

Geometries of all the molecules were first optimized using density functional three-parameter hybrid model (DFT/B3LYP).[46–48] The basis set for optimization is 6-31G(d,p). Single point energies were calculated on optimized geometries using DFT/B3LYP/6-311G+(d,p) level of theory to obtain the HOMO-LUMO energies in gas phase and solvent phase. For solvent phase calculation, polarizable continuum model was applied using the integral equation formalism variant (IEFPCM). All calculations were carried out using Gaussian03 Revision E.01 programme.[49]

3. Results and Discussion

Since experimental nucleophilicity values of a few 4-substituted pyridines are known in the literature,[25] initial study was carried out by taking examples of 4-substituted pyridines. Mayr has already determined the nucleophilicity values of six 4-substituted pyridines in dichloromethane. To verify the applicability of these theoritical methods, nucleophilicity indexs N, N′, N″ and N‴ were calculated in the gas phase based on the four methods I, II, III and IV, respectively, for all the 4-substituted pyridines for which the experimental nucleophilicity values were reported by Mayr.[25] The calculated values are listed in table 1. Leave one out cross validation and regression analysis by distributing the molecules in training and test sets indicated the validity of the methods (see Supplementary Information).

Calculated gas phase global nucleophilicity values determined by the method I, II, III and IV were plotted against Mayr's experimental nucleophilicity values (figure 1).

The regression coefficients (R^2) for Method I, II, III and IV are found to be 0.926, 0.930, 0.927 and 0.931, respectively. This result indicated that all the four methods generate similar correlation. It is well known that solvent plays an important role in nature for regulating the extent of interaction energy and reactivity

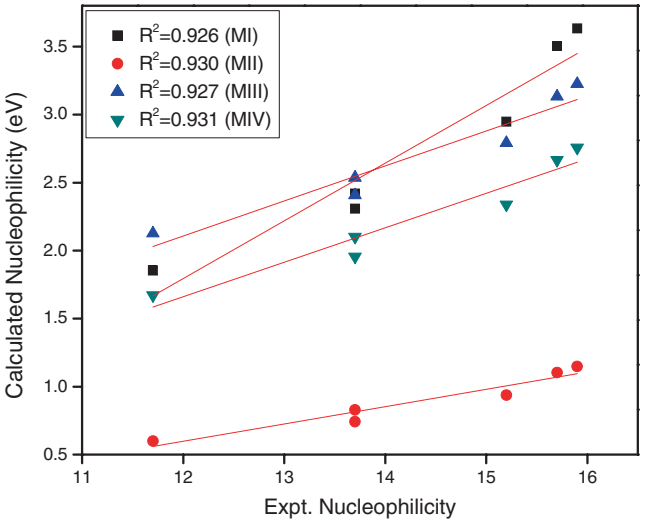

Figure 1. Gas phase nucleophilicity vs experimental nucleophilicity for 4-substituted pyridines.

Table 1. Calculated gas and solvent phase global nucleophilicity (eV) and Mayr's experimental values for six 4-substituted pyridines.

		N		N′		N″		N‴		N
Entry	Compound	Gas	Solvent	Gas	Solvent	Gas	Solvent	Gas	Solvent	Expt.[a]
1	4-chloropyridine	1.85	1.36	0.60	0.61	2.13	2.13	1.67	1.69	11.70
2	4-methylpyridine	2.31	1.69	0.74	0.72	2.41	2.34	1.95	1.90	13.70
3	4-methoxy pyridine	2.42	1.94	0.83	0.80	2.54	2.49	2.10	2.05	13.70
4	4-aminopyridine	2.95	2.64	0.94	0.95	2.79	2.83	2.34	2.37	15.20
5	4-(N,N-dimethylamino) pyridine	3.50	3.07	1.10	1.02	3.13	3.04	2.67	2.55	15.70
6	4-(pyrrolidino) pyridine	3.63	3.21	1.15	1.06	3.23	3.13	2.76	2.63	15.90

[a]Experimental values are taken from the literature[25]; Solvent=dichloromethane

amongst the molecule.[50–52] Since, experimental nucleophilicity values were obtained in dichloromethane, the global nucleophilicity parameters for all the six pyridines were calculated using the IEFPCM solvent model for dichloromethane (DCM) solution. The Calculated values are summarized in table 1.

The calculated solvent phase nucleophilicity values obtained by using the four methods were plotted against the experimental nucleophilicity values in the DCM solution (figure 2).

The R^2 values obtained for methods I, II, III and IV are found to be 0.919, 0.950, 0.933 and 0.943, respectively. Regression coefficients obtained from the above study indicate that inclusion of solvent model gives better correlation for method II, III and IV than gas phase calculation. For the method I, the R^2 value for solvent model decreases compared to gas phase calculation. However, these differences are negligible because of little difference in the nucleophilicity trends in gas phase and solvent phase calculation.

To verify the methods further, twelve commercially available 4-substituted pyridines for which Hammett substituent constant are known,[53] were chosen for nucleophilicity study. It has already been reported that the Hammett substituent constant can be taken as a standard for verification of the validity of the methods.[30,31] The gas phase global nucleophilicity were calculated using methods I, II, III and IV. A comparison of gas phase global nucleophilicity values with Hammett substituted constant (σ)values were summarized in table 2.

Further, the calculated gas phase global nucleophilicity values were plotted against the Hammett

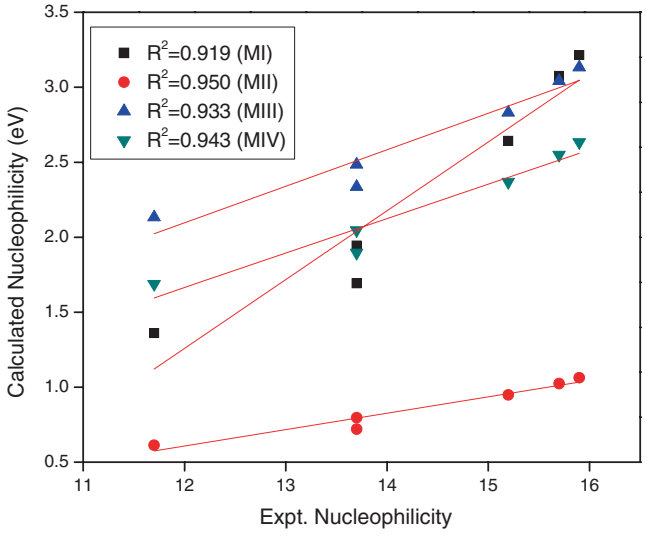

Figure 2. Calculated nucleophilicity in IEFPCM solvent model *vs.* expt. nucleophilicity for 4-substituted pyridines.

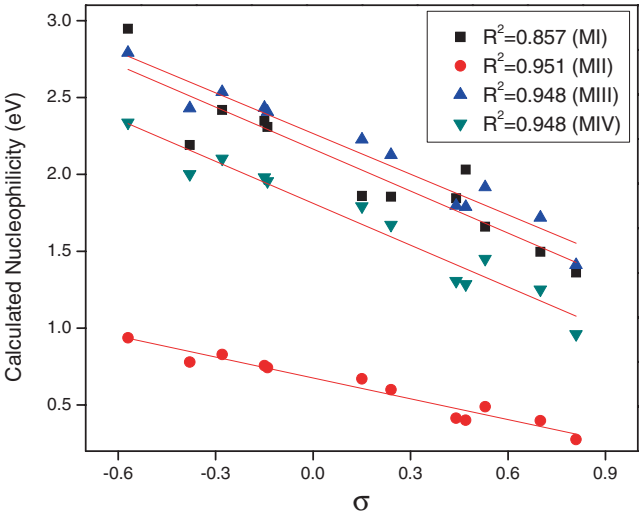

Figure 3. Gas phase Nucleophilicity *vs.* Hammett substituent constant (σ) for 4-substituted pyridines.

Table 2. Gas phase global nucleophilicity values for twelve 4-substituted pyridine and Hammett substituent constant[53] (σ) values.

Entry	Compound	N	N′	N″	N‴	σ
1	4-fluoropyridine	1.86	0.67	2.23	1.79	0.15
2	4-chloropyridine	1.85	0.60	2.13	1.67	0.24
3	4-nitropyridine	1.36	0.28	1.41	0.96	0.81
4	4-hydroxypyridine	2.19	0.78	2.43	2.00	−0.38
5	4-aminopyridine	2.95	0.94	2.79	2.34	−0.57
6	4-trifluoromethylpyridine	1.66	0.49	1.92	1.45	0.53
7	4-pyridinecarbonitrile	1.50	0.40	1.72	1.25	0.70
8	4-methylpyridine	2.31	0.74	2.41	1.95	−0.14
9	4-methoxypyridine	2.42	0.83	2.54	2.10	−0.28
10	4-acetylpyridine	2.03	0.40	1.79	1.29	0.47
11	4-tert-butylpyridine	2.35	0.76	2.43	1.98	−0.15
12	Isonicotinic acid	1.84	0.41	1.80	1.31	0.44

substituent constant (figure 3). For this case, the regression coefficients R^2 for the methods I, II, III and IV are found to be 0.857, 0.951, 0.948 and 0.948, respectively.

In this case also, the methods II, III and IV could generate better correlation with good regression coefficient as compared to method I. After having success in getting good correlation for nucleophilicity values for these substrates, another set of 36 commonly used 4-substituted pyridines were considered for predicting gas phase global nucleophilicity. Comparison of our theoretically calculated nucleophilicity values with the available experimental data revealed that the method II and IV are most successful with highest correlation value with experimental as well as Hammett substituent constant. Hence, method II and IV were applied for subsequent calculations of nucleophilicity values of these 36 numbers of 4-substituted pyridine analogues. Table 3 gives the nucleophilicity values applying both the methods.

Altogether, 50 numbers of 4-substituted pyridine nucleophiles were considered in this study. On the basis of gas phase global nucleophilicity value, the pyridines were arranged in such a way that the lowest nucleophilic pyridine is at the bottom of the scale (figure 4).

From this analysis, it can be concluded that 4-pyrrolidino pyridine has the highest nucleophilicity

Table 3. Gas phase global nucleophilicity values (eV) 36 commonly used 4-substituted pyridines calculated by method II and method IV.

Entry	Compound	N′	N‴
1	4-bromopyridine	0.59	1.66
2	4-pyridinecarboxaldehyde	0.36	1.18
3	Isonicotinamide	0.47	1.44
4	4-ethylpyridine	0.74	1.95
5	4-(1-aminoethyl)pyridine	0.75	1.99
6	4-(1H-pyrazol-4-yl)pyridine	0.63	1.79
7	4-(2-aminoethyl)pyridine	0.74	1.97
8	4-(3-phenylpropyl) pyridine	0.76	2.01
9	4-(4-formylphenyl)pyridine	0.38	1.24
10	4-(aminomethyl)pyridine	0.74	1.97
11	4-(boc-amino)pyridine	0.74	1.97
12	4-(bromomethyl)pyridine	0.50	1.49
13	4-(chloromethyl)pyridine	0.54	1.57
14	4-(ethylaminomethyl) pyridine	0.78	2.07
15	4-benzylpyridine	0.72	1.94
16	4-isobutylpyridine	0.74	1.95
17	1-(pyridin-4-ylmethyl) piperidine-3-carboxylic acid	0.77	2.07
18	(N,N-diethyl)-4-aminomethylpyridine	0.82	2.19
19	4-morpholinopyridine	0.93	2.38
20	4-phenylpyridine	0.57	1.68
21	4-pyridinemethanol	0.74	1.95
22	4-pyridinepropanol	0.77	2.01
23	4-pyridylacetic acid	0.67	1.83
24	4-pyridylacetonitrile	0.58	1.64
25	(4-pyridylthio)acetic acid	0.71	1.94
26	diphenyl-4-pyridylmethanol	0.69	1.89
27	diphenyl-4-pyridylmethane	0.72	1.95
28	Ethyl isonicotinate	0.45	1.40
29	Isonicotinoyl chloride	0.32	1.08
30	Ethyl 4-pyridylacetate	0.67	1.83
31	Methyl isonicotinate	0.45	1.38
32	Nialamide	0.55	1.63
33	1-(pyridine-4-yl)ethanol	0.74	1.95
34	1-(pyridin-4-ylmethyl) pyrrolidin-2-one	0.68	1.88
35	1-(pyridin-4-ylmethyl) piperidine-4-carboxylic acid	0.75	2.03
36	4-thionitrosopyridine	0.14	0.59

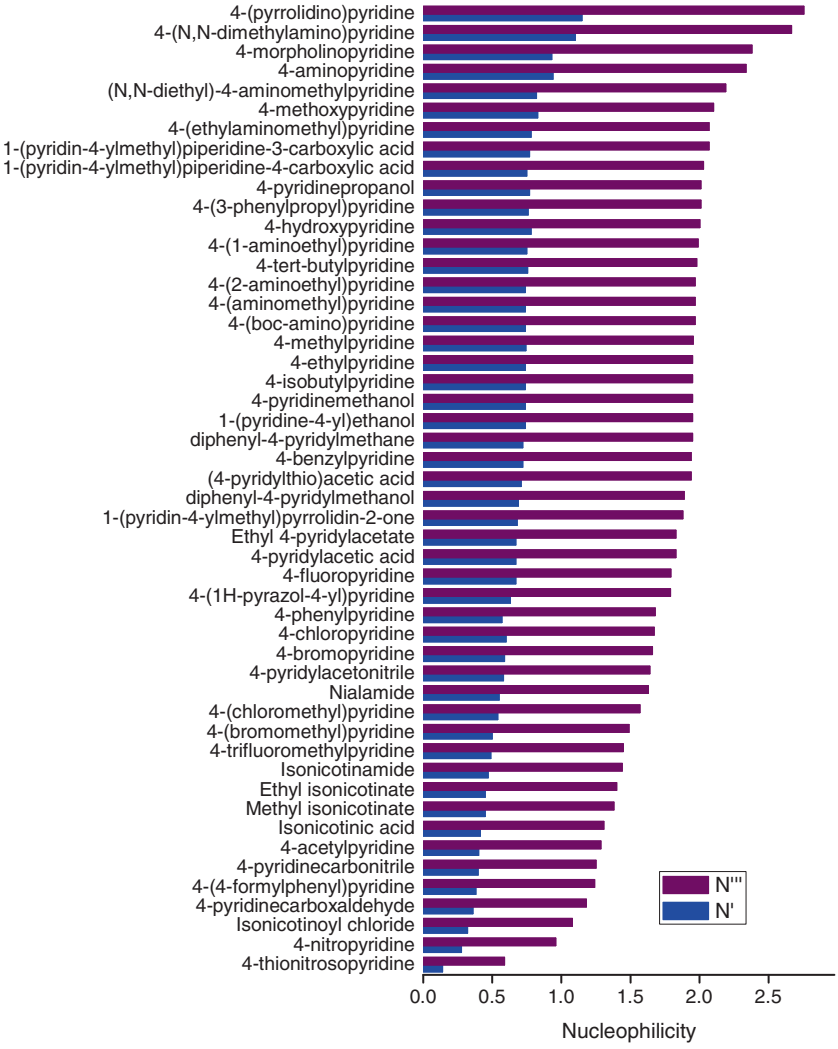

Figure 4. Nucleophilicity scale of 50 no. of 4-substituted pyridines based on gas phase calculation.

value among all 4-substituted pyridines. Both the experimental as well as theoretical methods placed it on the top of the scale in terms of nucleophilic behavior followed by 4-dimethylaminopyridine (DMAP). 4-Morpholinopyridine and 4-aminopyridine have similar values of nucleophilicity as predicted by method II

Table 4. Gas phase global nucleophilicity values (eV) of 12 no. of 3-substituted pyridines and Hammett substituent constant[53] (σ) values.

Entry	Compound	N	N′	N″	N‴	σ
1	3-fluoropyridine	1.96	0.60	2.14	1.68	0.34
2	3-chloropyridine	2.07	0.59	2.15	1.68	0.37
3	3-nitropyridine	1.39	0.30	1.47	1.01	0.71
4	3-hydroxypyridine	2.68	0.71	2.44	1.93	0.13
5	3-aminopyridine	3.30	0.82	2.74	2.20	−0.09
6	3-trifluoromethylpyridine	1.65	0.52	1.97	1.50	0.46
7	3-pyridinecarbonitrile	1.49	0.43	1.79	1.33	0.62
8	3-methylpyridine	2.33	0.71	2.37	1.91	−0.06
9	3-methoxypyridine	2.86	0.76	2.56	2.05	0.10
10	3-acetylpyridine	2.17	0.44	1.89	1.38	0.36
11	3-tert-butylpyridine	2.43	0.74	2.43	1.97	−0.09
12	Nicotinic acid	1.89	0.45	1.88	1.39	0.35

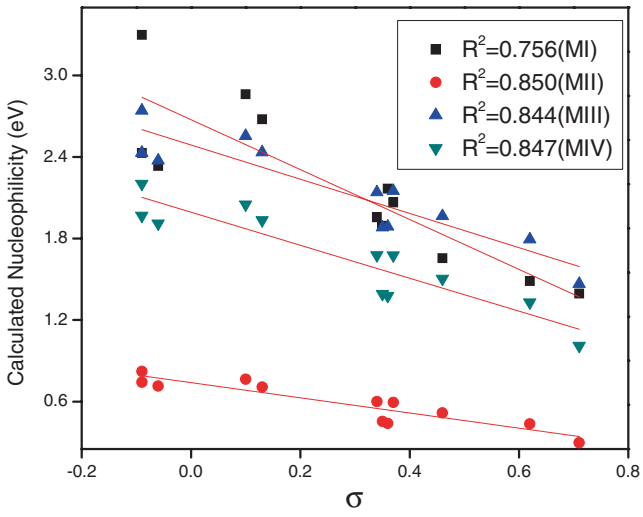

Figure 5. Gas phase nucleophilicity *vs.* Hammett substituent constant (σ) for 3-substituted pyridines.

and IV. The analysis further confirms the negative impact of electron withdrawing substituent by placing 4-thionitrosopyridine and 4-nitropyridine at the bottom and second from the bottom of the scale respectively. Encouraged by the positive correlation of our analysis with the experimental results for 4-substituted pyridines, we intended to extend our study for 3-substituted pyridines. However, no experimental data was found in the literature regarding the nucleophilicity value of 3-substituted pyridines. Accordingly, twelve 3-substituted pyridines having known values of Hammett substituent constant,[53] were considered for the determination of the gas phase global nucleophilicity. A comparative assessment of the nucleophilicities of 3-substituted pyridines using all the four methods and their Hammett substituent constant (σ) is summarized in table 4.

Table 5. Gas phase global nucleophilicity values (eV) of 32 commonly used 3-substituted pyridines calculated by methods II and IV.

Compound	N′	N‴
3-bromopyridine	0.59	1.69
Nicotamide	0.52	1.54
3-ethylpyridine	0.73	1.94
trans-3-(3-pyridyl)acrylic acid	0.38	1.25
3-pyridylacetonitrile	0.59	1.65
3-pyridylacetic acid	0.67	1.83
3-thionitrosopyridine	0.16	0.65
N-boc-3-aminomethylpyridine	0.69	1.87
Nicotinic hydrazide	0.51	1.51
Nicotinanilide	0.53	1.61
N,N-diethylnicotinamide	0.64	1.80
Methyl nicotinate	0.49	1.47
Ethyl 3-pyridylacetate	0.69	1.87
1-(pyridin-3-ylmethyl)piperidine-3-carboxylic acid	0.78	2.11
3-(pyrrol-1-ylmethyl)pyridine	0.72	2.04
3-(5-piperidin-4-yl-1,2,4-oxadiazol-3-yl)pyridine	0.53	1.61
3-pyridinepropanol	0.72	1.92
Ethyl nicotinate	0.50	1.49
Benzyl nicotinate	0.50	1.50
3-pyridinemethanol	0.72	1.94
3-pyridinealdoxime	0.51	1.56
3-picolylamine	0.76	2.02
3-ethynylpyridine	0.56	1.65
3-butylpyridine	0.74	1.95
3-benzoylpyridine	0.41	1.33
3-acetoxypyridine	0.66	1.80
3-(boc-amino)pyridine	0.75	2.04
3-pyridylpropanoic acid	0.67	1.82
3-isopropylpyridine	0.73	1.94
N,N-dimethyl-3-aminopyridine	0.94	2.47
(N,N-diethyl)-3-aminomethylpyridine	0.81	2.19
3-(pyrrolidino)pyridine	0.99	2.59

The calculated gas phase global nucleophilicity values were plotted against the Hammett substituent constant (figure 5). The regression coefficients for Methods I, II, III and IV were found to be 0.756, 0.850, 0.844 and 0.847, respectively. These methods could produce a moderate correlation of theoretical nucleophilicity trend of 3-substituted pyridines with respective Hammett substituent constants.

From the regression coefficient values (figure 5), it can be seen that Method II, III and IV produced similar results for 3-substituted pyridines, whereas method I showed somewhat poor correlation. Hence, methods II and IV, which produced the best fit, were considered for subsequent determination of nucleophilicity values of additional 32 commonly used 3-substituted pyridines. Results for the global nucleophilicity values are illustrated in table 5.

Finally, a total of 44 3-substituted pyridines were evaluated and a nucleophilicity scale has been constructed based on the results obtained from methods II and IV (figure 6). From this scale, it was found that 3-pyrrolidino pyridine has the the highest and 3-thionitrosopyridine has the lowest nucleophilicity value.

Mayr *et al.*,[26] recently synthesized highly nucleophilic 3,4,5-triamino-substituted pyridine and determined their nucleophilicity in acetonitrile solution. We therefore made an attempt to substantiate the best theoretical model for prediction of nucleophilicity for 3,4,5-substituted pyridines reported by Mayr.[26] The global nucleophilicity values are determined by gas phase calculation of HOMO-LUMO energy of the corresponding Mayr's 3,4,5-triamino-substituted pyridines. The results obtained using all the four methods are summarized in table 6.

The calculated global nucleophilicity values were plotted against the Mayr's experimental nucleophilicity values (figure 7).

The regression coefficient R^2 values were found to be 0.791, 0.743, 0.822 and 0.793 for method I, II, III and IV, respectively. From the regression coefficient

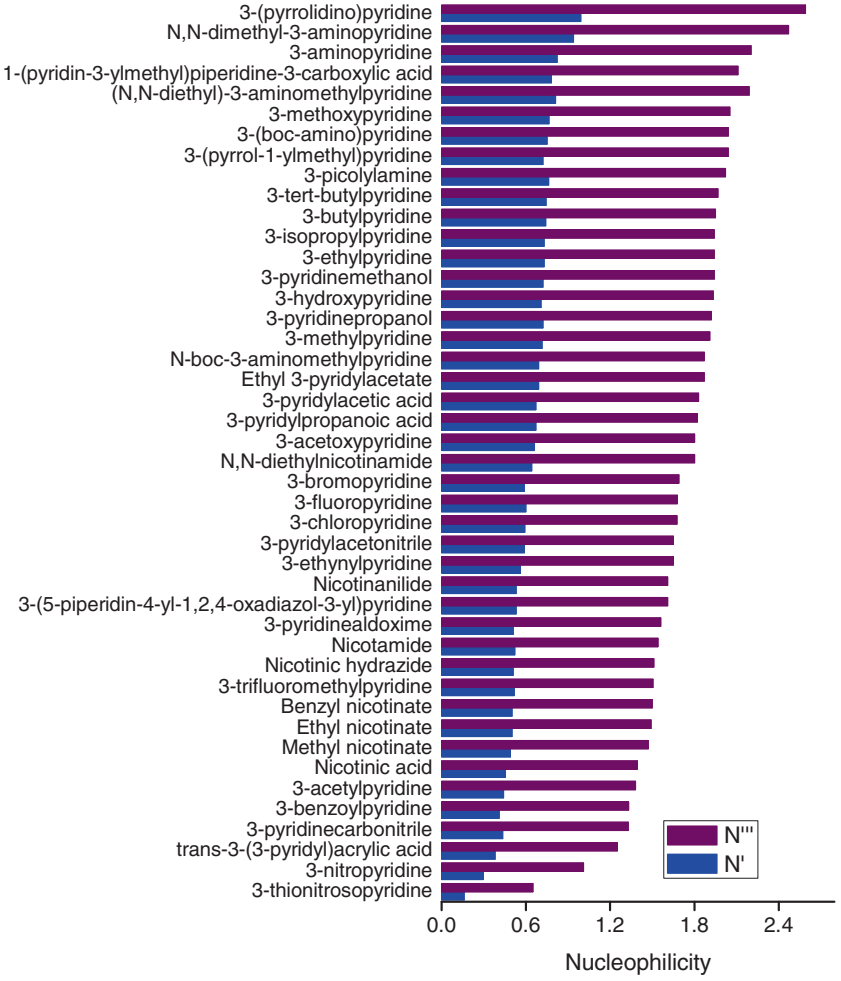

Figure 6. Nucleophilicity scale of 44 no. of 3-substituted pyridines based on gas phase calculation.

Table 6. Calculated gas and solvent phase global nucleophilicity (eV) and experimental values of Mayr's 3,4,5-substituted pyridine.

Entry	Compound		N		N′		N″		N‴		
			Gas	Solvent	Gas	Solvent	Gas	Solvent	Gas	Solvent	N Expt.[a]
1	M-2Bn	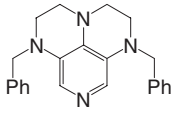	4.43	3.95	1.11	1.06	3.50	3.40	2.87	2.78	17.69
2	M-2Et	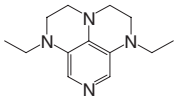	4.39	3.78	1.29	1.17	3.67	3.46	3.12	2.90	16.81
3	M-2Me	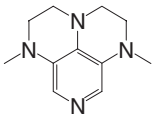	4.31	3.88	1.27	1.20	3.62	3.53	3.08	2.97	16.65
4	M-2Ac	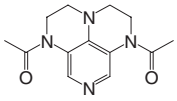	3.32	3.05	0.78	0.79	2.69	2.74	2.14	2.17	15.39
5	M-2Bz	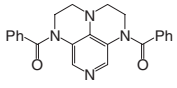	3.46	3.14	0.61	0.59	2.45	2.43	1.83	1.81	14.19

[a]Experimental values are taken from the literature[26]; Solvent=acetonitrile.

(R^2) analysis it was found that Method III gave the best fit compared to the other three methods. The linearity relation values were not decent for all the four methods compared to those obtained for 4-substituted pyridines. To check whether inclusion of solvent model in the calculation has any effect on linearity relation or not, the solvent phase global nucleophilicity of Mayr's 3,4,5-triamino-substituted pyridines were calculated. For the solvent phase calculation of nucleophilicity, acetonitrile was used as solvent and the IEFPCM as a model. Applying the four methods of calculation, the nucleophilicity values were tabulated (table 6).

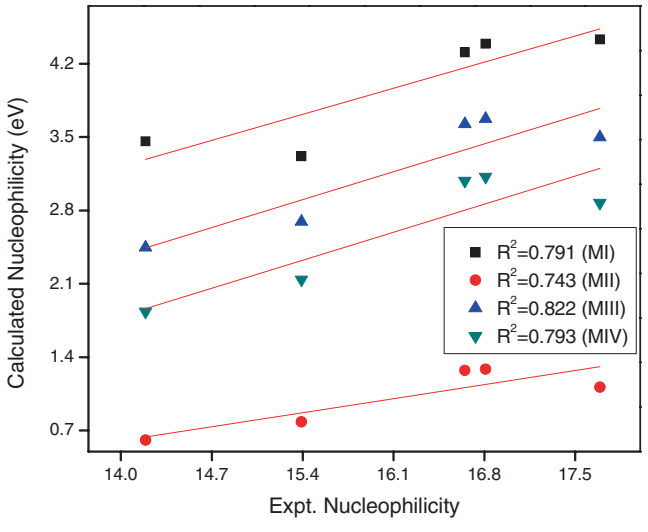

Figure 7. Gas phase Nucleophilicity *vs.* Expt. Nucleophilicity for 3,4,5-substituted pyridines.

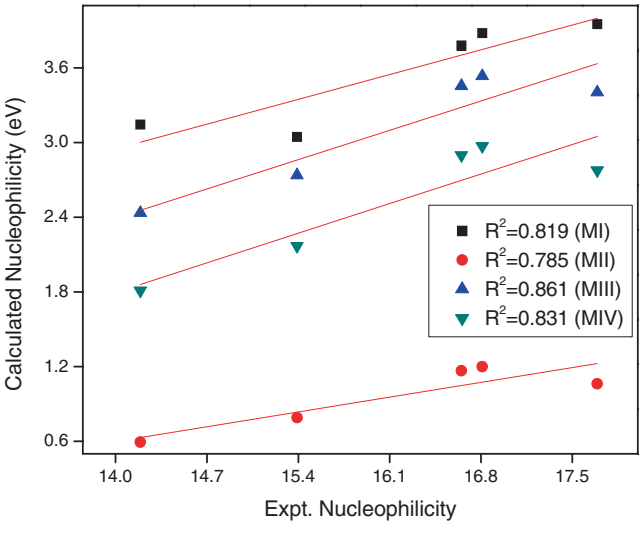

Figure 8. Calculated Nucleophilicity in IEFPCM solvent model vs Experimental Nucleophilicity for 3,4,5-substituted pyridines.

A graphical representation of the results of the calculated solvent phase nucleophilicities against Mayr's experimental nucleophilicity values is shown in figure 8. An interesting result came out of this study. As per experimental results, M-2Bn has the highest nucleophilicity value among all 5 experimentally synthesized pyridines. In our theoretical study, only method I is successful to predict the highest nucleophilicity value of M-2Bn. But it is unsuccessful to predict the trend of nucleohilicity for M-2Ac and M-2Bz. Whereas method II, III and IV were able to predict the correct trend of nucleophilicity of M-2Me, M-2Et, M-2Ac and M-2Bz, but particularly unsuccessful to predict the highest nucleophilicity value of M-2Bn.

In the solvent phase calculation, the regression coefficient (R^2) values were also analyzed. For all methods, it was found that the linearity relation value increases significantly. Method III generates the best fit for the solvent phase calculation also. The R^2 value increases in this case for Method III from 0.822 to 0.861. Therefore the gas phase global nucleophilicity for additional commonly available 26 3,4,5-substituted pyridines were also determined by applying method III. The gas phase global nucleophilicity values, calculated by method III are listed in table 7.

A nucleophilicity scale has been constructed (figure 9) for 31 numbers of 3,4,5-substituted pyridines. From the scale we found that 3,5-dimethyl-4-aminopyridine has the highest nucleophilicity value among the 26 pyridines considered in table 7.

3.1 *Construction of new molecules of 4-substituted pyridine*

Amongst the three categories of substituted pyridines considered in the present study, a good correlation of calculated values with experimental nucleophilicity values as well as Hammett substituent constant has been obtained only for 4-substituted pyridines. This study also supported by the experimental observation of superior nucleophilic character of 4-(pyrrolidino)pyridine,

Table 7. Gas phase global nucleophilicity values (eV) of 26 commonly available 3,4,5-substituted pyridine calculated by Method III.

Entry	Compound	N″
1	3,5-dichloro-4-pyridinecarbonitrile	1.58
2	3,5-dichloro-4-pyridinecarboxaldehyde	1.53
3	3,5-dichloropyridine-4-carboxylic acid	1.91
4	3,5-difluoro-4-formylpyridine	1.53
5	3,5-difluoropyridine-4-carboxylic acid	1.69
6	3.5-dimethyl-4-aminopyridine	2.98
7	Methyl 3,5-dichloropyridine-4-carboxylate	1.96
8	1-(3,5-dichloropyridin-4-yl)piperazine	2.48
9	3,4,5-trichloropyridine	1.96
10	3,5-dibromo-4-pyridinecarboxaldehyde	1.54
11	3-amino-4-chloro-5-methoxypyridine	2.59
12	3,5-dichloro-4-methylpyridine	2.13
13	4-bromo-3-chloro-5-nitropyridine	1.43
14	4-amino-3-bromo-5-chloropyridine	2.43
15	4-bromo-3,5-dichloropyridine	1.95
16	3-bromo-5-hydroxy-4-pyridinecarboxylic acid	1.73
17	3,4-dichloro-5-pyridinecarboxylic acid	1.73
18	4-amino-5-methyl-3-nitropyridine	1.65
19	5-chloro-3,4-diaminopyridine	2.82
20	5-bromo-3,4-diaminopyridine	2.81
21	3-bromo-5-methyl-4-nitropyridine	1.53
22	3-amino-5-methoxyisonicotinonitrile	2.15
23	4-amino-3,5-dichloropyridine	2.43
24	4-amino-5-bromo-3-methylpyridine	2.70
25	3,5-dichloro-4-nitropyridine	1.50
26	3-chloro-5-hydroxy-4-pyridinecarboxylic acid	1.73

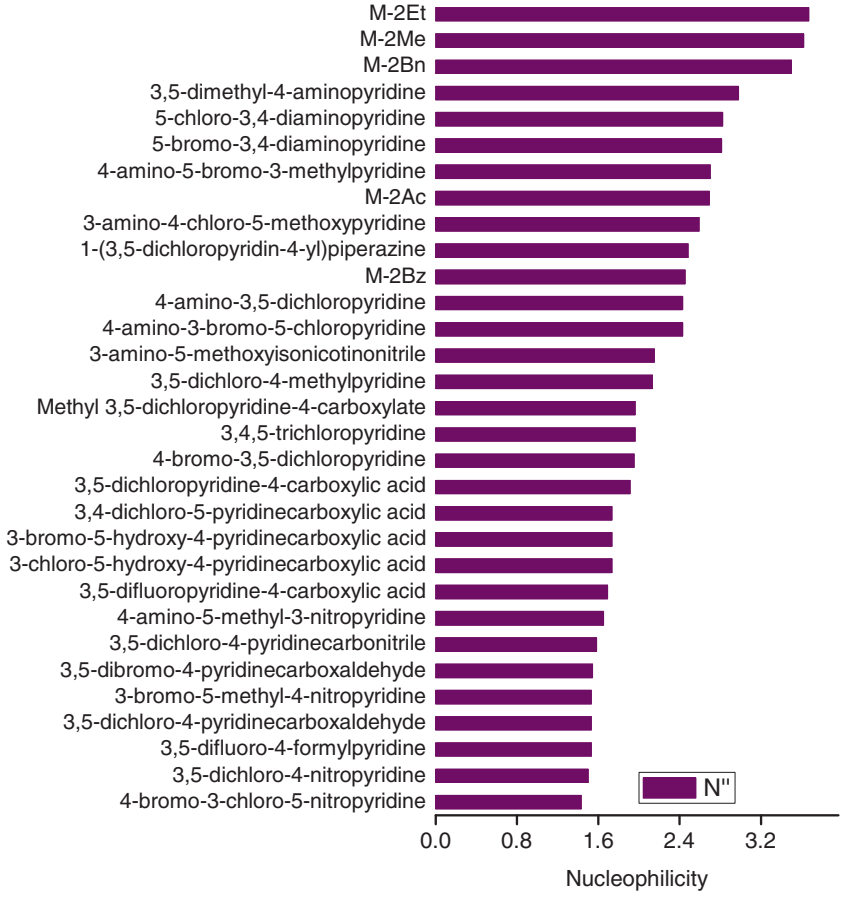

Figure 9. Nucleophilicity scale of 31 no. of 3,4,5-substituted pyridine based on gas phase calculation.

$\mathbf{T_1}$. However, it is highly desirable to construct pyridines having better nucleophilic property than $\mathbf{T_1}$. Hence, a total of 30 new 4-(N,N-disubstituted)pyridines having structural similarity with $\mathbf{T_1}$ have been proposed. To find out the best choice out of all these proposed pyridines, nucleophilicity values were computed using method IV. Method IV has been chosen because it gives good correlation value for experimental as well as Hammett substitution constant (σ) for 4-substituted pyridines. Furthermore, method IV is particularly consistent in predicting nucleophilicity trends among all categories of pyridines studied here. The nucleophilicity values calculated for newly proposed molecules obtained by using method IV are summarized in table 8.

It can be seen from table 8 that six molecules show better nucleophilic behavior than pyridine $\mathbf{T_1}$. Analysis of the results revealed that the nucleophilicity value decreases on expansion of the ring size (table 8, molecules $\mathbf{T_2}$ and $\mathbf{T_{11}}$). A similar trend was observed when molecules are proposed with decreasing ring size (table 8, molecules $\mathbf{T_8}$ and $\mathbf{T_9}$). Nucleophilicity of $\mathbf{T_2}$ decreases on substitution of dimethyl group in 2 and 6 position of the piperidine ring (table 8, molecule $\mathbf{T_{31}}$). But, nucleophilicity of $\mathbf{T_{11}}$ could be enhanced significantly by substituting -$(CH_2)_n$-group in 2 and 6 position of azepane ring, where n=3,4 (table 8, molecules $\mathbf{T_{28}}$ and $\mathbf{T_{29}}$). Substitution of dimethyl amino group in 2 and 5 position of the pyrrolidine ring (table 8, molecule $\mathbf{T_{13}}$) decreases nucleophilicity. Methyl and dimethyl substituent in 2 and 5 position of the pyrrolidine ring (table 8, molecules $\mathbf{T_{20}}$ and $\mathbf{T_{27}}$) increases the nucleophilicity. Substitution by -$(CH_2)_n$- increases the nucleophilicity for n=4 (molecule $\mathbf{T_{26}}$) but decreases the nucleophilicity for n=2 and 3 (table 8, molecules $\mathbf{T_{19}}$ and $\mathbf{T_{30}}$). Substitution of piperazine at 4-position of the pyridine ring does not increase the nucleophilicity of the pyridine ring (molecule $\mathbf{T_{10}}$). The nucleophilicity of T_{10} compared to T_1 can be enhanced by substitution, particularly for molecule $\mathbf{T_{24}}$. Other substituent does not increase the nucleophilicity of $\mathbf{T_{10}}$ (molecules $\mathbf{T_7}$, $\mathbf{T_{17}}$, $\mathbf{T_{22}}$, $\mathbf{T_{23}}$ and $\mathbf{T_{25}}$). A comparative evaluation of newly designed 4-(N, N-disubstituted)pyridines having nucleophilic profile better than $\mathbf{T_1}$ have been illustrated in figure 10.

Table 8. Gas phase global nucleophilicity values of constructed pyridine molecule based on Method IV.

No.	Compound	E_{HOMO}(au)	E_{LUMO}(au)	η(eV)	μ(eV)	ω^{-}(eV)	N'''(eV)
T_1	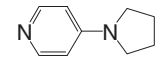	−0.21411	−0.01287	5.47602	3.088221	3.627974	2.756
T_2	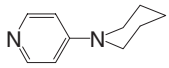	−0.22105	−0.02077	5.449897	3.290129	3.97195	2.518
T_3	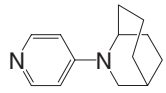	−0.21170	−0.01540	5.341596	3.089853	3.666106	2.728
T_4	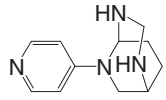	−0.21826	−0.01755	5.461598	3.208359	3.830246	2.611
T_5	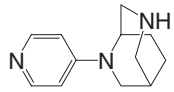	−0.21191	−0.01871	5.257241	3.137745	3.77019	2.652
T_6	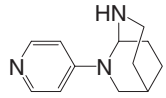	−0.21435	−0.01772	5.350576	3.157474	3.776431	2.648
T_7	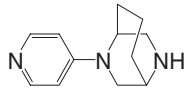	−0.21454	−0.01763	5.358195	3.158834	3.776542	2.648
T_8	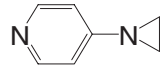	−0.24206	−0.02923	5.7914	3.691089	4.559984	2.193
T_9	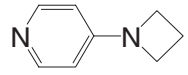	−0.22099	−0.01574	5.585138	3.220876	3.816947	2.620
T_{10}	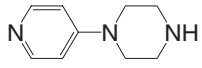	−0.21701	−0.01708	5.440373	3.184957	3.797071	2.634
T_{11}	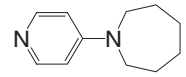	−0.21471	−0.01529	5.426495	3.12931	3.708397	2.697
T_{12}	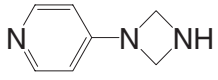	−0.23061	−0.02335	5.639833	3.455302	4.197068	2.383
T_{13}	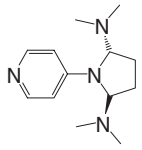	−0.21591	−0.01345	5.509218	3.120602	3.672239	2.723
T_{14}	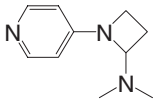	−0.22328	−0.01608	5.6382	3.256659	3.861784	2.589
T_{15}	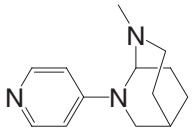	−0.21524	−0.01467	5.457788	3.128085	3.69799	2.704
T_{16}	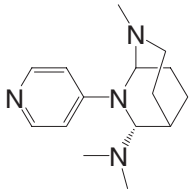	−0.22013	−0.01414	5.605274	3.187406	3.756532	2.662
T_{17}	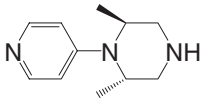	−0.21569	−0.01431	5.47983	3.12931	3.694167	2.707

Table 8. (continued)

No.	Compound	E_{HOMO}(au)	E_{LUMO}(au)	η(eV)	μ(eV)	ω^{-}(eV)	N'''(eV)
T_{18}	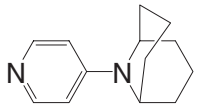	−0.21213	−0.01455	5.376426	3.084139	3.647285	2.742
T_{19}	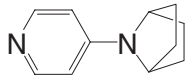	−0.22310	−0.01738	5.597927	3.271898	3.89819	2.565
T_{20}	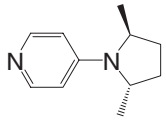	−0.21290	−0.01236	5.456972	3.064819	3.594775	2.782
T_{21}	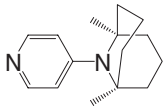	−0.21724	−0.03812	4.874104	3.47435	4.518387	2.213
T_{22}	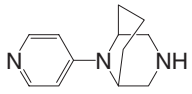	−0.21222	−0.01707	5.310303	3.11965	3.724423	2.685
T_{23}	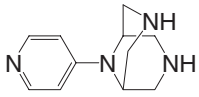	−0.20459	−0.01923	5.043903	3.045227	3.676395	2.720
T_{24}	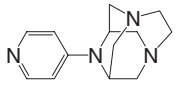	−0.20316	−0.01745	5.053427	3.001552	3.599429	2.778
T_{25}	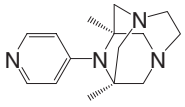	−0.19820	−0.03897	4.33287	3.226863	4.28741	2.332
T_{26}	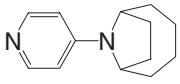	−0.21189	−0.01357	5.396563	3.06754	3.614721	2.766
T_{27}	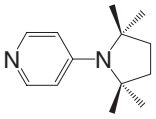	−0.21176	−0.01205	5.434387	3.045091	3.568473	2.802
T_{28}	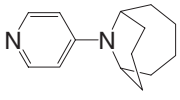	−0.21198	−0.01337	5.404454	3.066043	3.610221	2.770
T_{29}	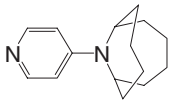	−0.21159	−0.01319	5.39874	3.058288	3.59903	2.779
T_{30}	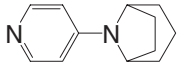	−0.21497	−0.01479	5.447176	3.126044	3.697456	2.705
T_{31}	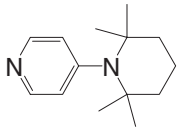	−0.21811	−0.03825	4.894241	3.487956	4.535614	2.205

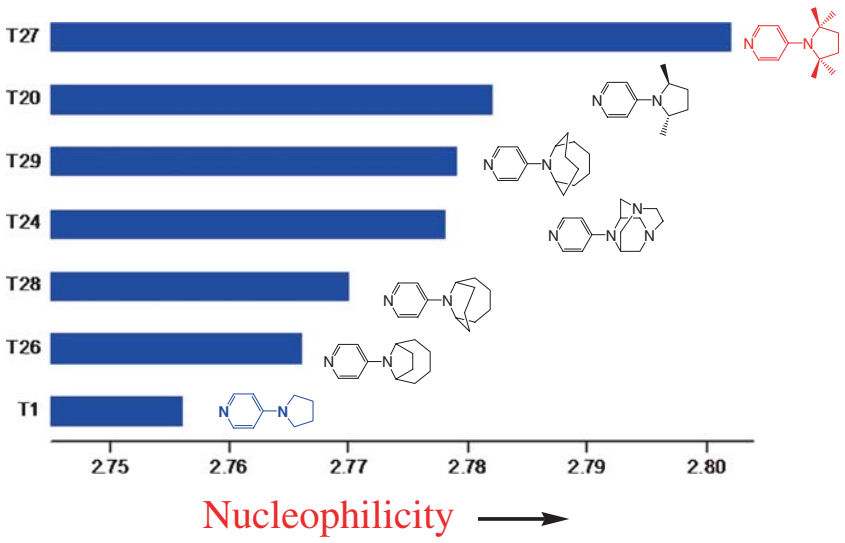

Figure 10. Nucleophilicity scale of the proposed molecules having nucleophilic profile better than $\mathbf{T_1}$ based on Method IV.

4. Conclusions

A theoretical study has been carried out to correlate the nucleophilic behavior of altogether 125 commonly available 3-substituted pyridines, 4-substituted pyridines and 3,4,5-substituted pyridines. Initially, the goodness and linearity of all the four methods of the present study for 3-substituted, 4-substituted and 3,4,5-substituted pyridines were established. Amongst the three categories of pyridines, only 4-substituted pyridines show very good correlation with experimental as well as Hammett substituent constant. The predictive performance of all the four models were found to follow a declining trend when substitutions are present in 3-position of the pyridine ring. This may be due to the different electronic effect operating in the pyridine ring for *meta*-substitution. Gas phase calculation for 4-substituted pyridines show that method I gives poor R^2 values with Hammett substituent constant, whereas R^2 values are similar for all methods with Mayr's experimental values. Inclusion of solvent model increases the linearity between calculated and experimental values for 4-substituted and 3,4,5-substituted pyridines. With the help of this model 30 new 4-substituted pyridine molecules were constructed and the gas phase nucleophilicity values were evaluated. The nature of substitution and ring size of the substituent have great influence on the nucleophilicity of 4-substituted pyridines. On the basis of our study, molecules $\mathbf{T_{20}}$, $\mathbf{T_{24}}$, $\mathbf{T_{26}}$, $\mathbf{T_{27}}$, $\mathbf{T_{28}}$ and $\mathbf{T_{29}}$ are found to be more nucleophilic in nature. These molecules deserve the experimental validation of nucleophilicity as well as effectiveness as organocatalyst.

Supplementary Information (SI)

Additional information pertaining to leave-one-out correlation and regression analysis by distribution of molecules into training and test sets is available in Supporting Information at www.ias.ac.in/chemsci.

Acknowledgements

Financial support from UGC (Grant No. 41-206/2012/SR) is gratefully acknowledged.

References

1. Ramsay W 1876 *Phil. Mag.* **2** 269
2. Wu W, Kong H, Li H, Ho Y, Gao Y, Hao J, Murphy M B, Lam M H, Wong K and Lee C 2011 *Eur. J. Org. Chem.* **26** 5054
3. Wu J, Kang S, Song B, Hu D, He M, Jin L and Yang S 2012 *Chem. Central J.* **62** 8
4. Di X, Liu Y, Liu Y, Yu X, Xiao H, Tian X and Gao R 2007 *Pesticide Biochem. Physiol.* **89** 81
5. Dorn F, Pfiffner A and Schlageter M 1991 *ACS Symposium Series* **443** 506
6. Lee L F, Stikes G L, Normansell J E, Molyneaux J M, Sing L Y L, Chupp J P, Parrish S K and Kaufmann J E 1991 *ACS Symposium Series* **443** 195
7. Peine G, Hoffmann P, Seifert G and Schilling G 1985 *Biochem. Physiol. Pflanzen* **180** 1
8. Harris R L N, Huppatz J L, Phillips J N and Teitei T 1979 In *Advances in Pesticide Science* H Geissbühler, G T Brooks and P C Kearney (Eds.) (Oxford: Pergamon) p. 99
9. Willand-Charnley R, Fisher T J, Johnson B M and Dussault P H 2012 *Org. Lett.* **14** 2242
10. Zhang Y, Zhang Y, Sun Y L, Du X, Shi J Y, Wang W D and Wang W 2012 *Chem. Eur. J.* **18** 6328

11. Ko K, Nakano K, Watanabe S, Ichikawa Y and Kotsuki H 2009 *Tetrahedron Lett.* **50** 4025
12. Xu X, Tang Z, Wang Y, Luo S, Cun L and Gong L 2007 *J. Org. Chem.* **72** 9905
13. List B 2007 *Chem. Rev.* **107** 5413
14. Cheong P H-Y, Legault C Y, Um J M, Çelebi-Ołcųm N and Houk K N 2011 *Chem. Rev.* **111** 5042
15. De Rycke N, Couty F and David O R P 2011 *Chem. Eur. J.* **17** 12852
16. Geerlings P, De Proft F and Langenaeker W 2003 *Chem. Rev.* **103** 1793
17. Ingold C K 1934 *Chem. Rev.* **15** 225
18. Swain C G and Scott C B 1953 *J. Am. Chem. Soc.* **75** 141
19. Edwards J O 1954 *J. Am. Chem. Soc.* **76** 1540
20. Edwards J O and Pearson R G 1962 *J. Am. Chem. Soc.* **84** 16
21. Bunnett J F 1963 *Ann. Rev. Phys. Chem.* **14** 271
22. Pearson R G, Sobel H and Songstad J 1968 *J. Am. Chem. Soc.* **90** 319
23. Legon A C and Millen D J 1987 *J. Am. Chem. Soc.* **109** 356
24. Legon A C and Millen D J 1987 *Acc. Chem. Res.* **20** 39
25. Brotzel F, Kempf B, Singer T, Zipse H and Mayr H 2007 *Chem. Eur. J.* **13** 336
26. De Rycke N, Berionni G, Couty F, Mayr H, Goumont R and David O R P 2011 *Org. Lett.* **13** 530
27. Campodonico P, Santos J G, Andres J and Contreras R 2004 *J. Phys. Org. Chem.* **17** 273
28. Contreras R, Andres J, Safont V S, Campodonico P and Santos J G 2003 *J. Phys. Chem. A* **107** 5588
29. Chattaraj P K and Maiti B 2001 *J. Phys. Chem. A* **105** 169
30. Pratihar S and Roy S 2010 *J. Org. Chem.* **75** 4957
31. Pratihar S and Roy S 2011 *Organometallics* **30** 3257
32. Domingo L R and Pérez P 2011 *Org. Biomol. Chem.* **9** 7168
33. Campodónico P R and Aizman A 2006 *Chem. Phys. Lett.* **422** 204
34. Deuri S and Phukan P 2012 *Comput. Theor. Chem.* **980** 49
35. Soliman S M 2012 *Comput. Theor. Chem.* **994** 105
36. Ess D H, Jones G O and Houk K N 2006 *Adv. Synth. Catal.* **348** 2337
37. Chattaraj P K, Sarkar U and Roy D R 2006 *Chem. Rev.* **106** 2065
38. Chattaraj P K and Roy D R 2007 *Chem. Rev.* **107** PR46
39. Chattaraj P K, Giri S and Duley S 2011 *Chem. Rev.* **111** PR43
40. Parr R G and Pearson R G 1983 *J. Am. Chem. Soc.* **105** 7512
41. Parr R G, Von Szentpaly L and Liu S 1999 *J. Am. Chem. Soc.* **121** 1922
42. Parr R G, Donnelly R A, Levy M and Palke W E 1978 *J. Chem. Phys.* **68** 3801
43. Gázquez J L, Cedillo A and Vela A 2007 *J. Phys. Chem. A* **111** 1966
44. Domingo L R, Chamorro E and Perez P 2008 *J. Org. Chem.* **73** 4615
45. Kohn W and Sham L J 1965 *Phys. Rev.* **140** 1133
46. Becke A D 1993 *J. Chem. Phys.* **98** 5648
47. Lee C, Yang W and Parr R G 1988 *Phys. Rev. B* **37** 785
48. Cohen A, Mori-Sánchez P and Yang W 2012 *Chem. Rev.* **112** 289
49. Frisch M J, Trucks G W, Schlegel H B, Scuseria G E, Robb M A, Cheeseman J R, Zakrzewski V G, Montgomery J A, Stratmann R E, Burant J C, Dapprich S, Millam J M, Daniels A D, Kudin K N, Strain M C, Farkas O, Tomasi J, Barone V, Cossi M, Cammi R, Mennucci B, Pomelli C, Adamo C, Clifford S, Ochterski J, Petersson G A, Ayala P Y, Cui Q, Morokuma K, Malick D K, Rabuck A D, Raghavachari K, Foresman J B, Cioslowski J, Ortiz J V, Baboul A G, Stefanov B B, Liu G, Liashenko A, Piskorz P, Komaromi I, Gomperts R, Martin R L, Fox D J, Keith T, Al- Laham M A, Peng C Y, Nanayakkara A, Gonzalez C, Challacombe M, Gill P M W, Johnson B, Chen W, Wong M W, Andres J L, Gonzalez C, Head Gordon M, Replogle E S and Pople J A 2004 GAUSSIAN 03, Revision E.01, (Gaussian Inc.: Wallingford, CT)
50. Swain C G, Swain M S, Powell A L and Alunni S 1983 *J. Am. Chem. Soc.* **105** 502
51. Um I-H, Lee E-J and Jeon S-E 2002 *J. Phys. Org. Chem.* **15** 561
52. Kim Y, Cramer C J and Truhlar D G 2009 *J. Phys. Chem. A* **113** 9109
53. Smith M B and March J 2007 In *Advanced Organic Chemistry: Reactions, Mechanism and Structure* 6th edn., (Hoboken- New Jersey: John Wiley)

THE JOURNAL OF PHYSICAL CHEMISTRY A

Article

pubs.acs.org/JPCA

Theoretical Insights on the Interaction of N-Heterocyclic Carbenes with Tetravalent Silicon Reagents

Dipanjali Pathak,[†] Sanjib Deuri,[‡] and Prodeep Phukan*[,†]

[†]Department of Chemistry, Gauhati University, Guwahati 781 001, Assam, India

[‡]Department of Chemistry, M. C. College, Barpeta 781 301, Assam, India

Supporting Information

ABSTRACT: Lewis acid−base type interaction between *N*-heterocyclic carbene (NHC) and tetravalent silicon reagent (SiR) has been investigated computationally. This NHC−Si interaction is of fundamental importance to the understanding of variety of NHC catalyzed organic transformations involving silicon compounds such as cyanosilylation, trifluoromethylsilylation, etc. Geometries of 24 NHCs, 10 silicon reagents, and their 61 Lewis acid−base complexes have been optimized using the B3LYP/6-31+G(d,p) and M05-2X/6-31+G(d,p) level of theory. The strength of NHC−Si interaction has been assessed in terms of binding energy of the complexes, charge transfer (CT) and the length of Si−C_{NHC} bond. Energy decomposition analysis (EDA) and natural bond orbital (NBO) analysis at M052X/6-31+G(d,p) level of theory has been carried out to get a deeper understanding of the nature of bonding and charge delocalization. Proton affinity of the NHCs and fluoride affinity of the SiRs have been calculated and correlated with the binding energy of the resulting complexes.

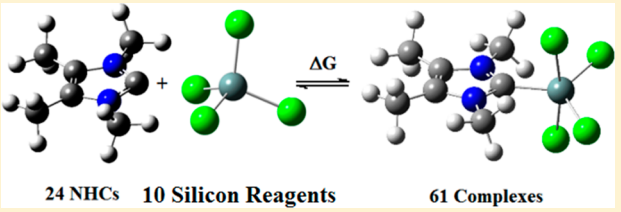

1. INTRODUCTION

Utility of *N*-heterocyclic carbenes (NHC) in various domains of chemistry is expanding very rapidly.[1] NHCs are found to be effective in many ways such as catalysts in organic transformations,[2] ligands for transition and main group chemistry,[3] etc. It is interesting to note that NHCs are found to act either as catalyst or as initiator in the case of reactions involving tetravalent silicon reagents.[4] Examples of reactions falling in this area include cyanosilylation[5,6] trifluoromethylation,[7] Mukaiyama aldol reaction,[8] aziridine addition reactions,[9] CO_2 reduction,[10] group transfer polymerization,[11] ring opening polymerization,[12] and dehydration of disilanol oligomers.[13] Usual mechanistic proposals of such reactions suggest the involvement of a Lewis acid−base type interaction between NHC and the silicon reagent.[4,6] Wang et al. has established the importance of NHC−Si interaction in the conversion of carbon dioxide into methanol by their computational study.[14] NHC−Si interaction has also been exploited in organometallic chemistry for the synthesis of a number of interesting compounds. Kuhn et al. synthesized pentacoordinate silicon compounds involving the interaction of "Arduengo-type" carbenes such as *N*-dialkyl-4,5-dimethylimidazol-2-ylidenes with $SiCl_4$, $SiCl_2Me_2$, and $SiCl_2Ph_2$.[15] Recently, Röschenthaler and co-workers[16] have presented a method for the synthesis of the adduct of 1,3-dimethylimidazolidin-2-ylidene with $SiCl_4$. Synthesis of NHC-stabilized compounds with a Si═Si, Si═O, and Si═Ge bond have also been reported.[17] NHC−Si interaction has its relevance also in explaining the observed stability of imidazol-2-ylidenes against hydrolysis and oxidation in silicone oils.[18]

Strategies employing NHCs for the activation of silicon compounds in organic transformation or for stabilization of main group element have a promising role to play in the future. In spite of so many experimental studies relying on NHC−Si interaction, there have been only a few computational studies involving NHC−Si systems. To understand the role played by NHC−Si interaction in the protection of NHCs by silicones, Baceiredo and co-workers[18] carried out DFT/B3LYP calculations using the 6-31G(d) basis set. Their calculations revealed the formation of complexes between NHCs and silicone oligomers to be exothermic by 2.6−5.4 kcal mol^{-1}, indicating a very weak NHC−Si interaction. Structure and stability of *penta*coordinate and *hexa*coordinate complexes of a number of carbenes with $SiCl_4$ and SiF_4 were studied by Nyulászi and co-workers.[19] This study also included a few complexes of "Arduengo-type" carbene. They suggested hexavalent complexes of imidazol-2-ylidene with $SiCl_4$ and SiF_4 as potential synthetic targets. Liu has analyzed the bonding situations in a few NHC−Si complexes using DFT methods.[20] There have also been many studies on the stable pentacoordinate Si compounds with ligands other than NHC. Dixon et al.[21] isolated a pentacoordinate siliconate by reversible addition of cyanide ion to trimethylsilyl cyanide in tetrahydrofuran (THF) and performed ab initio calculations to ascertain the position of CN group in its trigonal bipyramidal geometry. Gordon's group predicted the stability of a wide variety of pentacoordinate siliconates using MNDO and ab initio calculations in conjunction with experimental technique.[22] Heat of formation data of some diaminosilane adducts and their dehydrogenated

Received: September 5, 2015
Revised: December 11, 2015
Published: December 14, 2015

ACS Publications © 2015 American Chemical Society

DOI: 10.1021/acs.jpca.5b08676
J. Phys. Chem. A 2016, 120, 128−138

species were predicted by Dixon's group at the CCSD(T) and G3(MP2) levels.[23] However, having other objectives to fulfill, most of the computational works[18,19] focused mainly on the geometries, stabilities, and binding energies of very few NHC−Si compounds. Here, a thorough study on the NHC−Si interaction has been presented by taking a vast range of NHC−Si combinations. This study addresses some important issues like the origin of interaction energy, solvent effect on complex formation equilibrium, relevance of such interaction in NHC catalyzed organic transformations, etc.

The strength of the NHC−Si interaction has been interpreted here using several parameters such as binding energy of the complexes, charge transfer (CT) from the NHC (donor) to silicon reagent (acceptor), and bond length and Wiberg bond index of the bond between the carbene carbon of the NHC and the Si atom of the silicon reagent. Because the interaction between an NHC and silicon reagent is expected to be a Lewis acid−base type, variation of binding energy of the complex with respect to the proton affinity (PA) of the NHC and fluoride affinity (FA) of the SiR has been probed. Nature of the bond between NHC and SiR has been interpreted using energy decomposition analysis (EDA). Charge distribution in the complexes has been analyzed using both the frontier molecular orbital and NBO method. DFT calculations have been performed by taking a vast range of NHCs and SiRs. We have considered 24 NHCs out of which the first 11 are "Arduengo-type" and the rest are different variations of imidazolylidene, pyrazolylidene, triazolylidene, pyridylidene, isothiazolylidene, quinolidene, and Bertrand's NHCs (Scheme 1). All the NHCs have either alkyl groups or phenyl groups

Scheme 1. NHCs Considered in This Study

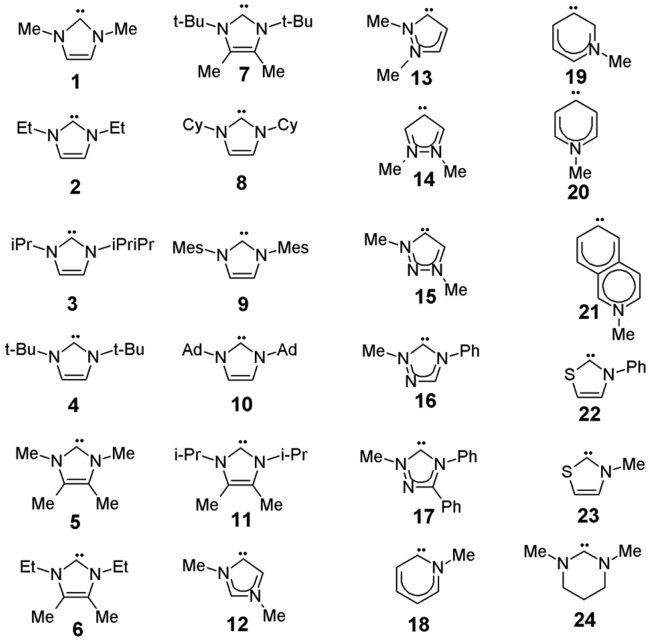

capable of exhibiting electronic and steric effect at key positions of the molecule. Most of these NHCs are employed as catalyst in many organic transformations.[5−8] NHCs **5**, **6**, **7**, and **11** having alkyl groups at the 4 and 5 positions are reported to interact strongly with some halosilanes ($SiCl_4$, Me_2SiCl_2, and Ph_2SiCl_2) to form very stable adducts.[15] All together, ten tetravalent SiRs (Scheme 2) have been selected on the basis of

Scheme 2. Silicon Reagents Considered in This Study

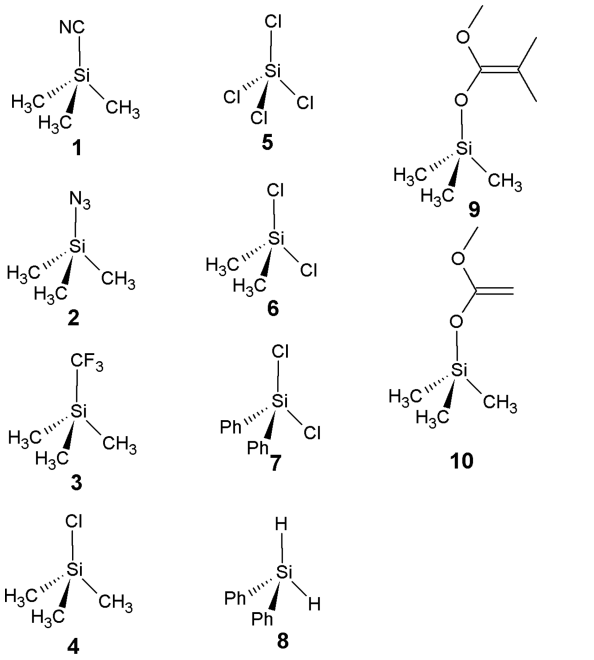

their reported use in organic transformations[5−10] and synthesis of stable adduct with NHC.[15] SiRs **1**, **2**, **3**, **9**, and **10** are reported to be employed in cyanosilylation,[5,6] trifluoromethylation,[7] aziridine addition,[9] Mukaiyama aldol reaction,[8] and group transfer polymerization[11] of the acrylate monomer, respectively. We have considered six sets of NHC−SiR complexes (altogether 61 complexes). In the first and second set of complexes, we have considered the interaction of all the imidazole-based NHCs (**1**−**11**) with the halosilanes $SiCl_4$ and Me_2SiCl_2, respectively. The third set consists of the complexes of Ph_2SiCl_2 with NHCs **1**−**8** and **11**. The fourth set includes the complexes of $SiCl_4$ with the NHCs **12**−**24**. Interactions of the 11 imidazole based NHCs with the same SiR TMSCN have been considered in the fifth set of complexes. In the sixth set, we have considered interaction of the same NHC, i.e., *N*,*N*-dimethylimidazol-2-ylidene (IMe_2), with the rest of the SiRs. Selection of these six sets of complexes have allowed us to study NHC−Si interaction ranging from very weak to very strong, having relevance in diverse areas of chemistry.

2. THEORY AND COMPUTATIONAL METHODS

All calculations were performed with the Gaussian 09 program package.[24] Geometry optimization of all the NHCs, SiRs, and the NHC−Si complexes considered in this study were performed using DFT with hybrid B3LYP functional[25,26] and a 6-31+G(d,p) basis set. As the M05-2X functional[27] is found to give a better performance in the description of Si-NHC chemistry,[14] optimizations were also carried out with the M05-2X functional using a 6-31+G(d,p) basis set. In all the cases, frequency calculations were performed at the same level of theory to ascertain the nature of the stationary state. The crystal structure of the stable adduct of *N*,*N*-diethyl-4,5-dimethylimidazol-2-ylidene (Me_2IEt_2) with $SiCl_4$ was established by Kuhn et al.[15] in their synthetic study. To test the performance of the two levels of theory, we compared the gas phase optimized geometries of this complex (Me_2IEt_2−$SiCl_4$) obtained from the two theories with the experimentally observed crystal structure in the solid state (Table 1). From Table 1 it is clear that the

DOI: 10.1021/acs.jpca.5b08676
J. Phys. Chem. A 2016, 120, 128−138

Table 1. Experimental and Calculated Bond Lengths and Bond Angles for the Adduct of Me_2IEt_2 with $SiCl_4$

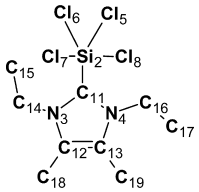

	experimental	B3LYP/6-31+G(d,p)	M0-52X/6-31+G(d,p)
	Bond Length (Å)		
Si2−C11	1.911	1.951	1.935
Si2−Cl5	2.045	2.102	2.090
Si2−Cl6	2.070	2.102	2.099
C11−N3	1.341	1.352	1.341
C12−C13	1.318	1.366	1.362
	Bond Angle (deg)		
N4−C11−N3	107.1	106.5	106.7
C11−Si2−Cl5	121.8	122.1	121.9
C11−Si2−Cl6	120.9	122.1	121.9
Cl5−Si2−Cl6	117.2	115.8	116.2
C11−N3−C12	108.5	110.1	110.1

M05-2X/6-31+G(d,p) level of theory has reproduced the experimentally observed structure more closely than the B3LYP/6-31+G(d,p) level. So in this study we have used the M05-2X/6-31+G(d,p) optimized geometries as model for analysis. BSSE corrected binding energies of the complexes of the Set 1, Set 2, Set 3, Set 4, Set 5, and Set 6 were calculated in terms of the thermodynamic parameters ΔE_0, ΔH_{298}, and ΔG_{298} for the change: NHC + SiR → NHC−SiR in the gas phase. BSSE corrections were performed using counterpoise method[28,29] at the M05-2X/6-31+G(d,p) optimized geometry.

Full geometry optimizations using solvent(THF) were also performed for some "strongly binding" and "weakly binding" complexes at the M05-2X/6-31+G(d,p) level using the integral equation formalism version of the polarizable continuum model (IEF-PCM).[30] Thermodynamic parameters for the complexes of Set 5 were also calculated in the solvent phase (THF) through single point energy calculations using the same method. Energy decomposition analysis was performed on the M05-2X/6-31+G(d,p) optimized structures of a few selected complexes with the LMOEDA[31] method implemented in GAMESS.[32]

Proton affinity (PA) was calculated as the negative of the enthalpy change (ΔH) at 298 K for the process: NHC(g) + H^+(g) → $NHCH^+$(g). Similarly, fluoride affinity (FA) was taken as the negative of enthalpy change for the process: SiR(g) + F^-(g) → $SiRF^-$(g). For the calculations of PA and FA we used M05-2X/6-31+G(d,p) level of theory.

Charge distribution on the important atoms of the complexes and Wiberg bond index for the C_{NHC}−Si bond were analyzed using NBO method.[33] NBO calculations were carried out at the M05-2X/6-31+G(d,p) level of theory using the NBO version implemented in Gaussian 09. Charge transfer (CT) from NHC to SiR was determined by taking the difference of the total NPA charge of the NHC molecule in the NHC−SiR complex and the total NPA charge of the NHC molecule in isolation.

3. RESULTS AND DISCUSSION

3.1. Classifying the Complexes as Strongly Binding and Weakly Binding. A complex resulting from the interaction of NHC with SiR may assume either a pentacoordinate structure or a hexacoordinate structure. Experimental evidence reported for an adduct of Me_2IEt_2 with $SiCl_4$ establishes a pentacoordinate geometry for similar NHC−Si interactions.[15] Pentacoordinate structure has also been reported for IMe_2−$SiCl_4$[16] and therefore we did not consider the hexacoordinate NHC−SiR complex in this study; however, a synthetic study on a hexacoordinate complex of SiF_4 with NHC is known.[34] Calculated binding energy, charge transfer, Si−C_{NHC} distance, Wiberg bond index (WBI), and dipole moment of the pentacoordinate complexes of $SiCl_4$ with the imidazole based NHCs (Set 1) are presented in Table 2 and those for the complexes of Set 2, Set 3, Set 4, Set 5, and Set 6 are presented in Table 3, Table 4, Table 5, Table 6 and Table 7, respectively. Most of the stable complexes reported by Kuhn and co-workers (Me_2IMe_2−$SiCl_4$, Me_2IEt_2−$SiCl_4$, $Me_2I^iPr_2$−$SiCl_4$, Me_2IEt_2−Me_2SiCl_2, and Me_2IEt_2−Ph_2SiCl_2) have negative ΔG_{298} values. The most stable complex in terms of ΔG_{298} among the reported complexes is Me_2IEt_2−$SiCl_4$, the one for which crystal structure was determined by Kuhn's group. It has a ΔG_{298} value of −6.48 kcal mol^{-1} (Table 2). The complex IMe_2−$SiCl_4$ synthesized by the Röschenthaler group[16] has a ΔG_{298} value of −3.18 kcal mol^{-1}. The lowest ΔG_{298} value among the complexes synthesized has been found to be 1.98 kcal mol^{-1} for $Me_2I^iPr_2$−Ph_2SiCl_2 (Table 4). Although it has a positive ΔG_{298} value in the gas phase, it has been found to be stabilized in the solvent phase by ∼4.0 kcal mol^{-1} (Table 8).

Table 2. Binding Energy[a] (BSSE Corrected), Charge Transfer (CT), Si−C_{NHC} Distance, Wiberg Bond Index (WBI), and Dipole Moment of the Complexes of $SiCl_4$ with the NHCs 1−11 (Set 1)

NHC	ΔE_0	ΔH_{298}	ΔG_{298}	CT (e)	Si−C_{NHC} distance (Å)	WBI	dipole moment (Debye)
NHC1(IMe_2)[c]	−16.37	−16.22	−3.18	0.341	1.931	0.5848	9.45
NHC2(IEt_2)	−18.30	−18.28	−3.72	0.343	1.937	0.5888	9.31
NHC3(I^iPr_2)	−18.18	−18.03	−3.86	0.345	1.938	0.5935	9.29
NHC4(I^tBu_2)	10.69	10.54	25.67	0.357	2.032	0.5840	10.39
NHC5(Me_2IMe_2)[b]	−17.74	−17.54	−4.69	0.351	1.929	0.5924	10.73
NHC6(Me_2IEt_2)[b]	−20.45	−20.32	−6.48	0.352	1.936	0.5961	10.48
NHC7($Me_2I^tBu_2$)	7.17	7.27	21.91	0.362	2.025	0.5941	10.59
NHC8(ICy_2)	−19.48	−19.21	−5.11	0.350	1.941	0.5981	9.00
NHC9($IMes_2$)	−15.77	−15.71	0.77	0.333	1.952	0.5856	8.53
NHC10(IAd_2)	−7.34	−7.14	6.27	0.344	1.947	0.5999	8.95
NHC11($Me_2I^iPr_2$)[b]	−15.82	−15.48	−1.97	0.354	1.946	0.6002	10.33

[a]Values in kcal mol^{-1}. [b]Synthesized by Kuhn et al.[15] [c]Synthesized by Röschenthaler et al.[16]

DOI: 10.1021/acs.jpca.5b08676
J. Phys. Chem. A 2016, 120, 128−138

Table 3. Binding Energy[a] (BSSE Corrected), Charge Transfer (CT), Si−C_{NHC} Distance, Wiberg Bond Index (WBI), and Dipole Moment of the Complexes of Me_2SiCl_2 with NHCs 1−11 (Set 2)

NHC	ΔE_0	ΔH_{298}	ΔG_{298}	CT (e)	Si−C_{NHC} distance (Å)	WBI	dipole moment (Debye)
NHC1(IMe_2)	−14.18	−14.37	−0.47	0.347	1.929	0.6176	6.66
NHC2(IEt_2)	−15.39	−15.60	−0.71	0.354	1.934	0.6197	6.47
NHC3(I^iPr_2)	−16.33	−16.45	−1.99	0.361	1.934	0.6235	6.45
NHC4(I^tBu_2)	4.95	4.27	20.95	0.369	1.991	0.6291	6.75
NHC5(Me_2IMe_2)	−15.88	−15.82	−2.62	0.357	1.929	0.6243	7.87
NHC6(Me_2IEt_2)[b]	−17.06	−17.14	−3.02	0.361	1.933	0.6264	7.53
NHC7($Me_2I^tBu_2$)	10.64	10.56	25.06	0.388	2.013	0.6296	7.50
NHC8(ICy_2)	−17.82	−17.85	−2.85	0.365	1.936	0.6269	6.35
NHC9($IMes_2$)	−15.21	−15.12	−0.39	0.331	1.952	0.6158	6.36
NHC10(IAd_2)	−5.50	−5.67	8.96	0.363	1.941	0.6287	6.31
NHC11($Me_2I^iPr_2$)[b]	−13.99	−13.91	0.10	0.370	1.939	0.6294	7.36

[a]Values in kcal mol^{-1}. [b]Synthesized by Kuhn et al.[15]

Table 4. Binding Energy[a] (BSSE Corrected), Charge Transfer (CT), Si−C_{NHC} Distance, Wiberg Bond Index (WBI), and Dipole Moment of the Complexes of Ph_2SiCl_2 with NHCs 1−8 and 11 (Set 3)

NHC	ΔE_0	ΔH_{298}	ΔG_{298}	CT (e)	Si−C_{NHC} distance (Å)	WBI	dipole moment (Debye)
NHC1(IMe_2)	−14.50	−15.15	1.39	0.348	1.929	0.6177	5.77
NHC2(IEt_2)	−15.81	−16.30	0.56	0.360	1.938	0.6199	5.73
NHC3(I^iPr_2)	−17.44	−17.80	−1.00	0.361	1.938	0.6250	5.57
NHC4(I^tBu_2)	6.85	5.93	24.96	0.361	1.997	0.6215	5.41
NHC5(Me_2IMe_2)	−16.81	−17.25	−1.23	0.373	1.932	0.6274	7.30
NHC6(Me_2IEt_2)[b]	−17.00	−17.38	−1.03	0.362	1.940	0.6254	6.57
NHC7($Me_2I^tBu_2$)	15.34	15.27	31.17	0.386	2.046	0.6200	7.24
NHC8(ICy_2)	−20.46	−20.79	−3.90	0.365	1.940	0.6295	5.30
NHC11($Me_2I^iPr_2$)[b]	−14.42	−14.73	1.98	0.371	1.946	0.6303	6.44

[a]Values in kcal mol^{-1}. [b]Synthesized by Kuhn et al.[15]

Table 5. Binding Energy[a] (BSSE Corrected), Charge Transfer (CT), Si−C_{NHC} Distance, Wiberg Bond Index (WBI), and Dipole Moment of the Complexes of NHCs 12−24 with $SiCl_4$ (Set 4)

NHC	ΔE_0	ΔH_{298}	ΔG_{298}	CT (e)	Si−C_{NHC} distance (Å)	WBI	dipole moment (Debye)
NHC12	−27.94	−27.77	−15.01	0.369	1.905	0.5981	14.08
NHC13	−23.94	−23.70	−11.23	0.350	1.915	0.5895	13.66
NHC14	−36.01	−35.89	−23.34	0.394	1.906	0.6094	17.93
NHC15	−20.30	−19.60	−7.94	0.347	1.913	0.5833	11.52
NHC16	−10.19	−9.79	2.32	0.311	1.933	0.5674	7.21
NHC17	−8.72	−8.24	5.57	0.308	1.934	0.5677	7.90
NHC18	−24.27	−24.13	−11.19	0.317	1.931	0.5787	10.62
NHC19	−33.76	−34.08	−20.44	0.357	1.914	0.5880	14.74
NHC20	−34.95	−35.67	−20.93	0.304	1.893	0.5850	15.34
NHC21	−43.16	−43.42	−29.71	0.348	1.895	0.6031	22.33
NHC22	−11.59	−11.03	0.75	0.282	1.934	0.5490	9.68
NHC23	−10.25	−9.95	2.20	0.280	1.935	0.6502	9.83
NHC24	−15.04	−14.84	−2.49	0.350	1.979	0.6416	10.16

[a]Values in kcal mol^{-1}.

We have regarded those NHC−SiR complexes as "strongly binding" for which ΔG_{298} values in the gas phase are greater in magnitude than 1.98 kcal mol^{-1}, which has been calculated for the "strongly binding" $Me_2I^iPr_2$−Ph_2SiCl_2. A total of 61 numbers of NHC−SiR complexes have been considered for this particular study. The analysis reveals that complexes with the halosilane ligands $SiCl_4$, Me_2SiCl_2, and Ph_2SiCl_2, are "strongly binding" according to this scale. Most of the strongly binding complexes identified here have stability comparable to that of the synthesized complexes; some of them even have higher stability, indicating the high possibility of their synthesis. On the other hand, all the combinations of TMSCN with the imidazole type NHCs (Set 4) have high positive ΔG_{298} values in both the gas and solvent phases (Table 6), confirming that no binding is favored. Interactions of the SiRs other than the halosilanes with IMe_2 have also been found to be very weak indicated by positive ΔG_{298} values of their corresponding complexes (Table 7). Some combinations with the halosilanes also do not favor any bonding; their complexes with I^tBu_2 and $Me_2I^tBu_2$ have positive ΔE_0, ΔH_{298}, and ΔG_{298} values. The complex of SiR6 with IAd_2 also has a ΔG_{298} value of +8.96 kcal mol^{-1}.

3.2. Strongly Binding Complexes of the SiRs with the Arduengo-Type NHCs. Optimized geometries of some of the

DOI: 10.1021/acs.jpca.5b08676
J. Phys. Chem. A 2016, 120, 128−138

Table 6. Binding Energy[a] (BSSE corrected), Charge Transfer (CT), Si−C_{NHC} Distance, Wiberg Bond Index (WBI), and Dipole Moment of the Complexes of TMSCN with NHCs 1−11 (Set 5)

	gas phase							solvent phase		
NHC	ΔE_0	ΔH_{298}	ΔG_{298}	CT (e)	Si−C_{NHC} distance (Å)	dipole moment (Debye)	WBI	ΔE_0	ΔH_{298}	ΔG_{298}
NHC1(IMe_2)	−4.68	−4.70	6.70	0.017	3.96	4.78	0.0055	−0.89	−0.91	10.48
NHC2(IEt_2)	−5.35	−4.91	5.98	0.018	3.96	4.45	0.0050	−1.24	−0.80	10.09
NHC3(I^iPr_2)	−5.16	−4.47	4.41	0.011	4.41	4.26	0.0005	−3.88	−3.19	5.69
NHC4(I^tBu_2)	−3.47	−3.08	7.62	0.010	4.52	7.61	0.0003	−5.15	−4.76	5.94
NHC5(Me_2IMe_2)	−4.80	−4.24	4.86	0.018	3.95	5.21	0.0059	−0.80	−0.24	8.86
NHC6(Me_2IEt_2)	−5.54	−4.96	4.79	0.018	4.07	4.88	0.0035	−1.34	−0.76	8.99
NHC7($Me_2I^tBu_2$)	−4.39	−4.19	6.82	0.009	4.57	7.97	0.0003	−2.47	−2.27	8.73
NHC8(ICy_2)	−56.79	−5.77	5.04	0.018	3.87	7.74	0.0089	−3.49	−2.95	7.86
NHC9($IMes_2$)	−8.21	−7.80	4.61	0.010	3.84	3.39	0.0066	−3.79	−3.38	9.03
NHC10(IAd_2)	−4.75	−4.35	7.12	0.006	4.35	4.49	0.0007	−1.83	−1.42	10.04
NHC11($Me_2I^iPr_2$)	−1.66	−1.60	10.09	0.014	4.00	4.82	0.0046	1.61	1.67	13.36

[a]Values in kcal mol^{-1}.

Table 7. Binding Energy[a] (BSSE Corrected), Charge Transfer (CT), Si−C_{NHC} Distance, Wiberg Bond Index (WBI), and Dipole Moment of the Complexes of IMe_2 with Some of the SIRs (Set 6)

SIR	ΔE_0	ΔH_{298}	ΔG_{298}	CT (e)	Si−C_{NHC} distance (Å)	WBI	dipole moment (Debye)
SiR2($TMSN_3$)	−3.93	−3.81	6.60	0.009	4.299	0.0017	4.31
SiR3($TMSCF_3$)	−4.22	−4.23	7.34	0.020	3.791	0.0112	6.91
SiR4(TMSCl)	−3.36	−2.60	4.99	0.013	4.240	0.0017	3.67
SiR8(Ph_2SiH_2)	−4.44	−3.86	6.84	0.024	3.364	0.0250	2.26
SIR9	−4.32	−4.34	7.39	0.017	4.122	0.0030	3.88
SIR10	−3.44	−2.73	6.70	0.007	4.338	0.0012	2.47

[a]Values in kcal mol^{-1}.

Table 8. Binding Energy[a] of Some Selected Complexes (BSSE Uncorrected) in the Solvent Phase (THF) along with the Corresponding Values in the Gas Phase

	solvent phase			gas phase		
NHC	ΔE_0	ΔH_{298}	ΔG_{298}	ΔE_0	ΔH_{298}	ΔG_{298}
IMe_2−iCl_4	−25.92	−25.92	−12.17	−20.62	−20.48	−7.43
Me_2IMe_2−$SiCl_4$	−27.17	−27.11	−13.54	−22.12	−21.91	−9.06
Me_2IEt_2−$SiCl_4$	−29.53	−29.45	−15.22	−25.14	−25.01	−11.18
ICy_2−$SiCl_4$	−27.42	−27.17	−12.89	−24.77	−24.51	−10.40
IMe_2−Me_2SiCl_2	−21.55	−21.74	−7.66	−17.02	−17.21	−3.31
$Me_2I^iPr_2$−Ph_2SiCl_2	−20.47	−20.14	−5.60	−17.92	−18.23	−1.52
IMe_2−TMSCN	−2.43	−1.96	7.98	−5.10	−5.11	6.28
IMe_2−$TMSN_3$	−1.38	−0.92	9.40	−4.50	−4.38	6.03
IMe_2−$TMSCF_3$	−2.86	−2.26	7.25	−4.62	−4.63	6.94
IMe_2−TMSCl	−2.86	−2.26	7.25	−3.73	−2.98	4.61
IMe_2−Ph_2SiH_2	−3.49	−3.03	8.00	−5.38	−4.81	5.90

[a]Values in kcal mol^{-1}.

strongly binding adducts are presented in Figure 1. In all the adducts the NHC occupies equatorial position in their pentacoordinate geometry making dihedral angles in the range 14−22° with the equatorial plane passing through the Si atom. The axial Cl atoms are found to be tilted toward the carbene carbon of the NHC. These optimized geometries are in accordance with the reported crystal structures.[15,16] Tilting of the axial Cl atoms results from somewhat stronger van der Waals repulsion from the equatorial Cl atoms than from the planar trigonal C atom of the NHC. Calculated ΔG_{298} value of the strongly binding NHC−$SiCl_4$ adducts ranges from +0.77 to −6.48 kcal mol^{-1} (Table 2). All the strongly binding NHC−$SiCl_4$ complexes have much shorter Si−C_{NHC} distances (ranging from 1.929 to1.952 Å) than the weakly binding ones. Both the steric and the electronic effects due to the groups present at the N atom of the NHC are found to be important for the stability of the complexes. In going from methyl (IMe_2) to isopropyl (I^iPr_2), the magnitude of the binding energy (ΔG_{298} value) of the complexes increases (from −7.43 to −8.78 kcal mol^{-1}) with the increasing electron donating effect of the *N*-substituents; however, with the introduction of the bulky *tert*-butyl group, the steric factor dominates over the electronic factor and the complex attains a high positive ΔG_{298} value (+25.67 kcal mol^{-1}). The electronic effect of the alkyl groups at the C4 and C5 positions of the imidazole ring is also significant. In the presence of methyl groups at the 4,5-positions (Me_2IMe_2), the complex becomes more stable compared to that of IMe_2; similar stabilization of the complex is also observed in the complex of Me_2IEt_2 relative to that of IEt_2 (ΔG_{298} value changes from −8.29 to −11.18 kcal

DOI: 10.1021/acs.jpca.5b08676
J. Phys. Chem. A 2016, 120, 128−138

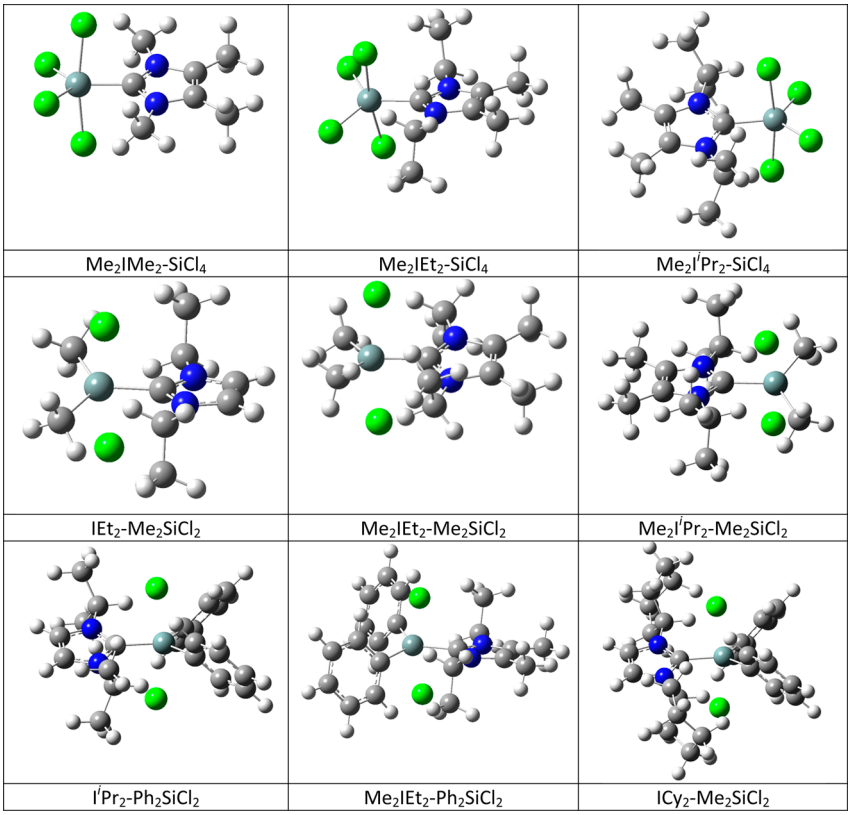

Figure 1. Optimized geometries of some strongly binding complexes.

mol^{-1}). However, in the presence of bulkier isopropyl and *tert*-butyl groups, destabilization due to steric effect becomes dominant over the stabilization effect of the methyl groups. Due to the presence of two methyl groups on the neighboring carbons, steric effects are even much worse here compared to those observed in the case of I^{i}Pr$_2$ and I^{t}Bu$_2$.

Charge transfer (CT) during the formation of the strongly binding NHC−SiCl$_4$ complexes has been plotted against $-\Delta G_{298}$ values in Figure 2. A very poor linear dependence of CT with ΔG_{298} has been obtained with a regression coefficient, R^2 = 0.471. The prominent outlier in the fit is the complex formed by Me$_2$I^{i}Pr$_2$, which in spite of having high CT, exhibits a relatively low ΔG_{298} value due to steric reason. Removing the Me$_2$I^{i}Pr$_2$ complex from the fit, a good linear dependence with

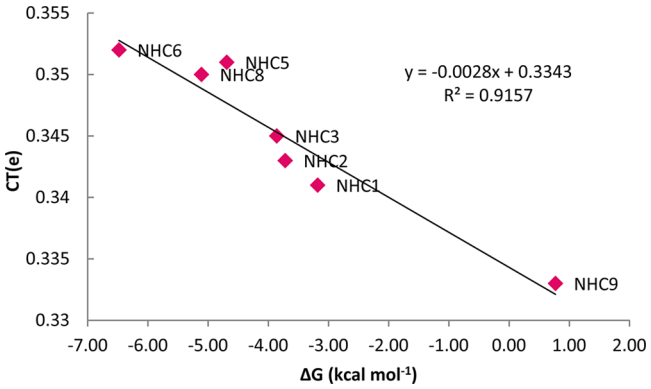

Figure 2. Linear correlation between the charge transfer (CT) values and binding energies of the complexes of NHCs with SiCl$_4$. The linear fit omits the complexes of NHCs I^{t}Bu$_2$, Me$_2$I^{t}Bu$_2$, IAd$_2$, and Me$_2$I^{i}Pr$_2$.

R^2 = 0.915 is obtained. Despite the highest values of CT, complexes of I^{t}Bu$_2$ and Me$_2$I^{t}Bu$_2$ with SiCl$_4$ are the weakest ones due to the dominance of steric factors.

All the complexes of Me$_2$SiCl$_2$ with NHC (Set 2) have lower binding energies (Table 3) than the corresponding complexes of SiCl$_4$ (Set 1). Similarly, all the complexes of Ph$_2$SiCl$_2$ with NHC (Set 3) have lower binding energies (Table 4) than the corresponding complexes of Me$_2$SiCl$_2$ except with ICy$_2$ (Set 2). Comparison of binding energies of the strongly binding NHC−SiR complexes of Set 1, Set 2, and Set 3 are displayed in Figure 3. Both SiCl$_4$ and Me$_2$SiCl$_2$ form their most stable complexes with Me$_2$IEt$_2$ whereas Ph$_2$SiCl$_2$ forms the stable complex with ICy$_2$.

To examine the variation of binding energy with the Lewis basicity of the NHCs, we calculated the proton affinity (PA) of the NHCs. The results are displayed in Table 9. As we move from IMe$_2$−SiCl$_4$ to I^{i}Pr$_2$−SiCl$_4$ (Table 2), the magnitude of binding energy gradually increases with an increase in PA. However, in the case of I^{t}Bu$_2$−TMSCN, the binding energy drops considerably although PA of the I^{t}Bu$_2$ is higher than the preceding ones. This may be due to steric effect of the bulky *tert*-butyl group. A good linear dependence of CT with $-\Delta G_{298}$ for the NHC−SiCl$_4$ complexes (Set 1) has been obtained with a regression coefficient, R^2 = 0.729 when the sterically demanding NHCs I^{t}Bu$_2$, Me$_2$I^{t}Bu$_2$, IMes$_2$, IAd$_2$, Me$_2$I^{i}Pr$_2$ are excluded from the correlation (Figure 4). Correlation of PA for the NHC−Me$_2$SiCl$_2$ complexes with $-\Delta G_{298}$ (Set 2) has been found to be more linear with a regression coefficient, R^2 = 0.934, when sterically demanding NHCs are excluded (Figure 5). Wiberg bond index values for the Si−C$_{NHC}$ bond of the NHC−Me$_2$SiCl$_2$ complexes are also found to correlate well (R^2 = 0.949) with the binding energy of the complexes (Figure 6).

DOI: 10.1021/acs.jpca.5b08676
J. Phys. Chem. A 2016, 120, 128−138

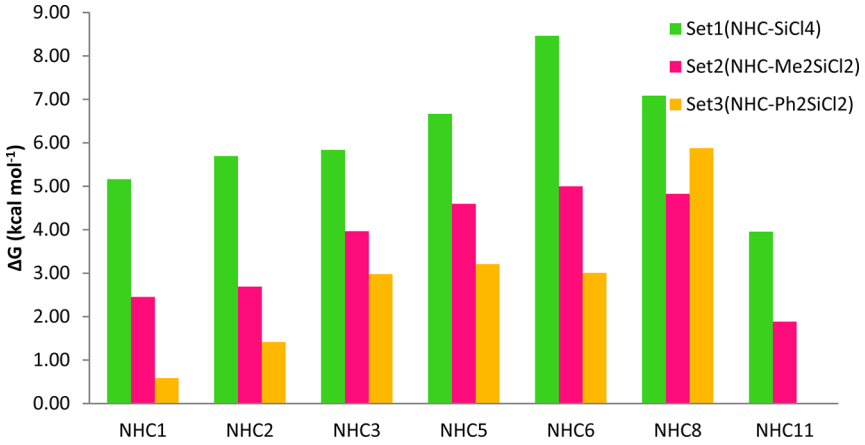

Figure 3. Comparison of stability of the strongly binding NHC−SiR complexes of Set 1, Set 2, and Set 3 in terms of relative binding energy values with respect to the least stable $Me_2I^iPr_2$−Ph_2 $SiCl_2$.

Table 9. Calculated Proton Affinity (PA) and Dipole Moment Values of the NHCs

NHC	PA (kcal mol $^{-1}$)	dipole moment (Debye)
NHC1(IMe_2)	258.74	2.63
NHC2(IEt_2)	261.37	2.52
NHC3(I^iPr_2)	263.77	2.13
NHC4(I^tBu_2)	267.27	2.04
NHC5(Me_2IMe_2)	264.96	3.29
NHC6(Me_2IEt_2)	266.68	3.11
NHC7($Me_2I^tBu_2$)	272.59	2.55
NHC8(ICy_2)	267.37	2.06
NHC9($IMes_2$)	267.84	2.10
NHC10(IAd_2)	272.18	1.67
NHC11($Me_2I^iPr_2$)	265.65	2.83
NHC12	278.71	6.20
NHC13	272.92	6.05
NHC14	289.73	8.40
NHC15	264.00	4.22
NHC16	248.15	1.57
NHC17	253.90	3.19
NHC18	269.53	3.93
NHC19	284.54	6.88
NHC20	286.60	7.79
NHC21	306.71	12.38
NHC22	252.58	3.98
NHC23	248.13	4.08
NHC24	267.04	3.16

From the comparison of binding energy data of all the SiRs in the present study, it is clear that $SiCl_4$ forms the most stable adducts with the NHCs (Tables 2−4). The highest binding energy observed in the case of NHC−$SiCl_4$ complexes can be correlated to the highest fluoride affinity of $SiCl_4$ (Table 10). In spite of having a higher fluoride affinity than Me_2SiCl_2, Ph_2SiCl_2 forms complexes (Set 3) with comparatively lower binding energies than those of the complexes of Set 2. All the strongly binding complexes formed by these three SiRs not only are the most Lewis acidic ones (in terms of fluoride affinity values) but also have the least steric bulk around the Si atom. Similarly, NHCs participating in these stable adduct formation also do not have much steric bulk around the carbene carbon.

Shapes of three important frontier molecular orbitals of the stable complex Me_2IMe_2−$SiCl_4$ have been constructed and displayed in Figure 7. The HOMO corresponds to the C−N π bonds and C−C π bond in the imidazole ring. The HOMO−2 corresponds to the Si−C_{NHC} σ bond, σ bonding in the imidazole ring, and localization of electron density on the axial Cl atoms. The HOMO−1 shows more electron density on the axial Cl atoms than on the equatorial ones.

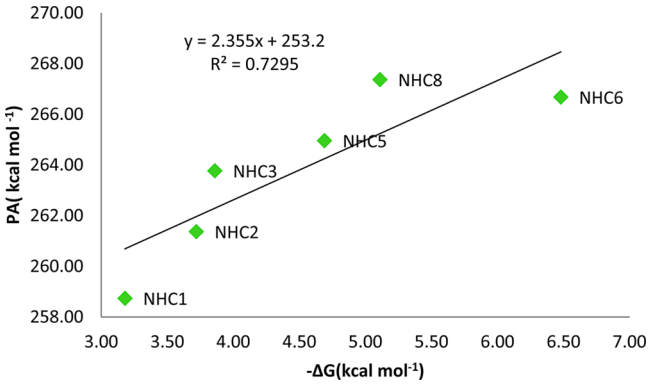

Figure 4. Linear correlation between the PA values of the NHCs and binding energies of the complexes of NHCs with $SiCl_4$. The linear fit omits the complexes of NHCs I^tBu_2, $Me_2I^tBu_2$, $IMes_2$, IAd_2, and Me_2I^iPr.

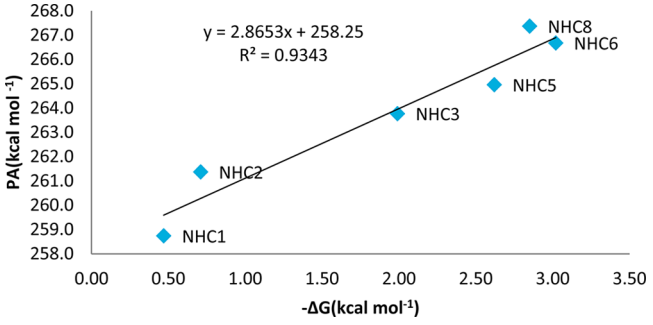

Figure 5. Linear correlation between the PA values of the NHCs and binding energies of the complexes of NHCs with Me_2SiCl_2. The linear fit omits the complexes of NHCs I^tBu_2, $Me_2I^tBu_2$, $IMes_2$, IAd_2, and Me_2I^iPr.

3.3. Strongly Binding Complexes of a Range of Diverse NHCs with $SiCl_4$. Optimized geometries of adducts of NHCs **12**−**24** are presented in Figure S1. Pentacoordinate geometries of the complexes of NHCs **12**−**24** with $SiCl_4$ are very much similar to those of the complexes of NHCs **1**−**11**.

DOI: 10.1021/acs.jpca.5b08676
J. Phys. Chem. A 2016, 120, 128−138

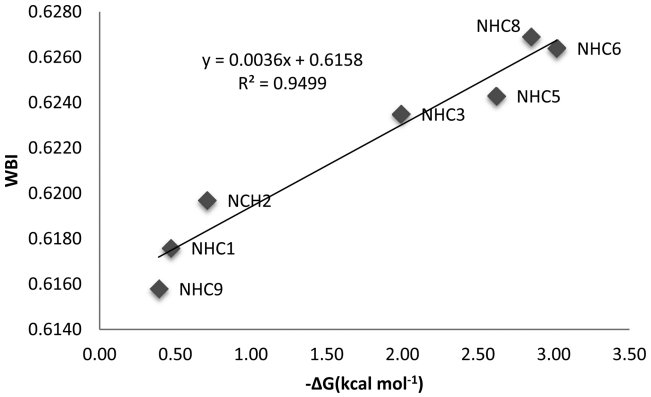

Figure 6. Linear correlation between the WBI values of the Si−C_{NHC} bond and binding energies of the complexes of NHCs with Me_2SiCl_2. The linear fit omits the complexes of NHCs I^tBu_2, $Me_2I^tBu_2$, IAd_2, and $Me_2I^iPr_2$.

Table 10. Calculated Fluoride Affinity (FA) and Dipole Moment Values of the SiRs

SiR	FA (kcal mol^{-1})	dipole moment (Debye)
SiR1(TMSCN)	58.61	4.58
SiR2($TMSN_3$)	59.32	3.03
SiR3($TMSCF_3$)	56.10	3.46
SiR4(TMSCl)	64.27	2.76
SiR5($SiCl_4$)	83.09	0.00
SiR6(Me_2SiCl_2)	66.52	2.98
SiR7(Ph_2SiCl_2)	72.85	3.43
SiR8(Ph_2SiH_2)	50.29	0.97
SiR9	48.92	0.97
SiR10	48.32	1.98

Calculated ΔG_{298} values of the strongly binding adducts range from −2.49 to −29.71 kcal mol^{-1} (Table 5). Binding energies of most of the complexes of this set are much higher than those of the complexes of set 1 (Table 2). The C-4 bound complex with NHC **12** is more stable than the normal C-2 bound complex of IMe_2 with $SiCl_4$, which was synthesized by Röschenthaler group,[16] because of the higher Lewis basicity of NHC **12** (Table 9). The ΔG_{298} value of the C-4 bound complex of pyrazole type NHC **14** is much larger in magnitude than the normal C-3 bound complex with NHC **13**. The NHC **14** having no adjacent N atom to the carbene C has a higher Lewis basicity than NHC **13** with one adjacent N. Among the triazole type NHCs **15**, **16**, and **17**, only NHC **15** forms a complex with negative ΔG_{298} value, clearly because of its higher Lewis basicity than the other two. The farther and lesser are the number of N centers (NHC **18**−**21**), the higher is the Lewis basicity of the NHCs, and hence the stronger is their binding with $SiCl_4$. Isothiazole-type NHCs with two adjacent heteroatoms (S and N) to the carbene C have very low Lewis basicity; hence their complexes with $SiCl_4$ are weakly binding. A very good linear dependence of PA with $-\Delta G_{298}$ has been obtained with a regression coefficient, R^2 = 0.915 (Figure 8).

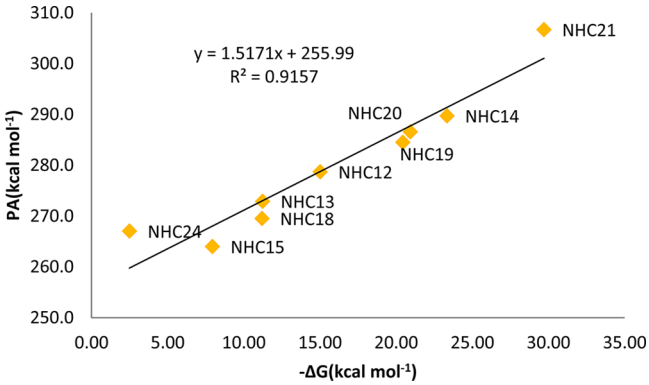

Figure 8. Linear correlation between the PA values of the NHCs and binding energies of the complexes of Set 4. The linear fit omits the complexes of NHCs **16**, **17**, **22**, and **23**.

3.4. Weakly Binding Complexes of the SiRs with the NHCs. All the combinations of TMSCN with NHCs (Set 4) have been found to favor very weak or no bonding at all. Pentacoordinate complexes of NHCs with TMSCN may have several possible isomers as shown in Scheme 3. For most of the

Scheme 3. Possible Isomers of Pentacoordinate Complexes of NHCs with TMSCN

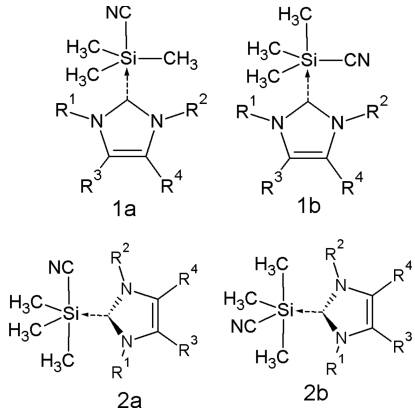

NHC−SiR combinations of the first set, the geometries **1a** and **1b** are found to be favored at B3LYP/6-31+G(d,p) level

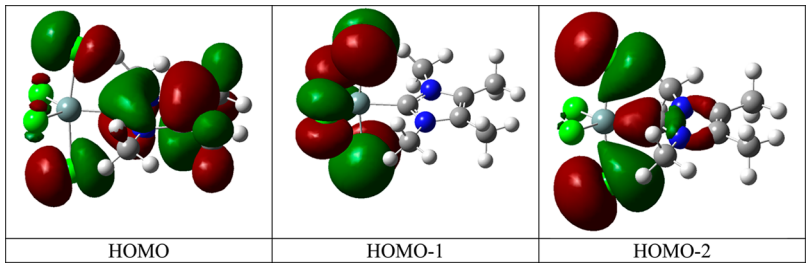

Figure 7. HOMO, HOMO−1, and HOMO−2 of the stable complex Me_2IMe_2−$SiCl_4$.

DOI: 10.1021/acs.jpca.5b08676
J. Phys. Chem. A 2016, 120, 128−138

Scheme 4. Mechanism Proposed by Song and Co-workers for NHC Catalyzed Cyanosilylation

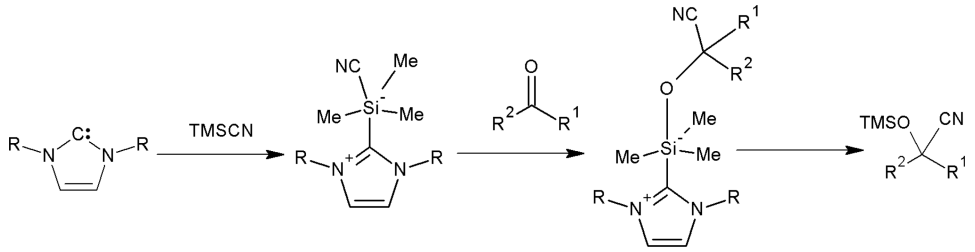

Table 11. Results of LMOEDA of Some Selected Strongly Binding Complexes of $SiCl_4$[a]

complex	ΔE_{el}	ΔE_{ex}	ΔE_{re}	ΔE_{pol}	ΔE_{dis}	ΔE
NHC1(IMe_2)	−177.83	−144.51	410.96	−135.77	−37.28	−84.43
NHC2(IEt_2)	−178.12	−145.70	415.82	−136.74	−41.42	−86.22
NHC3(I^iPr_2)	−179.60	−147.29	419.81	−139.06	−42.16	−88.30
NHC5(Me_2IMe_2)	−181.16	−146.51	416.10	−139.07	−37.49	−88.13
NHC12	−190.49	−148.92	418.34	−146.41	−32.89	−100.38
NHC13	−185.05	−145.80	411.71	−141.97	−33.45	−94.56
NHC14	−192.83	−146.04	407.65	−154.02	−30.86	−116.11
NHC19	−193.64	−146.87	413.42	−147.13	−31.69	−105.92

[a]Values are in kcal mol^{-1}.

(Figure S2). We further optimized the preferred conformation (found in B3LYP calculation) with the M05-2X/6-31+G(d,p) level of theory. Optimized geometries of the complexes of the NHCs with TMSCN are presented in Figure S3 of the Supporting Information. In the M05-2X/6-31+G(d,p) optimized geometries of the complexes of NHCs with TMSCN, NHC is found to take the axial position and the CN ligand prefers the equatorial position in eight out of the 11 complexes probably due to stabilization gained from a weak hydrogen bond interaction (CN···H). With I^tBu_2, $Me_2I^tBu_2$, and ICy_2, the CN ligand prefers the axial position due to steric repulsion with the bulky *tert*-butyl and cyclohexyl groups on the N atoms. Calculated binding energies, charge transfers, and Si−C_{NHC} distances of the complexes of TMSCN with all the NHCs (Set 4) are displayed in Table 6. All these complexes have positive ΔG_{298} values in both gas and solvent phases, indicating a very weak NHC−Si interaction. All the complexes have much longer Si−C_{NHC} distances (ranging from 3.84 to 4.57 Å) and much lower WBI values than observed for the stable cases, indicating that there is no significant interaction between Si and the carbene carbon. Charge transfers (CT) from the NHCs to the silicon reagent (TMSCN) during complex formation are also found to be very small.

Song and co-workers proposed a mechanism of NHC catalyzed cyanosilylation[6] involving a hypercoordinate NHC−TMSCN intermediate (Scheme 4). Our calculations show that such an adduct has a very low binding energy (positive ΔG_{298} value) in the gas phase. In the solution phase, the binding energy values are even much worse. We further verified this by optimizing two representative sets of strongly binding and weakly binding complexes using solvent (THF) at the M05-2X/6-31+G(d,p) level of theory. Binding energy data from these calculations are presented in Table 8, from which it is clear that strongly binding complexes are stabilized in the experimentally used solvent whereas weakly binding complexes get destabilized further. Therefore, this mechanistic proposal involving the NHC−Si interaction seems unlikely. The complexes of IMe_2 with $TMSN_3$, $TMSCF_3$, TMSCl, Ph_2SiH_2, and the silylenolates (**9** and **10**) which are relevant to many organic transformations also have high positive ΔG_{298} values and very low WBI values of the Si−C_{NHC} bond (Table 7), indicating weak or no NHC−Si interaction at all. In the complexes of $TMSCF_3$ and diphenylsilane with IMe_2, the carbene lone pairs are not even directed toward the Si center (Figure S4). Therefore, it seems unlikely that a NHC−SiR complex plays any significant role in the catalytic pathway.

3.5. LMOEDA and NBO Analysis. Results of LMOEDA analysis on a few strongly binding complexes of $SiCl_4$ are displayed in Table 11. In most of the strongly binding complexes of $SiCl_4$ with diverse NHCs considered for LMOEDA, the electrostatic interaction (ΔE_{el}) is found to be the most dominant term followed by the exchange (ΔE_{ex}), polarization (ΔE_{pol}), and dispersion (ΔE_{dis}) interactions. Electrostatic interaction mainly results from the large positive charge on the Si atom and the negative charges on the C atoms of the alkyl groups on the N atoms of the imidazole ring of the NHCs. The exchange stabilization term is large, but destabilization from repulsion is much larger for the complexes. In all the complexes polarization interaction is also a very important term; this results mainly from the charge transfer from the NHC to $SiCl_4$. In the complexes NHC **14** and NHC **19**, the polarization interaction term is the second most dominant term ahead of the exchange interaction due to very high charge transfer (Table 5). Stabilization from the dispersion interaction is very small compared to the other interactions.

We have also studied the redistribution of charge in the SiR as a result of adduct formation with NHC. For this purpose natural population analysis (NPA) based charges were examined. NPA charges on some selected atoms of the adducts were obtained from NBO analysis in Table 12. In all the adducts, the Si atom bears a positive charge. On complexation with NHC, NPA charges on the Si atom show very little decrease in certain cases and in some other cases they have been found to increase. However, negative charges on the axial Cl atoms bonded to the Si atom are found to be significantly high compared to that in the free $SiCl_4$ molecule. This may be correlated to the observance of higher electron density on the axial Cl atoms in the HOMO−1 and HOMO−2 (Figure 6).

DOI: 10.1021/acs.jpca.5b08676
J. Phys. Chem. A 2016, 120, 128−138

Table 12. NPA Charges on the Si and Its Neighboring Atoms in the Halosilanes and in Some of Their Stable Complexes

adduct	charge on Si atom	charge on axial Cl atom	charge on equatorial Cl/C atom[a]
$SiCl_4$	1.290	−0.322	−0.322
Me_2SiCl_2	1.583	−0.389	−1.271(C)
Ph_2SiCl_2	1.641	−0.372	−0.587(C)
IMe_2-SiCl_4	1.286	−0.471	−0.343
$I^iPr_2-SiCl_4$	1.279	−0.471	−0.342
$Me_2IMe_2-SiCl_4$	1.288	−0.474	−0.345
ICy_2-SiCl_4	1.277	−0.472	−0.344
$IMe_2-Me_2SiCl_2$	1.575	−0.569	−1.245(C)
$I^iPr_2-Me_2SiCl_2$	1.571	−0.572	−1.248(C)
$Me_2IMe_2-Me_2SiCl_2$	1.576	−0.572	−1.247(C)
$ICy_2-Me_2SiCl_2$	1.568	−0.572	−1.247(C)
$IMe_2-Ph_2SiCl_2$	1.636	−0.536	−0.562(C)
$I^iPr_2-Ph_2SiCl_2$	1.629	−0.538	−0.564(C)
$Me_2IMe_2-Ph_2SiCl_2$	1.631	−0.542	−0.563(C)
$ICy_2-Ph_2SiCl_2$	1.627	−0.539	−0.560(C)

[a](C) near the charge value indicates a carbon atom.

Therefore, the observed increase or very little decrease of positive charge on the Si atom may be attributed to the delocalization of electron density from the Si atom to its neighboring atoms. The Denmark group has made good use of this effect in Lewis base-catalyzed transformations.[35]

4. CONCLUSIONS

A variety of NHC−Si reagent adducts have been investigated using the M05-2X/6-31G+(d,p) level of theory. Most of the strongly binding complexes identified here (hitherto not synthesized) have stability comparable to that of the synthesized ones. High charge transfer has been observed with the formation of the stable adducts, which indicates the donor−acceptor nature of the complexes. A good linear correlation has been observed between charge transfer and binding energy for the complexes where steric effect is not dominant. The proton affinity values of the NHCs also correlate linearly with the binding energies of the complexes. These linear correlations suggest that the complex formation between the NHCs and the SiRs results from Lewis acid−base type interaction. Out of the ten SiRs considered, only three halosilanes form strongly binding NHC−SiR adducts. In the fluoride affinity scale, these three are the most Lewis acidic SiRs among the considered. Most of the SiRs used in NHC catalyzed organic transformation favor either very weak or no bonding with the NHCs. Therefore, the possibility of involvement of a NHC−SiR complex in the relevant NHC catalyzed processes is very low. The steric bulk around the NHC and SiR is the most decisive factor in forming a stable NHC−SiR adduct. The most stable adducts are produced by the most electrophilic SiRs having the least steric bulk. NHCs participating in these stable adduct formations also do not have much steric bulk around the carbene carbon. When the steric effect is not significant, electronic effects due to the alkyl groups at the C4, C5, and the N atoms of the NHC are found to be important for the stability of the complexes.

■ ASSOCIATED CONTENT

Supporting Information

The Supporting Information is available free of charge on the ACS Publications website at DOI: 10.1021/acs.jpca.5b08676.

Energies, structures, coordinates, and frequency data of all the M0-52X/6-31+G(d,p) optimized geometries (PDF)

■ AUTHOR INFORMATION

Corresponding Author

*P. Phukan. E-mail: pphukan@yahoo.com. Phone: +91-361-2570535 (o). Fax: +91-361-2700311 (o).

Notes

The authors declare no competing financial interest.

■ ACKNOWLEDGMENTS

Financial Support from UGC, India (Grant No. 41-206/2012-SR), is gratefully acknowledged.

■ REFERENCES

(1) Hopkinson, M. N.; Richter, C.; Schedler, M.; Glorius, F. An Overview of N-Heterocyclic Carbenes. *Nature* **2014**, *510*, 485−496.

(2) Enders, D.; Niemeier, O.; Henseler, A. Organocatalysis by N-Heterocyclic Carbenes. *Chem. Rev.* **2007**, *107*, 5606−5655.

(3) Díez-González, S.; Marion, N.; Nolan, S. P. N-Heterocyclic Carbenes in Late Transition Metal Catalysis. *Chem. Rev.* **2009**, *109*, 3612−3676.

(4) Fuchter, M. J. N-Heterocyclic Carbene Mediated Activation of Tetravalent Silicon Compounds: a Critical Evaluation. *Chem. - Eur. J.* **2010**, *16*, 12286−12294.

(5) Suzuki, Y.; Abu Bakar, M. D.; Muramatsu, K.; Sato, M. Cyanosilylation of Aldehydes Catalyzed by N-Heterocyclic Carbenes. *Tetrahedron* **2006**, *62*, 4227−4231.

(6) Song, J. J.; Gallou, F.; Reeves, J. T.; Tan, Z.; Yee, N. K.; Senanayake, C. H. Activation of TMSCN by N-Heterocyclic Carbenes for Facile Cyanosilylation of Carbonyl Compounds. *J. Org. Chem.* **2006**, *71*, 1273−1276.

(7) Song, J. J.; Tan, Z.; Reeves, J. T.; Gallou, F.; Yee, N. K.; Senanayake, C. H. N-Heterocyclic Carbene Catalyzed Trifluoromethylation of Carbonyl Compounds. *Org. Lett.* **2005**, *7*, 2193−2196.

(8) Song, J. J.; Tan, Z.; Reeves, J. T.; Yee, N. K.; Senanayake, C. H. N-Heterocyclic Carbene-Catalyzed Mukaiyama Aldol reactions. *Org. Lett.* **2007**, *9*, 1013−1016.

(9) Wu, J.; Sun, X.; Ye, S.; Sun, W. N-Heterocyclic Carbene: a Highly Efficient Catalyst in the Reactions of Aziridines with Silylated Nucleophiles. *Tetrahedron Lett.* **2006**, *47*, 4813−4816.

(10) Riduan, S. N.; Zhang, Y.; Ying, J. Y. Conversion of Carbon dioxide into Methanol with Silanes over N-Heterocyclic Carbene Catalysts. *Angew. Chem., Int. Ed.* **2009**, *48*, 3322−3325.

(11) Raynaud, J.; Ciolino, A.; Baceiredo, A.; Destarac, M.; Bonette, F.; Kato, T.; Gnanou, Y.; Taton, D. Harnessing the Potential of N-Heterocyclic Carbenes for the Rejuvenation of Group-Transfer Polymerization of (Meth)Acrylics. *Angew. Chem., Int. Ed.* **2008**, *47*, 5390−5393.

(12) Rodriguez, M.; Marrot, S.; Kato, T.; Stérin, S.; Fleury, E.; Baceiredo, A. Catalytic Activity of N-Heterocyclic Carbenes in Ring Opening Polymerization of Cyclic Siloxanes. *J. Organomet. Chem.* **2007**, *692*, 705−708.

(13) Marrot, S.; Bonnette, F.; Kato, T.; Saint-Jalmes, L.; Fleury, E.; Baceiredo, A. N-. Heterocyclic Carbene Catalyzed Dehydration of α,ω-Disilanol Oligomers. *J. Organomet. Chem.* **2008**, *693*, 1729−1732.

(14) Huang, F.; Lu, G.; Zhao, L.; Li, H.; Wang, Z.-X. The Catalytic Role of N-Heterocyclic Carbene in a Metal-free Conversion of Carbon Dioxide into Methanol: A Computational Mechanism Study. *J. Am. Chem. Soc.* **2010**, *132*, 12388−12396.

(15) Kuhn, N.; Kratz, T.; Bläser, D.; Boese, R. Derivate des Imidazols, XIII. Carben-Komplexe des Siliciums und Zinns. *Chem. Ber.* **1995**, *128*, 245−250.

(16) Böttcher, T.; Bassil, B. S.; Zhechkov, L.; Heine, T.; Röschenthaler, G. V. $(NHC^{Me})SiCl_4$: a Versatile Carbene Transfer

DOI: 10.1021/acs.jpca.5b08676
J. Phys. Chem. A 2016, 120, 128−138

Reagent − Synthesis from Silicochloroform. *Chem. Sci.* **2013**, *4*, 77−83.
(17) Yao, S.; Xiong, Y.; Driess, M. N-Heterocyclic Carbene (NHC)-stabilized Silanechalcogenones: NHC→Si(R_2) = E (E = O, S, Se, Te). *Chem. - Eur. J.* **2010**, *16*, 1281−1288.
(18) Bonnette, F.; Kato, T.; Destarac, M.; Mignani, G.; Cosso, F. P.; Baceiredo, A. Encapsulated N-Heterocyclic Carbenes in Silicones without Reactivity Modification. *Angew. Chem., Int. Ed.* **2007**, *46*, 8632−8635.
(19) Hollczki, O.; Nyulászi, L. Stability and Structure of Carbene-Derived Neutral Penta- and Hexacoordinate Silicon Complexes. *Organometallics* **2009**, *28*, 4159−4164.
(20) Liu, Z. Chemical Bonding in Silicon−Carbene Complexes. *J. Phys. Chem. A* **2009**, *113*, 6410−6414.
(21) Dixon, D. A.; Hertler, W. R.; Chase, D. B.; Farnham, W. B.; Davidson, F. Pentacoordinate Cyanosiliconates. *Inorg. Chem.* **1988**, *27*, 4012−4018.
(22) Damrauer, R.; Burggraf, L. W.; Davis, L. P.; Gordon, M. S. Gas-Phase and Computational Studies of Pentacoordinate Silicon. *J. Am. Chem. Soc.* **1988**, *110*, 6601−6606.
(23) Grant, D. J.; Arduengo, A. J., III; Dixon, D. A. Diammoniosilane: Computational Prediction of the Thermodynamic Properties of a Potential Chemical Hydrogen Storage System. *J. Phys. Chem. A* **2009**, *113*, 750−755.
(24) Frisch, M. J.; Trucks, G. W.; Schlegel, H. B.; Scuseria, G. E.; Robb, M. A.; Cheeseman, J. R.; Scalmani, G.; Barone, V.; Mennucci, B.; Petersson, G. A.; et al. *Gaussian 09*, Revision C.01; Gaussian, Inc.: Wallingford, CT, 2010.
(25) Becke, A. D. Density-Functional Thermochemistry. III. The Role of Exact Exchange. *J. Chem. Phys.* **1993**, *98*, 5648−5652.
(26) Lee, C.; Yang, W.; Parr, R. G. Development of the Colle-Salvetti Conelation Energy Formula into a Functional of the Electron Density. *Phys. Rev. B: Condens. Matter Mater. Phys.* **1988**, *37*, 785−789.
(27) Zhao, Y.; Schultz, N. E.; Truhlar, D. G. Design of Density Functionals by Combining the Method of Constraint Satisfaction with Parametrization for Thermochemistry, Thermochemical Kinetics, and Noncovalent Interactions. *J. Chem. Theory Comput.* **2006**, *2*, 364−382.
(28) Boys, S. F.; Bernardi, F. Calculation of Small Molecular Interactions by Differences of Separate Total Energies - Some Procedures with Reduced Errors. *Mol. Phys.* **1970**, *19*, 553−566.
(29) Simon, S.; Duran, M.; Dannenberg, J. J. How Does Basis Set Superposition Error Change the Potential Surfaces for Hydrogen Bonded Dimers? *J. Chem. Phys.* **1996**, *105*, 11024−11031.
(30) Tomasi, J.; Mennucci, B.; Cammi, R. Quantum Mechanical Continuum Solvation Models. *Chem. Rev.* **2005**, *105*, 2999−3093.
(31) Su, P.; Li, H. Energy Decomposition Analysis of Covalent Bonds and Intermolecular Interactions. *J. Chem. Phys.* **2009**, *131*, 014102−014115.
(32) Schmidt, M. W.; Baldridge, K. K.; Boatz, J. A.; Elbert, S.; Gordon, M. S.; Jensen, J. J.; Koseki, S.; Matsunaga, N.; Nguyen, K. A.; Su, S. J.; et al. General Atomic and Molecular Electronic Structure System. *J. Comput. Chem.* **1993**, *14*, 1347−1363.
(33) Reed, A. E.; Curtiss, L. A.; Weinhold, F. Intermolecular Interactions from a Natural Bond Orbital, Donor-Acceptor Viewpoint. *Chem. Rev.* **1988**, *88*, 899−926.
(34) Ghadwal, R. S.; Sen, S. S.; Roesky, H. W.; Tavcar, G.; Merkel, S.; Stalke, D. Neutral Penta- and Hexacoordinate N-Heterocyclic Carbene Complexes Derived from SiX_4 (X = F, Br). *Organometallics* **2009**, *28*, 6374−6377.
(35) Denmark, S. E.; Beutner, G. L. Lewis Base Catalysis in Organic Synthesis. *Angew. Chem., Int. Ed.* **2008**, *47*, 1560−1638.

DOI: 10.1021/acs.jpca.5b08676
J. Phys. Chem. A 2016, 120, 128−138